Mathematical modelling of microbial cross-feeding on hydrogen in the human colon

A thesis presented in partial fulfilment of the requirements for the degree of

Doctor of Philosophy

in

Nutritional Science

at

Massey University

Palmerston North

New Zealand

Nick William Smith

2020

Abstract

The microbial population of the human colon contains three subgroups that cross-feed on hydrogen produced during microbial metabolism of carbohydrates: methanogens, sulphate-reducing bacteria (SRB) and reductive acetogens. These microbes and their activities have been linked to various host physiological and health outcomes. This thesis aimed to construct mathematical models for the growth and metabolism of colonic hydrogenotrophs to investigate key factors in hydrogenotroph metabolism and population dynamics that would be difficult to study experimentally.

Monoculture models based on Monod kinetics were developed for *Methanobrevibacter smithii*, *Desulfovibrio vulgaris*, and *Blautia hydrogenotrophica*, as representatives of colonic methanogens, SRB and reductive acetogens. The models were parameterised and validated using experimental data. The monoculture models were combined to examine interactions between these microbes, before incorporation into an existing microbial community model, microPop. Adaptations were made to microPop to enable simulation of the colonic environment, investigating the role of hydrogenotrophs in the colon.

The *D. vulgaris* model provided similarly accurate predictions to an existing thermodynamics-based model. The *B. hydrogenotrophica* model estimated a hydrogen uptake threshold of 86 mM and provided supportive evidence for the confounding effect of growth media on reductive acetogenesis. Growth yield parameters for SRB and methanogenic strains were reduced in co-culture compared to monoculture, while tri-culture modelling identified conditions necessary for the survival of each hydrogenotroph. Substrate competition prevented survival of all three together in continuous culture. The community model predicted colonic pH, short chain fatty acid gradient and dominant microbial groups but could not accurately predict other experimental metabolite and microbial abundance measurements. Investigating the role of colonic sulphate availability showed contrasting predictions: sulphate availability positively correlated with SRB and sulphide concentrations and negatively correlated with methanogen abundance using a continuous representation of the colon, but no effect was predicted using a compartmental representation.

This research demonstrates that modelling can extract additional information from existing experimental data. The community model provides a basis for the computational study of the microbiota and hydrogen cross-feeding dynamics in the colon, which can complement or even accelerate experimental research on the influences of the microbiome on the host.

Acknowledgements

The greatest thanks for the completion of this thesis must go to my supervisors. Dr Paul Shorten was always available to resolve modelling difficulties and suggest new techniques, as well as being a calming influence in the early stages. Thanks to Dr Amy Van Wey Lovatt for excellent criticism and always challenging me to prove that I knew what I was talking about, and most sincerely for convincing me to start the PhD in the first place. Dr Eric Altermann gave extremely thoughtful and thought-provoking feedback on all material. His short questions at the end of any draft would often provoke days of further study, to the great benefit of the draft. Prof Nicole Roy was always quick in resolving my questions and any difficulties around management of the PhD, as well as encouraging me to travel further and meet more people than I would have attempted to otherwise. Thanks to Prof Warren McNabb for well-timed and inspiring encouragement. I enjoyed both his and the other supervisors' pleasure at seeing things occasionally go wrong for me as the PhD progressed, when it had all seemed so easy at the start. My supervisors must also be thanked for the flexibility allowed to me in where I based myself, trusting me to work effectively from overseas while spending time with family.

I am grateful to the Tertiary Education Commission for funding this PhD project through the Riddet Institute Centre of Research Excellence and Massey University. I also acknowledge the many contributions from the Riddet Institute, including the Riddet Institute Travel Grant that enabled me to present my research internationally. Despite being at distance from the core body of Riddet students, I felt part of the 'Riddet family' and the student colloquia were some of the most enjoyable meetings I attended. I thank the Riddet students and staff for being so welcoming and inclusive on my irregular meetings with them around the country.

I also thank AgResearch Ltd. for housing and supporting me throughout my studies, and for letting me tag along as part of various science teams and projects that took my interest. I immediately felt at home on the Ruakura campus thanks to the welcoming nature of the people working there. They formed the foundations of my social activities in a new city, from sports teams to housemates, and I thank them for the many enjoyable distractions that they have provided.

Several people also directly contributed to this thesis through advice, discussion and encouragement. In this respect, I must thank Indrakumar Vetharaniam for his coding assistance and insightful modelling advice. Further, I thank Rafael Munoz-Tamayo for hosting me in Paris, Helen Kettle for hosting me in Edinburgh, and the researchers at APC Microbiome for hosting me in Cork.

Thank you to my overseas and New Zealand family and friends for providing timely holidays over the last three years, particularly those who travelled to New Zealand for this purpose. Special thanks to those of you who have made the effort to read far more gut and modelling research than you ever deserved to. Another important thank you to my newly adopted Tauwhare family, who have made me feel at home in the Waikato from the start with their generosity, hospitality and games. Thanks Mel: you have been supportive and encouraging throughout, made sure I celebrated milestones along the way, and kept me from turning into too much of a nerd.

Finally, I thank all those experimental scientists whose data I have 'borrowed' in my research. Without data to validate them, the models presented here would be entirely theoretical and far less useful. I hope mathematical modelling continues to be of use in guiding experimental work in the future, to return the favour.

Contents

Abstract ii
Acknowledgements iv
Contents vi
List of Figures x
List of Tables xii
Abbreviations xiii
Publications xv
Note to the reader xv
Chapter 1: Introduction 1
References 4
Chapter 2: Literature Review 6
2.1 Introduction 6
2.2 Classification of microbial cross-feeding 11
2.2.1 Cross-feeding in one direction 12
2.2.2 Cross-feeding in both directions 14
2.3 Evolution of microbial cross-feeding 17
2.3.1 Specialisation 18
2.3.2 The Black Queen Hypothesis 21
2.3.3 Mutual cross-feeding 24
2.3.4 Augmented cross-feeding 26
2.3.5 The influence of spatial structure on cross-feeding evolution 29
2.3.6 Stability and persistence of cross-feeding relationships 33
2.4 Future directions for cross-feeding terminology and evolution research 36
2.5 Short chain fatty acid production via cross-feeding on carbohydrates in the colon 37
2.5.1 Butyrate production via cross-feeding 38
2.5.2 Beyond co-culture: short chain fatty acid cross-feeding in more diverse consortia 40
2.6 The relationship between pH and cross-feeding interactions 44
2.7 The hydrogenotrophic functional groups of the human colon 48
2.7.1 Methanogens 50
2.7.2 Sulphate-reducing bacteria 52
2.7.3 Acetogens 54
2.7.4 Competition between the hydrogenotrophic functional groups 56
2.7.5 The balance between hydrogenotrophic functional groups in the colon 59
2.8 The health implications of hydrogen in the colon 65
2.8.1 Health impacts of hydrogen cross-feeding on the host 65
2.8.2 Mitigation of the harmful effects of hydrogen cross-feeding 68
2.9 Mathematical modelling of the human colonic microbiota 70
2.10 Future directions for colonic hydrogenotroph research 75

2.11 Conclusions 75
2.12 Aims of the thesis 76
References 80
Chapter 3: Mathematical models for the growth and hydrogenotrophic metabolism of *Methanobrevibacter smithii* 95
Abstract 95
3.1 Introduction 95
3.2 Methodology 97
3.2.1 Mathematical models 97
3.2.2 Biological assumptions 101
3.2.3 Data capture 102
3.2.4 Model fitting 102
3.3 Results 103
3.3.1 Model calibration 103
3.3.2 Model validation 107
3.4 Discussion 109
3.5 Conclusions 111
References 111
Chapter 4: A mathematical model for the growth of the sulphate-reducing bacterium *Desulfovibrio vulgaris* 115
Abstract 115
4.1 Introduction 116
4.2 Methodology 118
4.2.1 Assumptions 118
4.2.2 Mathematical model 119
4.2.3 Data capture 123
4.2.4 Model fitting 123
4.2.5 Statistical analysis 123
4.3 Results 124
4.3.1 Model calibration 124
4.3.2 Model validation 130
4.4 Discussion 134
4.5 Conclusions 138
References 139
Chapter 5: Mathematical modelling of the reductive acetogen *Blautia hydrogenotrophica* supports the existence of a threshold hydrogen concentration and media-dependent yields 144
Abstract 144
5.1 Introduction 144
5.2 Methodology 146
5.2.1 Assumptions 146
5.2.2 Data capture 146

5.2.3 Model fitting 147
5.2.4 Mathematical model 147
5.3 Results 152
5.3.1 Model calibration 152
5.3.2 Model validation 154
5.4 Discussion 155
5.5 Conclusions 160
References 161
Chapter 6: Mathematical modelling of sulphate-reducing bacteria and methanogenic archaea shows differences in metabolic parameter values between monoculture and co-culture 165
Abstract 165
6.1 Introduction 166
6.2 Methodology 167
6.2.1 Mathematical model 167
6.2.2 Experimental data 169
6.2.3 Model fitting 169
6.3 Results 171
6.3.1 Comparison of model predictions to experimental data using monoculture-derived parameters 171
6.3.2 Comparison of model predictions to experimental data using fitted metabolic parameters 178
6.4 Discussion 188
6.5 Conclusions 191
References 191
Chapter 7: Competition for hydrogen prevents coexistence of human gastrointestinal hydrogenotrophs in a continuous culture environment 194
Abstract 194
7.1 Introduction 195
7.2 Methodology 196
7.2.1 Mathematical model 196
7.2.2 Numerical simulations 198
7.3 Results 200
7.3.1 Analysis of the model under batch culture conditions 200
7.3.2 Analysis of the model under continuous culture conditions 205
7.3.3 Numerical analysis of the model under continuous culture conditions 213
7.4 Discussion 217
7.5 Conclusions 220
References 220
Chapter 8: Adaptation of the microbial community model microPop for the study of hydrogenotrophs of the human colon 225
Abstract 225
8.1 Introduction 226

8.2 Methodology 227
8.2.1 Consideration of hydrogen cross-feeding in microPop 227
8.2.2 Comparison of microPop to experimental data 228
8.2.3 Adaptation of microPop to the human colonic environment 228
8.2.4 Computation 231
8.3 Results 231
8.3.1 Comparison of model predictions to experimental data 231
8.3.2 Simulation of the colonic microbiota 245
8.4 Discussion 258
8.5 Conclusions 268
References 269
Chapter 9: General discussion 274
9.1 Summary 274
9.2 Future perspectives 280
References 284
Appendix A 287
Appendix B 289
B1: Monoculture sulphate-reducing bacteria model 289
B2: Monoculture methanogen model 289
B3: Supplementary tables 291
References 293
Appendix C 294
C1: microPop equations 294
C2: Summary of parameter values and metabolic pathways for the three hydrogenotrophic microbial functional groups 297
C3: Metabolite influx rates for comparison to experimental data 298
C4: Microbial abundance calculations 300
C5: Addition of mucin and alterations to Bacteroides microbial functional group 305
C6: pH modelling 305
C7: Supplementary figures 308
C8: Parameter values for the Beta parameter set 309
References 311
Appendix D 313

List of Figures

Figure 2.1. Overview diagram of hydrogen production and cross-feeding in the colon..... 9
Figure 2.2. Diagrammatic examples of cross-feeding classifications..... 13
Figure 2.3. Venn diagram illustrating the nature of mutual and augmented cross-feeding..... 15
Figure 2.4. Diagrammatic example of evolution via the Black Queen Hypothesis..... 22
Figure 2.5. Tri-culture cross-feeding dynamics from experimentation by Moens et al. (2017)..... 42
Figure 2.6. Hydrogenotrophic methanogenesis diagram..... 51
Figure 2.7. Lactate and sulphate metabolic pathways in *Desulfovibrio vulgaris*..... 53
Figure 2.8. Wood-Ljungdahl pathway diagram..... 55
Figure 2.9. Overview of the thesis structure..... 79

Figure 3.1. *Methanobrevibacter smithii* monoculture data from Khelaifia et al. (2013)..... 102
Figure 3.2. Comparison of methanogen growth rate models to calibration data..... 103
Figure 3.3. Comparison of methanogen growth rate models to calibration data with inclusion of a lag phase..... 105
Figure 3.4. *Methanobrevibacter smithii* monoculture data from Muñoz-Tamayo et al. (2019)..... 107
Figure 3.5. Comparison of methanogen growth rate models to validation data..... 108
Figure 3.6. Comparison of methanogen growth rate models to validation data with inclusion of a lag phase..... 109

Figure 4.1 Structure of the sulphate-reducing bacteria mathematical model..... 120
Figure 4.2. Model fits to lactate and sulphate calibration data from Noguera et al. (1998)..... 127
Figure 4.3. Model fits to lactate only calibration data from Noguera et al. (1998)..... 127
Figure 4.4. Model fits to sulphate and hydrogen validation data from Noguera et al. (1998)..... 130
Figure 4.5. Model fits to first lactate and sulphate validation data from Noguera et al. (1998)..... 132
Figure 4.6. Model fits to second lactate and sulphate validation data from Noguera et al. (1998)..... 132
Figure 4.7. Model fits to lactate and sulphate validation data from da Silva et al. (2013)..... 134

Figure 5.1. Comparison of Monod kinetics with first order kinetics when fit to monoculture data for *Blautia hydrogenotrophica*..... 149
Figure 5.2. Comparison of model fits to calibration data from Bernalier et al. (1996)..... 152
Figure 5.3. Comparison of model fits to validation data from Groher and Weuster-Botz (2016b) using General Acetogen medium..... 154
Figure 5.4. Comparison of model fits to validation data from Groher and Weuster-Botz (2016b) using DSMZ medium..... 155
Figure 5.5. Example model prediction for *Blautia hydrogenotrophica* growth on DSMZ medium with the inclusion of yeast extract metabolism..... 159

Figure 6.1 Model fit to co-culture data of *Desulfovibrio vulgaris* and *Methanococcus maripaludis* from Stolyar et al. (2007) using monoculture parameters..... 172
Figure 6.2. Model fit to co-culture data of *Desulfovibrio vulgaris* and *Methanococcus maripaludis* from Walker et al. (2009) using monoculture parameters..... 173
Figure 6.3. Model fit to co-culture data of *Desulfovibrio alaskensis* and *Methanococcus maripaludis* from Meyer et al. (2013) using monoculture parameters..... 174
Figure 6.4. Model fit to the data of Meyer et al. (2013) using six fitting parameters..... 180
Figure 6.5. Model fit to the data of Meyer et al. (2013) using nine fitting parameters..... 181
Figure 6.6. Model fit to the data of Stolyar et al. (2007) using six-parameter set values..... 182
Figure 6.7. Model fit to the data of Walker et al. (2009) using six-parameter set values..... 183
Figure 6.8. Model fit to the data of Stolyar et al. (2007) using nine-parameter set values..... 184
Figure 6.9. Model fit to the data of Walker et al. (2009) using nine-parameter set values..... 185

Figure 7.1. Early stages of batch tri-culture with lactate the sole added substrate..... 201
Figure 7.2. Late stages of batch tri-culture with lactate the sole added substrate..... 202

Figure 7.3. Conditions necessary for an acetogen growth rate above 0.1 g L^{-1} h^{-1} 203
Figure 7.4. Comparison of steady state hydrogen concentrations achieved by the methanogen and the reductive acetogen 206
Figure 7.5. Conditions necessary for sulphate-reducing bacteria survival in the absence of lactate…. 207
Figure 7.6. Conditions necessary for sulphate-reducing bacteria survival in the absence of sulphate. 208
Figure 7.7. Maximum dilution rates under which only the acetogen survives continuous culture……. 214
Figure 7.8. Minimum dilution rates under which only the methanogen survives continuous culture. 215
Figure 7.9. Maximum dilution rates under which only the sulphate-reducing bacterium survives continuous culture 216
Figure 7.10. Dilution rates under which both the methanogen and the sulphate-reducing bacterium survive continuous culture 217

Figure 8.1. Model prediction compared with experimental data from Walker et al. (2005) for continuous culture of a faecal microbial community with 0.6% w/v peptide 232
Figure 8.2. Model prediction compared with experimental data from Walker et al. (2005) for continuous culture of a faecal microbial community with 0.1% w/v peptide. 233
Figure 8.3. Model prediction compared with experimental data from Walker et al. (2005) for continuous culture of a faecal microbial community (Donor 1) with a pH shift. 234
Figure 8.4. Model prediction compared with experimental data from Walker et al. (2005) for continuous culture of a faecal microbial community (Donor 2) with a pH shift. 235
Figure 8.5. Model predictions for short chain fatty acid production compared to data from Belenguer et al. (2011) for faecal cultures at pH 5.5 235
Figure 8.6. Model predictions for short chain fatty acid production compared to data from Belenguer et al. (2011) for faecal cultures at pH 6 237
Figure 8.7. Short chain fatty acid concentrations in the three fermenter compartments over the course of experiment A of Payne et al. (2012a) 239
Figure 8.8. A comparison of observed and modelled microbial relative abundances in each compartment in experiment A of Payne et al. (2012a) 240
Figure 8.9. Short chain fatty acid concentrations in the three fermenter compartments over the course of experiment B of Payne et al. (2012a) 241
Figure 8.10. A comparison of observed and modelled microbial relative abundances in each compartment in experiment B of Payne et al. (2012a) 242
Figure 8.11. Diagrammatic explanation of the major adaptations made to microPop in the development of microPop:Colon. 245
Figure 8.12. pH dynamics over the first ten days of the discrete microPop:Colon simulation 246
Figure 8.13. Microbial functional group dynamics in the proximal compartment over the first ten days of the discrete microPop:Colon simulation 247
Figure 8.14. Short chain fatty acid dynamics in the distal compartment over the first ten days of the discrete microPop:Colon simulation 247
Figure 8.15. pH dynamics over a day of colonic transit simulated with the continuous microPop:Colon model 250
Figure 8.16. Microbial functional group dynamics over a day of colonic transit simulated with the continuous microPop:Colon model 251
Figure 8.17. Short chain fatty acid dynamics over a day of colonic transit simulated with the continuous microPop:Colon model 252

Figure 9.1. Summary of the main results of the thesis. 279

List of Tables

Table 2.1. Cell, gene and relative abundance of hydrogenotrophic microbial functional groups measured in samples from healthy individuals..... 49
Table 2.2. Summary of selected mathematical models for the colonic microbiome 74

Table 3.1. Mathematical notation for the methanogen monoculture model 100
Table 3.2. Best fit parameter estimates for the four methanogen model structures considered . 104
Table 3.3. Best fit parameter estimates for the four methanogen model structures considered after inclusion of a lag phase 106

Table 4.1. Sulphate-reducing bacteria model parameter values. 125
Table 4.2. Analysis of sulphate-reducing bacteria model fits to calibration data 128
Table 4.3. Akaike information criterion calculation values for the newly developed sulphate-reducing bacteria model and that of Noguera et al. (1998) 128
Table 4.4. Comparison of model parameter estimate confidence intervals when half-saturation constants were included or excluded from the estimation 130
Table 4.5. Mathematical notation for the sulphate-reducing bacteria monoculture model..... 139

Table 5.1. Best fit parameter values for the acetogen monoculture model..... 153
Table 5.2. Mathematical notation for the acetogen monoculture model..... 161

Table 6.1. Comparison of model fits to experimental co-culture data using biological parameters determined from monoculture fitting..... 176
Table 6.2. Parameter values obtained via model fitting to co-culture data for the six- and nine-parameter sets..... 187

Table 7.1. Mathematical notation for the tri-culture model 199
Table 7.2. Outcomes of batch tri-culture under various initial conditions 204
Table 7.3. Outcomes of continuous tri-culture under various initial conditions..... 211

Table 8.1. Mean bias of the microPop model fits to short chain fatty acid data sets 243
Table 8.2. Comparison of simulation predictions from the discrete and continuous microPop:Colon models..... 254
Table 8.3. Summary of changes in predicted microbiota and metabolite concentrations with varied sulphate influx and transit times in the continuous microPop model..... 258

Abbreviations

ADM1	Anaerobic Digestion Model No. 1
AIC(c)	(corrected) Akaike information criterion
AXOS	Arabinoxylan oligosaccharides
CCC	Concordance correlation coefficient
CDW	Cell dry weight
COBRA	Constraint-based reconstruction and analysis
CRC	Colorectal cancer
FBA	Flux balance analysis
FOS	Fructooligosaccharides
GA	General acetogen
GIT	Gastrointestinal tract
H_2S	Hydrogen sulphide
HE	High-energy (in reference to growth medium in Chapter 8)
HighS	High sulphate availability (in reference to colonic conditions investigated in Chapter 8)
IBD	Inflammatory Bowel Disease
IBS(-C)	Irritable Bowel Syndrome (with constipation)
LE	Low-energy (in reference to growth medium in Chapter 8)
LTEE	Long-term evolution experiment
MCMC	Markov chain Monte Carlo
MFG	Microbial functional group
MTC	Mass transfer coefficient
NE	Normal-energy (in reference to growth medium in Chapter 8)
NormS	Normal sulphate availability (in reference to colonic conditions investigated in Chapter 8)

NoS	No sulphate availability (in reference to colonic conditions investigated in Chapter 8)
NSP	Non-starch polysaccharide
OD	Optical density
ODE	Ordinary differential equation
OF	Oligofructose
RS	Resistant starch
SCFA	Short chain fatty acid
SRB	Sulphate-reducing bacteria
TIM-2	TNO Intestinal Model 2

Publications

Smith NW, Shorten PR, Altermann EH, Roy NC, McNabb WC (2018): Hydrogen cross-feeders of the human gastrointestinal tract. Gut Microbes 10(3): 270-288. https://doi.org/10.1080/19490976.2018.1546522

Smith NW, Shorten PR, Altermann E, Roy NC, McNabb WC (2019): The Classification and Evolution of Bacterial Cross-Feeding. Frontiers in Ecology and Evolution 7:153. https://doi.org/10.3389/fevo.2019.00153

Smith NW, Shorten PR, Altermann E, Roy NC, McNabb WC (2019): A Mathematical Model for the Hydrogenotrophic Metabolism of Sulphate-Reducing Bacteria. Frontiers in Microbiology 10:1652. https://doi.org/10.3389/fmicb.2019.01652

Smith NW, Shorten PR, Altermann E, Roy NC, McNabb WC (2020): Mathematical modelling supports the existence of a threshold hydrogen concentration and media-dependent yields in the growth of a reductive acetogen. Bioprocess and Biosystems Engineering. https://doi.org/10.1007/s00449-020-02285-w

Smith NW, Shorten PR, Altermann E, Roy NC, McNabb WC (2020): Competition for hydrogen prevents coexistence of human gastrointestinal hydrogenotrophs in continuous culture. Frontiers in Microbiology 11:1073. https://doi.org/10.3389/fmicb.2020.01073

Smith NW, Shorten PR, Altermann E, Roy NC, McNabb WC (Submitted to Ecological Modelling): Co-culture modelling of a sulphate-reducing bacterium and a methanogen shows altered metabolic parameters compared to monoculture.

Smith NW, Shorten PR, Altermann E, Roy NC, McNabb WC (In preparation for submission to Microbiome): Examination of hydrogen cross-feeders using a colonic microbiota model.

Note to the reader

The practice for presenting and discussing mathematics differs from that of biology. It is conventional to describe biological methodology and results in the past tense, whereas mathematics is usually presented in the present tense. As the topic of this thesis includes both biology and mathematics, it was necessary to use the appropriate convention for both fields: biological material is discussed in the past tense, whereas mathematical models are described in the present tense.

The data to support the conclusions of this thesis can be found under the following link: https://drive.google.com/open?id=1RSULthw86TF9Fh_MXCAgry2ntyJhvWRs

Chapter 1: Introduction

The human gastrointestinal tract (GIT) microbiome has attracted increasing attention from both the scientific community and the general public due to clear evidence that GIT microbes influence host physiology and metabolism, and thus human health and wellbeing (Cani, 2018). The term 'microbiome', in reference to a community of microbes, is defined as "the entire habitat, including the microorganisms […] their genomes […] and the surrounding environmental conditions" (Marchesi and Ravel, 2015), with 'microbiota' used to refer to the microbial component of the microbiome. The human GIT microbiome encompasses all microbes and host GIT cells, as well as diet-, host- and microbially-derived molecules, against the background physiology and biochemistry of the GIT. The term 'microbiome' has been in use for decades to describe small ecological communities (see review by Prescott (2017)), but since its application to the human GIT, research mentioning this term has increased exponentially, with 80% of GIT microbiome research publications between 1977 and 2017 having been published since 2013 (Cani, 2018).

During this bloom of interest and research, the microbiome has been linked to numerous aspects of host nutrition, digestive physiology, metabolism and health. Notable examples include: determining the yield of energy and important nutrients obtained by the host (see review by Treuren and Dodd (2020)); roles in pathogenic infections and diseases of the GIT such as inflammatory bowel disease (IBD) and colorectal cancer (CRC); links to disease in distal regions of the body, including the heart and brain (see review by Illiano et al. (2020)); and even links between the microbiome and the brain, which extend to influences on cognition, mood, stress response and neurological development (see review by Butler et al. (2019)).

Perhaps the most widely studied organisms of the GIT microbiome are those species inhabiting the colon that metabolise resistant carbohydrates (resistant here meaning resistant to human digestive enzymes in the stomach and small intestine), which are the primary substrate class to reach the distal colon (Payling et al., 2020). These saccharolytic organisms produce a range of products during carbohydrate metabolism, including the widely studied short chain fatty acids (SCFAs; den Besten et al., 2013). Another product of carbohydrate metabolism that has received less

attention is hydrogen, despite its important role in determining the thermodynamic viability of many carbohydrate metabolic pathways. The anaerobic breakdown of carbohydrates in the colon usually takes place via the reduction of cofactors such as NAD, which must then be reoxidised for further use; this reoxidation results in the formation of H_2. The thermodynamic favourability of cofactor reoxidation is partly determined by the local concentration of hydrogen, with reoxidation increasingly inhibited as the hydrogen concentration increases (see Stams (1994) and Van Lingen et al. (2016) for detailed descriptions of the thermodynamics of cofactor oxidation in carbohydrate breakdown). Thus, an effective hydrogen removal system is required for efficient carbohydrate metabolism. In the colon, this removal is performed by host absorption and excretion of hydrogen, but also by hydrogenotrophic microbes that utilise hydrogen as a metabolic substrate. As well as their influence on colonic hydrogen concentration, the products formed by these hydrogenotrophs have demonstrated impacts on the host, including roles in host energy yield, colonic transit time and GIT disease development (Samuel and Gordon, 2006; Sahakian et al., 2010; Carbonero et al., 2012). The hydrogenotrophic members of the microbiome form the focal point of this thesis.

To date, experimental research on the microbiome has taken many forms, with common examples including isolation and culture of single strains, the use of animal models associated with human colonic microbes, and observational or interventional studies with human subjects coupled with genomic, metabolomic and proteomic profiling of faecal samples. The main advantage of experimentation is that the information extracted from experiments is limited only by the currently available analytical technology, which can already provide information as detailed as detection and quantification of nucleic acids at concentrations as low as 10^{-15} moles (Degliangeli et al., 2014), and differentiation between more than 6,000 faecal metabolites (Karu et al., 2018).

The disadvantages of the experimental approaches are the financial and time investments required in their execution. Moreover, animal and human studies are ethically constrained and can be invasive or disruptive to the lives of the subjects. Microbiome sampling can be limited by the difficulty of obtaining samples and data directly from the colon, with faecal analysis only a proxy for the distal region of the colon. As such, it is advantageous to extract as much information as possible from data generated in experimental research to reduce repetition of similar experiments with different goals. It is here that computational biology and bioinformatics can complement

experimental research by extracting further information from data, in addition to the testing of the original hypothesis.

Mathematical modelling is one computational method for the interrogation of data generated from both *in vitro* and direct study of the microbiome. The construction of a mechanistic mathematical model involves making assumptions about the behaviour of a system (be this a single microbe in culture or the diverse microbiome population) based on existing knowledge of the system. This set of assumptions is then expressed mathematically, and both model and predictions are inspected and compared to experimental data to determine relevance. Once validated, a model can be used to computationally investigate experimental data, provide theoretical hypothesis tests and suggest avenues for further research. The greater the number of independent data sets that the model is validated against, the greater its value in providing predictions, thus there is a clear advantage to using both experimental and modelling techniques together.

The work of Muñoz-Tamayo et al. (2019) exemplifies this. These researchers cultured three methanogenic microbial strains in monoculture to investigate the energetics of their metabolism of hydrogen. This work allowed them to estimate the thermodynamic properties of the reactions carried out by each strain. Next, the authors constructed mathematical models for each of the three microbes, parameterised using the monoculture data. These models were then used to investigate competition between the three methanogens under various conditions, finding that the surviving strain differed between environmental conditions, even when these conditions were similar. The use of the model allowed for investigation of co-culture that would have been challenging to conduct and monitor experimentally. The additional degree of insight taken from the model demonstrates the value of including the computational approach in microbiology research.

In this thesis, mathematical modelling is applied to gain new insights into the role of the hydrogen cross-feeding microbes of the human colon. These microbes have a demonstrated role in human nutrition and health, as highlighted in the review of the literature in Chapter 2. However, understanding of the dietary and host factors that determine their population size in each individual is lacking. This thesis seeks to provide mathematical models that can be used to interrogate existing experimental data for hydrogenotroph metabolism and growth in monoculture and when competing or cross-feeding with other microbes of the human colonic microbiota. Moreover, these models

should provide a means to simulate and predict the results of experimental or interventional research, providing information not easily obtained experimentally.

References

Butler, M.I., Cryan, J.F., and Dinan, T.G. (2019). Man and the Microbiome: A New Theory of Everything? Ann. Rev. Clin. Psych. 15(1), 371-398. doi: 10.1146/annurev-clinpsy-050718-095432.

Cani, P.D. (2018). Human gut microbiome: hopes, threats and promises. Gut 67(9), 1716. doi: 10.1136/gutjnl-2018-316723.

Carbonero, F., Benefiel, A.C., Alizadeh-Ghamsari, A.H., and Gaskins, H.R. (2012). Microbial pathways in colonic sulfur metabolism and links with health and disease. Front. Physiol. 3:448. doi: 10.3389/fphys.2012.00448.

Degliangeli, F., Kshirsagar, P., Brunetti, V., Pompa, P.P., and Fiammengo, R. (2014). Absolute and Direct MicroRNA Quantification Using DNA–Gold Nanoparticle Probes. J. Am. Chem. Soc. 136(6), 2264-2267. doi: 10.1021/ja412152x.

den Besten, G., Van Eunen, K., Groen, A.K., Venema, K., Reijngoud, D.J., and Bakker, B.M. (2013). The role of short-chain fatty acids in the interplay between diet, gut microbiota, and host energy metabolism. J. Lipid Res. 54(9), 2325-2340. doi: 10.1194/jlr.R036012.

Illiano, P., Brambilla, R., and Parolini, C. (2020). The mutual interplay of gut microbiota, diet and human disease. FEBS J. 287, 833-855. doi: 10.1111/febs.15217.

Karu, N., Deng, L., Slae, M., Guo, A.C., Sajed, T., Huynh, H., et al. (2018). A review on human fecal metabolomics: Methods, applications and the human fecal metabolome database. Anal. Chim. Acta 1030, 1-24. doi: https://doi.org/10.1016/j.aca.2018.05.031.

Marchesi, J.R., and Ravel, J. (2015). The vocabulary of microbiome research: a proposal. Microbiome 3(1), 31. doi: 10.1186/s40168-015-0094-5.

Muñoz-Tamayo, R., Popova, M., Tillier, M., Morgavi, D.P., Morel, J.P., Fonty, G., et al. (2019). Hydrogenotrophic methanogens of the mammalian gut: Functionally similar, thermodynamically different-A modelling approach. PLoS ONE 14(12). doi: 10.1371/journal.pone.0226243.

Payling, L., Fraser, K., Loveday, S.M., Sims, I., Roy, N., and McNabb, W. (2020). The effects of carbohydrate structure on the composition and functionality of the human gut microbiota. Trends Food Sci. Technol. 97, 233-248. doi: 10.1016/j.tifs.2020.01.009.

Prescott, S.L. (2017). History of medicine: Origin of the term microbiome and why it matters. Hum. Microbiome J. 4, 24-25. doi: https://doi.org/10.1016/j.humic.2017.05.004.

Sahakian, A.B., Jee, S.-R., and Pimentel, M. (2010). Methane and the Gastrointestinal Tract. Digest. Dis. Sci. 55(8), 2135-2143. doi: 10.1007/s10620-009-1012-0.

Samuel, B.S., and Gordon, J.I. (2006). A humanized gnotobiotic mouse model of host-archaeal-bacterial mutualism. Proc. Natl. Acad. Sci. U. S. A. 103(26), 10011-10016. doi: 10.1073/pnas.0602187103.

Stams, A.J.M. (1994). Metabolic interactions between anaerobic bacteria in methanogenic environments. Anton. Leeuw. 66(1-3), 271-294. doi: 10.1007/BF00871644.

Treuren, W.V., and Dodd, D. (2020). Microbial Contribution to the Human Metabolome: Implications for Health and Disease. Annu. Rev. Pathol.-Mech. 15(1), 345-369. doi: 10.1146/annurev-pathol-020117-043559.

Van Lingen, H.J., Plugge, C.M., Fadel, J.G., Kebreab, E., Bannink, A., and Dijkstra, J. (2016). Thermodynamic driving force of hydrogen on rumen microbial metabolism: A theoretical investigation. PLoS ONE 11(10). doi: 10.1371/journal.pone.0161362.

The following chapter contains material from an accepted manuscript of an article published by Taylor & Francis in Gut Microbes on 18 December 2018, available online: http://www.tandfonline.com/10.1080/19490976.2018.1546522. The full reference is given below:

Smith NW, Shorten PR, Altermann EH, Roy NC, McNabb WC (2018): Hydrogen cross-feeders of the human gastrointestinal tract. Gut Microbes 10(3): 270-288.
https://doi.org/10.1080/19490976.2018.1546522

The following chapter also contains material from:

Smith NW, Shorten PR, Altermann E, Roy NC, McNabb WC (2019): The Classification and Evolution of Bacterial Cross-Feeding. Frontiers in Ecology and Evolution 7:153.
https://doi.org/10.3389/fevo.2019.00153

Chapter 2: Literature Review

2.1 Introduction

Human health has been a priority of scientific research for centuries, but it is only since the late 19th century that the role of nutrition as a vital and disease-preventing component of human health has emerged (Stipanuk and Caudill, 2018). Determining what constitutes a healthy diet and how this diet is digested by the human body has since been the subject of much research. However, increasing attention is being dedicated to the contribution to digestion made by microbes (Cani, 2018). The majority of the microbes living in the human body occupy the colon, estimated to contain over 10^{13} microbial cells (Sender et al., 2016). The actions of these microbes are increasingly found to be linked to human health and nutritional outcomes, prompting the desire in the scientific community for greater understanding of GIT microbial metabolism.

The microbial community in the GIT is estimated to contain around 4×10^{13} individual cells (Sender et al., 2016). This population is commonly described taxonomically, so an overview of the major taxa of the microbiota is given here.

At the kingdom level, bacteria dominate the GIT, with microbes from other kingdoms (predominantly methanogenic archaea) usually forming less than 1% of the total microbial population (Qin et al., 2010; Rajilić-Stojanović and de Vos, 2014). A typical individual harbours at least 160 distinct bacterial species, at varied abundances (Qin et al., 2010). The Firmicutes (35-55%), Bacteroidetes (15-50%), Proteobacteria (5-45%) and Actinobacteria (5-25%) phyla represent almost the entire bacterial population, although relative abundance of taxa varies between individuals (Frank et al., 2007; Cho and Blaser, 2012; Sankar et al., 2015). At lower taxonomic levels, the Bacteroidales (Bacteroidetes) and Clostridiales (Firmicutes) orders are the most abundant (Frank et al., 2007). Both the Bacteroidales and the Clostridiales are commonly studied for their involvement in carbohydrate breakdown and the production of SCFAs (Thomas et al., 2011; Lopetuso et al., 2013).

The GIT population exhibits a high degree of functional redundancy in the metabolism of dietary substrates (Moya and Ferrer, 2016; Reichardt et al., 2018). Although diet, and thus the feed

available, and the taxonomic profile of the microbiota varies over time and between individuals, the metabolic capacity of the microbiota is relatively stable. The core bacterial species and metabolic functionality are also shared between individuals, allowing for generalised study of microbiota metabolism (Tap et al., 2009; Qin et al., 2010).

All microbes require an energy source for maintenance of cellular functions, growth, and reproduction, although these sources may differ between species and between strains. Although microbes compete for nutrients, products of one microbe's metabolism may become substrates for another, in a process termed 'metabolic cross-feeding'. Due to the variety in feeding preferences displayed by different microbial strains, cross-feeding relationships between microbes can be complex. While much study of cross-feeding between microbial strains focusses on the present state of these relationships, it is important to also consider their evolutionary history. With an understanding of how cross-feeding interactions have been selected for, and have then propagated in a population, we may better predict how a population will respond to changes in nutrient availability, or how new interactions might emerge, be this naturally or by synthetic means. Such an understanding often involves interdisciplinary research between evolutionary biology, ecology, and microbiology, making accurate communication across the fields of study vital.

In any discussion of microbial interaction, it is essential that terminology is unambiguously defined and in line with published literature. Although this can be challenging when the body of literature is large and varied, drawn as it is from many different scientific fields, the importance of clarity cannot be understated. In this chapter, a framework of terminology will be provided that can be applied in the discussion of cross-feeding dynamics, since there are currently inconsistencies of language both within and between fields (West et al., 2007b).

Under the established framework, it is possible to discuss sequentially how increasingly complex cross-feeding relationships may evolve. Alongside this, research must go beyond the first instance of trait evolution and consider factors influencing their subsequent persistence. Studying evolution is experimentally challenging, particularly in large and increasingly complex cross-feeding networks, such as those found in the human colon.

Direct study of the human colonic microbiome can be achieved via several means, including study of the recently deceased, ingestion of telemetric capsules or biopsies from the colon (for

example Macfarlane et al. (1992), Berean et al. (2018) and Nava et al. (2012a)). Other methods, such as using faecal samples as a proxy for colonic material, using animals as model organisms, or the construction of *in vitro* systems designed to replicate conditions in the colon have also been used as alternatives to the invasive nature and limited sampling volumes inherent in direct study (Proctor et al., 2019). However, these abstractions of the *in vivo* environment are limited in how accurately they reflect the colon; for example, faecal samples have been shown to differ from colonic samples (Momozawa et al., 2011), and animal and *in vitro* models cannot replicate every aspect of human colonic anatomy and physiology.

A full analysis of each technique for studying the microbiome is beyond the scope of this chapter, but clearly the microbiome can be studied in a variety of ways. Due to the difficulty in studying complex systems experimentally, mathematical modelling is a powerful tool for inference when experimental systems are less manageable. In this chapter, both the experimental and theoretical evolutionary literature are drawn upon, to give a more complete perspective on the evolution of different cross-feeding types.

As well as considering the different types of cross-feeding, the different molecules involved in these interactions must also be discussed. The nutrients required by each microbial strain in the colon vary, as do the metabolites produced. Much research has been undertaken into the mechanics and characteristics of cross-feeding relationships between colonic microbes, particularly with regard to microbial cross-feeding on the products of carbohydrate fermentation and SCFA production (Belenguer et al., 2006; Falony et al., 2006; De Vuyst and Leroy, 2011; Rios-Covian et al., 2015; Rivière et al., 2015; Louis and Flint, 2017; Moens et al., 2017). SCFAs are organic acids with an aliphatic tail containing two to six carbon molecules (Tan et al., 2014). Acetate, propionate and butyrate are the major SCFAs found in the distal GIT (Cummings et al., 1987; Cummings and Macfarlane, 1991). Many characteristics of SCFAs have been widely studied due to associated benefits to the host, such as in appetite regulation and a role in glucose homeostasis (see Morrison and Preston (2016) for a recent review of the impact of SCFAs on health). In particular, butyrate has attracted much attention. It forms a major source of energy for colonic epithelial cells (Clausen and Mortensen, 1995) and has a well-studied, though still not entirely understood, role in colonic cancer prevention (Lupton, 2004; Donohoe et al., 2012; Pant et al., 2017). The benefits of SCFAs

experienced by the host are dependent upon their production via cross-feeding pathways in the colon. As common metabolic products of many colonic microbes, SCFA cross-feeding relationships are likely widespread in the human colon, only a subset of which have been studied experimentally. In this chapter, the literature on SCFAs as cross-fed metabolites is summarised.

An important yet understudied product of microbial metabolism involved in SCFA-producing metabolic pathways is hydrogen. It is also targeted by cross-feeding microbes (Figure 2.1) and has a range of implications for the nutrition and health of the host.

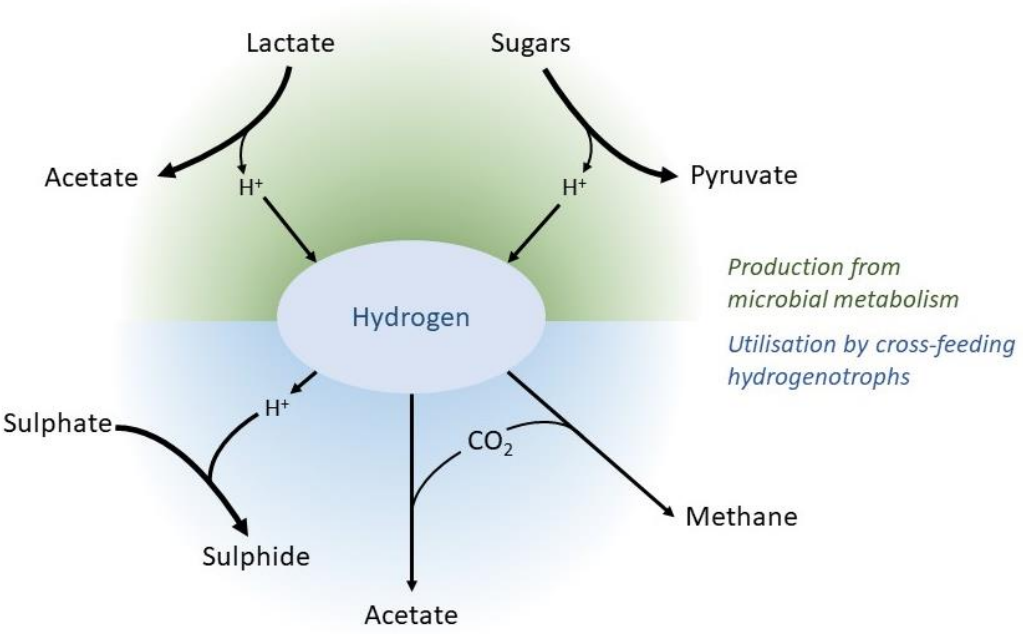

Figure 2.1. Selected sources of hydrogen production in the colon and microbial cross-feeding pathways by which it is removed.

Molecular hydrogen is a common metabolite found within the human colon, produced through widely used microbial carbohydrate breakdown pathways, including glycolysis (Moss et al., 2000; Carbonero et al., 2012). The hydrogen produced in these reactions acts as an electron sink, allowing for the disposal of reducing power (Gibson et al., 1993a). Electron sink products are a necessary part of microbial metabolism, which allow for the disposal of free electrons produced during substrate catabolism.

Hydrogen is a major and efficient electron sink product in the colon, alongside other fermentation products such as ethanol, lactate, and succinate (Nakamura et al., 2010). However, the quantity of hydrogen produced in the colon is dependent upon the population structure of the

microbiota in each individual. The two major phyla of the colonic microbiota are the Firmicutes and the Bacteroidetes, which together form over 85% of the total colonic bacterial population in adults (Hold et al., 2002; Eckburg et al., 2005). The relative proportions of these phyla have been shown to vary between individuals (Schwiertz et al., 2010; Healey et al., 2017) and according to diet (David et al., 2014). Of the Firmicutes and Bacteroidetes, culture-based studies suggest that free hydrogen is mainly produced by the former (for a review, see Carbonero et al. (2012)). The concentration of hydrogen in the colon will depend in part upon the balance between those microbes that produce hydrogen during fermentation and those that do not.

The hydrogen concentration in the colon affects both the microbiota and the host. High hydrogen concentrations can impair the metabolism of both hydrogen-producing and non-producing microbes. A high hydrogen partial pressure inhibits the regeneration of the coenzyme NAD^+ from NADH, slowing the rate of substrate catabolism and thus hindering microbial growth (Thauer et al., 1977; Wolin and Miller, 1983). The partial pressure of hydrogen also determines the thermodynamic favourability of SCFA production. The production of acetate and butyrate results in a greater release of free hydrogen than does propionate formation, thus the latter is more thermodynamically favourable at high ambient hydrogen concentrations (Janssen, 2010).

In addition, hydrogen can have a detrimental effect on the human host, with proposed roles in various GIT disorders, which will be discussed later in this review, and include Irritable Bowel Syndrome (IBS), IBD and obesity.

Hydrogen is removed from the colon in several ways, mediated by both the host and the microbiota. Some hydrogen is expelled directly from the colon as flatus and some is absorbed into the bloodstream (Nakamura et al., 2010). The remaining hydrogen can be converted into other metabolites by hydrogenotrophic members of the microbiota, in sufficient quantities to influence the host. Major gaps exist in our understanding of the mechanisms behind the interindividual differences observed in hydrogenotroph colonisation and metabolism. Without this knowledge, it is impossible to make strong inference about the role of hydrogenotrophs in disease, nor to propose remedial strategies based on the control of the microbiota.

In this chapter, the inconsistencies in the language used to describe distinct cross-feeding relationships are summarised and a set of terms for use in this thesis is defined. Thereafter, the way

each of these cross-feeding relationships may have evolved and persisted is discussed. Studies on microbial cross-feeding leading to the production of SCFAs in the colon are then reviewed. Finally, the current understanding of hydrogenotrophic microbes, the nature of their cross-feeding relationships, their occurrence and prevalence in the microbiota, and their associated health impacts are discussed.

2.2 Classification of microbial cross-feeding

There are many forms of nutrient exchange between microbes and the language used to classify these interactions is not always consistent in the literature. Such variation in terminology can lead to different definitions for a single term, or multiple terms being used to describe the same interaction. This is particularly true of terminology related to metabolic cross-feeding, which is not consistent across the literature and has several suggested subclasses. A small number of publications studying cross-feeding have merely termed it 'interaction' or 'symbiotic interaction' (Helling et al., 1987; Hansen et al., 2007). 'Incidental cross-feeding' has also been used to describe certain one-way interactions (Bull and Harcombe, 2009), and there are also those who only use cross-feeding if the interaction studied involves a two-way exchange of nutrients (West et al., 2006; Sun et al., 2019). In this thesis, **metabolic cross-feeding** is defined as an interaction between microbial strains in which molecules resulting from the metabolism of one strain are further metabolised by another strain. In general, the term 'metabolic cross-feeding' is used according to this definition in the literature, although not further sub-divided according to characteristics of the relationship, as will be done here (Porcher et al., 2001; Doebeli, 2002; Duncan et al., 2002; Belenguer et al., 2006; Belenguer et al., 2008; MacLean et al., 2010; Egan et al., 2014; Rivière et al., 2015; Pacheco et al., 2019).

Closely related to cross-feeding is the term 'syntrophy', which has been defined as "obligately mutualistic metabolism" (Morris et al., 2013). This definition is inclusive of behaviour such as detoxification of the environment by one strain, if that detoxification is necessary for the metabolism of the mutualist partner (Oliveira et al., 2014). Such relationships have also been referred to as reciprocal syntrophy (Kim et al., 2008) or syntrophic cooperation (Hillesland and Stahl, 2010). Alternatively, Pande and Kost (2017) defined syntrophic interactions to be those "in which two or more microorganisms obligately exchange essential metabolites", which would not include

detoxification. In a recent review, Hillesland (2018) stated that this condition of dependence on the relationship is not fixed, and that only some organisms are obligately syntrophic. Another definition of syntrophy in the literature describes the combined capabilities of two or more organisms being necessary for degradation of an otherwise unavailable substrate (Stams and Plugge, 2009), while yet another corresponds to any two-way exchange of nutrients (Gudelj et al., 2016). This evidence of variation in the use of terminology in the field encourages the formulation of an explicitly defined set of terms for the discussion of metabolic cross-feeding.

2.2.1 Cross-feeding in one direction

To begin to address the lack of consistent terminology, experimental examples of cross-feeding in one direction only are described, which are separated into two distinct classes. For the first class, the observations of Belenguer et al. (2006) are considered: these authors observed a *Eubacterium hallii* strain utilising lactate produced by *Bifidobacterium* strain in co-culture. Importantly, lactate could not be further metabolised by the *Bifidobacterium*. Correspondingly, **metabolite cross-feeding** is defined as the feeding of one microbial strain on molecules produced by another, given that these molecules cannot be further metabolised by the producing bacterium, and are therefore waste products. The second class is exemplified by the growth of bifidobacterial strains on partially degraded oligofructose (OF) or inulin, resultant from the metabolism of *Bacteroides thetaiotaomicron* in co-culture (Falony et al., 2009a). Extracellular degradation of the carbon source by *B. thetaiotaomicron* resulted in the accumulation of shorter chain sugars in the environment, which were substrates for both *B. thetaiotaomicron* and the bifidobacteria. Correspondingly, **substrate cross-feeding** is defined as the feeding of one strain on molecules produced by the metabolic actions of another, which may still be further metabolised by either strain (Figure 2.2). These relationships were described in the mathematical modelling work of Van Wey et al. (2016) and, since all these strains are found in the human colon, these examples of cross-feeding may be expected to occur there.

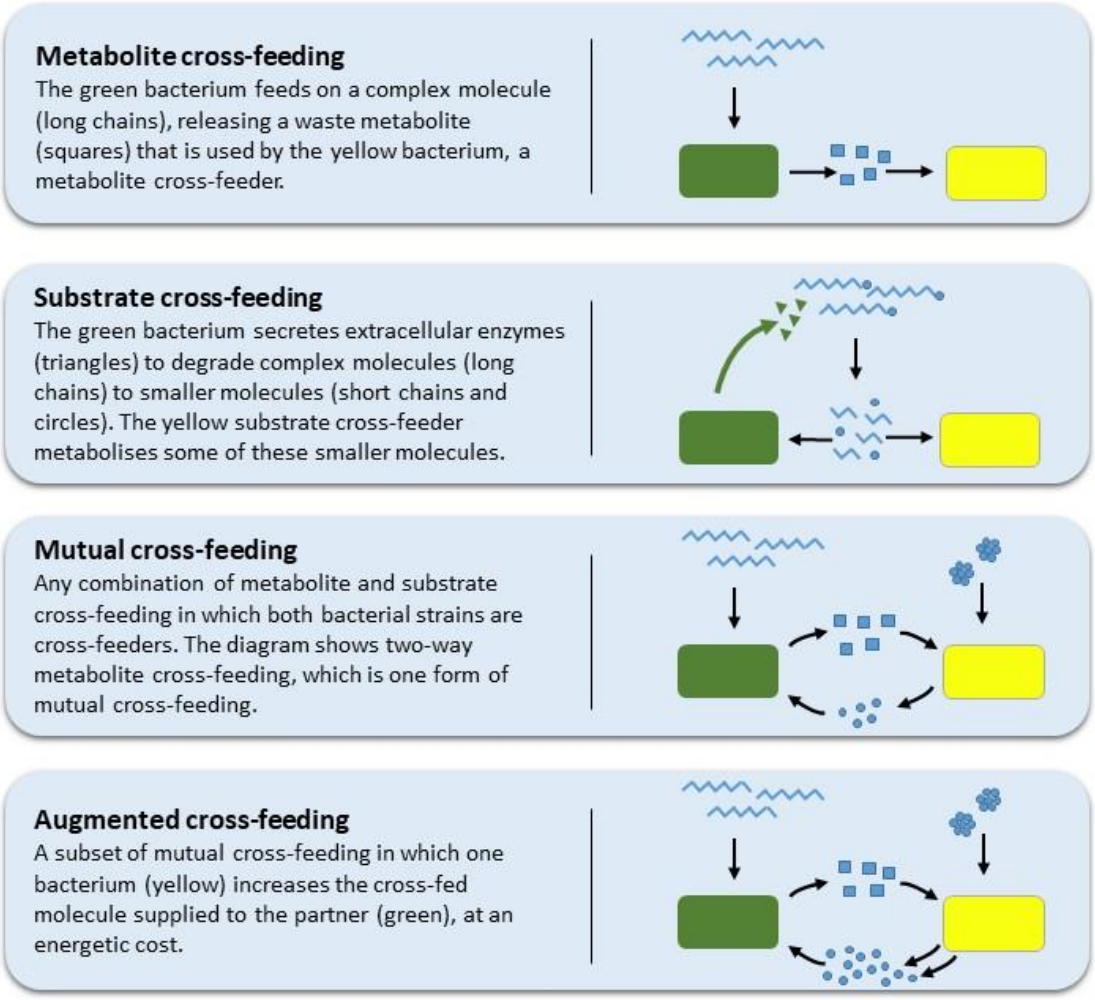

Figure 2.2. Diagrammatic examples of each of the four forms of cross-feeding discussed in the text. Note that the example for augmented cross-feeding is identical to that of mutual cross-feeding, but for the increased metabolite production by the yellow bacterium. This is reflective of the fact that augmented cross-feeding is mutual cross-feeding with the condition that one or both strains involved must increase the supply of metabolite to their partner, at some energetic cost.

Combinations of both these forms of cross-feeding are also observed. The colonic bacterium *Anaerostipes caccae* has been shown to utilise both fructose and lactate as energy sources (Moens et al., 2017). Separately, *Lactobacillus acidophilus*, when grown on OF as the sole added carbon source, liberated free fructose via extracellular degradation of OF, before importing this sugar for further metabolism. *L. acidophilus* then produced lactate as a metabolic end-product. When in co-culture on OF, *A. caccae* was able to use both the liberated fructose and the secreted lactate produced by *L. acidophilus*, displaying both substrate and metabolite cross-feeding.

Disposal of waste is a necessary action; thus, metabolite cross-feeding does not negatively affect the excretor. The same is not true of substrate cross-feeding. As mentioned above, many microbes produce extracellular enzymes for the purpose of degrading a complex molecule to simpler

constituents, which can subsequently be imported into the microbial cell for further metabolism (see, for example, Rossi et al. (2005) and Amaretti et al. (2007)). In the intervening period between breakdown and uptake by the primary degrader, these constituents are also available to other microbes in the immediate environment. This can create competition for the breakdown products. Thus, it may be that an extracellular enzyme producer may show reduced growth when growing in co-culture with a substrate cross-feeder, as compared to growing in monoculture. This has been shown between two colonic sugar degraders. A *Bifidobacterium breve* strain, previously able to achieve only limited growth on colonic mucins, showed improved growth on mucins when in co-culture with *Bifidobacterium bifidum* (Egan et al., 2014). This was due to the extracellular degradation of mucin by *B. bifidum*, resulting in the release of galactose-containing oligosaccharides into the medium. However, *B. bifidum* showed reduced growth in co-culture with *B. breve* compared to monoculture, thought to be a result of the competitive substrate cross-feeding.

2.2.2 Cross-feeding in both directions

Continuing the classification of interactions and avoiding the inconsistencies around the term syntrophy, **mutual cross-feeding** is defined to be the case in which both microbial strains involved are engaged in cross-feeding on metabolites produced during the metabolism of the other (Figure 2.3; (Rivière et al., 2015)). Mutual cross-feeding is a subset of mutualism in which all benefits are nutritional. An example of such a feeding strategy has been shown in *Escherichia coli* populations that are auxotrophic (unable to synthesise critical organic compounds required for survival). Mee et al. (2014) engineered several strains, each unable to synthesise a certain essential amino acid. No strains were able to grow in monoculture, but certain co-cultures of two strains with differing auxotrophies achieved growth due to two-way exchange of the necessary amino acids, via secretion into the extracellular environment.

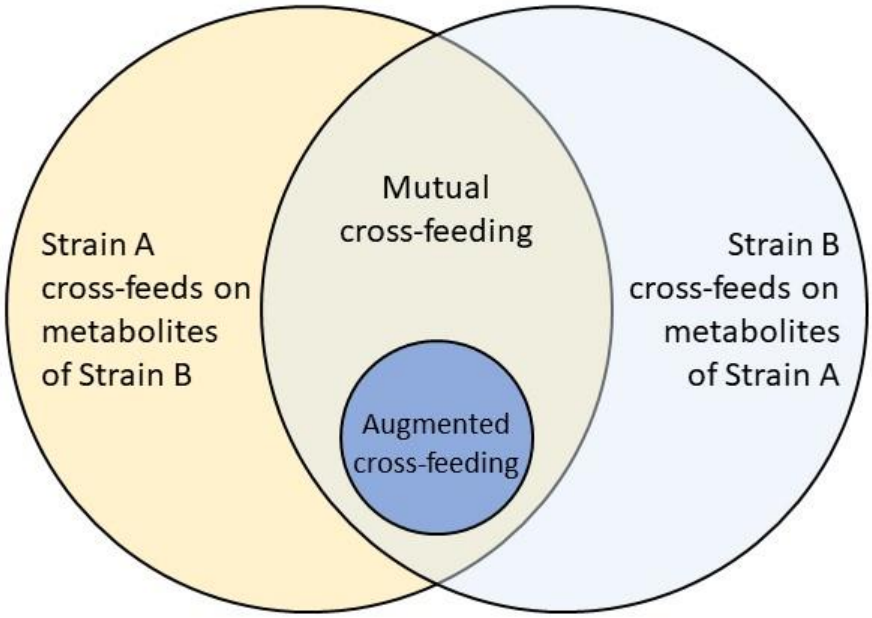

Figure 2.3. A Venn diagram illustrating the nature of mutual and augmented cross-feeding. Mutual cross-feeding requires that each strain is cross-feeding on products produced in the metabolism of the other. Each partner must be engaged in metabolite and/or substrate cross-feeding. Augmented cross-feeding relationships form a subset of mutual cross-feeding relationships.

Before presenting the final cross-feeding classification discussed in this chapter, the concept of cooperation in ecology must be reviewed. Among the enormous quantity of ecological and biological studies mentioning cooperation, there are two widely referenced publications that define it. Sachs et al. (2004) would consider all forms of cross-feeding to be cooperation. Their definition of cooperation – action that is beneficial to the recipient regardless of its effect on the donor – is used by many (Velicer and Vos, 2009; Nadell et al., 2010; Wintermute and Silver, 2010a; Damore and Gore, 2012; Sachs and Hollowell, 2012; Momeni et al., 2013). However, West et al. (2006) have given a tighter definition, stating that selection for the beneficial trait in the donor must, at least partially, be due to its beneficial effect on the recipient. This definition has also been widely adopted in the literature (Bull and Harcombe, 2009; Estrela and Gudelj, 2010; Foster and Bell, 2012; Pande et al., 2014; Douglas et al., 2016; Germerodt et al., 2016; Pande et al., 2016), and would include only certain forms of mutual cross-feeding. It may be challenging to classify interactions as cooperative under this definition due to the type of information required. For example, two microbial strains may be engaged in mutual cross-feeding, each utilising a metabolic end-product of the other; is selection for this relationship purely due to the need to excrete waste, or is increased

excretion for the strengthening of the mutualism present? Although not a naturally evolved relationship, the question may still be asked whether the mutual cross-feeding observed by Mee et al. (2014) is cooperative, i.e. will the exchange of amino acids be further selected due to its benefit to the auxotrophic partner? This seems unlikely given the strains' independent origin, but it would be non-trivial to prove (De Mazancourt et al., 2005). This issue is compounded by the fact that, in similar work with engineered auxotrophic *E. coli* strains, the secretion of amino acids by one of the strains was shown to increase over the course of mere hours in co-culture, but not in monoculture (Hosoda et al., 2011). This increase is likely due to the observed upregulation of many genes involved in anabolic metabolism, rather than selection for individual strains that produce more amino acids. Such phenotypic plasticity makes classification of cooperative behaviour yet more difficult.

Additionally, the argument could be made that the term cooperation implies some degree of communication or coordination between individuals. Microbial communication, especially quorum sensing, has received much attention in recent years and has been implicated in microbial metabolism (see review by Goo et al. (2015)). However, the addition of communication to any definition of cooperation would present further challenges to its classification. For these reasons, care must be taken with the use and interpretation of this term.

Despite the difficulties around cooperation as a classification of microbial interactions, there exists a further cross-feeding interaction, in referring to which many authors have used the term 'cooperative cross-feeding' (Bull and Harcombe, 2009; Estrela and Gudelj, 2010; Pande et al., 2014; Germerodt et al., 2016; Pande et al., 2016). These interactions are a subset of mutual cross-feeding (Figure 2.3) in which one or both partners undertake an activity at energetic cost that increases the supply of the cross-fed molecule to the partner (Figure 2.2). Other authors have termed this 'by-product reciprocity' (Connor, 1995; Sachs et al., 2004; West et al., 2006; West et al., 2007b), which avoids the previously stated difficulties around the term cooperation. A recent review considering the role of cross-feeding in bacterial 'unculturability' uses both 'by-product reciprocity' and 'cooperative cross-feeding' to refer to mutual cross-feeding in which the interaction is energetic in one or both directions, respectively (Pande and Kost, 2017). To imply the increased energetic investment present in these interactions, the term **augmented cross-feeding** is preferred in this

chapter, defined as a mutual cross-feeding relationship in which the production of the cross-fed molecules (in one or both directions) incurs an energetic cost to the producing strain. This costly production would be disadvantageous to the producer in the absence of the mutualism, which could be tested by comparing its monoculture growth to that of an ancestor that does not perform the costly production.

An example of augmented cross-feeding is again provided by genetically engineered *E. coli*. Comparably to Mee et al. (2014), auxotrophy for one amino acid was combined with overproduction of another amino acid in each engineered strain (Pande et al., 2014). However, in this case many more permutations of auxotrophy and overproduction were investigated. These strains were constructed and paired in culture in such a way that the auxotrophy of one partner corresponded to the overproduction of the other. Many of these augmented cross-feeding cultures were successful in terms of growth, even though overproduction was shown to come at a fitness cost to the bacterium when compared to its wild type ancestor.

Augmented cross-feeding is the final cross-feeding term defined in this chapter. These classifications allow for easy comparison between observations of cross-feeding, without the need to delve into the biological details of each individual interaction. Next, the literature on the evolution of the defined interactions is reviewed.

2.3 Evolution of microbial cross-feeding

Ecologists have heavily studied inter-species interactions for many decades and a well-developed theory exists for how these interactions may have evolved. Microbes are particularly attractive for the study of evolution due to their rapid asexual reproduction, the ease with which their genetic code can be artificially altered, and the ability to control environmental variables in cultures (Elena and Lenski, 2003; West et al., 2007a; Hillesland, 2018). There is also the possibility of time-shift experiments, in which strains from different stages in evolutionary history may be co-cultured to investigate the change in relative fitness over generations. Such experiments can also facilitate study of coevolution, where the two strains involved in a cross-feeding relationship may adapt to one another (see review by Hillesland (2018)). Alongside *in vitro* approaches, mathematical modelling is popular among evolutionary biologists, since the extended time periods necessary for

evolution can often be simulated *in silico* in mere minutes to provide further insight into observed results (Widder et al., 2016). These mathematical models can be used to test theories and identify new experiments and hypotheses on the nature and evolution of microbial interactions.

An important phenomenon in ecology is the occurrence of multiple different species feeding upon a single resource. This observation should be precluded by the competitive exclusion principle, whereby, if two species are in direct competition for a single resource, the population should converge to a single species with the greatest fitness to survive on that resource (Hardin, 1960). The existence of cross-feeding interactions in which multiple species may persist in a single resource environment demonstrates a possible exception to this principle, as will now be explored.

2.3.1 Specialisation

In addition to observing the evolution of microbial populations, it is also useful to observe how these evolutionary changes persist over time. The Long-Term Evolution Experiment (LTEE), early results of which were reported by Lenski et al. (1991), has now been conducted for more than 25 years, involving over 60,000 generations of the cultured *E. coli* population (Lenski, 2017). One result of this experiment was the emergence, from an originally clonal population, of two phenotypically and genotypically distinct strains, small and large (S and L, respectively), differentiable by their colony formation morphology and cell size (Rozen and Lenski, 2000). Since their first isolation, these strains have been shown to coexist for over 12,000 generations (Rozen et al., 2005). Not only are these strains visibly different, but strain L also shows a greater maximum growth rate on glucose, whereas strain S has increased relative fitness in co-culture after glucose depletion. When S was grown in monoculture on a combination of glucose and cell-free supernatant of L, it achieved a higher growth rate than when grown on glucose alone. This implies cross-feeding by S on one or more molecules produced by L (Rozen and Lenski, 2000).

Genetic analysis of bacterial samples obtained periodically throughout the LTEE demonstrated that the L strain emerged first, before the subsequent emergence of the newly evolved S strain, from which point the two have coexisted (Rozen and Lenski, 2000; Rozen et al., 2005; Lenski, 2017). Importantly, the S strain appears not to have evolved from the L strain, but from a shared ancestral strain, which was outcompeted by the evolved L and S strains (Rozen et al., 2005).

Similar dynamics have been discussed elsewhere (Rosenzweig et al., 1994; Treves et al., 1998), and the evolutionary route hypothesised by the authors is as follows. Strain L evolved from the ancestral strain with an increased growth rate on glucose, giving it an advantage and allowing it to persist in the ancestral population. However, the fact that the L strain did not outcompete its ancestor implies some mechanism by which the two were able to coexist. This mechanism was thought to be a trade-off between glucose uptake and the use of some unknown metabolic intermediate molecule that could be utilised by either strain. Accordingly, the L strain's increased glucose usage resulted in more of this intermediate molecule being released into the medium, which could be better utilised by the ancestral strain. This increase in concentration of the intermediate molecule provided an advantage for a second mutant, S, which attained better growth on this molecule than either the ancestor or the L strain. As a result, the S strain was also able to persist in the population but did not dominate due to its dependency on the intermediate molecule (Lenski, 2017).

More recent follow-up experimentation has provided supportive evidence for the trade-off between growth efficiency on glucose and the unknown intermediate molecule when experimenting with historical LTEE samples (Großkopf et al., 2016). These authors gave evidence that acetate was the molecule upon which S had a growth advantage, whereas L specialised in glucose uptake, resulting in increased acetate excretion. It has been proposed that the excretion of acetate frees phosphoryl groups in the cell, which are required for glucose uptake (Rosenzweig et al., 1994). Thus, increased acetate excretion by strain L would facilitate increased glucose uptake. This has been supported by more recent experimental and modelling studies (Treves et al., 1998; Kumari et al., 2000; Großkopf et al., 2016; Enjalbert et al., 2017). If, as has been suggested (Großkopf et al., 2016; Lenski, 2017), strain L has lost the ability to metabolise acetate, then L and S have a metabolite cross-feeding relationship, although this has not been fully elucidated and continued evolution may result in this classification changing over time.

To examine abstractly how diversification such as that observed in the LTEE may occur, Doebeli (2002) presented a mathematical model for the evolution of cross-feeding on metabolic intermediates. In this model, a single-species microbial population converted an initial molecule to an intermediate, before further converting it to a final end-product. The bacteria were constrained by a trade-off function between efficient metabolism of the initial molecule and the intermediate.

Mutation in the system was restricted to changes in the maximum growth rates achieved on the initial and intermediate molecules. From these assumptions, the model exhibited branching divergence of a single population into two increasingly distinct strains. One strain metabolised the initial molecule efficiently, while being less efficient at metabolising the intermediate and thus released increased amounts of the intermediate into the environment. The second strain more efficiently degraded the intermediate than the initial molecule, thus cross-fed on that which was released by the first strain.

Pfeiffer and Bonhoeffer (2004) produced a similar model, containing a more extended metabolic pathway for complete degradation of an initial molecule with several distinct steps, each with a catalysing enzyme. They assumed that bacteria maximise ATP production – this production being possible only at specific steps of the metabolic pathway – whilst minimising concentrations of enzymes and intermediate compounds. In a homogeneous population that metabolised the initial molecule entirely, the model introduced mutation, whereby a mutant produced more of the earlier enzymes in the pathway than the original strain, and less of the later. As seen in the previous model, this resulted in the subsequent evolution of a cross-feeding strain, specialising on an intermediate molecule produced by the first mutant, with eventual extinction of the ancestor.

Both theoretical models achieved results reflective of those observed in the LTEE. A notable point on which the two models differed is the manner in which new strains were established: the first model involved gradual speciation from a single population over an extended time period, whereas the second considered the occurrence of phenotypically distinct mutants, which quickly increased in number due to their growth advantage. The latter is more readily comparable with the long-term observations of the LTEE, in which the relative proportions of S and L strains vary widely across generations. The hypothesised cause of the generational fluctuation in population proportions is the invasion of new, fitter derivatives of each strain, which then rapidly altered the relative abundance of each strain at steady state (Rozen and Lenski, 2000; Lenski, 2017). In addition, neither model allowed for the accumulation of more than one intermediate molecule and the possible complex cross-feeding dynamics that might ensue. Is, therefore, a two-strain cross-feeding dynamic the most favourable on a single resource? If not, would it be possible to evolve a stable cross-feeding population of three or more strains utilising different intermediate molecules of the

same metabolic pathway? The dynamics studied in these models could conceivably take place in already complex microbial communities, such as the human colon, increasing the number of exchanged molecules and the diversity of the population.

A separate question posed by Pfeiffer and Bonhoeffer (2004), was whether a cross-feeding relationship is the result of mutation leading to the loss or alteration of a function, or simply due to phenotypic plasticity. An example of such plasticity is the switching between glucose and acetate metabolism as the former becomes depleted, resulting in the diauxic growth of *E. coli* described by Friesen et al. (2004). In an environment in which glucose concentration is maintained at an abundant level, such a switching would not occur, but this does not imply that the microbes have lost the ability to switch. It should always be asked when studying cross-feeding relationships, whether the microbes involved have evolved complete dependence on cross-feeding or are merely behaving in the most energetically efficient manner for their current environment. The answer to this question is likely case-dependent (Pande et al., 2014), and may qualitatively change as a population evolves, due to processes such as adaptive gene loss.

2.3.2 The Black Queen Hypothesis

A different, but complementary perspective for the evolution of cross-feeding dependencies is provided by the Black Queen Hypothesis (Morris et al., 2012). The hypothesis is that there are "conditions under which it is advantageous for an organism to stop performing a function", via loss of a functional gene. This phenomenon is also termed adaptive gene loss or reductive evolution and relates to a permanent change in the phenotype. If a microbe must expend energy to perform a function, but the end-product of this function is freely available in the environment, it would be beneficial to the microbe to utilise the available product and desist in performing the function itself. A strongly related concept is streamlining theory, the idea that selection can favour the "minimisation of cell size and complexity" (Giovannoni et al., 2014; Mas et al., 2016). An example of such a function is the production of extracellular enzymes for the degradation of complex carbohydrates (Figure 2.4). Such enzymes perform a beneficial function for all microbes in the immediate environment since the resulting simpler sugars are available to all microbes in the vicinity. Thus, under the Black Queen Hypothesis, it would be selectively

advantageous for a microbe in this environment to not synthesise the extracellular enzyme, whilst still maintaining the same feeding strategy on the released sugars. Any mutant unable to synthesise the extracellular enzyme could have an immediate growth advantage via such energy saving, and thus this trait would propagate in the population, provided that other members of the population continue to synthesise the enzyme. The Black Queen Hypothesis applies in any case where an individual performs a function that is to some degree 'leaky' by nature, meaning that its benefits are also available to other individuals.

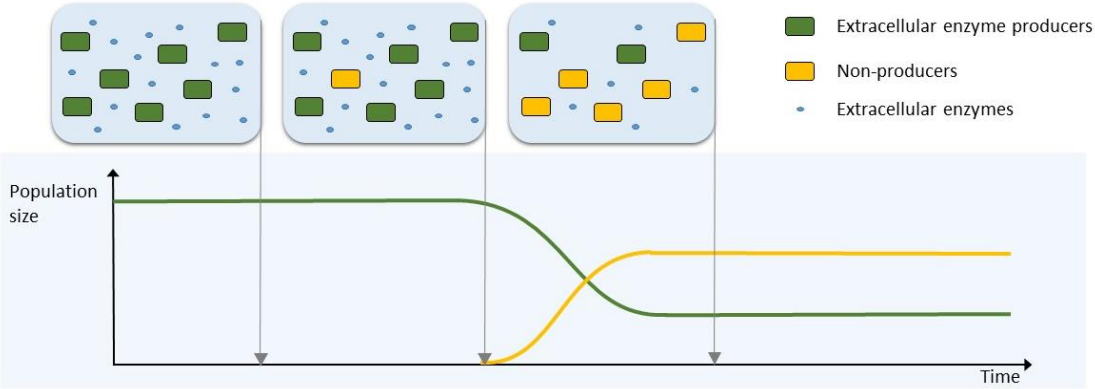

Figure 2.4. Diagrammatic example of evolution via the Black Queen Hypothesis, where the function lost is the production of an extracellular enzyme for the degradation of a complex molecule. Initially, all microbes produce the extracellular enzyme, resulting in an abundance of available breakdown products. Mutation produces an individual unable to synthesise this enzyme, therefore giving it a growth advantage via energy saving, but making it entirely dependent on the ancestor. The mutant proportion of the population increases until, at some critical point, the population growth of the mutants is halted, since the reduced overall enzyme production by the population results in reduced availability of breakdown products. The enzyme producers are maintained via negative frequency dependent selection.

The potential for improved growth through reductive evolution is exemplified by studies on auxotrophic *E. coli* and *Acinetobacter baylyi* strains (D'Souza et al., 2014). Engineered auxotrophs for a specific essential nutrient were created via gene deletion. Many of these auxotrophs achieved greater growth than their prototrophic ancestor in competition experiments on growth medium containing the essential nutrient. Although the level of advantage varied between nutrients and was concentration-dependent, this shows that lack-of-function can be advantageous when the product of the function is readily available. In this study, lack-of-function was not due to loss-of-function via adaptive gene loss, but the single gene deletions necessary to achieve the observed growth advantage support the Black Queen Hypothesis. The authors did investigate the relative advantages of different gene deletions within the same biosynthetic pathway, but no investigation was carried out to ascertain whether further genome reduction would spontaneously occur once the pathway

was made redundant by the artificial deletion. Moreover, in a large-scale analysis of metabolic networks and sequenced bacterial genomes, more than 60% of the GIT-inhabiting microbes tested were predicted to be auxotrophic for at least one of the amino acids, nucleosides and vitamins considered, with a median of two auxotrophies per strain (D'Souza et al., 2014). This analysis showed that most of the GIT strains studied had lost almost all the genes for the biosynthetic pathway corresponding to their auxotrophy. Together, these results suggest that it is possible that cross-feeding dependencies emerging from gene loss may be widespread in complex communities such as the colon, and that a single gene loss is likely followed by the loss of other genes within the same biosynthetic pathway. Longer-term studies with these *E. coli* auxotrophs would then be expected to show further adaptive gene loss, but this remains to be confirmed.

In much simpler populations than that of the human colon, cross-feeding via adaptive gene loss shows potential for stability. In this scenario, evolution under the Black Queen Hypothesis would not necessarily lead to the extinction of the original, prototrophic strain. If the newly evolved strain was dependent upon the costly function performed by the ancestor, then extinction of the ancestor would be followed by extinction of the new strain (Mas et al., 2016). In the case of cross-feeding, if the cross-feeder is entirely dependent upon its partner for the provision of some essential molecule, then the newly evolved cross-feeder cannot drive the ancestral strain to extinction, despite its energetic advantage (Figure 2.4). If repeated loss of function occurs in a population, an ancestral strain, which retains those functions and upon which all others depend, may become a 'keystone' strain (see 'Shooting the Moon' (Morris et al., 2012; Morris, 2015)). Loss of the keystone strain is avoided by negative frequency-dependent selection, since the dependent strains experience reduced relative fitness as the keystone population decreases (Ze et al., 2013). Several studies have identified and discussed candidate keystone species in the colonic microbiota. Often, these have been *Bacteroides* strains with broad metabolic capabilities, but not always strains that are at high abundances in the colon (Bäckhed et al., 2005; Ze et al., 2012; Ze et al., 2013; Fisher and Mehta, 2014; Cockburn and Koropatkin, 2016).

An intriguing point is what population composition is reached at steady state, if after gene loss the cross-feeder is not *entirely* dependent on its ancestor? In this case, negative frequency-dependent selection may not be powerful enough to preserve the ancestor, potentially leading to

the loss of the original function in the population. The consequences of such an eventuality are difficult to predict. It would be assumed that the cross-feeder will survive, but, without the benefit of the cross-feeding molecule, may show reduced growth. After this point, it is interesting to consider in which direction selection pressure will drive the remaining strain, especially in the presence of some third-party competitor. Mathematical modelling could be applied to study the conditions that might lead to such a scenario, and the population dynamics that would ensue.

The two routes to cross-feeding discussed thus far, divergence due to specialisation or by adaptive gene loss, are not mutually exclusive. Combinations of both routes are entirely plausible, but difficult to identify. Even with knowledge of a microbial population's evolutionary history, the root cause of an evolutionary shift is elusive, as shown by the LTEE. These difficulties are compounded once cross-feeding relationships in which resources are exchanged in a more complex manner are considered.

2.3.3 Mutual cross-feeding

Although the term mutualism is broad and applicable across taxonomic kingdoms, here the subset relating to microbial metabolism is considered. Mutual cross-feeding has been observed in several microbial communities (for examples, see Harcombe (2010), Rivière et al. (2015) and Marchal et al. (2017)) and it is interesting to question how these two-way interactions may have arisen in initially self-sufficient populations. The answer to this lies in the cross-feeding relationships discussed previously.

For example, consider a pair of microbial strains, one of which is a metabolite cross-feeder on some waste product of the other (molecule A). If a mutation occurred in a cross-feeding bacterium that caused it to excrete, at no detriment to itself, some metabolite (molecule B) required by the primary degrader, this mutation would be favoured. By supplementing the ambient availability of molecule B for the primary degrader, the mutation in the cross-feeder would benefit the growth of the primary degrader. This would result in subsequently increased availability of molecule A for the cross-feeder, in a positive feedback mechanism that would lead to increased growth of both. This description of evolution from a nutritional one-way benefit to mutualism is consistent with the hypothesised emergence of mutualism described by Connor (1995) and repeated

in the literature (Sachs et al., 2004; Foster and Wenseleers, 2006; Harcombe, 2010; Wintermute and Silver, 2010a; Estrela and Brown, 2013). Although not specific to nutritional mutualisms, or to microbes, the framework of Connor (1995) is a potential route by which mutual cross-feeding may evolve.

An example of mutual cross-feeding is again provided by experimental culture using engineered auxotrophic *E. coli* (Harcombe, 2010). In this instance, an *E. coli* strain with engineered methionine auxotrophy was partnered with a *Salmonella typhimurium* strain, which displayed cross-feeding on products of lactose metabolism released by wild type *E. coli*. Initially the auxotrophic *E. coli* and the cross-feeder were unable to grow in co-culture on lactose since neither was supplying its partner with the essential molecule. However, upon treatment with ethionine, a methionine antagonist, and selection of *Salmonella* strains displaying ethionine resistance, a novel strain evolved. This strain excreted methionine and could enable growth of both strains in co-culture. Although this evolution involved a degree of interference from the experimenters, this did not extend to genome editing of the *Salmonella* strain, and the ultimate emergence of methionine excretion was via mutation. Methionine secretion was even favoured in the presence of a wild-type *Salmonella* strain, which was unable to become established in a population of methionine-secreting *Salmonella* and auxotrophic *E. coli*, perhaps due to the effects of spatial structure discussed later in this chapter. It would be expected that the wild type *E. coli* would not become established in culture with the mutual cross-feeding partners, since the energetic cost of producing methionine would put it at a disadvantage compared to the auxotrophic strain. As would be expected, in the absence of either *E. coli* the methionine excreting *Salmonella* strain lost its advantage over the ancestral strain, since this advantage was entirely dependent on the mutualism. The relationship observed here shows the gaining of a function to support cross-feeding, but mutual cross-feeding may also emerge from loss-of-function.

An alternative perspective to the framework of Connor (1995) is provided by the adaptive gene loss of the Black Queen Hypothesis. Consider a cross-feeder that is dependent, due to adaptive gene loss, upon a molecule produced by its prototrophic ancestor. Morris (2015) proposed a scenario in which this ancestor also undergoes adaptive gene loss and becomes dependent on the cross-feeder for provision of some other nutrient. Both strains would then be dependent on one

another for a specific product, thus forming an obligate mutual cross-feeding partnership. This specialisation is supported by the biological market model of Schwartz and Hoeksema (1998): nations profit more by specialising in the production and export of certain products, whilst importing others, than by producing all they need internally. The model applied this principle to biology and found further support for the benefits of mutualistic interactions.

This chapter has thus far focussed upon the evolution of one-way and mutual cross-feeding in an initially identical population or a population that has been artificially constructed to perform cross-feeding. It is also entirely possible that two strains of microbes will engage incidentally in cross-feeding when grown together. When feeding preferences and waste production coincide, microbes may be predisposed to such behaviour (Sachs et al., 2004). Investigations using genome-scale metabolic models found that simulations under anoxic conditions, such as those in the colon, were more conducive to mutual cross-feeding and the secretion of central carbon intermediates than simulations with available oxygen (Pacheco et al., 2019). Although the evolutionary background was not included, only molecules that were secreted at no detriment to growth were considered, ensuring that only passive relationships were studied. This form of cross-feeding does not necessarily require any evolutionary process to emerge, merely coexistence. However, further evolution via routes such as adaptive gene loss and specialisation would still be possible in these more general cases, as they are based upon passive production of metabolites. Passive interactions, which require no more energetic investment from either party than would be seen in the absence of interaction, do not account for all forms of cross-feeding. Instances in which microbes actively invest in some action at an individual cost, to the benefit of others, have also been observed.

2.3.4 Augmented cross-feeding

Within the established group of mutual cross-feeding interactions, there are those that are beyond the boundaries of direct individual benefits. From an evolutionary perspective, investment in an unrelated individual should be precluded by natural selection (Darwin, 1859; Sachs et al., 2004; Penders et al., 2006). However, augmented cross-feeding is sustainable because ultimately, though not directly, the investor does receive benefit.

As discussed previously, an existing metabolite or substrate cross-feeding relationship may lead to the evolution of mutual cross-feeding (Connor, 1995; Sachs et al., 2004). In most cases, it seems reasonable to assume that augmented cross-feeding, a subset of mutual cross-feeding, will emerge when one of a mutualist pair begins to energetically increase its contribution to its partner (Pande and Kost, 2017). The example of mutual cross-feeding given in the previous section, between an *E. coli* auxotroph and a *Salmonella* strain, fits the criteria for augmented cross-feeding since methionine excretion was shown to be costly (Harcombe, 2010). More recent follow-up experimentation found a variety of levels of methionine excretion on the part of different *Salmonella* strains (Douglas et al., 2016; Douglas et al., 2017). Higher production of the essential amino acid resulted in slower growth of *Salmonella*, but faster growth of *E. coli* auxotrophs, as would be expected. Although higher methionine production resulted in greater consortia growth, the *Salmonella* strains reached lower proportions in the population due to the high cost involved in this production.

The concept of cost and benefit is important in the evolution of augmented cross-feeding. The cost-benefit ratio is a widely used term in the literature and is vital to the interaction (Trivers, 1971; Yamamura et al., 2004; Foster and Wenseleers, 2006; Harcombe, 2010; Nadell et al., 2010; Wintermute and Silver, 2010b; Damore and Gore, 2012; Oliveira et al., 2014; Germerodt et al., 2016). Clearly, the benefits of investing must outweigh the costs if an investing mutant is to invade a non-investing population.

The cost-benefit ratio was studied by Wintermute and Silver (2010b) in their auxotrophic *E. coli* experiments. Paired co-cultures of 46 *E. coli* strains with differing auxotrophies showed that several of these combinations could grow successfully in media that did not support monoculture growth, as a result of mutual cross-feeding. It was found that it was most frequently molecules of low cost to produce that were involved in successful mutual cross-feeding combinations, as would be expected.

Pande et al. (2014) took a similar line of study and genetically altered auxotrophic *E. coli* strains to overproduce the amino acid required by their co-culture partner. Many of these combinations were shown to have a growth advantage over prototrophic monocultures, achieving higher growth rates than their ancestors. The cost of overproducing one amino acid was less than

the benefit of not needing to synthesise both. While both studies involved genetically engineered bacteria so that the cross-feeding mechanism could be fully controlled, they provide evidence that augmented cross-feeding on specific molecules can be a successful growth strategy.

Examples of augmented cross-feeding relationships in the less controlled and more diverse environment of the colon are rare. Rakoff-Nahoum et al. (2016) demonstrated the costly production of extracellular enzymes by the bacterium *Bacteroides ovatus* that were not required for its own growth, but which were beneficial to other colonic microbes. It was shown that *B. ovatus* received some growth advantage in return when performing this action in co-cultures; however, the mechanism by which *B. ovatus* benefitted has not yet been established. The authors suggested cross-feeding of some other molecules and detoxification as possible mechanisms of the mutualism. It seems likely that cross-feeding occurs in both directions, which could make this an example of augmented cross-feeding by colonic microbes, but this remains to be proven. Furthermore, understanding the evolution of such a relationship will also require more complete knowledge of its current nature.

Augmented cross-feeding has been achieved artificially in the colon of gnotobiotic mice (Ziesack et al., 2019). Again, using engineered amino acid auxotrophies coupled with complementary overproduction, a consortium of four strains became successfully established in the mouse colon, with higher population evenness but smaller overall population size than was achieved using the equivalent wild type consortium.

The experiments with synthetic consortia discussed here show that strains native to the colon are capable of augmented cross-feeding interactions, but only under strict conditions. Furthering the difficulty of evolving augmented cross-feeding, mathematical modelling has found that this phenotype is only favoured at intermediate population densities, due to a lack of sufficient reciprocation in sparse populations and competition for space in dense populations (Bull and Harcombe, 2009). The tight constraints on augmented cross-feeding might lead one to believe that it must be vanishingly rare. However, there are several factors that increase selection for positive interaction, foremost being the physical structure of the population.

2.3.5 The influence of spatial structure on cross-feeding evolution

In discussing mixed microbial systems, Wintermute and Silver state that: "In well-mixed systems, shared metabolites are easily lost" (Wintermute and Silver, 2010a). This is true for unstructured populations, but microbes living in such a planktonic manner are only a subset of microbial populations, especially in the colon (Macfarlane et al., 2011). Biofilm populations abound, so spatial analysis must be applied to the study of cross-feeding and its evolution (Tolker-Nielsen and Molin, 2000; Nadell et al., 2010; Wintermute and Silver, 2010a; Macfarlane et al., 2011; Van Wey et al., 2011).

Before adding the context of cross-feeding evolution, the terminology of structured and unstructured environments must be qualified. A well-mixed culture implies little or no aggregation of cells and equal availability of nutrients to all individuals. In a biofilm however, dynamics that are more complex must be allowed for. Diffusion in a biofilm is hampered by the density of cells and extra-cellular polymeric substances, as well as the three-dimensional biofilm structure (Wanner et al., 2006; Van Wey et al., 2011; Van Wey et al., 2012). Nutrient transport is slower in a biofilm than an unstructured medium, resulting from hindered diffusion, thereby decreasing the rate of resource exchange between nearby biofilm-dwelling cross-feeders.

An observed result of this reduced mixing is increased genetic diversity. Rainey and Travisano (1998) compared the genetic variation from static or shaken monocultures of *Pseudomonas fluorescens*, a strain known for its rapid evolutionary capabilities. In static cultures, the *P. fluorescens* population diverged to multiple genetically different strains, many of which were able to coexist over several days of culture. The novel strains were direct competitors, exploiting a niche only available due to the spatial separation between them. In contrast, the mixed culture saw no genetic differentiation over the same time period.

More recent experimentation compared the success of a cross-feeding pair when grown in structured or unstructured media (Hansen et al., 2007). An *Acinetobacter* strain converted benzyl alcohol to benzoate, which could then be utilised by *Pseudomonas putida*. When grown as a biofilm, the relationship evolved from mere proximity of populations to *P. putida* forming a covering layer over aggregates of the *Acinetobacter* strain. *P. putida* achieved greater population growth in the

resultant co-culture arrangement, and such adaptation was not observed in the mixed chemostat environment, demonstrating that the biofilm structure was necessary for the evolution of increased productivity.

It is especially fruitful when the study of evolutionary processes is carried out in an environment where spatial structure can be varied. Long-term culture of *Burkholderia cenocepacia*, a pathogenic bacterium known for biofilm formation, gave rise to three morphologically and genetically different strains (Poltak and Cooper, 2011; Traverse et al., 2013). This work was carried out under a regime of daily recolonisation in a new biofilm environment, and planktonic control experiments showed markedly less diversification. Subsequent growth assays for each strain on cell-free supernatant of the others was suggestive of cross-feeding dynamics, though the most pronounced differences between the novel strains was in their biofilm formation. Imaging of these biofilm structures showed growth similar to that observed by Hansen et al. (2007), in that the different strains grew in proximity and achieved better growth as a result. Both these observations support the authors' assertion that cross-feeding was present and beneficial to the biofilm strains.

The fact that cells remain in proximity to one another in a biofilm is promotive of the evolution of positive interactions. Any newly arising mutant that gains a selective advantage from molecules produced by the surrounding population will only succeed if it remains in the environment that gives it that advantage. Structure, and the ability to interact continuously with a consistent group of neighbours is more conducive to cross-feeding evolution than a well-mixed environment (Trivers, 1971; Wintermute and Silver, 2010a), and it is important in mutual and augmented cross-feeding that the microbes are able to remain in proximity to their partners (Germerodt et al., 2016). One difficulty in the evolution of augmented cross-feeding is the fact that any mutant that evolves overproduction of the focal molecule at an energetic cost should be selected against, as it is at a disadvantage compared to its ancestors (Marchal et al., 2017). In a well-mixed population, any increased mutual exchange promoted by overproduction will also benefit the non-investing ancestor. In contrast, a spatially structured environment allows the benefits of overproduction to be more readily available to the overproducing bacterium, and thus is more likely to encourage the evolution of augmented cross-feeding (Bull and Rice, 1991; Doebeli and Knowlton, 1998; Foster and Wenseleers, 2006; Kim et al., 2008).

A mathematical formulation for the impact of spatial structure can be derived from Hamilton's rule (Hamilton, 1964). It states that sustained interaction of a costly nature requires that

$$rb > c$$

where *c* is the cost of a beneficial act, *b* is the benefit of the act to the receiver, and *r* is the relatedness of the individuals involved. Although simplistic and originally posed for genetic relatedness, Hamilton's rule is flexible and intuitive.

Nadell et al. (2010) adapted the relatedness term in their study of evolution with spatial structure. They considered a mathematical model population divided into individuals that perform the costly production of a public good, and those that do not, grown in a spatially structured environment. For the purpose of this model, Hamilton's relatedness term can simply be seen as the proportion of the benefits of producing the public good that are shared with other producers, as opposed to non-producers (Nadell et al., 2010; Damore and Gore, 2012). Thus, in terms of Hamilton's rule, the proportion of the benefit of producing the public good accrued to other producers must be greater than the cost of producing. For a wide range of parameter values favouring public good production, the model displayed the producers forming segregated colonies, excluding the non-producers.

This segregation in a structured environment has been shown experimentally between unrelated microbial species (Pande et al., 2016). *E. coli* and *A. baylyi* were each engineered for obligate augmented cross-feeding, the focal molecules being two essential amino acids. In tri-cultures including a strain without the overproduction characteristic, segregation of the population was observed, with the overproducing pair excluding those cells that did not overproduce. Further experimentation and accompanying mathematical modelling found that the overproducing cross-feeders were well mixed. Meanwhile, small colonies of the non-producers were excluded to the edge of the much larger and more successful overproducing colony. Similar results have been published based on experimentation and modelling of yeast populations (Momeni et al., 2013), and in both cases, repeat experimentation under mixed conditions resulted in domination by the non-overproducing strain. The similarity between model simulations and experimental observations in the work of both groups is clear and encourages the use of further modelling of spatial self-organisation in naturally occurring communities such as biofilms.

However, it would be incorrect to generalise completely and state that structured groups of cross-feeders always attain greater growth than heterogeneously mixed groups. Interactions between differing microbial species are complex, as exemplified by Kim et al. (2008). These authors found that when an engineered three-member obligate mutualist group was grown in mixed culture, one strain dominated at the expense of the others. However, all three strains showed increased growth when kept separated using a microfluidic device, with resources - but not cells - able to pass between colonies. This increased growth was only seen at intermediate separation distances (600-1200 µm); increasing distance between strain colonies resulted in a decline in the growth of all three populations. While this specific interaction of these three strains is not observed in nature, the results are enough to urge researchers to co-culture microbes in various spatially structured media, before declaring that the combinations are unculturable.

A similar result was recently found by Shitut et al. (2019), who observed that exchange of amino acids between overproducing and auxotrophic *E. coli* strains was prevented when the two were separated by a membrane. Even though amino acids could diffuse through this membrane, growth of the auxotrophic strains under separation was negligible. Nanotubes (thin, membrane-based structures linking individual cells (Pande et al., 2015; Shitut et al., 2019)) were found to be facilitating the exchange of amino acids in mixed co-culture but could not be formed through the separating membrane. Contrary to the results of Kim et al. (2008), separation was preventative of co-culture growth here, highlighting the differing outcomes of spatial structure in specific cross-feeding combinations.

Although several of the experiments and models discussed in this section are not specifically focussed on cross-feeding, the conclusions generalise to a range of microbial interactions. Routes by which cross-feeding interactions may emerge have been presented and conditions that may favour their evolution discussed. However, persistence of these relationships in a population is also important. Once cross-feeding has evolved, it must be resilient to fluctuations in levels of nutrients, competitors, and inconsistent cross-feeding partners to remain sustainable.

2.3.6 Stability and persistence of cross-feeding relationships

Not all evidence credits cross-feeding with persistence and enhanced growth over many generations. There is the argument that adaptive gene loss and interdependence between species may lead to reduced overall growth. Oliveira et al. (2014) found in their mathematical model that a cross-feeding community was less productive than a corresponding prototrophic population and stated that a given strain that relies upon another strain for the provision of essential nutrients is vulnerable to extinction if the other strain is lost. Network modelling of microbial community stability has been used to derive a similar conclusion: that the entire community is less stable as mutual cross-feeding increases (Coyte et al., 2015). A precarious population structure is formed, in which the loss of a single strain may cause the collapse of much or all the population, particularly if the strain lost is a keystone strain.

Alongside the difficulties of inter-species dependency, there is also the problem of inconsistent nutrient supply. This is a factor of importance in the colon, where host diet plays a crucial role in determining the availability of resources for microbes. Cross-feeding microbes are dependent on the actions of primary degraders, who themselves require enough energy source for growth if the population is to survive. Gudelj et al. (2016) presented a mathematical model simulating two *E. coli* strains that have the capacity for cross-feeding but are also both able to feed on the primary resource. This dynamic is comparable to that of strains L and S in the LTEE literature, however the simulation was carried out for continuous culture conditions, parameterised using data from Rosenzweig et al. (1994). The model showed that the strains maintained a stable cross-feeding relationship when the concentration of the initial molecule was high. Low or intermediate concentrations resulted in the eventual extinction of one strain, for all but a narrow range of population densities. Which strain was lost was determined by the initial conditions. Regardless, a large event such as a reduction in resource availability would seriously challenge a cross-feeding relationship. Significant dietary changes have been shown in numerous cases to result in rapid alterations in the colonic population (for example, (Walker et al., 2011; Korpela et al., 2014; Salonen et al., 2014)). Although this is not necessarily due to the availability of resources for microbial metabolism, as other factors such as colonic pH are partially determined by diet (Flint et al., 2014),

cross-feeding relationships in the colon must also be affected by the resultant changes in resource and strain concentrations.

By contrast, mutual cross-feeding may be favoured by low environmental resource availabilities, by selecting for greater resource exchange in the face of adverse conditions. Experimentation using two mutual cross-feeding yeast strains has observed that continued cross-feeding is determined by the level of dependency on the cross-fed molecules (Müller et al., 2014). It was found that the cross-feeders, which were homogenously mixed initially, showed increased separation as the plate culture expanded radially. An even mixing of the two strains was only observed when the environmental availability of the cross-fed molecules was low, increasing inter-dependency.

In a study of augmented cross-feeding relationships, data from a pair of *E. coli* strains, engaged in obligate augmented cross-feeding for essential amino acids, were used to fit a computational model (Germerodt et al., 2016). The model predicted that limiting the addition of amino acids to the population would select for augmented cross-feeding, as this encouraged auxotrophs to support their partners. When the focal amino acids were abundantly available, augmented cross-feeding was no longer advantageous due to the cost of overproduction and cells that did not overproduce were at an advantage. At this point, the term cheat is introduced, to describe such individuals. Formally, a cheat is a member of a population that benefits from a function, but does not pay the full cost of performing this function, thus decreasing the fitness of those individuals that do (Hamilton, 1964; Trivers, 1971; Axelrod and Hamilton, 1981; Ferriere et al., 2002; West et al., 2007a; Ghoul et al., 2014). Naturally, in some cases individuals may be investing to various degrees, at which point deciding what level constitutes cheating becomes difficult. Examples from the literature most frequently deal with the binary case in which cheats invest nothing into the beneficial function.

Intuitively, an individual that reaps all the benefits of augmented cross-feeding, at no individual cost, will have a fitness advantage over those paying the cost, so could be expected to thrive. Much research has investigated the persistence of mutually beneficial interactions in the presence of cheats. Most commonly, these studies assess what conditions are necessary for a cheat to invade a reciprocating population. Pande et al. (2014) introduced cheats into their co-cultures of

reciprocating *E. coli* strains and found that, although the cheats exhibited negative frequency-dependent growth and increased their population size, augmented cross-feeding persisted. All three strains could stably coexist in these experiments. This result has also been obtained in mathematical models that emphasise the importance of the cost-benefit ratio (Yamamura et al., 2004; Estrela and Gudelj, 2010; Sun et al., 2019). The stochastic model of Yamamura et al. (2004) showed that a cheat could invade an augmented cross-feeding population only when the cost of overproduction was high relative to its benefits – the opposite of the ideal conditions for the evolution of augmented cross-feeding. Sun et al. (2019) recently published a mathematical investigation of cheat invasion and persistence, in a framework that can be easily adapted to multiple species and multiple exchanged resources. This model structure could be parameterised from experimental data to facilitate the study of cheat dynamics in more complex populations.

Revisiting Germerodt et al. (2016), the observed clustering of the augmented cross-feeders in the model proved resistant to cheats, as the benefits of cross-feeding sought by the cheats were not as readily available outside these clusters. Diffusion of the essential amino acids produced during augmented cross-feeding was limited, thus encouraging cluster formation by the producers. It is conceivable that this spatial separation may also be promoting stronger mutual cross-feeding by individuals in the clusters. There is also evidence that quorum sensing among microbes may decrease the expression of extracellular enzymes in the presence of cheats, thereby achieving maximum productivity only when cheats are absent (Allen et al., 2016). The selection pressure caused by the presence of a cheat may also drive higher levels of cross-feeding under certain conditions (Ferriere et al., 2002; MacLean et al., 2010). In yeast experimentation and accompanying mathematical modelling, the presence of cheats that did not produce the extracellular carbohydrate-degrading enzyme invertase improved population fitness, subject to strict conditions on: the balance between invertase production and carbohydrate availability; the trade-off between carbohydrate availability and efficiency of use, as discussed for the cross-feeding observed in the LTEE; and the now common necessity for imperfect mixing due to spatial structure (MacLean et al., 2010). The intriguing concept that cheats may positively affect cross-feeding relationships deserves further physical and theoretical study.

The factors consistently found to promote the evolution of augmented cross-feeding - low cost-benefit ratio and spatial structure - also contribute to its persistence in adversity. However, the studies of stability reviewed here consider only a small number of strains with distinct phenotypes, whereas in the colon there are a multitude of different species, and wide genetic variation within species. Although the influencing factors discussed here will also likely be decisive in larger cross-feeding systems, more complex experimentation and mathematical modelling will no doubt identify further characteristics that are key to cross-feeding persistence in more complex networks. For example, the host would be expected to have a role in determining selection pressure on members of the colonic microbiota. How the host immune system has coevolved with the microbiota remains unclear. However, it is important to accept that members of the microbiota are not evolving in a constant environment, but rather one that also responds and adapts (Maynard et al., 2012).

2.4 Future directions for cross-feeding terminology and evolution research

Whether and in what manner other forms of nutrient exchange fit within the discussed definitions of cross-feeding types pose individual and intriguing questions. The framework proposed here primarily provides a means for quick and consistent comparison of cross-feeding relationships observed in separate experiments.

Using the terminology framework as a base, possible evolutionary origins for the four forms of microbial cross-feeding defined initially have been discussed and factors influencing their emergence and subsequent persistence listed. It is notable that mainly consortia of only a few different strains engaged in few interactions were considered here, as this is what is available in the literature. In the environment of the human colon, the variety of the microbiota implies that far more complex networks are likely active (Pande and Kost, 2017; Sung et al., 2017). Illustrating this, Sung et al. (2017) published the NJS16 model for metabolite exchange within the colonic microbiota, which involved 244 metabolic compounds and 567 microbial species. The average metabolite was imported by a median seven species and exported by a median four species. This complex cross-feeding network, coupled with ongoing evolution and changing environmental conditions, makes

these systems an enormous yet enticing challenge to the researcher. One area which stands out as requiring further research is the how cross-feeding may continue to evolve once established, particularly in complex cross-feeding networks (Hillesland, 2018). The abstract techniques reviewed here to examine evolutionary dynamics often provide further insight when in conjunction with experimentation, and ever more widespread use of mathematical modelling in evolutionary biology can be foreseen, to predict mechanisms of action as the level of complexity in experimental studies increases. Translating the results of synthetic experiments and mathematical models to *in situ* microbial metabolism is a challenge, but rewarded by a greater understanding of important communities such as the colonic microbiota.

There exist several documented cross-feeding relationships between members of the colonic microbiota, only a small subset of which has been discussed thus far in an evolutionary context. Many observed colonic cross-feeding relationships centre around SCFA production. The quantity of research on these relationships merits discussion in this literature review, and several key relationships and their classifications are presented next.

2.5 Short chain fatty acid production via cross-feeding on carbohydrates in the colon

SCFA production from carbohydrates is not a straightforward conversion, but rather comprises many interlinked metabolic pathways involving cross-feeding interactions. These processes are not uniform along the length of the colon; concentrations of SCFAs are higher in the proximal colon, where primary substrate sources and overall microbial growth are greatest (Cummings et al., 1987; Macfarlane et al., 1992). Reasons behind this gradient are absorption by the host and further conversion due to cross-feeding (Ruppin et al., 1980; den Besten et al., 2013). Highlighting the non-trivial nature of SCFA production: the substrates most often found to be butyrogenic *in vivo* (such as resistant starch and inulin), are often indigestible by butyrate-producing strains cultured *in vitro* (Pryde et al., 2002; Scott et al., 2014). This implies some form of interaction between those microbes that can degrade the butyrogenic substrates and the butyrate producers that cannot (Pryde et al., 2002; De Vuyst and Leroy, 2011; Rivière et al., 2016). Many authors have

shown that cross-feeding butyrate producers are responsible for the butyrogenic effect of various substrates (Duncan et al., 2004; Falony et al., 2006; Morrison et al., 2006; Scott et al., 2014).

2.5.1 Butyrate production via cross-feeding

The microbial community involved in the production of butyrate is broad. Beginning with the well-studied bifidobacteria: these organisms principally convert carbohydrates to lactate and acetate, along with lesser amounts of formate, ethanol and succinate under certain conditions (Van Der Meulen et al., 2004; Falony et al., 2006; Van Der Meulen et al., 2006). Variations in the proportions of these products exist, but all are waste products to the bifidobacteria, allowing for metabolite cross-feeding by lactate- and acetate-utilisers.

Duncan et al. (2004) investigated the relationship between the resistant starch degrader *Bifidobacterium adolescentis* and two butyrate-producers, *E. hallii* and *A. caccae*. *B. adolescentis* degraded starch, the sole added carbon substrate, and produced lactate. In co-culture with either butyrate-producer, lactate concentrations were reduced to near zero, with butyrate the major product found at the end of incubation. *B. adolescentis* growth was unaffected by the co-culture, implying metabolite cross-feeding on lactate by the butyrate-producers.

Several butyrogenic bacterial strains can metabolise certain carbohydrates only in the presence of acetate. For example, when grown in co-culture with *B. adolescentis* on fructooligosaccharides (FOS), *Faecalibacterium prausnitzii* produced higher levels of butyrate than were seen in this bacterium's monoculture metabolism of FOS (Rios-Covian et al., 2015). It was determined, by the change in the SCFA production profile, that *F. prausnitzii* used the acetate produced by *B. adolescentis*, allowing *F. prausnitzii* to metabolise both FOS and acetate simultaneously (Duncan et al., 2002; Duncan et al., 2004). The authors hypothesised a more complex cross-feeding relationship was also present: *F. prausnitzii* was aided by the acetate produced by *B. adolescentis*, and it is suggested that the breakdown of the sole added substrate by *F. prausnitzii* also released short chain sugars beneficial to *B. adolescentis*. Such a relationship would constitute mutual cross-feeding but was not explicitly demonstrated experimentally.

Further evidence for mutual cross-feeding by the same pair of species has been shown elsewhere, however co-cultures with closely related strains have achieved different results. *F.*

prausnitzii, when grown in co-culture with various bifidobacteria, displayed relationships ranging from competition to mutualism (Moens et al., 2016). The selection of these strains by the authors was to provide representatives of each of four inulin-type fructan-degrading clusters previously described by Falony et al. (2009b). Furthering the earlier results, *B. adolescentis* was observed to consume only short chain OF, whereas *F. prausnitzii* degraded all lengths of the tested OF fractions with equal preference. This released further short chain sugars for the *Bifidobacterium* strain, and butyrate was produced in high concentrations by this mutual cross-feeding partnership. The authors stated that competition for the sole added substrate OF was mostly avoided due to the preferences of the two bacteria. Contrastingly, other co-cultures between *F. prausnitzii* and either *Bifidobacterium angulatum* or *Bifidobacterium longum* both displayed non-preferential degradation of OF by all strains, resulting in a rapid depletion of the substrate. The bifidobacteria released acetate into the medium, but only a limited amount of butyrate was produced by *F. prausnitzii* in this more competitive scenario. The contrast between the effect of each *Bifidobacterium* strain upon the co-culture emphasises that cross-feeding differs at the strain level.

The difficulty of predicting co-culture dynamics is enhanced by the range of substrates that may be degraded by bifidobacteria. Mutual cross-feeding has been observed between *B. longum* and *Eubacterium rectale* grown in co-culture on arabinoxylan oligosaccharides (AXOS; (Rivière et al., 2015)). In monoculture with added acetate, *E. rectale* preferentially degraded long-chain AXOS, producing large quantities of free xylose. *B. longum* consumed only the simpler sugars, including xylose, in monoculture, producing high concentrations of acetate. In co-culture, the xylose released by *E. rectale* was metabolised by *B. longum*, resulting in the production of acetate and smaller quantities of other metabolites. Analogously to the previous experimentation, acetate produced by *B. longum* was used by *E. rectale* in the production of butyrate, forming a mutual cross-feeding exchange. Previous experimentation with 36 bifidobacterial strains has shown that these strains may be divided into 5 groups according to their AXOS degradation capabilities (Rivière et al., 2014). These groups do not, however, correspond to those previously defined by Falony et al. (2009b) for the breakdown of fructose, OF and inulin. The prediction of co-culture dynamics is therefore specific to the substrate used, as well as to the strains cultured.

Despite the challenges posed by the variation in butyrate-producing interactions by colonic microbes, study in this area must continue if the health benefits of butyrate and other microbially-produced molecules are to be fully exploited.

2.5.2 Beyond co-culture: short chain fatty acid cross-feeding in more diverse consortia

Although co-culture experimentation demonstrates the mechanism of a cross-feeding relationship at the simplest level, it only enables the study of one facet of the entire colonic community. The diversity of the microbiota is difficult to study *in vitro*, and as the scope of an experiment increases, drawing direct conclusions from data becomes increasingly more difficult.

An investigation of the cross-feeding interactions of *B. longum*, two *Lactobacillus* strains and the butyrate producers *A. caccae* and *E. hallii*, illustrated how moving from co-culture to tri-culture increases the uncertainty surrounding cross-feeding relationships (Moens et al., 2017). The primary degraders in this experiment were the lactobacilli and the *Bifidobacterium*, producing predominantly lactate and acetate, respectively. *E. hallii* and *A. caccae* were chosen due to their inability to degrade the added substrates inulin and OF. Instead, these two butyrate producers show rapid use of lactate and carbohydrate monomers produced by the primary degraders. The presence of acetate was required for successful metabolism of lactate by both *A. caccae* and *E. hallii*. Several culture combinations were constructed, of which only a selection is discussed.

In co-culture on OF medium with added acetate, both *L. acidophilus* and *A. caccae* strains grew from initial time, with negligible lag phases. However, in the absence of acetate, *A. caccae* growth was limited until the 6-hour point, at which point there was enough free fructose produced by *L. acidophilus* to support growth of the cross-feeder. The dominant end-products also changed between cultures: co-cultures supplemented with acetate had high final butyrate concentrations, whereas in the absence of added acetate, lactate was the major end-product. This is reflective of the types of cross-feeding occurring in each culture: in co-culture with supplemented acetate, both metabolite cross-feeding on lactate and substrate cross-feeding on fructose are performed by *A. caccae;* however, in the absence of added acetate, only substrate cross-feeding on fructose is

possible, since *A. caccae* requires acetate in order to metabolise lactate. In tri-cultures between *B. longum*, *Lactobacillus paracasei*, and either of the butyrate-producers on inulin, initial breakdown of the substrate by the primary degraders resulted in the production of free fructose, acetate, and lactate. These were then converted to butyrate, which was the dominant end-product of the culture, with no residual lactate.

This experiment is particularly interesting as several instances of cross-feeding have occurred (Figure 2.5). Exact dynamics remain unclear as to the extent to which substrate cross-feeding is occurring between primary degraders *B. longum* and *L. paracasei* on breakdown products of the sole added substrate. It is also unclear in what proportion the butyrate-producer performs each of its possible types of cross-feeding. It may be that over the course of the culture, metabolite cross-feeding and both competitive and non-competitive substrate cross-feeding occur, and that these relationships shift as the substrate concentration is reduced over time. As in the previously discussed co-culture of *B. adolescentis* and *F. prausnitzii*, computational approaches using the time-series data documented in this paper may further elucidate the results. Either of the primary degraders in this experiment could support the butyrate producers in co-culture, however in some cases a single strain may be decisive in determining the success of a diverse population.

Such is the case for *Ruminococcus bromii*, the presence of which can be the deciding factor in whether a microbial population can degrade certain resistant starch species (Ze et al., 2012; Ze et al., 2013). In *in vitro* studies with this bacterium, two significant results were obtained. The first was that the combination of *R. bromii* in co-culture with a variety of other colonic bacteria allowed for improved growth of the partner on resistant starch compared to monoculture. *R. bromii* was shown to degrade resistant starch to reducing sugars, which, though largely useless to the degrader, were cross-fed by *B. thetaiotaomicron*, *E. rectale* and *B. adolescentis*, improving their growth. Secondly, in a mixed faecal consortium with poor starch degradation capabilities, addition of *R. bromii* more than doubled the percentage of starch that was utilised by the end of culture. The *R. bromii* strain studied is potentially a keystone species, but the authors noted that it is far more likely that keystone groups are responsible for such essential functions *in vivo* (Ze et al., 2013). Perhaps the most accurate approach would be the discussion of keystone *functions* in the colon, followed by those strains which are able to perform them.

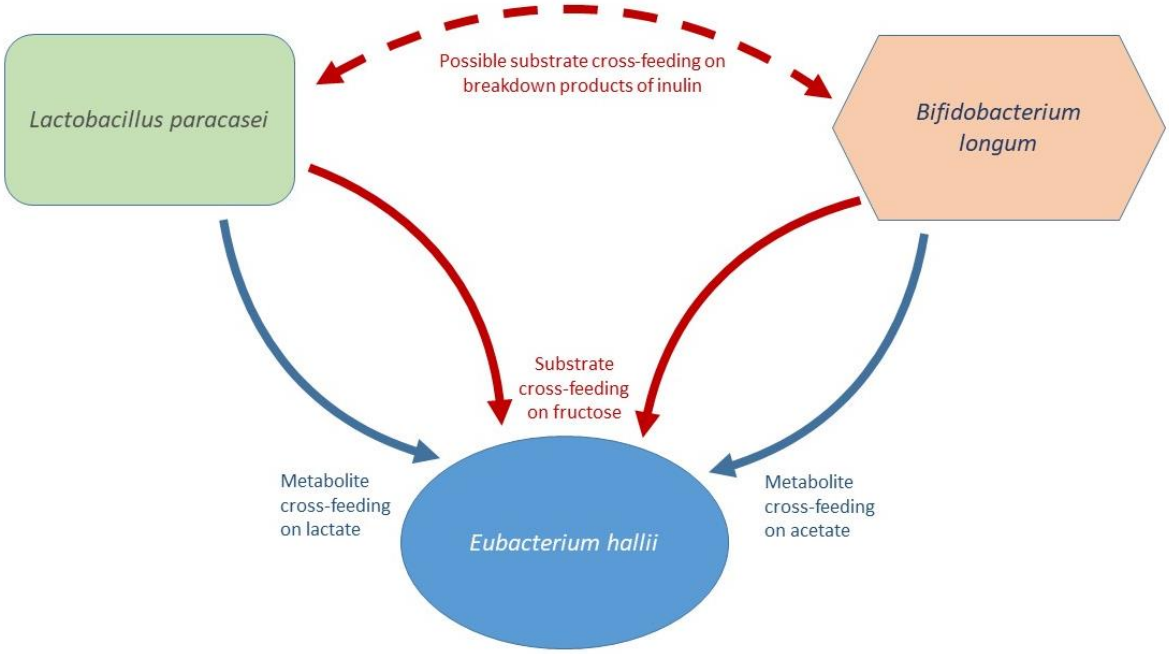

Figure 2.5. Tri-culture cross-feeding dynamics from experimentation by Moens et al. (2017). The butyrate producer *Eubacterium hallii* was shown to simultaneously metabolise lactate and acetate, obtained by metabolite cross-feeding. *E. hallii* also utilised free fructose released by both *Lactobacillus paracasei* and *Bifidobacterium longum* during the degradation of inulin, via substrate cross-feeding. Separately, both *L. paracasei* and *B. longum* could grow on fructose and short chain sugars from inulin breakdown. In co-culture with *L. paracasei*, *B. longum* cross-fed on these short chain sugars, and *L. paracasei* may also have cross-fed on free fructose released by *B. longum*. It was not shown in what proportion each of the three strains utilised the free products of inulin breakdown released by the two primary degraders, or whether competition for these products increased as inulin concentration decreased. Mathematical modelling using the time series data for the experimentation could reveal more about this interaction.

Functions which improve the success of a population are not always easy to identify, as exemplified in the work on substrate cross-feeding by Rakoff-Nahoum et al. (2016). The competitive substrate cross-feeding between *B. breve* and *B. bifidum* on mucins was previously discussed, when providing demonstrative examples for the cross-feeding classifications. The primary degrader, *B. bifidum*, was limited in co-culture by the loss of some substrate to the cross-feeder (Egan et al., 2014). Such cross-feeding on the products of extracellular substrate degradation has been observed in multiple members of the Bacteroidales order, which express extracellular hydrolysing enzymes for the breakdown of complex carbohydrates (Rakoff-Nahoum et al., 2016). In order to assess the proportion of the breakdown products which were used by the enzyme producer, mutant strains were engineered without the capability to produce certain extracellular enzymes, reminiscent of the discussion of cheating and reductive evolution earlier in this chapter. Co-culture experiments with these mutants returned a mixture of anticipated and unintuitive results. When grown in

monoculture on amylopectin or levan, *B. thetaiotaomicron* mutants were unable to grow, as expected. When in co-culture with the functional *B. thetaiotaomicron*, the mutants exhibited growth in the order of 1 $\log_{10}$ CFU ml^{-1}, showing that substrate cross-feeding on breakdown products was occurring, but to a limited extent.

By contrast, the dynamics of *B. ovatus* grown on inulin were surprising and show beneficial, although not keystone, functionality for the population. The bacterium expressed several enzymes which did not appear necessary for their growth on inulin, since mutants unable to synthesise these enzymes grew just as well as the original strain. It was hypothesised that perhaps these enzymes are expressed to the benefit of other species, which by their presence then confer some mutual benefit on *B. ovatus*. This would be in accordance with previous study, in which substrate cross-feeding has been displayed by *B. adolescentis* on xylan degradation products of *B. ovatus* (Rogowski et al., 2015).

The hypothesis was tested by inoculation of gnotobiotic mice with both the wild type *B. ovatus* and the mutant, to assess their behaviour when coexisting in the colon. Both could become established in the mice for 14 days, over which period the wild type fraction of the population gradually declined. However, upon further inoculation of the mice with a third bacterium, *Bacteroides vulgatus*, the wild type *B. ovatus* universally showed a resurgence against the mutant strain. The wild type gained proportional dominance over the mutant strain by 21 days in all but one of the tested mice. Moreover, *in vitro* plate cultures of each of the two *B. ovatus* strains with the *B. vulgatus* partner, demonstrated that the co-culture containing the original, enzyme-producing *B. ovatus* always showed greater growth of the partner strain than the mutant *B. ovatus* co-cultures. This increase in the partner strain came at no significant growth detriment to *B. ovatus*. There is clearly some community benefit which the mutant did not perform to the same degree as the wild type strain. Since all strains showed increased growth in co-culture compared to monoculture, there is clearly mutual benefit, but the exact mechanism of the mutualism is unknown. If the benefit which the *B. ovatus* strain obtains in co-culture is nutritional, then the costly nature of producing extracellular enzymes would make the relationship between *B. ovatus* and *B. vulgatus* an instance of naturally occurring augmented cross-feeding. However, the chromatographic analyses performed by the authors could not isolate a metabolite which might be cross-fed by *B. ovatus*, so the exact nature of the mutualism remains unknown.

Bifidobacterial populations in mouse models have exhibited similar behaviour. Those mice inoculated with a pair of bifidobacterial strains showed higher caecal bifidobacterial counts than those inoculated with a single strain, accompanied by significant upregulation of genes involved in glycan degradation pathways (Turroni et al., 2016). This again displays a mutually beneficial relationship between the introduced strains, but whether this is based upon cross-feeding has not been proven. The uncertain nature of the final classification of these relationships in the mouse emphasises the difficulty in drawing conclusions from *in vivo* data, increasing our reliance on *in vitro* experimentation and computational approaches.

2.6 The relationship between pH and cross-feeding interactions

Besides the health effects resulting from the absorbance and further use of microbially produced SCFAs, production itself has the effect of reducing the pH of the colonic environment (Hernot et al., 2009). Decreases in pH from a near-neutral level to values around pH 5.5 have been observed between the terminal ileum and proximal colon, where SCFA production is highest, followed by an increase to neutral pH in the distal colon and rectum (Cummings and Macfarlane, 1991; Macfarlane et al., 1992; Nugent et al., 2001). Discussion of the increasing pH gradient in the colon has been a feature of the literature for many years (Cummings et al., 1987; Evans et al., 1988; Macfarlane et al., 1992), but only more recently has the relationship between colonic pH and microbial cross-feeding been investigated.

In their investigation of metabolite and substrate cross-feeding between *B. adolescentis* and prominent butyrate producers, Belenguer et al. (2006) observed that lactate utilisation and butyrate production occurred at a higher rate at pH 6.5 than at pH 5.7. Increased lactate and decreased SCFA concentrations in faeces are factors associated with ulcerative colitis (Vernia et al., 1988), thought to be due to a build-up of lactate in the colon potentially associated with a disturbed microbiota (Vernia et al., 1988; Belenguer et al., 2007). The experimental results linking pH to lactate concentrations, along with the knowledge of the pH gradient in the colon, prompted further study into the effect of pH on lactate cross-feeding.

Belenguer et al. (2007) assessed the effects of differing pH on lactate levels in mixed faecal slurries. A mixture of polysaccharides was added to cultures at pH values of 5.2, 5.9 and 6.4.

Bifidobacteria became the dominant species in polysaccharide culture at pH 5.2. This was also the only culture in which lactate was present in the medium after 24 hours. The dominance of the bifidobacteria was not due to increased bifidobacterial growth, which did not change significantly between the three pH levels, but rather due to reduced growth by other members of the culture. The cross-feeding *E. hallii* group achieved high proportions in the cultured population at the higher pH values, accompanied by a decrease in lactate and an increase in SCFA concentrations. These results are reflective of metabolite cross-feeding by *E. hallii* and other butyrate-producers on lactate, as discussed previously.

Two possibilities exist for the observed lactate accumulation at low pH: either greater lactate production by the bifidobacterial group occurred, or there was reduced utilisation of lactate by cross-feeders. Low pH has been shown to stimulate lactate production by bifidobacteria and mixed faecal cultures (Belenguer et al., 2006; Belenguer et al., 2011), which supports the former explanation. However, more recent work by the same group demonstrated that lactate utilisation by cross-feeders down to pH 5.5 should exceed production (Belenguer et al., 2011). Therefore, it was hypothesised that the lactate build-up observed at pH 5.2 was due to increased lactate production by bifidobacteria, with inhibition of butyrate production at this level of acidity a possible contributing factor. Further experimentation at pH values below 5.5 to ascertain the relative activity of lactate producers and utilisers could be useful in gaining an understanding of the role of this metabolite in ulcerative colitis.

Alongside changes in the production of lactate at different pH values, the products of lactate metabolism shift with acidity. Whilst acetate and butyrate were the main SCFAs produced in culture on polysaccharides, this was not the case for all substrates. In faecal cultures grown at pH 6.4 with lactate as the sole added substrate, propionate was the dominant end-product (Belenguer et al., 2007). Corresponding butyrate production in lactate cultures was low, implying that both pH and the availability of polysaccharides are important variables in the production of this SCFA. A comparable switching between greater butyrate production at pH 5.5 and greater propionate production at pH 6.5 has previously been shown in faecal cultures grown on polysaccharides (Walker et al., 2005). As is common in cross-feeding experimentation, the extent to which butyrate production is achieved via metabolite cross-feeding on lactate, or via metabolism of sugars, is

unclear. However, continuous culture in chemostats with carbon-labelled substrates estimated that up to 20% of butyrate carbon was derived from lactate, the rest assumed to have been produced directly from carbohydrate, but again with variation between pH levels (Belenguer et al., 2011). It is impossible to draw general conclusions about the production of butyrate in the colon from faecal cultures, since these do not necessarily reflect the population or dynamics of the proximal colon (Macfarlane and Macfarlane, 2007) and display wide variation between donors (Belenguer et al., 2007; Belenguer et al., 2011; Salonen et al., 2014); however, pH has a decisive role in determining the SCFA production profile.

pH is also reflective of the changing population composition of the microbiota along the length of the colon. Individual bacterial growth assays have previously shown that several *Bacteroides* strains, including *B. thetaiotaomicron*, were unable to grow at pH 5.5 (Duncan et al., 2009). Contrastingly, *B. adolescentis* and the butyrate producers *Roseburia intestinalis*, *E. hallii*, and another *Roseburia* strain, all showed growth rates above 0.4 h^{-1} at this pH value. Growth of *B. thetaiotaomicron* was further limited when an SCFA mixture was present in the medium. In particular, the addition of acetate and lactate in concentrations comparable to those in the colon completely inhibited growth of *B. thetaiotaomicron* at pH 5.5, but had less effect at the higher pH values, indicating that this inhibition is pH dependent. Together, these results imply that this strain, and perhaps other closely related strains, may be inhibited by the SCFAs produced via cross-feeding in the low pH environment of the proximal colon. Indeed, continuous fermentation with a consortium of faecal microbes, maintained at either pH 5.5 or 6.5, showed dominance by the Bacteroidetes at the higher pH and dominance by the butyrate-producing *Roseburia* and *E. rectale* group at the lower pH. These results are supported by similar, more recent experimentation which showed that decreasing pH negatively affects the Bacteroidetes phylum, whilst the Firmicutes thrive (Chung et al., 2016). In a cross-feeding context, the ratio of Bacteroidetes to Firmicutes can also affect the SCFA production profile in the colon, with many health implications (Ley et al., 2006; Schwiertz et al., 2010; Payne et al., 2011; Bervoets et al., 2013; Cerdó et al., 2017).

Ascertaining the interaction between the microbiota and colonic pH is challenging experimentally, but can also be investigated using mathematical modelling. Kettle et al. (2015) used the faecal continuous culture data at changing pH produced by Walker et al. (2005) for comparison

to their mathematical model for a colonic microbial community. Whilst the model was accurate in predicting microbial counts and SCFA concentrations for the two different pH values, the model would benefit from adding a dependency of pH on the production of SCFAs, as considered in a preceding model (Kettle et al., 2014). As acknowledged by the authors, the exact manner and extent to which SCFA production alters colonic pH is not known, due to absorption and buffering actions by the host (Kettle et al., 2014), and is a subject for future modelling investigations. Whilst the metabolic cross-feeding pathways by which SCFAs are produced are well-documented, the activity of these pathways in the dynamic environment of the human colon requires continued study.

Since butyrate is widely accepted as a desirable product of the colonic microbiota, continued efforts will likely be made to enhance the butyrogenic qualities of food. While assaying faecal samples for their response to certain prebiotics provides information on what foods are particularly butyrogenic, cross-feeding co-cultures provide the best mechanistic information for butyrate production. Upscaling these experiments to several strains comes with difficulties in both the experimental design and in drawing inference from data. Computational approaches should be utilised to isolate the key interactions of such complex cultures.

Many of the mathematical models which have been used to study cross-feeding in the past have not considered the effect of SCFA production on colonic pH. Although this may be an acceptable simplification for some models, pH does have a dramatic effect on the SCFA production profile, and the relative abundance and metabolic activity of certain microbial genera. A relationship between SCFA concentrations and pH should therefore be incorporated into future models.

The production of hydrogen in the SCFA cross-feeding experiments reviewed here was not a focus of the research. However, many of these cross-feeding interactions would have resulted in significant hydrogen production, which may have influenced the outcomes of the experiments via partial inhibition of metabolic pathways. In the more diverse community of the colonic microbiota, further cross-feeding interactions will be present utilising hydrogen as a substrate. The following sections detail the current knowledge on hydrogenotrophic microbes of the colon.

2.7 The hydrogenotrophic functional groups of the human colon

Hydrogenotrophic microbes in the colon largely fall into three functional groups, determined principally by the products of their hydrogen metabolism: methanogens, which produce methane; sulphate-reducing bacteria (SRB), which convert free sulphate to sulphide compounds; and acetogens, which produce acetate. Each utilise hydrogen to varying degrees under certain conditions and all have been shown to coexist in the human colon (Doré et al., 1995; Chassard et al., 2008; Nava et al., 2012a). Microbiome data shows that although functional genes from all three hydrogenotrophic groups are consistently found throughout the colon, they form a numerically minor part of the microbiota (Table 2.1). Arumugam et al. (2011) suggested that the three enterotypes into which they could separate individuals in their microbiome sequencing work may be influenced by the dominant form of hydrogenotrophy occurring in each enterotype. However, confirming this hypothesis was prevented by the low abundance of genetic material from the hydrogenotrophic functional groups obtained in samples and deserves further investigation.

The role of hydrogenotrophic microbes in reducing the partial pressure of hydrogen in the colon lessens the associated inhibitory effect on carbohydrate metabolism (Stams, 1994; Chassard et al., 2010; Janssen, 2010). The relationship between hydrogen producers and consumers therefore constitutes a mutualism, beneficial to both. However, it does not satisfy the established definition of mutual cross-feeding unless some molecule produced by the hydrogenotroph is metabolised by the hydrogen producer. In most cases discussed in this review, the relationship between the hydrogenotroph and the hydrogen producer is metabolite cross-feeding since hydrogen is a waste product for the producer.

Table 2.1. Cell, gene and relative abundance of hydrogenotrophic microbial functional groups measured in samples from healthy individuals		
Functional group	**Abundance**	**Source**
Methanogens	Below detection (<10^2 cells g^{-1} faeces) to $10^{9.9}$ cells g^{-1} faeces	Culture-based estimation from faecal samples Pochart et al. (1992)
	Below detection (<10^2 cells g^{-1} faeces) to $10^{9.8}$ cells g^{-1} faeces	Culture-based estimation from faecal samples (Doré et al., 1995)
	0.0143 to 6.605 mg DNA per gram wet weight	Targeted PCR on faecal samples (Abell et al., 2006)
	3×10^2 to 4.5×10^9 gene copy numbers per gram tissue	Targeted qPCR on colonic mucosal biopsy samples (Nava et al., 2012a)
	Mean $10^{3.78}$ gene copies per ml	Targeted qPCR on faecal samples (Million et al., 2012)
Sulphate-reducing bacteria	$10^{5.3}$ to $10^{10.7}$ cells per gram dry weight	Culture-based estimation from faecal samples (Gibson et al., 1988c)
	$10^{6.1}$ to $10^{7.9}$ cells per gram	Culture-based estimation from faecal samples Pochart et al. (1992)
	$10^{5.6}$ to $10^{9.2}$ cells per gram	Culture-based estimation from faecal samples (Doré et al., 1995)
	$10^{6.5}$ to $10^{9.9}$ gene copies per gram wet weight (*Desulfovibrio* only)	Targeted qPCR from faecal samples (Bartosch et al., 2004)
	0.145 ± 0.145% relative abundance (*Desulfovibrio* only)	Re-analysis of faecal metagenomic data set (White et al., 2009)
	1.8×10^2 to 1.4×10^9 gene copy numbers per gram tissue	Targeted qPCR on colonic mucosal biopsy samples (Nava et al., 2012a)
Acetogens	Below detection (<10^2 cells g^{-1} faeces) to $10^{8.4}$ cells g^{-1} faeces	Culture-based estimation from faecal samples (Doré et al., 1995)
	0 to 10% relative abundance (*Blautia* only)	Metanalysis of multiple faecal metagenomic data sets (Arumugam et al., 2011)
	1.8×10^3 to 3.8×10^7 gene copy numbers per gram tissue	Targeted qPCR on colonic mucosal biopsy samples (Nava et al., 2012a)
(q)PCR: (quantitative) polymerase chain reaction.		

2.7.1 Methanogens

The Archaeon *Methanobrevibacter smithii* is the most abundant and, in some cases, the sole methanogen found within the human colon (Miller et al., 1982; Eckburg et al., 2005; Dridi et al., 2009; Million et al., 2012; Nava et al., 2012a; Faith et al., 2013). *Methanosphaera stadtmanae* is also commonly observed (Dridi et al., 2009; Hansen et al., 2011). *M. smithii* converts CO_2 and hydrogen into methane (CH_4; Moss et al., 2000) in the following reaction (Figure 2.6):

$CO_2 + 4H_2 \rightarrow CH_4 + 2H_2O$

M. smithii is also able to utilise formate (HCO_2^-) in the same manner because the similar reduction potentials of formate and hydrogen make interconversion between the two manageable (da Silva et al., 2013). Expression levels of genes involved in formate utilisation by *M. smithii* has been shown to be increased in the presence of formate-producing bacteria (Samuel et al., 2007). Samuel et al. (2007) also found evidence to support minor levels of ethanol and methanol uptake by this archaeon as lesser energy sources, as well as acetate uptake, for use in an incomplete tricarboxylic acid cycle (Samuel et al., 2007). They suggest that these latter pathways are responsible for biomass accumulation.

Methanogen growth is limited by low pH, even in the range found within the proximal colon, which can be as low as pH 5.5 (Gibson et al., 1990; Cummings and Macfarlane, 1991). They are also limited by their inability to degrade sugars (Robert and Bernalier-Donadille, 2003; Samuel et al., 2007) and are therefore obligate cross-feeders, dependent upon the products of carbohydrate degraders for survival.

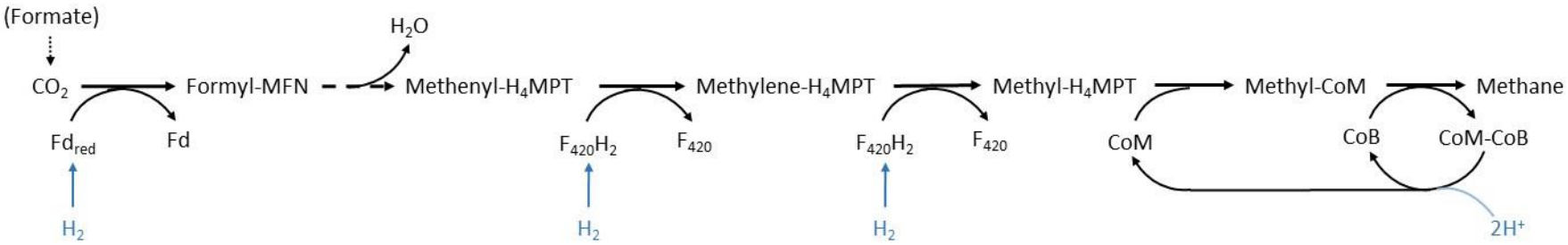

Figure 2.6. Simplified diagram for hydrogenotrophic methanogenesis. The dashed arrow represents multiple reactions and intermediates. Formate may be a precursor but is converted to CO_2 for methanogenesis. Formyl-MFN = formyl-methanofuran; H_4MPT = tetrahydromethanopterin; Fd = ferredoxin; Fd_{red} = reduced ferredoxin; F_{420} = coenzyme F_{420}; CoM/CoB = coenzyme M/B. See Samuel et al. (2007) and Enzmann et al. (2018) for full pathway descriptions.

2.7.2 Sulphate-reducing bacteria

The SRB show greater taxonomic diversity in the microbiota than the methanogens and can utilise a wider range of substrates for growth. Most commonly it is *Desulfovibrio* that is the dominant SRB genus in the colon (Gibson et al., 1990; Nava et al., 2012a), members of which can reduce sulphate compounds to hydrogen sulphide (H_2S), whilst simultaneously oxidising lactate to acetate. *Desulfovibrio piger* has an obligate requirement for sulphate in order to oxidise lactate (Marquet et al., 2009), and interestingly was able to reduce sulphate effectively at pH 5.5 - substantially more acidic conditions than the neutral pH supportive of colonic methanogens. Other SRB species are able to metabolise substrates such as the SCFAs acetate, butyrate and propionate, as well as ethanol and pyruvate (Willis et al., 1997), although these genera are usually absent or found at low counts in humans (Gibson et al., 1988b; Gibson et al., 1988c; Barton and Fauque, 2009; Nava et al., 2012a; Nava et al., 2012b). A standard stoichiometric equation for sulphate reduction is as follows (Thauer et al., 1977):

$4H_2 + SO_4^{2-} + H^+ \rightarrow HS^- + 4H_2O$

or

$2\ CH_3CHOHCOO^- + SO_4^{2-} \rightarrow 2\ CH_3COO^- + 2\ HCO_3^- + H_2S$

(2 Lactate + Sulphate → 2 Acetate + 2 Bicarbonate + Hydrogen Sulphide)

with the inclusion of the lactate to acetate conversion (Figure 2.7; Noguera et al., 1998; Keller and Wall, 2011; Rowland et al., 2017). Both lactate oxidation and sulphate reduction are energy yielding pathways for SRB and use of intermediates of the lactate oxidation pathway as carbon sources for growth can be expected to alter the stoichiometry of these reactions (Keller and Wall, 2011).

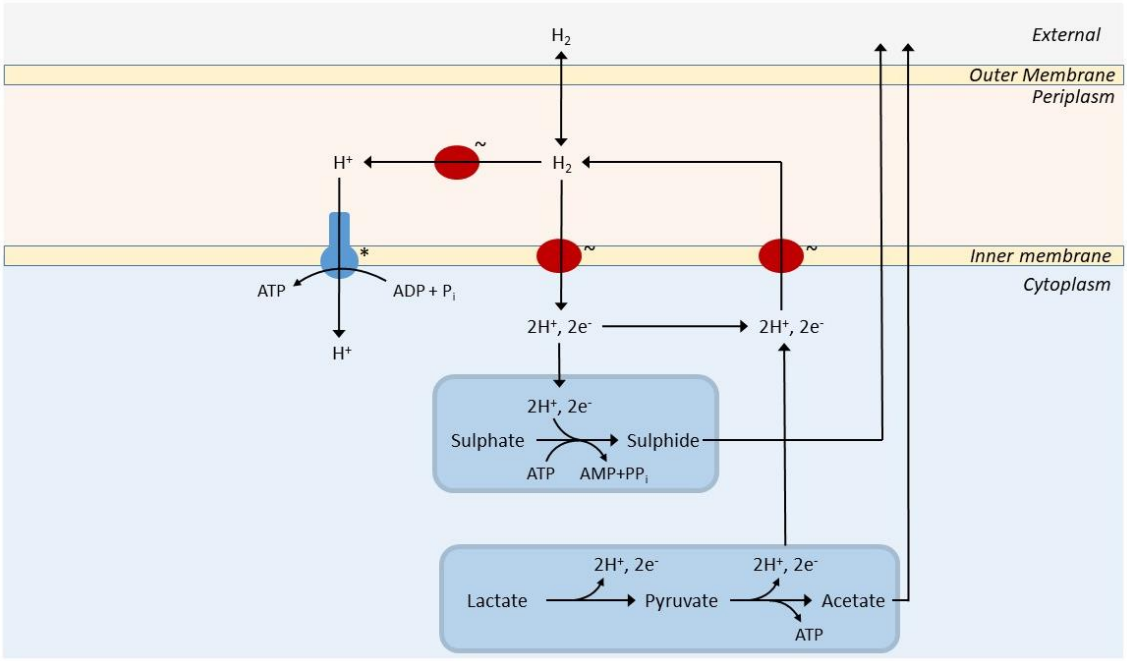

Figure 2.7. Simplified diagram for the simultaneous oxidation of lactate and reduction of sulphide by sulphate-reducing bacteria (SRB), based on data for the prominent SRB *Desulfovibrio vulgaris*. Both lactate oxidation and sulphate reduction occur in the cell cytoplasm. The protons and electrons produced during lactate oxidation are acted upon by several hydrogenase enzymes, with interconversion between H_2, and $2H^+ + 2e^-$. A proton gradient is maintained across the cytoplasmic membrane, enabling the synthesis of ATP by membrane-bound ATPase. * = ATP synthase; ~ = hydrogenase enzyme. See da Silva et al. (2013), Keller and Wall (2011), Noguera et al. (1998) and Heidelberg et al. (2004) for full pathway descriptions.

Sulphate may be derived in the colon from several dietary sources, particularly high-protein foods such as animal products, which contain the sulphur amino acids cysteine, methionine and taurine, as well as the inorganic sulphate present in *Brassica* vegetables (Magee et al., 2000). Sulphate may also be generated from the breakdown of endogenous sulphur-containing mucins (Willis et al., 1996; Windey et al., 2012). However, SRB are unable to degrade mucins, so rely on other members of the microbiota to release free sulphate during their metabolism of mucins (Gibson et al., 1993a). Willis et al. (1996) investigated the cross-feeding actions of the SRB *Desulfovibrio desulfuricans* on free sulphate produced by *Bacteroides fragilis* during mucin breakdown. Both *D. desulfuricans* cell counts and the sulphide produced were increased in co-culture compared to SRB monoculture, clearly displaying a cross-feeding relationship. The sulphate-reduction pathway of SRB is dependent on the availability of sulphate, and thus is often dependent on cross-feeding for this substrate.

Although the metabolism of hydrogen by SRB puts them in competition with other hydrogenotrophic microbes, the broader metabolic capabilities of the SRB allow them to compete

with other functional groups of the microbiota, metabolising more complex substrates. *D. piger* has been shown to cross-feed on lactate produced by *B. adolescentis* (Marquet et al., 2009), and to effectively compete for this substrate against the butyrate-producers *E. hallii* and *A. caccae*. Butyrate production was decreased in all co-cultures containing the SRB, as were cell counts for *E. hallii* and *A. caccae*, due to competition for lactate. By contrast, *D. piger* cell counts were unaffected by the presence or absence of either or both butyrate producers, potentially due to more effective lactate scavenging by the SRB. The authors hypothesised that the hydrogen produced by the other bacteria in the co-cultures may have given a further advantage to *D. piger*, which is supported by the increased final sulphide concentrations in the co-cultures. However, this is impossible to determine explicitly, since only initial and final cell counts were measured in this experiment, leaving no way to ascertain growth rates or the time taken to reach steady state. Moreover, both the butyrate-producing species studied here have been shown to metabolise sugars as well as lactate (Moens et al., 2017), a dynamic that was not analysed in this study. Nevertheless, the behaviour exhibited by *D. piger* shows more complex cross-feeding interactions than those of the methanogens.

2.7.3 Acetogens

Acetate is produced via several microbial metabolic pathways, however in the context of hydrogen cross-feeding, only the acetate formed via reductive acetogenesis is considered (Figure 2.8; Thauer et al., 1977):

$$4H_2 + 2CO_2 \rightarrow CH_3COO^- + H^+ + 2H_2O$$

Reductive acetogenesis uses the Wood-Ljungdahl metabolic pathway. Another common and pertinent term found in the literature is “homoacetogenesis”, but the definition is not uniform across the field of study. Homoacetogenesis has been defined as the formation of acetate as the sole reduced end-product in the metabolism of a substrate (Drake, 1994), but discordantly as the “production of more than 2 mol of acetate per mol of sugar consumed” (Bernalier et al., 1996b). Use of the term homoacetogenesis is avoided here and in the remainder of this thesis the use of the term acetogen is restricted to bacteria producing acetate via the Wood-Ljungdahl pathway. This also excludes SRB, which, as previously noted, are acetate producers but do not perform reductive acetogenesis.

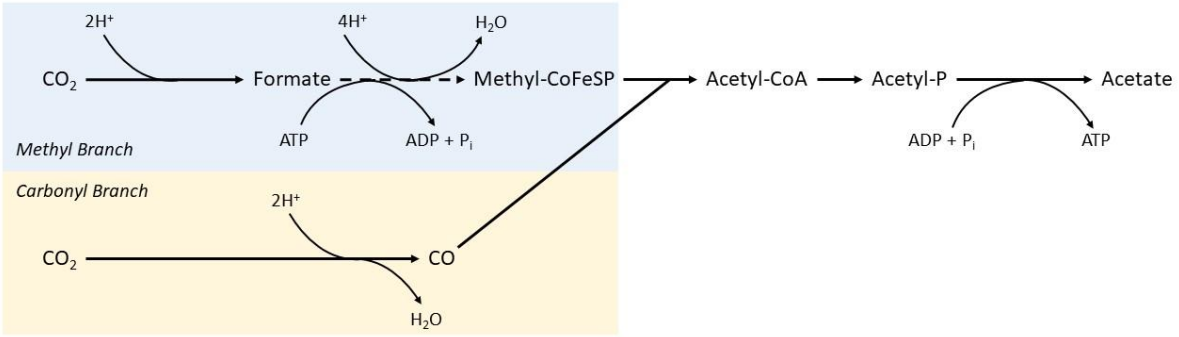

Figure 2.8. Simplified diagram of the Wood-Ljungdahl pathway. The dashed arrow indicates multiple reactions with several intermediates, leading to the formation of Methyl-CoFeSP (Co/Fe-containing corrinoid iron-sulphur protein). See Nakamura et al. (2010) and Schiel-Bengelsdorf and Dürre (2012) for full pathway descriptions.

Genome sequenced acetogens possess the genes necessary for the metabolism of a greater range of substrates than either SRB or methanogens (Carbonero et al., 2012; Kelly et al., 2016). The colonic acetogen *Blautia hydrogenotrophica* (previously *Ruminococcus hydrogenotrophicus*, but since reclassified (Bernalier et al., 1996b; Liu et al., 2008)) has been shown to metabolise a range of mono- and disaccharides, as well as hydrogen and CO_2, required for reductive acetogenesis (Bernalier et al., 1996b). Work culturing the hydrogen producer *Ruminococcus albus* with a colonic acetogen resulted in acetate concentrations of around three times that recorded for *R. albus* alone (Miller and Wolin, 1995). Hydrogen was near undetectable after five days of co-culture, due to its conversion to acetate via the Wood-Ljungdahl pathway.

Acetogens have a positive impact on the human body in terms of energy harvest, since acetate can be absorbed by the colon for use as a host energy source (Morrison and Preston, 2016). Acetate produced via the Wood-Ljungdahl pathway has been shown to account for up to 33% of acetate produced by faecal cultures (Miller and Wolin, 1996). Moreover, acetogens may provide benefits to other microbial groups. An *in vitro* mutual cross-feeding interaction has been observed between *R. intestinalis* and *B. hydrogenotrophica* when the pair were grown on xylan (Chassard and Bernalier-Donadille, 2006). *R. intestinalis* converted xylan to butyrate, releasing hydrogen for acetogenesis. Also observed was cross-feeding by *R. intestinalis* on the acetate produced by the acetogen, resulting in higher butyrate production by the co-culture than the monoculture.

2.7.4 Competition between the hydrogenotrophic functional groups

The competition between the hydrogenotrophic functional groups can be investigated by considering the biochemistry of the reactions performed by each group. Sulphate reduction is thermodynamically the most favourable of the three, having a Gibbs free energy change of -152.2 kJ mol^{-1}, compared to -130 kJ mol^{-1} for methanogenesis and -95 kJ mol^{-1} for acetogenesis (Thauer et al., 1977; Gibson et al., 1993a; Bernalier et al., 1996a). Moreover, of the three functional groups, SRB have the greatest affinity for hydrogen (lowest half-saturation constant, K_S (Kristjansson and Schönheit, 1983)). Methanogens have a far lower hydrogen concentration threshold than acetogens for growth on this substrate (a minimum of 116 ± 20 ppm for *M. smithii*, compared to a minimum 1,100 ± 200 ppm for acetogens, although this number varies between strains (Leclerc et al., 1997)), which together demonstrate the hierarchical nature of hydrogen usage capability between the three functional groups. SRB should be favoured in an environment with abundant substrate, however a lack of sufficient sulphate has been shown to negate their advantage (Gibson et al., 1988b). Between methanogens and acetogens, the methanogenic population should reduce the concentration of hydrogen to such an extent as to be unavailable for use in the Wood-Ljungdahl pathway (Bernalier et al., 1996a). However, as shown by observational studies, low pH can improve selection for SRB and acetogens due to its inhibitory effect on methanogens (Gibson et al., 1990).

The hydrogenotrophic dominance of SRB in mixed faecal cultures was demonstrated more than 30 years ago. Gibson et al. (1988a) found significant methane production by faecal cultures sampled from individuals with a positive methane breath test. However, when these cultures were mixed with non-methanogenic faecal cultures, methane production was almost completely inhibited, with high sulphide production recorded instead. Methane production was recoverable only when sulphate reduction was chemically inhibited. Acetate production was not measured but could be expected to have remained relatively consistent between cultures, as reductive acetogenesis should not be favourable in competition with sulphate-reduction and methanogenesis. This result is in contrast with that of a later experiment that showed, when following a similar protocol, that methanogenesis dominated cultures grown from a mixture of methanogenic and non-methanogenic faecal samples (Strocchi et al., 1994b). As stated by the authors of the second

publication, the two results are difficult to reconcile. They hypothesised that the thermodynamic advantages of SRB may be incorrect for all species in the colon, however there is also the possibility that pH played a role. pH was not recorded in the work of Gibson et al. (1988a), whereas it remained at pH 6.8 or higher in the experiments of Strocchi et al. (1994b). It is therefore possible that pH was lower in the earlier experimentation, which would have been more favourable to the SRB.

Limited data exist on the direct co-culture combination of the hydrogenotrophic functional groups. However, some inference can be made from studies in gnotobiotic mice. As described by Samuel and Gordon (2006), mice colonised with *B. thetaiotaomicron* and either the methanogen *M. smithii* or the SRB *D. piger*. *B. thetaiotaomicron* produced mainly acetate when combined with *M. smithii*. This association rapidly reached much higher population densities than the SRB combination, as well as increasing host adiposity compared with both the SRB combination and mono-association with *B. thetaiotaomicron*. Gene expression changes were detected in *B. thetaiotaomicron* when in combination with *M. smithii*, including increased expression levels of genes involved in the production of the enzyme pyruvate-formate lyase. This points to increased production of formate, which can be utilised by *M. smithii*. This was combined with a shift to more acetate production in the methanogenic association, with reduced propionate and butyrate. The cause of this change was thought to be the observed reduction in the caecal NADH/NAD^+ ratio, which indicated that the metabolism of *M. smithii* created a more favourable environment for the breakdown of sugars by *B. thetaiotaomicron*. By contrast, only minimal gene expression changes were detected in the SRB association. Unfortunately, no association with both the methanogen and the SRB was undertaken to ascertain direct competition dynamics. Thus, it cannot be determined whether the effect of *M. smithii* upon *B. thetaiotaomicron* metabolism would persist in the presence of *D. piger*, or which of the hydrogenotrophs would dominate the colonic environment in this case. From a biochemistry perspective, the extinction of *M. smithii* due to competitive exclusion would be expected. However, the more successful association observed between the methanogen and *B. thetaiotaomicron* casts doubt upon this hypothesis.

Acetogen cross-feeding in mice has also been demonstrated between *B. thetaiotaomicron* and *B. hydrogenotrophica*, a combination that increased the efficiency of fermentation by *B. thetaiotaomicron* (Rey et al., 2010). Similarly to the *M. smithii* bi-associations of Samuel and Gordon

(2006), the presence of the acetogen reduced the NADH/NAD^+ ratio in faecal samples, implying that the regeneration of NAD^+ is facilitated by the reductive acetogenesis carried out by *B. hydrogenotrophica*. There is currently no evidence to support the reduction of the NADH/NAD^+ ratio by SRB in mice or humans. This may be due to the scarcity of studies of this nature but may also imply that SRB are of little benefit in the facilitation of more efficient substrate breakdown by carbohydrate degraders.

It is important to note that the three functional groups will not always be in competition, since hydrogen is only essential to the methanogens. A mutualistic relationship has been observed between the SRB *D. vulgaris* and the methanogen *Methanococcus maripaludis in vitro* (Hillesland and Stahl, 2010). The SRB converted lactate to acetate, CO_2, and hydrogen, whilst the methanogen utilised the released CO_2 and hydrogen for methane production. This cross-feeding reduced the partial pressure of hydrogen, creating a more favourable metabolic environment for the SRB. In this combination, *D. vulgaris* acted as a net hydrogen producer, indicating that competition between the functional groups is environmentally dependent. Sulphate was not present in the medium in sufficient quantity for metabolism by *D. vulgaris*, thus preventing competitive interaction.

More recently, Rey et al. examined the behaviour of *D. piger* using both mouse models and *in vitro* study (Rey et al., 2013). The SRB was introduced to gnotobiotic mice that had been associated with a consortium of eight non-hydrogenotrophic human colonic bacteria. The authors hypothesised that the observed enhanced growth of *D. piger* was due to both hydrogen production and the degradation of sulphur-containing host mucins by other members of the consortium, providing free sulphate and hydrogen for *D. piger*. This relationship was confirmed with *in vitro* cultures of *D. piger* and the mucin degrader *B. thetaiotaomicron*. Cultured on the supernatant of wild type *B. thetaiotaomicron* grown in medium supplemented with chondroitin sulphate (a sulphated glycan that cannot be metabolised by SRB), the SRB were able to grow and produce H_2S. However, using an engineered *B. thetaiotaomicron* strain unable to synthesise a certain sulfatase enzyme resulted in reduced overall SRB growth and sulphide production. Neither bacterium could release free sulphate from the chondroitin sulphate compound. Applying this to mucin in the colonic environment, *D. piger* grew better in mice associated with the wild type *B. thetaiotaomicron* than those harbouring the sulfatase mutant. This provides compelling evidence for cross-feeding by *D.*

piger on sulphate released by the mucin degradation of *B. thetaiotaomicron in vivo*. Moreover, additional sulphate supplemented to the diets of these mice showed little effect on *D. piger* growth, implying that it obtains enough sulphate from host secretions in the presence of the mucin degrader. It would be expected that in the bi-association including the *B. thetaiotaomicron* sulfatase mutant, supplementary sulphate would enhance the growth of *D. piger* only, but this scenario does not appear to have been investigated.

The lack of any published data regarding the direct *in vivo* or *in vitro* competition between all three hydrogenotrophic functional groups means that it is impossible to conclude which is likely to dominate in the colon. Moreover, the relatively inaccessible nature of the human colon means that direct measurement of hydrogen flux between members of the microbiota is difficult. One recently posed strategy for tracking hydrogen *in vitro* and *in vivo* is the use of stable isotope probing coupled with Raman spectroscopy to analyse the flux of labelled hydrogen (for a review, see Wang et al. (2016)). This technique has to date only been explored in a few experiments but has the potential to be an important tool in microbiota experimentation. Promise is also being shown by telemetric capsules, which can measure luminal gas concentrations throughout the GIT in real time (Berean et al., 2018). This technique will likely be applied for the study of colonic hydrogenotrophy and methane production in the future.

The current lack of experimental data on hydrogenotroph competition encourages the construction of an *in vivo* or culture-based model for such a combination. Alternatively, mathematical modelling could be used to make predictions of co-culture dynamics based on monoculture data, but any such approach would benefit from the construction of the experimental system for verification of model results. Although these data are currently unavailable, there exists a wealth of literature concerning the hydrogenotrophic population of human faecal samples, upon which many etiological hypotheses have been based.

2.7.5 The balance between hydrogenotrophic functional groups in the colon

There have been a number of studies, particularly over the past 30 years, which have attempted to ascertain the balance between the three hydrogenotrophic functional groups in the human microbiota. Most of these studies have relied upon analysis of faecal samples or faecal

cultures, coupled with breath-testing for hydrogen and methane. The results of breath tests are then used to classify individuals as methane positive or negative.

2.7.5.1 Evidence for mutual exclusivity of methanogens and SRB

Several observational studies suggested that methanogens and SRB were mutually exclusive, or nearly so, in the colon due to competition for hydrogen, the only mutual substrate of the two. Gibson et al. (1988c) studied two groups of 20 individuals from the UK and South Africa to determine the methanogenic and sulphate-reducing potential of each. Differences in the dominant functional group were found between the two locations, with most of the rural South Africans being predominantly methanogenic, whereas the UK cohort had higher levels of SRB in their faeces. In both sample groups, individuals who were methane producers rarely had SRB detected in their faeces, and those with high concentrations of SRB did not produce methane. However, enumeration of microbes was performed solely *via* culture-based methods in this work, and methane status was determined by breath testing, a technique that has been shown to give negative results in individuals who carry methanogens in low concentrations (Stewart et al., 2006), and therefore is inconclusive in determining the presence of methanogens in the colon (Dridi et al., 2009; Sahakian et al., 2010; Carbonero et al., 2012).

In a later assessment of 30 South African volunteers, cultured samples from methane-positive individuals were shown to have lower rates of both sulphate-reduction and acetogenesis than those from methane-negative individuals (Gibson et al., 1990). Further work by the same authors with a larger cohort of volunteers allowed for separation of individuals into three distinct classes: methanogenic with no SRB detected in faeces; methanogenic with low numbers of SRB detected in faeces; and non-methanogenic with high SRB counts in faeces (Gibson et al., 1993b). Of the 87 individuals tested in this later study, only nine were the second class, providing further evidence for the mostly mutually exclusive nature of SRB and methanogens.

At a similar time, (Macfarlane et al., 1992) found that the colonic contents of sudden death victims followed the same pattern, harbouring predominately either a methanogenic or a sulphate-reducing community. Although only two individuals were examined, the more complete examination

of the colonic microbiota possible in sudden death victims agreed with the classing of individuals proposed by Gibson et al. (1993b).

2.7.5.2 Evidence against mutual exclusivity of methanogens and SRB

There exist counter-examples to the mutual exclusivity hypothesis. Most of the volunteers in the cohort tested by Pochart et al. (1992) were shown to harbour both methanogens and SRB. Following a similar protocol to Gibson et al. (1988c), the volunteers were split into methane-excreting and non-excreting groups by means of breath-testing before faecal analysis was performed. All the methane-positive individuals harboured both methanogens and SRB, as did most of the methane-negative individuals. There were those individuals who had SRB but no methanogens in their samples, so the cohort could be divided in the manner of Gibson et al. (1993b), but with different proportions of the cohort in each class. The methanogen-free group was in the minority in this study, at 21%. The sample size of 19 was small, but this group later assayed another cohort of 19, and found no significant difference in SRB counts between individuals who excreted methane and those who did not (Doré et al., 1995). (El Oufir et al., 1996) found that, although SRB cell counts differed significantly between methane-positive and negative individuals in their study cohort, and negatively correlated with methanogen counts, every individual tested had detectable SRB in their faeces (at least 10^6 cells g^{-1}), regardless of methane excretor status. Suarez et al. (1997) found that methane and sulphide were both present in the flatus of their study subjects, giving further evidence against mutual exclusivity.

Such contrasting results from many separate studies indicate that there is potentially a complex pattern to hydrogenotroph colonisation that has not yet been clearly identified. The possibility that the varied conclusions from different investigations are influenced by the different geographic and ethnic backgrounds of the individuals studied cannot be discounted, as observed by Gibson et al. (1988c). More recent comparative analysis of microbiome data from a number of countries indeed found higher similarity in the microbiota composition of individuals from the same country than from different countries (Nishijima et al., 2016). In recent times, due to new evidence and the contradictory nature of previous data, the hypothesis of mutual exclusion has been discounted. No relationship between the presence or abundance of methanogens and SRB was

found by Hansen et al. (2011) when sequencing faecal samples from 68 sets of twins. However, they did find a relationship between the presence of methanogens and the abundance of several clusters within the Firmicutes phylum, which may be explained by the high hydrogen production of strains in these clusters, suggesting a further possible variable affecting hydrogenotroph colonisation.

2.7.5.3 Associations between hydrogenotrophs and other colonic variables

The work of Hansen et al. (2011) was not the first instance of positive associations between specific hydrogenotrophs and other microbial functional groups (MFGs) studied. In examining the earlier hypothesis that high methanogen counts were related to increased counts of cellulolytic bacteria (Robert et al., 2001), Chassard et al. (2010) sampled a larger group of volunteers and observed a positive relationship between the two. Although increased cellulolytic activity was not found on all cellulose sources, it was observed that methane-negative faecal samples tended to contain a greater proportion of Gram-negative bacteria, whereas methane positive samples were associated with more Gram-positive bacteria. This may be reflective of the greater hydrogen production by the Gram-positive Firmicutes, resulting in higher concentrations of available substrate for methanogens (Chassard et al., 2005). However, microbial isolation was performed in samples taken from only 7 of the 49 volunteers originally sampled (3 methane negative and 4 methane positive). Therefore, while there is evidence for some link between methanogen concentrations and the presence of the cellulolytic strains targeted by these authors, drawing a conclusion about a dominant cellulolytic phylum associated with methanogenesis requires a larger study. There was also no investigation on the effect of these cellulolytic bacteria on the other hydrogenotrophic functional groups. Correlations between functional groups observed in studies such as that of Hansen et al. (2011) ought to bring more culture-based studies of the kind performed by Chassard et al. (2010), to better understand the mechanism driving the positive association.

Separate to the relationship between SRB and methanogen colonisation, there may be an observable relationship between these functional groups and the acetogens. A negative correlation has been documented between acetogens and methanogens, implying that perhaps there exists some competition between these two functional groups, not necessarily involving SRB (Doré et al., 1995). Similar relationships between acetogen and methanogen abundance have been found

elsewhere (Lajoie et al., 1988; Bernalier et al., 1996a; Pitcher et al., 2000; Chassard et al., 2008). Recent microbiome data analysis of faecal samples from 106 Japanese individuals was unable to detect *M. smithii* in 92% of individuals (Nishijima et al., 2016). This constituted lower methanogen colonisation than was found in all eleven other countries considered in this study and was coupled with an increased abundance of members of the genus *Blautia*. SRB, by contrast, did not vary greatly between countries. Bernalier et al. (1996a) found that although SRB counts did not vary between the individuals tested in their experiment, mean acetogen counts were lower in individuals with high methanogen counts. Moreover, when methanogens were chemically inhibited in faecal cultures from methane-producing individuals, total acetate production by the culture was threefold greater than that of the original faecal culture. This implies that while the methanogens competed effectively for hydrogen, acetogens were always present in these samples, and converted hydrogen to acetate in detectable concentrations only in the absence of competition for hydrogen. This is consistent with the thermodynamic and threshold hydrogen concentration restrictions presented earlier.

Aside from the direct competition between functional groups, there may also be non-microbial factors that strongly influence the relative abundance of each group. El Oufir et al. (1996) found that treatment of volunteers with an antidiarrheal drug increased methanogen counts and decreased SRB counts in faeces, with the converse true during treatment with a laxative. Their findings point to a link between transit time and the predominant mechanism of hydrogen consumption. The observed slow growth rates of methanogens support the hypothesis that faster colonic transit negatively affects their population size (Khelaifia et al., 2013).

In considering the colonisation of the colon by hydrogenotrophs, spatial variables must also be considered, as environmental conditions are not uniform throughout the colon. An *in vitro* 3-stage model of the human colon was inoculated with a faecal slurry containing both methanogenic and SRB to analyse their *in situ* competition and the effect of endogenous mucins on this interaction (Gibson et al., 1988b). The three vessels were of different volumes, arranged in sequence and maintained at fixed pH levels. Methane production was consistently greater in the latter two vessels, representative of the transverse and distal colon, where the pH was higher (pH 6.5 and 7). However, once the continuous infusion of sulphated mucins to the model was initiated, methanogenesis was

inhibited. Sulphide production increased upon addition of mucins due to the increased availability of sulphate, most notably in the latter two vessels, where methanogenesis had been highest previously. Therefore, the availability of sulphated mucins in the colon will affect the dominance of SRB.

In contrast, a recent study of mice inoculated with *M. smithii* found that methanogen counts were highest in the small intestine, in disagreement with previous studies (Mathur et al., 2013). To add to the lack of consensus in the observed data, a study using biopsy samples to examine the population of hydrogenotrophs present in the colonic mucosa at various sites in 25 healthy individuals concluded that, although gene copies from each of the three hydrogenotrophic functional groups were present in every volunteer tested, there was no obvious pattern of spatial colonisation (Nava et al., 2012a). A further contrast with previous results was the finding that SRB gene copies were higher than those of acetogenic bacteria in the proximal colon, with the opposite found in the distal colon. Methanogenic genes showed the greatest variation between sites and individuals, from undetectable to 10^8 copies g^{-1}, with no clear pattern.

The contrasting results on the balance of hydrogenotrophs obtained in different experiments require better explanation. Although there is now irrefutable evidence to show that all three functional groups coexist in the human colon, competition for hydrogen is likely still a driving force in determining the relative population sizes of each group (Sahakian et al., 2010). Also, if an individual appears to harbour predominantly one hydrogenotroph at one sampling, this does not necessarily imply that the situation will remain so, as dominant functional groups have been shown to change over time (Strocchi et al., 1994a). The great influence of diet on hydrogenotroph population also cannot be ignored in this area of research. Changes in dietary sulphate, for example, have been shown to transiently alter both methanogen and SRB population sizes in the colon (Christl et al., 1992), an aspect that is not always included in the discussion of hydrogenotroph colonisation. Despite more than 35 years of research on hydrogenotrophs of the human colon, there is still an insufficient understanding of the underlying causes for both the spatial distribution and inter-individual differences of hydrogenotrophic colonisation in this environment. Without this knowledge, deriving the distribution of hydrogenotrophs most conducive to optimal nutrition and health remains a challenge.

2.8 The health implications of hydrogen in the colon

Hydrogen itself has been shown to have both beneficial and detrimental health impacts. The build-up of hydrogen gas is a source of discomfort in both adults and infants (Chassard et al., 2005; Pham et al., 2017). However, hydrogen gas can also be used as a therapeutic agent, particularly when administered in drinking water. Drinking of hydrogen-dissolved water has been shown to reduce oxidative stress via the removal of reactive oxygen species, with related effects such as reducing the symptoms of obesity, metabolic syndrome and Parkinson's disease (for reviews, see Ohta (2014) and Ostojic (2018)). Furthermore, hydrogen is a stable and safe molecule, making it an attractive treatment (Ohta, 2014). The fact that patients with Parkinson's disease have a lower abundance of hydrogen-producing bacteria in their faecal microbiota suggests some link between the hydrogen produced in the colon and the aetiology of this degenerative disease (Scheperjans et al., 2015; Ostojic, 2018). The removal of hydrogen by hydrogenotrophs contributes to the balance of hydrogen, which must be considered alongside the health impacts of the products of these cross-feeders.

2.8.1 Health impacts of hydrogen cross-feeding on the host

The products of hydrogen cross-feeding have been implicated in a variety of disease states, justifying the study of hydrogenotrophic microbes from a medical perspective. Lactate and hydrogen build-up in the GIT has been linked to colic symptoms in a study of 40 infants (Pham et al., 2017). Although it was difficult to obtain reliable information from their infant cohort study, mainly due to the difficulty in diagnosing colic and the variation in symptoms between individuals, the accompanying *in vitro* studies provide data on SRB in co-culture with hydrogen producers. Large volumes of hydrogen were produced by the prominent infant microbiota bacterium *Veillonella ratti* in monoculture, which the authors suggested contributed to discomfort. However, co-cultures of this hydrogen producer with the hydrogen utilising SRB *D. piger* resulted in reduced hydrogen concentrations. Any therapeutic reduction in hydrogen levels must be weighed up against the increased H_2S concentrations caused by the SRB. Whether a similar effect, without the production of H_2S, could be achieved by methanogens has not been investigated. Methanogens have been isolated

from both the gastric juice of newborns (Grine et al., 2017), and from infant faecal samples (Stewart et al., 2006; Dridi et al., 2009). It is thought that colonisation of the infant by *M. smithii* originates from the mother, potentially through breast-feeding. However, analysis of breastmilk from 20 women found archaeal sequences in only 8 (Jiménez et al., 2015), implying that inoculation from other sources may be responsible.

The study of hydrogenotrophs, and cross-feeding in general, in the infant colon is quite new. It is well-established that the infant microbiota is different to that of adults and shows significant interindividual variation (for a review, see Collado et al. (2012)), but current data on the relationship between SRB and methanogens in this environment, and any health impacts of this relationship, are not available.

Moving to the adult microbiome, H_2S and/or the SRB that produce it have been found at higher concentrations in patients suffering from IBS (King et al., 1998; Chassard et al., 2012), ulcerative colitis (Roediger et al., 1997; Pitcher et al., 2000; Khalil et al., 2014; although this could not be confirmed in all studies (Fite et al., 2004)) and CRC (Louis et al., 2014; Song and Chan, 2017). H_2S is also implicated in increased risk of DNA damage (Attene-Ramos et al., 2006; Attene-Ramos et al., 2010) and increased risk of developing CRC (Cai et al., 2010).

However, there are also are potentially health-promoting effects of H_2S, such as maintaining colonic mucous layer integrity (Motta et al., 2015) and a potential cardioprotective role (for a review, see Tomasova et al. (2016)). It should also be noted that H_2S is not exclusively produced by SRB. A variety of human cells, including GIT cells, also produce H_2S, predominantly as a signalling molecule, which is kept at or below micromolar concentrations *via* oxidation in the mitochondria (for a review, see Wallace and Wang (2015)). This oxidation contributes electrons to the electron transport chain, therefore both human and bacterially produced sulphide may also be an energy source for the host (Goubern et al., 2007). Furthermore, microbial fermentation of sulphur-containing amino acids, such as cysteine, can also lead to H_2S formation, and may, in some individuals, be a more significant source of sulphide than sulphate reduction (Yao et al., 2018).

Methane also has links to health issues, although the literature is sparser on this topic in comparison to H_2S. Higher methane production has been associated with constipation, including IBS-related constipation (IBS-C; Chatterjee et al., 2007; Furnari et al., 2012; Ghoshal et al., 2016; Wolf et

al., 2017) and increased GIT transit time (El Oufir et al., 1996). However, microbiome analysis has shown that the abundance of methanogens was lower in IBS individuals, particularly those with IBS-related constipation (Rajilić–Stojanović et al., 2011). These studies only show associations and not causality, and a consensus has not been reached on the role of methanogens in IBS (for reviews, see Chaudhary et al. (2018), Wolf et al. (2017) and Jalanka and Spiller (2017)). However, infusion of methane into the small intestinal lumen of dogs has been shown to increase transit time by affecting muscular motility (Pimentel et al., 2006) and methanogen counts have been shown to positively correlate with increased transit time (El Oufir et al., 1996). It is possible that a positive feedback loop may exist between increased transit time and increased methanogen counts, but this requires experimental validation.

A separate area that has received much attention is the role of methanogenesis in obesity (for a review, see Pimentel et al. (2013)). Turnbaugh et al. (2006) found that genetically obese mice harboured higher levels of methanogens than their lean litter mates. It was hypothesised that the uptake of hydrogen by methanogens improved the efficiency of carbohydrate metabolism by the microbiota, resulting in the observed increase in SCFA concentrations. Mice harbouring high concentrations of methanogens therefore received a greater energy yield from their diet, which was confirmed by the lower residual energy found in their faeces. This effect, due to the consumption of hydrogen in the GIT, may also result from the action of other hydrogenotrophs. Indeed, enzymes involved in reductive acetogenesis were enriched in genetically obese mice. The most impressive result of this study was the fact that lean mice, when inoculated with the microbiota of an obese littermate, showed significant weight gain with no greater chow consumption. However, methanogens were one of many functional groups that varied between the lean and obese microbiota. Further work with mice inoculated with methanogens has implicated a high-fat diet as a cause for increases in both faecal methanogen counts and bodyweight but does not provide evidence that methanogens are causative of obesity (Mathur et al., 2013).

Contrastingly, two large studies involving qPCR analysis of faeces from lean and obese humans showed depleted *M. smithii* counts in obese individuals, though did not pose direct mechanisms by which this species influences host adiposity (Schwiertz et al., 2010; Million et al., 2012). Moreover, a meta-analysis of 16S rRNA gene-based surveys of the colonic microbiota showed

that the *Methanobrevibacter* genus was negatively correlated with body mass index, but positively correlated with the abundance of *Christensenella*, a hydrogen producing genus (Ruaud et al., 2020). Co-culture studies revealed reduced butyrate production by *Christensenella* strains when *M. smithii* was present, leading to the authors' hypothesis that the presence of the methanogen resulted in less energy available to the host in the form of absorbed SCFAs. Due to the directly contrasting results of these studies, the impact of methanogenesis on obesity remains far from clear.

2.8.2 Mitigation of the harmful effects of hydrogen cross-feeding

There have been several attempts to counter the negative health effects related to hydrogen metabolism in the colon. The simplest interventions are dietary. Longer chain length prebiotics (substrates that are selectively utilized by host microorganisms conferring a health benefit (Gibson et al., 2017)) have been shown to produce less gases and at a reduced rate in *in vitro* faecal cultures compared to short chain prebiotics (Hernot et al., 2009). Moreover, faecal cultures grown with prebiotics such as resistant starch and FOS showed reduced H_2S generation (Yao et al., 2018).

If methane reduction in humans becomes a desirable health outcome, then full advantage should also be taken of the results of studies conducted towards lessening the environmental impact of agriculture through reducing methane emissions from ruminants. Knapp et al. (2014) reviewed a number of methane-reducing techniques applied in the dairy industry, such as: increasing starch intake in the diet, which may shift microbial fermentation in the rumen towards a higher propionate production, thus reducing the hydrogen available to methanogens; decreasing the passage time through the GIT, thus inhibiting methanogen population growth; and biological controls such as immunisation, which directly target methanogens. Supplementing the diets of methanogen-positive humans with additional sulphate has been shown to reduce methanogenesis in half of the individuals tested, although whether this effect would last longer than the 10 days of the study was not investigated (Christl et al., 1992). There have also been experiments in which acetogens have been used to reduce the formation of methane in the rumen or *in vitro*, but with limited success (Lopez et al., 1999; Morgavi et al., 2010). Whether such techniques will be necessary or effective in humans is yet to be determined.

Methanogenesis and sulphate reduction both have links to negative health outcomes, making acetogenesis appear the more attractive way to dispose of enteric hydrogen. The formation of acetate from free hydrogen constitutes a more energy efficient metabolic pathway for the host, as acetate may be absorbed into the bloodstream and used as an energy source (Morrison and Preston, 2016). Study of the kangaroo foregut, which bears similarity to the rumen, has shown that reductive acetogenesis can prevail over methanogenesis, despite its thermodynamic deficiency (Godwin et al., 2014). Methane production by the kangaroo microbiota in both *in situ* assays using stable isotope probing and *in vitro* fermentations was minimal, while abundant incorporation of CO_2 into acetate was also shown. Several differences exist between the bovine and kangaroo microbiota, but of note is that the acetogen *Blautia coccoides* was found in samples from all kangaroos tested, whereas only 40% of bovine samples contained this bacterium, and at a lower mean abundance. Acetogens can clearly perform the role of principal hydrogen consumer effectively and have also been shown to be a viable replacement for methanogens in the lamb rumen (Fonty et al., 2007). However, the mechanism by which methanogenesis is repressed in the kangaroo is unclear and no efficient mechanism for continued methanogen control in the rumen is currently available (Patra et al., 2017).

Although this means that human nutrition cannot immediately benefit from animal research, cooperation between researchers on microbial hydrogen cross-feeding in the human and animal fields should be encouraged, as similar challenges and questions are faced by each. The motivation for study may differ between the two, with human health the focus of one and methane emission reduction often the goal of the other, but it can be expected that progress in one will aid progress in the other.

The research thus far reviewed in this chapter has predominantly been experimental rather than computational in nature. While several small-scale mathematical models from the evolutionary and cross-feeding literature were discussed, large-scale models for the colonic microbial community are reviewed and compared next.

2.9 Mathematical modelling of the human colonic microbiota

Several mathematical models for the colonic microbiome have been developed over the last ten years, which can usually be divided by the nature of the approach. Bottom-up approaches utilise detailed information on individual microbial strains, often from genomic data, and combine these to form complex models. Top-down approaches on the other hand make overarching assumptions about the microbiome, with model complexity introduced via assigning of specific functions to subsets of the microbiota. Table 2.2 gives an overview of selected models of both types, which are reviewed in more detail in this section.

An increasingly common bottom-up technique for modelling the metabolism of both individual microbes and communities is known as constraint-based reconstruction and analysis (COBRA). This technique involves using genomic data to reconstruct the metabolic pathways available to an organism, before associating rate terms to each step in the pathway and running simulations in which flux along every available pathway is modelled, subject to some optimisation objective (often the maximising of biomass; (Magnúsdóttir and Thiele, 2018)). Hundreds of such reconstructions now exist for human colonic strains, as well as community-level models for the colonic microbiota.

An example COBRA model is BacArena (Bauer et al., 2017). This R tool is applicable to any number of environments and populations, taking genome reconstructions for microbes as its input and running a spatial and temporal flux balance analysis (FBA) simulation of community dynamics. The original authors applied it to the colon using a seven-member representative consortium and investigated the role of host glycan secretion on the population near the mucous layer. They observed that the *Bacteroides* representative dominated near the epithelium upon addition of the mucous glycans, with a more balanced population present further from the glycan source.

Van Hoek and Merks (2017) presented a similar model, but instead of using representative strains for their colon model, they instead designed a supra-organism: one with the metabolic capability covering the most common colonic microbial pathways, focussed on glucose and glucose breakdown product metabolism. Each individual microbe in the cellular automaton model then had a random subset of these pathways available to it, with this subset able to change over time. What

emerged was a population that fed independently on glucose (the sole added substrate) in the proximal colon, but became increasingly reliant on cross-feeding distally, due to increased concentrations of secondary metabolites in this region. While this was an intuitive result, it is unclear how well it correlates with the observed microbiota distribution in the colon, and such a comparison is difficult to draw given the lack of matching between the modelled organisms and living taxa.

A great step forward in the application of these COBRA-based models has recently been developed by Heinken and Thiele (2019). These authors created personalised community models for the microbiota of each individual in an IBD cohort. They used these models to predict the metabolic dynamics of the microbiota with validation against metabolomic data. The use of personalised models using genome-based reconstructions could have many benefits, including use in diagnosis and understanding of diseases, as investigated by these authors, but also in the field of personalised nutrition, guiding dietary information specific to an individual's microbiota. However, these personalised models do not yet allow for general conclusions to be made about microbiota behaviour under differing non-dietary conditions, such as host factors. Moreover, the bottom-up approach requires extensive data sets for metabolic reconstructions and are usually computationally intensive due to the number of variables included. A top-down approach avoids these difficulties by being more general, at the expense of making less realistic representations of the microbiome.

The more coarse-grained top-down methods for modelling the colonic microbiota require less in the way of large genomic data sets and rely instead on assumptions about the overall capabilities of microbial strains, utilising rate parameters taken from culture observations. Many such models cite the Anaerobic Digestion Model No. 1 (ADM1; Batstone et al., 2002) as their basis, which was originally developed for the simulation of industrial anaerobic reactors, but easily repurposed to the anaerobic environment of the colon. The ADM1-based model of Muñoz-Tamayo et al. (2010) represented the colonic microbiome using three sequential compartments, four functional groups, ten dissolved metabolites and three gaseous metabolites. The strength of this model was its consideration of the mucous layer and gaseous phase, but the metabolic pathways modelled were less diverse than those of other community models, and pH was held fixed in each compartment.

This model was recently unified with the peristaltic movement modelling work of Cremer et al. (2017) by Labarthe et al. (2019). The result was a comprehensive but computationally taxing model, allowing an even greater range of influencing factors on the colon to be varied. An important prediction of the model was that the inclusion of microbial active swimming, even at low rates compared to colonic transit speed, significantly affected the population structure. The major difficulty cited by the authors was in finding suitable data for validation, due to the simple nature of the four-member community used and the need for invasive measurements of the living colon for comparison to the spatial aspects of their model.

Greater diversity in microbes and metabolic pathways was present in the model of Motelica-Wagenaar et al. (2014). This model was developed for the proximal colon only. The model included ten MFGs and was parameterised using results of the *in vitro* TNO Intestinal Model 2 (TIM-2; Venema, 2015), before validation against data from a separate TIM-2 experiment. Greater consideration of protein degradation and breakdown products was included, and again transfer between the aqueous and gaseous phases was modelled. Since the TIM-2 model included a dialysis membrane to simulate metabolite absorption, the *in silico* model also featured a concentration-dependent absorption term for several metabolites, including SCFAs. These authors tackled the difficulty of an uncertain proximal colonic microbiota by evenly distributing the initial microbial biomass across the ten functional groups, and observed washout of several at physiological dilution rates. Notably, the methanogen and acetogen functional groups were among the first to be lost as the dilution rate was increased, and only one of these groups could survive in the model in any one simulation. SRB were not included in the model.

Also including ten MFGs but applied to faecal culture data, the versatile microbial community modelling tool microPop could easily be applied to the colon (Kettle et al., 2017). This model builds on the structure of a previous faecal culture model (Kettle et al., 2015) and ten functional groups are involved in the degradation or production of 17 metabolites. The model gave accurate results when applied to faecal culture data, but, as is common to all the models discussed here, was not focussed on hydrogen cross-feeding. Similarly to Motelica-Wagenaar et al. (2014), methanogens and acetogens were included, but SRB were not. However, microPop was designed to

be easily adapted for other populations and environments, so future iterations of the model could put greater emphasis on hydrogenotrophs.

The models reviewed here represent the principal contributions to colonic microbiome research from a mathematical modelling perspective. Other models which consider smaller subsets of the microbiome or were similar predecessors to the discussed models were omitted from the discussion, but were recently reviewed by Magnúsdóttir and Thiele (2018) for COBRA-based approaches and by Widder et al. (2016) for microbial communities in general. While the existing models are important tools for microbiome research, insufficient modelling study of hydrogenotrophs in the colon has thus far been performed. Each of the existing models could be used as a basis to address this gap in the modelling literature.

Table 2.2. Summary of selected mathematical models for the colonic microbiome			
Publication (model name)	**No. of MFGs/strains**	**No. of metabolites**	**Key features**
Muñoz-Tamayo et al. (2010)	4	13	Lumen, mucous and gaseous compartments for three colonic sections
Motelica-Wagenaar et al. (2014)	10	24	Proximal colon only, adaptation of Muñoz-Tamayo et al. (2010) Parameterised from *in vitro* model data Impact of transit time, feed, pH, presence of methanogens investigated
Moorthy et al. (2015)	4 (multiple strains within microbial functional group)	10	One-dimensional spatially continuous adaptation of Muñoz-Tamayo et al. (2010) Only carbohydrate substrates considered No gaseous phase Varied transit times, fibre intakes and number of strains in the primary degrader MFG investigated
Bauer et al. (2017) (BacArena)	7	50+	Two-dimensional cellular automaton COBRA model Includes cellular motility and mucin layer
van Hoek and Merks (2017)	Single supra-organism used	50+	Two-dimensional cellular automaton COBRA model Evolutionary component of metabolic pathway gain/loss No specific MFGs, rather organisms with widely varied metabolic capabilities Varied transit times investigated
Cremer et al. (2017)	2	7	One-dimensional mechanistic model Includes relationship between short chain fatty acid production, pH and microbial growth Models water absorption and peristaltic movement of the colon wall
Kettle et al. (2017) (microPop)	10	17	Protein included Sequential compartments Easily adapted
Labarthe et al. (2019)	4	12	A unification of Muñoz-Tamayo et al. (2010) with Cremer et al. (2017), also including microbial active motion Diet, mucous, chemotaxis and peristalsis variations investigated
COBRA: constraint-based reconstruction and analysis. MFG: microbial functional group.			

2.10 Future directions for colonic hydrogenotroph research

Although many studies of microbial cross-feeding leading to the production of SCFAs have been published, few have considered the impact of hydrogen removal by hydrogenotrophic cross-feeders. It is unclear whether different results may have been obtained in these experiments if a hydrogenotrophic microbe had been included. In some cases, SCFA production may have increased, due to the beneficial action of reducing the partial pressure of hydrogen performed by hydrogenotrophs. However, it is possible that the relationship would be more complex. It is conceivable, for example, that the inclusion of an SRB in an SCFA cross-feeding experiment may result in competitive cross-feeding for intermediates such as lactate, resulting in reduced SCFA yields, as observed by Marquet et al. (2009). The versatile nature of many hydrogenotrophic strains makes prediction of the outcome of such cultures difficult. However, existing data from separate experiments could be combined into a predictive model, to give structured analytical validation to predictions.

The clear impacts of hydrogen cross-feeding on human health and nutrition should lead to further investigation of colonic hydrogenotrophs. The effect of both hydrogen and its subsequent metabolites on areas such as digestive discomfort in infants, functional GIT disorders in adults, and energy yield from food, are not well understood. The first step in the greater understanding of these effects is to ascertain how the three functional groups behave in co-culture, and in the wider community of the microbiota.

2.11 Conclusions

In this chapter, the literature covering several aspects of microbial cross-feeding as it pertains to the human colon has been reviewed. The need for clear definitions for use in the discussion of cross-feeding has been justified and fulfilled with a set of four classifications for these interactions. These classifications allowed the literature on the evolution of cross-feeding to be subdivided according to the type of interaction studied, and the resilience of these cross-feeding types to change, both in the colon and other environments, was considered.

It is also important to consider what role cross-feeding plays in the wider field of microbial interactions. Recent genome-scale metabolic modelling of 800 bacterial communities, drawn from a variety of natural environments including the colon, analysed the metabolic relationships within each (Zelezniak et al., 2015). Competitive interactions dominated these relationships, but significant signs of metabolic dependencies and cross-feeding were also present. Evidence also exists for widespread auxotrophy across many bacterial environments (D'Souza and Kost, 2016). The implication of cross-feeding is clear, but competition should be accepted as the dominant form of interaction between microbes in any environment (Foster and Bell, 2012; Pacheco et al., 2019). Moreover, all examples of augmented cross-feeding discussed in this review were artificially induced, not involving naturally occurring interactions. There is doubt as to the existence of naturally occurring microbial relationships that satisfy the definition stated here for augmented cross-feeding, and any empirical evidence for it should be rigorously examined with the aid of mathematical modelling to ascertain the true mechanism behind observed data.

Moving to relationships specific to the colon, the commonly studied routes to SCFA production, often reliant on cross-feeding, have been described. Those leading to butyrate production have attracted the most attention in the literature to date due to the widely accepted health benefits associated with this molecule. These organic acids are mostly produced in the colon from carbohydrate substrates, with concomitant release of hydrogen, which itself is a cross-feeding substrate for hydrogenotrophic members of the microbiota. These lesser studied organisms were the subject of the latter sections of this chapter, and there remain several unanswered questions around the benefits, harms and distribution of hydrogenotrophs in each individual.

Throughout this chapter, the important role for computational approaches such as mathematical modelling in the study of microbial interactions has been highlighted. The remainder of this thesis is focussed on the greater understanding of the hydrogenotrophic microbes of the colon using a mathematical modelling approach.

2.12 Aims of the thesis

It is clear from the review of the literature that many questions remain around the nature of individual microbial cross-feeding relationships and their importance to the microbiome. The

evidence that these relationships influence human health and wellbeing makes answering these questions even more urgent. The review of the literature established that several types of cross-feeding relationships exist, each of which must be understood at an individual level. The research in this thesis seeks to better understand the metabolism and cross-feeding relationships of the hydrogenotrophic microbes of the human colon both at an individual level and as part of the wider microbiome.

Understanding the role of hydrogenotrophs as members of the colonic microbiota requires detailed knowledge of these microbes at the monoculture level. Therefore, the first goal of this thesis was to develop monoculture mathematical models for the growth and hydrogenotrophic metabolism of each of the three major hydrogenotrophic functional groups of the human colon. These were to be dynamic models parameterised from experimental data, including the major substrates and products of hydrogenotrophic metabolism, as well as resultant population growth over time. These deterministic models were chosen as they were well-suited to the available data and readily comparable to existing models in the literature.

Chapters 3, 4 and 5 detail the development of these monoculture models for the three major hydrogenotrophic functional groups of the colon, namely the methanogens, SRB and acetogens, respectively. In Chapter 3, the ability of several growth models to capture methanogen data was compared. In Chapter 4, a Monod model for SRB dynamics was developed and compared with an existing, more complex model in the literature. In Chapter 5, multiple modelling techniques were compared, in this instance to capture the dynamics of reductive acetogen growth and metabolism. The model was then used to investigate the suitability of two experimental growth media for the production of acetate from hydrogen by an acetogenic strain.

The second goal of this thesis was to provide information on the relative capabilities of each hydrogenotroph in metabolising hydrogen and their interactions with one another. Therefore, the monoculture modes were combined into co- and tri-culture models. Firstly, in Chapter 6, the ability of a combined methanogen and SRB model to reproduce experimentally observed co-culture dynamics was evaluated. The model was used to identify key parameter values that changed between monoculture and co-culture. In Chapter 7, all three monoculture models were combined

into a tri-culture model, which was then assessed both analytically and computationally to establish conditions necessary for the survival of each hydrogenotroph.

The final goal of the thesis was to investigate hydrogenotroph growth and metabolism in the colon. To address this, the monoculture models were included in an existing model for the dynamics of the human colonic microbiota, microPop (Kettle et al., 2017) in Chapter 8. Further additions were made to the existing microbiota model to better reflect the colonic environment, and the predictive capabilities of the model were tested against experimental data. Finally, the model was used to investigate the role of colonic sulphate availability on the relative abundance of the three hydrogenotrophs. It is hoped that this model will be used in the future as a tool to complement experimental work by aiding in the design and analysis of *in vitro* experimentation.

A summary and discussion of the important results presented in this thesis is given in Chapter 9.

	Chapter 1	General introduction
	Chapter 2	Literature review
Research chapters	Chapter 3	Methanogen model • Investigation of suitable models for *Methanobrevibacter smithii* dynamics • Validation against experimental data
	Chapter 4	Sulphate-reducing bacteria (SRB) model • Development of model for *Desulfovibrio vulgaris* dynamics • Validation against experimental data • Comparison to an existing *D. vulgaris* model
	Chapter 5	Acetogen model • Investigation of suitable model for *Blautia hydrogenotrophica* dynamics • Validation against experimental data • Application to *B. hydrogenotrophica* growth in differing media
	Chapter 6	Co-culture model for methanogen and SRB • Combination of *M. smithii* and *D. vulgaris* models • Analysis of metabolic parameter changes in co-culture using experimental data
	Chapter 7	Tri-culture hydrogenotroph model • Combination of all three monoculture models • Analytical and numerical investigation into survival conditions for each hydrogenotroph
	Chapter 8	Microbial community and colon models • Incorporation of all three monoculture models into existing microbial community model • Development of colon model • Comparison to experimental data sets • Investigation into the role of sulphate availability on colonic hydrogenotroph population
	Chapter 9	General discussion

Figure 2.9. Overview of the thesis structure.

References

Abell, G.C.J., Conlon, M.A., and McOrist, A.L. (2006). Methanogenic archaea in adult human faecal samples are inversely related to butyrate concentration. Microb. Ecol. Health Dis. 18(3-4), 154-160. doi: 10.1080/08910600601048969.

Allen, R.C., McNally, L., Popat, R., and Brown, S.P. (2016). Quorum sensing protects bacterial co-operation from exploitation by cheats. ISME J. 10(7), 1706-1716. doi: 10.1038/ismej.2015.232.

Amaretti, A., Bernardi, T., Tamburini, E., Zanoni, S., Lomma, M., Matteuzzi, D., et al. (2007). Kinetics and metabolism of *Bifidobacterium adolescentis* MB 239 growing on glucose, galactose, lactose, and galactooligosaccharides. Appl. Environ. Microbiol. 73(11), 3637-3644. doi: 10.1128/aem.02914-06.

Arumugam, M., Raes, J., Pelletier, E., Le Paslier, D., Yamada, T., Mende, D.R., et al. (2011). Enterotypes of the human gut microbiome. Nature 473(7346), 174-180. doi: 10.1038/nature09944.

Attene-Ramos, M.S., Nava, G.M., Muellner, M.G., Wagner, E.D., Plewa, M.J., and Gaskins, H.R. (2010). DNA damage and toxicogenomic analyses of hydrogen sulfide in human intestinal epithelial FHs 74 Int cells. Environ. Mol. Mutag. 51(4), 304-314. doi: 10.1002/em.20546.

Attene-Ramos, M.S., Wagner, E.D., Plewa, M.J., and Gaskins, H.R. (2006). Evidence That Hydrogen Sulfide Is a Genotoxic Agent. Mol. Cancer Res. 4(1), 9.

Axelrod, R., and Hamilton, W.D. (1981). The evolution of cooperation. Science 212(4489), 1390-1396.

Bäckhed, F., Ley, R.E., Sonnenburg, J.L., Peterson, D.A., and Gordon, J.I. (2005). Host-bacterial mutualism in the human intestine. Science 307(5717), 1915-1920. doi: 10.1126/science.1104816.

Barton, L.L., and Fauque, G.D. (2009). "Biochemistry, Physiology and Biotechnology of Sulfate-Reducing Bacteria," in Adv. Appl. Microbiol.: Academic Press, 41-98.

Bartosch, S., Fite, A., Macfarlane, G.T., and McMurdo, M.E.T. (2004). Characterization of Bacterial Communities in Feces from Healthy Elderly Volunteers and Hospitalized Elderly Patients by Using Real-Time PCR and Effects of Antibiotic Treatment on the Fecal Microbiota. Appl. Environ. Microbiol. 70(6), 3575. doi: 10.1128/AEM.70.6.3575-3581.2004.

Batstone, D.J., Keller, J., Angelidaki, I., Kalyuzhnyi, S.V., Pavlostathis, S.G., Rozzi, A., et al. (2002). The IWA Anaerobic Digestion Model No 1 (ADM1). Water Sci. Technol. 45(10), 65-73.

Bauer, E., Zimmermann, J., Baldini, F., Thiele, I., and Kaleta, C. (2017). BacArena: Individual-based metabolic modeling of heterogeneous microbes in complex communities. PLoS Comp. Biol. 13(5). doi: 10.1371/journal.pcbi.1005544.

Belenguer, A., Duncan, S.H., Calder, A.G., Holtrop, G., Louis, P., Lobley, G.E., et al. (2006). Two routes of metabolic cross-feeding between *Bifidobacterium adolescentis* and butyrate-producing anaerobes from the human gut. Appl. Environ. Microbiol. 72(5), 3593-3599. doi: 10.1128/aem.72.5.3593-3599.2006.

Belenguer, A., Duncan, S.H., Holtrop, G., Anderson, S.E., Lobley, G.E., and Flint, H.J. (2007). Impact of pH on lactate formation and utilization by human fecal microbial communities. Appl. Environ. Microbiol. 73(20), 6526-6533. doi: 10.1128/aem.00508-07.

Belenguer, A., Duncan, S.H., Holtrop, G., Flint, H.J., and Lobley, G.E. (2008). Quantitative analysis of microbial metabolism in the human large intestine. Curr. Nutr. Food Sci. 4(2), 109-126. doi: 10.2174/157340108784245957.

Belenguer, A., Holtrop, G., Duncan, S.H., Anderson, S.E., Calder, A.G., Flint, H.J., et al. (2011). Rates of production and utilization of lactate by microbial communities from the human colon. FEMS Microbiol. Ecol. 77(1), 107-119. doi: 10.1111/j.1574-6941.2011.01086.x.

Berean, K.J., Ha, N., Ou, J.Z., Chrimes, A.F., Grando, D., Yao, C.K., et al. (2018). The safety and sensitivity of a telemetric capsule to monitor gastrointestinal hydrogen production in vivo in healthy subjects: a pilot trial comparison to concurrent breath analysis. Aliment. Pharmacol. Ther. 48(6), 646-654. doi: 10.1111/apt.14923.

Bernalier, A., Lelait, M., Rochet, V., Grivet, J.P., Gibson, G.R., and Durand, M. (1996a). Acetogenesis from H2 and CO2 by methane- and non-methane-producing human colonic bacterial communities. FEMS Microbiol. Ecol. 19(3), 193-202. doi: 10.1016/0168-6496(96)00004-9.

Bernalier, A., Willems, A., Leclerc, M., Rochet, V., and Collins, M.D. (1996b). *Ruminococcus hydrogenotrophicus* sp. nov., a new H2/CO2-utilizing acetogenic bacterium isolated from human feces. Arch. Microbiol. 166(3), 176-183. doi: 10.1007/s002030050373.

Bervoets, L., Van Hoorenbeeck, K., Kortleven, I., Van Noten, C., Hens, N., Vael, C., et al. (2013). Differences in gut microbiota composition between obese and lean children: A cross-sectional study. Gut Pathog. 5(1). doi: 10.1186/1757-4749-5-10.

Bull, J.J., and Harcombe, W.R. (2009). Population dynamics constrain the cooperative evolution of cross-feeding. PLoS ONE 4(1), e4115. doi: 10.1371/journal.pone.0004115.

Bull, J.J., and Rice, W.R. (1991). Distinguishing mechanisms for the evolution of co-operation. J. Theor. Biol. 149(1), 63-74. doi: https://doi.org/10.1016/S0022-5193(05)80072-4.

Cai, W.-J., Wang, M.-J., Ju, L.-H., Wang, C., and Zhu, Y.-C. (2010). Hydrogen sulfide induces human colon cancer cell proliferation: Role of Akt, ERK and p21. Cell Biol. Int. 34(6), 565-572. doi: 10.1042/CBI20090368.

Cani, P.D. (2018). Human gut microbiome: hopes, threats and promises. Gut 67(9), 1716. doi: 10.1136/gutjnl-2018-316723.

Carbonero, F., Benefiel, A.C., and Gaskins, H.R. (2012). Contributions of the microbial hydrogen economy to colonic homeostasis. Nat. Rev. Gastroenterol. Hepatol. 9, 504. doi: 10.1038/nrgastro.2012.85.

Cerdó, T., Ruiz, A., Jáuregui, R., Azaryah, H., Torres-Espínola, F.J., García-Valdés, L., et al. (2017). Maternal obesity is associated with gut microbial metabolic potential in offspring during infancy. J. Physiol. Biochem., 1-11. doi: 10.1007/s13105-017-0577-x.

Chassard, C., and Bernalier-Donadille, A. (2006). H2 and acetate transfers during xylan fermentation between a butyrate-producing xylanolytic species and hydrogenotrophic microorganisms from the human gut. FEMS Microbiol. Lett. 254(1), 116-122. doi: 10.1111/j.1574-6968.2005.00016.x.

Chassard, C., Dapoigny, M., Scott, K.P., Crouzet, L., Del'Homme, C., Marquet, P., et al. (2012). Functional dysbiosis within the gut microbiota of patients with constipated-irritable bowel syndrome. Aliment. Pharmacol. Ther. 35(7), 828-838. doi: 10.1111/j.1365-2036.2012.05007.x.

Chassard, C., Delmas, E., Robert, C., and Bernalier-Donadille, A. (2010). The cellulose-degrading microbial community of the human gut varies according to the presence or absence of methanogens. FEMS Microbiol. Ecol. 74(1), 205-213. doi: 10.1111/j.1574-6941.2010.00941.x.

Chassard, C., Gaillard-Martinie, B., and Bernalier-Donadille, A. (2005). Interaction between H2-producing and non-H2-producing cellulolytic bacteria from the human colon. FEMS Microbiol. Lett. 242(2), 339-344. doi: 10.1016/j.femsle.2004.11.029.

Chassard, C., Scott, K.P., Marquet, P., Martin, J.C., Del'homme, C., Dapoigny, M., et al. (2008). Assessment of metabolic diversity within the intestinal microbiota from healthy humans using combined molecular and cultural approaches. FEMS Microbiol. Ecol. 66(3), 496-504. doi: 10.1111/j.1574-6941.2008.00595.x.

Chatterjee, S., Park, S., Low, K., Kong, Y., and Pimentel, M. (2007). The Degree of Breath Methane Production in IBS Correlates With the Severity of Constipation. Am. J. Gastroenterol. 102, 837. doi: 10.1111/j.1572-0241.2007.01072.x.

Chaudhary, P.P., Conway, P.L., and Schlundt, J. (2018). Methanogens in humans: potentially beneficial or harmful for health. Appl. Microbiol. Biotechnol. 102(7), 3095-3104. doi: 10.1007/s00253-018-8871-2.

Cho, I., and Blaser, M.J. (2012). The human microbiome: at the interface of health and disease. Nat. Rev. Genet. 13, 260-270.

Christl, S.U., Gibson, G.R., and Cummings, J.H. (1992). Role of dietary sulphate in the regulation of methanogenesis in the human large intestine. Gut 33(9), 1234-1238.

Chung, W.S.F., Walker, A.W., Louis, P., Parkhill, J., Vermeiren, J., Bosscher, D., et al. (2016). Modulation of the human gut microbiota by dietary fibres occurs at the species level. BMC Biol. 14(1). doi: 10.1186/s12915-015-0224-3.

Clausen, M.R., and Mortensen, P.B. (1995). Kinetic studies on colonocyte metabolism of short chain fatty acids and glucose in ulcerative colitis. Gut 37(5), 684-689.

Cockburn, D.W., and Koropatkin, N.M. (2016). Polysaccharide Degradation by the Intestinal Microbiota and Its Influence on Human Health and Disease. J. Mol. Biol. 428(16), 3230-3252. doi: 10.1016/j.jmb.2016.06.021.

Collado, M.C., Cernada, M., Baüerl, C., Vento, M., and Pérez-Martínez, G. (2012). Microbial ecology and host-microbiota interactions during early life stages. Gut Microbes 3(4).

Connor, R.C. (1995). The Benefits of Mutualism: A Conceptual Framework. Biol. Rev. 70(3), 427-457. doi: 10.1111/j.1469-185X.1995.tb01196.x.

Coyte, K.Z., Schluter, J., and Foster, K.R. (2015). The ecology of the microbiome: Networks, competition, and stability. Science 350(6261), 663.

Cremer, J., Arnoldini, M., and Hwa, T. (2017). Effect of water flow and chemical environment on microbiota growth and composition in the human colon. P. Natl. Acad. Sci. USA 114(25), 6438.

Cummings, J.H., and Macfarlane, G.T. (1991). The control and consequences of bacterial fermentation in the human colon. J. Appl. Bacteriol. 70(6), 443-459. doi: 10.1111/j.1365-2672.1991.tb02739.x.

Cummings, J.H., Pomare, E.W., Branch, H.W.J., Naylor, C.P.E., and MacFarlane, G.T. (1987). Short chain fatty acids in human large intestine, portal, hepatic and venous blood. Gut 28(10), 1221-1227. doi: 10.1136/gut.28.10.1221.

D'Souza, G., and Kost, C. (2016). Experimental Evolution of Metabolic Dependency in Bacteria. PLoS Genet. 12(11), e1006364. doi: 10.1371/journal.pgen.1006364.

D'Souza, G., Waschina, S., Pande, S., Bohl, K., Kaleta, C., and Kost, C. (2014). Less is more: Selective advantages can explain the prevalent loss of biosynthetic genes in bacteria. Evolution 68(9), 2559-2570. doi: 10.1111/evo.12468.

da Silva, S.M., Voordouw, J., Leitão, C., Martins, M., Voordouw, G., and Pereira, I.A.C. (2013). Function of formate dehydrogenases in *Desulfovibrio vulgaris* Hildenborough energy metabolism. Microbiology (UK) 159(8), 1760-1769. doi: 10.1099/mic.0.067868-0.

Damore, J.A., and Gore, J. (2012). Understanding microbial cooperation. J. Theor. Biol. 299, 31-41. doi: 10.1016/j.jtbi.2011.03.008.

Darwin, C. (1859). The Origin of Species. John Murray, London.

David, L.A., Maurice, C.F., Carmody, R.N., Gootenberg, D.B., Button, J.E., Wolfe, B.E., et al. (2014). Diet rapidly and reproducibly alters the human gut microbiome. Nature 505(7484), 559-563. doi: 10.1038/nature12820.

De Mazancourt, C., Loreau, M., and Dieckmann, U.L.F. (2005). Understanding mutualism when there is adaptation to the partner. J. Ecol. 93(2), 305-314. doi: 10.1111/j.0022-0477.2004.00952.x.

De Vuyst, L., and Leroy, F. (2011). Cross-feeding between bifidobacteria and butyrate-producing colon bacteria explains bifdobacterial competitiveness, butyrate production, and gas production. Int. J. Food Microbiol. 149(1), 73-80. doi: 10.1016/j.ijfoodmicro.2011.03.003.

den Besten, G., Lange, K., Havinga, R., van Dijk, T.H., Gerding, A., van Eunen, K., et al. (2013). Gut-derived short-chain fatty acids are vividly assimilated into host carbohydrates and lipids. Am. J. Physiol. Gastrointest. Liver Physiol. 305(12), G900-G910. doi: 10.1152/ajpgi.00265.2013.

Doebeli, M. (2002). A model for the evolutionary dynamics of cross-feeding polymorphisms in microorganisms. Popul. Ecol. 44(2), 59-70. doi: 10.1007/s101440200008.

Doebeli, M., and Knowlton, N. (1998). The evolution of interspecific mutualisms. Proc. Natl. Acad. Sci. USA 95(15), 8676-8680.

Donohoe, D.R., Collins, L.B., Wali, A., Bigler, R., Sun, W., and Bultman, S.J. (2012). The Warburg Effect Dictates the Mechanism of Butyrate Mediated Histone Acetylation and Cell Proliferation. Mol. Cell 48(4), 612-626. doi: 10.1016/j.molcel.2012.08.033.

Doré, J., Pochart, P., Bernalier, A., Goderel, I., Morvan, B., and Rambaud, J.C. (1995). Enumeration of H2-utilizing methanogenic archaea, acetogenic and sulfate-reducing bacteria from human feces. FEMS Microbiol. Ecol. 17(4), 279-284. doi: 10.1016/0168-6496(95)00033-7.

Douglas, S.M., Chubiz, L.M., Harcombe, W.R., and Marx, C.J. (2017). Identification of the potentiating mutations and synergistic epistasis that enabled the evolution of inter-species cooperation. PLoS ONE 12(5), e0174345. doi: 10.1371/journal.pone.0174345.

Douglas, S.M., Chubiz, L.M., Harcombe, W.R., Ytreberg, F.M., and Marx, C.J. (2016). Parallel mutations result in a wide range of cooperation and community consequences in a two-

species bacterial consortium. PLoS ONE 11(9), e0161837. doi: 10.1371/journal.pone.0161837.
Drake, H.L. (1994). "Acetogenesis, Acetogenic Bacteria, and the Acetyl-CoA "Wood/Ljungdahl" Pathway: Past and Current Perspectives," in Acetogenesis, ed. H.L. Drake. (Boston, MA: Springer US), 3-60.
Dridi, B., Henry, M., El Khéchine, A., Raoult, D., and Drancourt, M. (2009). High Prevalence of *Methanobrevibacter smithii* and *Methanosphaera stadtmanae* Detected in the Human Gut Using an Improved DNA Detection Protocol. PLoS ONE 4(9), e7063. doi: 10.1371/journal.pone.0007063.
Duncan, S.H., Barcenilla, A., Stewart, C.S., Pryde, S.E., and Flint, H.J. (2002). Acetate utilization and butyryl coenzyme A (CoA): Acetate-CoA transferase in butyrate-producing bacteria from the human large intestine. Appl. Environ. Microbiol. 68(10), 5186-5190. doi: 10.1128/aem.68.10.5186-5190.2002.
Duncan, S.H., Louis, P., and Flint, H.J. (2004). Lactate-utilizing bacteria, isolated from human feces, that produce butyrate as a major fermentation product. Appl. Environ. Microbiol. 70(10), 5810-5817. doi: 10.1128/aem.70.10.5810-5817.2004.
Duncan, S.H., Louis, P., Thomson, J.M., and Flint, H.J. (2009). The role of pH in determining the species composition of the human colonic microbiota. Environ. Microbiol. 11(8), 2112-2122. doi: 10.1111/j.1462-2920.2009.01931.x.
Eckburg, P.B., Bik, E.M., Bernstein, C.N., Purdom, E., Dethlefsen, L., Sargent, M., et al. (2005). Microbiology: Diversity of the human intestinal microbial flora. Science 308(5728), 1635-1638. doi: 10.1126/science.1110591.
Egan, M., O'Connell Motherway, M., Kilcoyne, M., Kane, M., Joshi, L., Ventura, M., et al. (2014). Cross-feeding by *Bifidobacterium breve* UCC2003 during co-cultivation with *Bifidobacterium bifidum* PRL2010 in a mucin-based medium. BMC Microbiol. 14(1), 0282. doi: 10.1186/s12866-014-0282-7.
El Oufir, L., Flourié, B., Bruley des Varannes, S., Barry, J.L., Cloarec, D., Bornet, F., et al. (1996). Relations between transit time, fermentation products, and hydrogen consuming flora in healthy humans. Gut 38(6), 870-877.
Elena, S.F., and Lenski, R.E. (2003). Evolution experiments with microorganisms: The dynamics and genetic bases of adaptation. Nat. Rev. Gen. 4(6), 457-469. doi: 10.1038/nrg1088.
Enjalbert, B., Millard, P., Dinclaux, M., Portais, J.-C., and Létisse, F. (2017). Acetate fluxes in Escherichia coli are determined by the thermodynamic control of the Pta-AckA pathway. Sci. Rep. 7, 42135. doi: 10.1038/srep42135
Enzmann, F., Mayer, F., Rother, M., and Holtmann, D. (2018). Methanogens: biochemical background and biotechnological applications. AMB Express 8(1), 1. doi: 10.1186/s13568-017-0531-x.
Estrela, S., and Brown, S.P. (2013). Metabolic and Demographic Feedbacks Shape the Emergent Spatial Structure and Function of Microbial Communities. PLoS Comp. Biol. 9(12), e1003398. doi: 10.1371/journal.pcbi.1003398.
Estrela, S., and Gudelj, I. (2010). Evolution of Cooperative Cross-Feeding Could Be Less Challenging Than Originally Thought. PLoS ONE 5(11), e0014121. doi: 10.1371/journal.pone.0014121.
Evans, D.F., Pye, G., Bramley, R., Clark, A.G., Dyson, T.J., and Hardcastle, J.D. (1988). Measurement of gastrointestinal pH profiles in normal ambulant human subjects. Gut 29(8), 1035.
Faith, J.J., Guruge, J.L., Charbonneau, M., Subramanian, S., Seedorf, H., Goodman, A.L., et al. (2013). The long-term stability of the human gut microbiota. Science 341(6141). doi: 10.1126/science.1237439.
Falony, G., Calmeyn, T., Leroy, F., and De Vuyst, L. (2009a). Coculture fermentations of bifidobacterium species and *Bacteroides thetaiotaomicron* reveal a mechanistic insight into the prebiotic effect of inulin-type fructans. Appl. Environ. Microbiol. 75(8), 2312-2319. doi: 10.1128/aem.02649-08.
Falony, G., Lazidou, K., Verschaeren, A., Weckx, S., Maes, D., and De Vuyst, L. (2009b). In vitro kinetic analysis of fermentation of prebiotic inulin-type fructans by Bifidobacterium species reveals four different phenotypes. Appl. Environ. Microbiol. 75(2), 454-461. doi: 10.1128/aem.01488-08.
Falony, G., Vlachou, A., Verbrugghe, K., and De Vuyst, L. (2006). Cross-feeding between *Bifidobacterium longum* BB536 and acetate-converting, butyrate-producing colon bacteria

during growth on oligofructose. Appl. Environ. Microbiol. 72(12), 7835-7841. doi: 10.1128/aem.01296-06.
Ferriere, R., Bronstein, J.L., Rinaldi, S., Law, R., and Gauduchon, M. (2002). Cheating and the evolutionary stability of mutualisms. Proc. R. Soc. Lond. B. Biol. Sci. 269(1493), 773.
Fisher, C.K., and Mehta, P. (2014). Identifying Keystone Species in the Human Gut Microbiome from Metagenomic Timeseries Using Sparse Linear Regression. PLoS ONE 9(7), e102451. doi: 10.1371/journal.pone.0102451.
Fite, A., Macfarlane, G.T., Cummings, J.H., Hopkins, M.J., Kong, S.C., Furrie, E., et al. (2004). Identification and quantitation of mucosal and faecal desulfovibrios using real time polymerase chain reaction. Gut 53(4), 523-529. doi: 10.1136/gut.2003.031245.
Flint, H.J., Duncan, S.H., Scott, K.P., and Louis, P. (2014). Links between diet, gut microbiota composition and gut metabolism. Proc. Nutr. Soc. 760. doi: 10.1017/s0029665114001463.
Fonty, G., Joblin, K., Chavarot, M., Roux, R., Naylor, G., and Michallon, F. (2007). Establishment and Development of Ruminal Hydrogenotrophs in Methanogen-Free Lambs. Appl. Environ. Microbiol. 73(20), 6391-6403. doi: 10.1128/AEM.00181-07.
Foster, K.R., and Bell, T. (2012). Competition, not cooperation, dominates interactions among culturable microbial species. Curr. Biol. 22(19), 1845-1850. doi: 10.1016/j.cub.2012.08.005.
Foster, K.R., and Wenseleers, T. (2006). A general model for the evolution of mutualisms. J. Evol. Biol. 19(4), 1283-1293. doi: 10.1111/j.1420-9101.2005.01073.x.
Frank, D.N., St. Amand, A.L., Feldman, R.A., Boedeker, E.C., Harpaz, N., and Pace, N.R. (2007). Molecular-phylogenetic characterization of microbial community imbalances in human inflammatory bowel diseases. Proc. Natl. Acad. Sci. USA. 104, 13780.
Friesen, M.L., Saxer, G., Travisano, M., and Doebeli, M. (2004). Experimental evidence for sympatric ecological diversification due to frequency-dependent competition in Escherichia coli. Evolution 58(2), 245-260.
Furnari, M., Savarino, E., Bruzzone, L., Moscatelli, A., Gemignani, L., Gianini, E.G., et al. (2012). Reassessment of the role of methane production between irritable bowel syndrome and functional constipation. J. Gastrointestin. Liver Dis. 21(2), 157-163.
Germerodt, S., Bohl, K., Lück, A., Pande, S., Schröter, A., Kaleta, C., et al. (2016). Pervasive Selection for Cooperative Cross-Feeding in Bacterial Communities. PLoS Comp. Biol. 12(6), e1004986. doi: 10.1371/journal.pcbi.1004986.
Ghoshal, U., Shukla, R., Srivastava, D., and Ghoshal, U.C. (2016). Irritable bowel syndrome, particularly the constipation-predominant form, involves an increase in *Methanobrevibacter smithii*, which is associated with higher methane production. Gut Liver 10(6). doi: 10.5009/gnl15588.
Ghoul, M., Griffin, A.S., and West, S.A. (2014). Toward an evolutionary definition of cheating. Evolution 68(2), 318-331. doi: 10.1111/evo.12266.
Gibson, G.R., Hutkins, R., Sanders, M.E., Prescott, S.L., Reimer, R.A., Salminen, S.J., et al. (2017). Expert consensus document: The International Scientific Association for Probiotics and Prebiotics (ISAPP) consensus statement on the definition and scope of prebiotics. Nat. Rev. Gastroenterol. Hepatol. 14, 491-502.
Gibson, G.R., Cummings, J.H., and Macfarlane, G.T. (1988a). Competition for hydrogen between sulphate-reducing bacteria and methanogenic bacteria from the human large intestine. J. Appl. Bacteriol. 65(3), 241-247. doi: doi:10.1111/j.1365-2672.1988.tb01891.x.
Gibson, G.R., Cummings, J.H., and Macfarlane, G.T. (1988b). Use of a three-stage continuous culture system to study the effect of mucin on dissimilatory sulfate reduction and methanogenesis by mixed populations of human gut bacteria. Appl. Environ. Microbiol. 54(11), 2750-2755.
Gibson, G.R., Cummings, J.H., Macfarlane, G.T., Allison, C., Segal, I., Vorster, H.H., et al. (1990). Alternative pathways for hydrogen disposal during fermentation in the human colon. Gut 31(6), 679-683.
Gibson, G.R., Macfarlane, G.T., and Cummings, J.H. (1988c). Occurrence of sulphate-reducing bacteria in human faeces and the relationship of dissimilatory sulphate reduction to methanogenesis in the large gut. J. Appl. Microbiol. 65(2), 103-111.
Gibson, G.R., MacFarlane, G.T., and Cummings, J.H. (1993a). Sulphate reducing bacteria and hydrogen metabolism in the human large intestine. Gut 34(4), 437-439.

Gibson, G.R., Macfarlane, S., and Macfarlane, G.T. (1993b). Metabolic interactions involving sulphate-reducing and methanogenic bacteria in the human large intestine. FEMS Microbiol. Ecol. 12(2), 117-125.
Giovannoni, S.J., Thrash, C.J., and Temperton, B. (2014). Implications of streamlining theory for microbial ecology. ISME J. 8(8), 1553-1565. doi: 10.1038/ismej.2014.60.
Godwin, S., Kang, A., Gulino, L.M., Manefield, M., Gutierrez-Zamora, M.L., Kienzle, M., et al. (2014). Investigation of the microbial metabolism of carbon dioxide and hydrogen in the kangaroo foregut by stable isotope probing. ISME J. 8(9), 1855-1865. doi: 10.1038/ismej.2014.25.
Goo, E., An, J.H., Kang, Y., and Hwang, I. (2015). Control of bacterial metabolism by quorum sensing. Trends Microbiol. 23(9), 567-576. doi: 10.1016/j.tim.2015.05.007.
Goubern, M., Andriamihaja, M., Nübel, T., Blachier, F., and Bouillaud, F. (2007). Sulfide, the first inorganic substrate for human cells. FASEB J. 21(8), 1699-1706. doi: 10.1096/fj.06-7407com.
Grine, G., Boualam, M.A., and Drancourt, M. (2017). *Methanobrevibacter smithii*, a methanogen consistently colonising the newborn stomach. Eur. J. Clin. Microbiol. Infect. Dis. 36(12), 2449-2455. doi: 10.1007/s10096-017-3084-7.
Großkopf, T., Consuegra, J., Gaffé, J., Willison, J.C., Lenski, R.E., Soyer, O.S., et al. (2016). Metabolic modelling in a dynamic evolutionary framework predicts adaptive diversification of bacteria in a long-term evolution experiment. BMC Evol. Biol. 16(1), 163. doi: 10.1186/s12862-016-0733-x.
Gudelj, I., Kinnersley, M., Rashkov, P., Schmidt, K., and Rosenzweig, F. (2016). Stability of Cross-Feeding Polymorphisms in Microbial Communities. PLoS Comp. Biol. 12(12). doi: 10.1371/journal.pcbi.1005269.
Hamilton, W.D. (1964). The genetical evolution of social behaviour. I & II. J. Theor. Biol. 7(1), 1-52.
Hansen, E.E., Lozupone, C.A., Rey, F.E., Wu, M., Guruge, J.L., Narra, A., et al. (2011). Pan-genome of the dominant human gut-associated archaeon, *Methanobrevibacter smithii*, studied in twins. Proc. Natl. Acad. Sci. USA. 108(SUPPL. 1), 4599-4606. doi: 10.1073/pnas.1000071108.
Hansen, S.K., Rainey, P.B., Haagensen, J.A.J., and Molin, S. (2007). Evolution of species interactions in a biofilm community. Nature 445(7127), 533-536. doi: http://www.nature.com/nature/journal/v445/n7127/suppinfo/nature05514_S1.html.
Harcombe, W. (2010). Novel cooperation experimentally evolved between species. Evolution 64(7), 2166-2172. doi: 10.1111/j.1558-5646.2010.00959.x.
Hardin, G. (1960). The Competitive Exclusion Principle. Science 131(3409), 1292.
Healey, G.R., Murphy, R., Brough, L., Butts, C.A., and Coad, J. (2017). Interindividual variability in gut microbiota and host response to dietary interventions. Nutr. Rev. 75(12), 1059-1080. doi: 10.1093/nutrit/nux062.
Heidelberg, J.F., Seshadri, R., Haveman, S.A., Hemme, C.L., Paulsen, I.T., Kolonay, J.F., et al. (2004). The genome sequence of the anaerobic, sulfate-reducing bacterium *Desulfovibrio vulgaris* Hildenborough. Nat. Biotechnol. 22, 554. doi: 10.1038/nbt959.
Helling, R.B., Vargas, C.N., and Adams, J. (1987). Evolution of *Escherichia coli* during growth in a constant environment. Genetics 116(3), 349-358.
Heinken, A., and Thiele, I. (2019). Systematic interrogation of the distinct metabolic potential in gut microbiomes of inflammatory bowel disease patients with dysbiosis. bioRxiv, 640649. doi: 10.1101/640649.
Hernot, D.C., Boileau, T.W., Bauer, L.L., Middelbos, I.S., Murphy, M.R., Swanson, K.S., et al. (2009). In vitro fermentation profiles, gas production rates, and microbiota modulation as affected by certain fructans, galactooligosaccharides, and polydextrose. J. Agric. Food Chem. 57(4), 1354-1361. doi: 10.1021/jf802484j.
Hillesland, K.L. (2018). Evolution on the bright side of life: microorganisms and the evolution of mutualism. Ann. N. Y. Acad. Sci. 1422(1), 88-103. doi: 10.1111/nyas.13515.
Hillesland, K.L., and Stahl, D.A. (2010). Rapid evolution of stability and productivity at the origin of a microbial mutualism. Proc. Natl. Acad. Sci. USA. 107(5), 2124-2129. doi: 10.1073/pnas.0908456107.
Hold, G.L., Pryde, S.E., Russell, V.J., Furrie, E., and Flint, H.J. (2002). Assessment of microbial diversity in human colonic samples by 16S rDNA sequence analysis. FEMS Microbiol. Ecol. 39(1), 33-39. doi: 10.1016/s0168-6496(01)00190-8.

Hosoda, K., Suzuki, S., Yamauchi, Y., Shiroguchi, Y., Kashiwagi, A., Ono, N., et al. (2011). Cooperative Adaptation to Establishment of a Synthetic Bacterial Mutualism. PLoS ONE 6(2), e17105. doi: 10.1371/journal.pone.0017105.

Jalanka, J., and Spiller, R. (2017). Role of microbiota in the pathogenesis of functional disorders of the lower GI tract: Work in progress. Neurogastroenterol. Motil. 29(10), e13194. doi: doi:10.1111/nmo.13194.

Janssen, P.H. (2010). Influence of hydrogen on rumen methane formation and fermentation balances through microbial growth kinetics and fermentation thermodynamics. Anim. Feed Sci. Technol. 160(1), 1-22. doi: https://doi.org/10.1016/j.anifeedsci.2010.07.002.

Jiménez, E., Javier de, A., Marina, M., Pablo, P.-T., Raquel, T., Juan, F.M.-B., et al. (2015). Metagenomic Analysis of Milk of Healthy and Mastitis-Suffering Women. J. Hum. Lact. 31(3), 406-415. doi: 10.1177/0890334415585078.

Keller, K., and Wall, J. (2011). Genetics and Molecular Biology of the Electron Flow for Sulfate Respiration in *Desulfovibrio*. Front. Microbiol. 2(135). doi: 10.3389/fmicb.2011.00135.

Kelly, W.J., Henderson, G., Pacheco, D.M., Li, D., Reilly, K., Naylor, G.E., et al. (2016). The complete genome sequence of *Eubacterium limosum* SA11, a metabolically versatile rumen acetogen. Stand. Genom. Sci. 11(1). doi: 10.1186/s40793-016-0147-9.

Kettle, H., Donnelly, R., Flint, H.J., and Marion, G. (2014). pH feedback and phenotypic diversity within bacterial functional groups of the human gut. J. Theor. Biol. 342, 62-69. doi: 10.1016/j.jtbi.2013.10.015.

Kettle, H., Holtrop, G., Louis, P., and Flint, H.J. (2017). microPop: Modelling microbial populations and communities in R. Methods Ecol. Evol. 9, 399–409. doi: 10.1111/2041-210x.12873.

Kettle, H., Louis, P., Holtrop, G., Duncan, S.H., and Flint, H.J. (2015). Modelling the emergent dynamics and major metabolites of the human colonic microbiota. Environ. Microbiol. 17(5), 1615-1630. doi: 10.1111/1462-2920.12599.

Khalil, N.A., Walton, G.E., Gibson, G.R., Tuohy, K.M., and Andrews, S.C. (2014). In vitro batch cultures of gut microbiota from healthy and ulcerative colitis (UC) subjects suggest that sulphate-reducing bacteria levels are raised in UC and by a protein-rich diet. Int. J. Food Sci. Nutr. 65(1), 79-88. doi: 10.3109/09637486.2013.825700.

Khelaifia, S., Raoult, D., and Drancourt, M. (2013). A Versatile Medium for Cultivating Methanogenic Archaea. PLoS ONE 8(4), e61563. doi: 10.1371/journal.pone.0061563.

Kim, H.J., Boedicker, J.Q., Choi, J.W., and Ismagilov, R.F. (2008). Defined spatial structure stabilizes a synthetic multispecies bacterial community. Proc. Natl. Acad. Sci. USA 105(47), 18188-18193. doi: 10.1073/pnas.0807935105.

King, T.S., Elia, M., and Hunter, J.O. (1998). Abnormal colonic fermentation in irritable bowel syndrome. Lancet 352(9135), 1187-1189. doi: https://doi.org/10.1016/S0140-6736(98)02146-1.

Knapp, J.R., Laur, G.L., Vadas, P.A., Weiss, W.P., and Tricarico, J.M. (2014). Invited review: Enteric methane in dairy cattle production: Quantifying the opportunities and impact of reducing emissions. J. Dairy Sci. 97(6), 3231-3261. doi: https://doi.org/10.3168/jds.2013-7234.

Korpela, K., Flint, H.J., Johnstone, A.M., Lappi, J., Poutanen, K., Dewulf, E., et al. (2014). Gut microbiota signatures predict host and microbiota responses to dietary interventions in obese individuals. PLoS ONE 9(3). doi: 10.1371/journal.pone.0090702.

Kristjansson, J.K., and Schönheit, P. (1983). Why do sulfate-reducing bacteria outcompete methanogenic bacteria for substrates? Oecologia 60(2), 264-266. doi: 10.1007/bf00379530.

Kumari, S., Beatty, C.M., Browning, D.F., Busby, S.J.W., Simel, E.J., and Hovel-Miner, G. (2000). Regulation of acetyl coenzyme A synthetase in *Escherichia coli*. J. Bacteriol. 182(15), 4173-4179. doi: 10.1128/JB.182.15.4173-4179.2000.

Labarthe, S., Polizzi, B., Phan, T., Goudon, T., Ribot, M., and Laroche, B. (2019). A mathematical model to investigate the key drivers of the biogeography of the colon microbiota. J. Theor. Biol. 462, 552-581. doi: 10.1016/j.jtbi.2018.12.009.

Lajoie, S.F., Bank, S., Miller, T.L., and Wolin, M.J. (1988). Acetate production from hydrogen and [13C]carbon dioxide by the microflora of human feces. Appl. Environ. Microbiol. 54(11), 2723-2727.

Leclerc, M., Bernalier, A., Donadille, G., and Lelait, M. (1997). H2/CO2 Metabolism in Acetogenic Bacteria Isolated From the Human Colon. Anaerobe 3(5), 307-315. doi: https://doi.org/10.1006/anae.1997.0117.

Lenski, R.E. (2017). Experimental evolution and the dynamics of adaptation and genome evolution in microbial populations. ISME J. 11(10), 2181-2194. doi: 10.1038/ismej.2017.69.
Lenski, R.E., Rose, M.R., Simpson, S.C., and Tadler, S.C. (1991). Long-term experimental evolution in *Escherichia coli*. I. Adaptation and divergence during 2000 generations. Am. Nat. 138(6), 1315-1341. doi: 10.1086/285289.
Ley, R.E., Turnbaugh, P.J., Klein, S., and Gordon, J.I. (2006). Microbial ecology: Human gut microbes associated with obesity. Nature 444(7122), 1022-1023. doi: 10.1038/4441022a.
Liu, C., Finegold, S.M., Song, Y., and Lawson, P.A. (2008). Reclassification of *Clostridium coccoides*, *Ruminococcus hansenii*, *Ruminococcus hydrogenotrophicus*, *Ruminococcus luti*, *Ruminococcus productus* and *Ruminococcus schinkii* as *Blautia coccoides* gen. nov., comb. nov., *Blautia hansenii* comb. nov., *Blautia hydrogenotrophica* comb. nov., *Blautia luti* comb. nov., *Blautia producta* comb. nov., *Blautia schinkii* comb. nov. and description of *Blautia wexlerae*. Int. J. Syst. Evol. Microbiol. 58(8), 1896-1902. doi: 10.1099/ijs.0.65208-0.
Lopetuso, L.R., Scaldaferri, F., Petito, V., and Gasbarrini, A. (2013). Commensal Clostridia: leading players in the maintenance of gut homeostasis. Gut Pathog. 5, 23.
Lopez, S., McIntosh, F.M., Wallace, R.J., and Newbold, C.J. (1999). Effect of adding acetogenic bacteria on methane production by mixed rumen microorganisms. Anim. Feed Sci. Technol. 78(1), 1-9. doi: https://doi.org/10.1016/S0377-8401(98)00273-9.
Louis, P., and Flint, H.J. (2017). Formation of propionate and butyrate by the human colonic microbiota. Environ. Microbiol. 19(1), 29-41. doi: 10.1111/1462-2920.13589.
Louis, P., Hold, G.L., and Flint, H.J. (2014). The gut microbiota, bacterial metabolites and colorectal cancer. Nat. Rev. Microbiol. 12(10), 661-672. doi: 10.1038/nrmicro3344.
Lupton, J.R. (2004). Microbial Degradation Products Influence Colon Cancer Risk: The Butyrate Controversy. J. Nutr. 134(2), 479-482.
Macfarlane, G.T., Gibson, G.R., and Cummings, J.H. (1992). Comparison of fermentation reactions in different regions of the human colon. J. Appl. Bacteriol. 72(1), 57-64. doi: 10.1111/j.1365-2672.1992.tb04882.x.
Macfarlane, G.T., and Macfarlane, S. (2007). Models for intestinal fermentation: association between food components, delivery systems, bioavailability and functional interactions in the gut. Curr. Opin. Biotechnol. 18(2), 156-162. doi: 10.1016/j.copbio.2007.01.011.
Macfarlane, S., Bahrami, B., and Macfarlane, G.T. (2011). "Mucosal biofilm communities in the human intestinal tract", in: Adv. Appl. Microbiol. doi: 10.1016/B978-0-12-387046-9.00005-0
MacLean, R.C., Fuentes-Hernandez, A., Greig, D., Hurst, L.D., and Gudelj, I. (2010). A Mixture of "Cheats" and "Co-Operators" Can Enable Maximal Group Benefit. PLoS Biol. 8(9), e1000486. doi: 10.1371/journal.pbio.1000486.
Magee, E.A., Richardson, C.J., Hughes, R., and Cummings, J.H. (2000). Contribution of dietary protein to sulfide production in the large intestine: an in vitro and a controlled feeding study in humans. Am. J. Clin. Nutr. 72(6), 1488-1494. doi: 10.1093/ajcn/72.6.1488.
Magnúsdóttir, S., and Thiele, I. (2018). Modeling metabolism of the human gut microbiome. Curr. Opin. Biotechnol. 51, 90-96. doi: 10.1016/j.copbio.2017.12.005.
Marchal, M., Goldschmidt, F., Derksen-Müller, S.N., Panke, S., Ackermann, M., and Johnson, D.R. (2017). A passive mutualistic interaction promotes the evolution of spatial structure within microbial populations. BMC Evol. Biol. 17(1), 106. doi: 10.1186/s12862-017-0950-y.
Marquet, P., Duncan, S.H., Chassard, C., Bernalier-Donadille, A., and Flint, H.J. (2009). Lactate has the potential to promote hydrogen sulphide formation in the human colon. FEMS Microbiol. Lett. 299(2), 128-134. doi: 10.1111/j.1574-6968.2009.01750.x.
Mas, A., Jamshidi, S., Lagadeuc, Y., Eveillard, D., and Vandenkoornhuyse, P. (2016). Beyond the Black Queen Hypothesis. ISME J. 10(9), 2085-2091. doi: 10.1038/ismej.2016.22.
Mathur, R., Kim, G., Morales, W., Sung, J., Rooks, E., Pokkunuri, V., et al. (2013). Intestinal *Methanobrevibacter smithii* but not total bacteria is related to diet-induced weight gain in rats. Obesity 21(4), 748-754. doi: 10.1002/oby.20277.
Maynard, C.L., Elson, C.O., Hatton, R.D., and Weaver, C.T. (2012). Reciprocal interactions of the intestinal microbiota and immune system. Nature 489(7415), 231-241. doi: 10.1038/nature11551.
Mee, M.T., Collins, J.J., Church, G.M., and Wang, H.H. (2014). Syntrophic exchange in synthetic microbial communities. Proc. Natl. Acad. Sci. USA. 111(20), E2149-E2156. doi: 10.1073/pnas.1405641111.

Miller, T.L., and Wolin, M.J. (1995). Bioconversion of cellulose to acetate with pure cultures of *Ruminococcus albus* and a hydrogen-using acetogen. Appl. Environ. Microbiol. 61(11), 3832-3835.
Miller, T.L., and Wolin, M.J. (1996). Pathways of acetate, propionate, and butyrate formation by the human fecal microbial flora. Appl. Environ. Microbiol. 62(5), 1589-1592.
Miller, T.L., Wolin, M.J., De Macario, E.C., and Macario, A.J.L. (1982). Isolation of *Methanobrevibacter smithii* from human feces. Appl. Environ. Microbiol. 43(1), 227-232.
Million, M., Maraninchi, M., Henry, M., Armougom, F., Richet, H., Carrieri, P., et al. (2012). Obesity-associated gut microbiota is enriched in Lactobacillus reuteri and depleted in *Bifidobacterium animalis* and *Methanobrevibacter smithii*. Int. J. Obesity 36(6), 817-825. doi: 10.1038/ijo.2011.153.
Moens, F., Verce, M., and De Vuyst, L. (2017). Lactate- and acetate-based cross-feeding interactions between selected strains of lactobacilli, bifidobacteria and colon bacteria in the presence of inulin-type fructans. Int. J. Food Microbiol. 241, 225-236. doi: 10.1016/j.ijfoodmicro.2016.10.019.
Moens, F., Weckx, S., and De Vuyst, L. (2016). Bifidobacterial inulin-type fructan degradation capacity determines cross-feeding interactions between bifidobacteria and *Faecalibacterium prausnitzii*. Int. J. Food Microbiol. 231, 76-85. doi: 10.1016/j.ijfoodmicro.2016.05.015.
Momeni, B., Waite, A.J., and Shou, W. (2013). Spatial self-organization favors heterotypic cooperation over cheating. eLife 2, e00960. doi: 10.7554/eLife.00960.
Momozawa, Y., Deffontaine, V., Louis, E., and Medrano, J.F. (2011). Characterization of Bacteria in Biopsies of Colon and Stools by High Throughput Sequencing of the V2 Region of Bacterial 16S rRNA Gene in Human. PLoS ONE 6(2), e16952. doi: 10.1371/journal.pone.0016952.
Moorthy, A.S., Brooks, S.P.J., Kalmokoff, M., and Eberl, H.J. (2015). A spatially continuous model of carbohydrate digestion and transport processes in the colon. PLoS ONE 10(12). doi: 10.1371/journal.pone.0145309.
Morgavi, D.P., Forano, E., Martin, C., and Newbold, C.J. (2010). Microbial ecosystem and methanogenesis in ruminants. animal 4(7), 1024-1036. doi: 10.1017/S1751731110000546.
Morris, B.E.L., Henneberger, R., Huber, H., and Moissl-Eichinger, C. (2013). Microbial syntrophy: Interaction for the common good. FEMS Microbiol. Rev. 37(3), 384-406. doi: 10.1111/1574-6976.12019.
Morris, J.J. (2015). Black Queen evolution: The role of leakiness in structuring microbial communities. Trends Genet. 31(8), 475-482. doi: 10.1016/j.tig.2015.05.004.
Morris, J.J., Lenski, R.E., and Zinser, E.R. (2012). The black queen hypothesis: Evolution of dependencies through adaptive gene loss. mBio 3(2). doi: 10.1128/mBio.00036-12.
Morrison, D.J., Mackay, W.G., Edwards, C.A., Preston, T., Dodson, B., and Weaver, L.T. (2006). Butyrate production from oligofructose fermentation by the human faecal flora: What is the contribution of extracellular acetate and lactate? Br. J. Nutr. 96(3), 570-577. doi: 10.1079/bjn20061853.
Morrison, D.J., and Preston, T. (2016). Formation of short chain fatty acids by the gut microbiota and their impact on human metabolism. Gut Microbes 7(3), 189-200. doi: 10.1080/19490976.2015.1134082.
Moss, A.R., Jouany, J.-P., and Newbold, J. (2000). Methane production by ruminants: its contribution to global warming. Ann. Zootech. 49(3), 231-253.
Motelica-Wagenaar, A.M., Nauta, A., van den Heuvel, E.G.H.M., and Kleerebezem, R. (2014). Flux analysis of the human proximal colon using anaerobic digestion model 1. Anaerobe 28, 137-148. doi: 10.1016/j.anaerobe.2014.05.008.
Motta, J.-P., Flannigan, K.L., Agbor, T.A., Beatty, J.K., Blackler, R.W., Workentine, M.L., et al. (2015). Hydrogen Sulfide Protects from Colitis and Restores Intestinal Microbiota Biofilm and Mucus Production. Inflamm. Bowel Dis. 21(5), 1006-1017. doi: 10.1097/MIB.0000000000000345.
Moya, A., and Ferrer, M. (2016). Functional Redundancy-Induced Stability of Gut Microbiota Subjected to Disturbance. Trends Microbiol. 24, 402-413.
Müller, M.J.I., Neugeboren, B.I., Nelson, D.R., and Murray, A.W. (2014). Genetic drift opposes mutualism during spatial population expansion. P. Natl. Acad. Sci. 111(3), 1037-1042. doi: 10.1073/pnas.1313285111.

Muñoz-Tamayo, R., Laroche, B., Walter, T., Doré, J., and Leclerc, M. (2010). Mathematical modelling of carbohydrate degradation by human colonic microbiota. J. Theor. Biol. 266(1), 189-201. doi: 10.1016/j.jtbi.2010.05.040.

Nadell, C.D., Foster, K.R., and Xavier, J.B. (2010). Emergence of Spatial Structure in Cell Groups and the Evolution of Cooperation. PLoS Comp. Biol. 6(3), e1000716. doi: 10.1371/journal.pcbi.1000716.

Nakamura, N., Lin, H.C., McSweeney, C.S., MacKie, R.I., and Rex Gaskins, H. (2010). Mechanisms of microbial hydrogen disposal in the human colon and implications for health and disease. Annu. Rev. Food Sci. Technol. 1(1), 363-395. doi: 10.1146/annurev.food.102308.124101.

Nava, G.M., Carbonero, F., Croix, J.A., Greenberg, E., and Gaskins, H.R. (2012a). Abundance and diversity of mucosa-associated hydrogenotrophic microbes in the healthy human colon. ISME J. 6(1), 57-70. doi: 10.1038/ismej.2011.90.

Nava, G.M., Carbonero, F., Ou, J., Benefiel, A.C., O'Keefe, S.J., and Gaskins, H.R. (2012b). Hydrogenotrophic microbiota distinguish native Africans from African and European Americans. Environ. Microbiol. Rep. 4(3), 307-315. doi: 10.1111/j.1758-2229.2012.00334.x.

Nishijima, S., Suda, W., Oshima, K., Kim, S.-W., Hirose, Y., Morita, H., et al. (2016). The gut microbiome of healthy Japanese and its microbial and functional uniqueness. DNA Res. 23(2), 125-133. doi: 10.1093/dnares/dsw002.

Noguera, D.R., Brusseau, G.A., Rittmann, B.E., and Stahl, D.A. (1998). A unified model describing the role of hydrogen in the growth of *Desulfovibrio vulgaris* under different environmental conditions. Biotechnol. Bioeng. 59(6), 732-746. doi: 10.1002/(SICI)1097-0290(19980920)59:6<732::AID-BIT10>3.0.CO;2-7.

Nugent, S.G., Kumar, D., Rampton, D.S., and Evans, D.F. (2001). Intestinal luminal pH in inflammatory bowel disease: Possible determinants and implications for therapy with aminosalicylates and other drugs. Gut 48(4), 571-577. doi: 10.1136/gut.48.4.571.

Ohta, S. (2014). Molecular hydrogen as a preventive and therapeutic medical gas: initiation, development and potential of hydrogen medicine. Pharmacol. Ther. 144(1), 1-11. doi: https://doi.org/10.1016/j.pharmthera.2014.04.006.

Oliveira, N.M., Niehus, R., and Foster, K.R. (2014). Evolutionary limits to cooperation in microbial communities. Proc. Natl. Acad. Sci. USA 111(50), 17941-17946. doi: 10.1073/pnas.1412673111.

Ostojic, S.M. (2018). Inadequate Production of H2 by Gut Microbiota and Parkinson Disease. Trends Endocrin. Met. 29(5):286-288. doi: https://doi.org/10.1016/j.tem.2018.02.006.

Pacheco, A.R., Moel, M., and Segrè, D. (2019). Costless metabolic secretions as drivers of interspecies interactions in microbial ecosystems. Nat. Commun. 10(1), 103. doi: 10.1038/s41467-018-07946-9.

Pande, S., Kaftan, F., Lang, S., Svato, A., Germerodt, S., and Kost, C. (2016). Privatization of cooperative benefits stabilizes mutualistic cross-feeding interactions in spatially structured environments. ISME J. 10(6), 1413-1423. doi: 10.1038/ismej.2015.212.

Pande, S., and Kost, C. (2017). Bacterial Unculturability and the Formation of Intercellular Metabolic Networks. Trends Microbiol. 25(5), 349-361. doi: https://doi.org/10.1016/j.tim.2017.02.015.

Pande, S., Merker, H., Bohl, K., Reichelt, M., Schuster, S., De Figueiredo, L.F., et al. (2014). Fitness and stability of obligate cross-feeding interactions that emerge upon gene loss in bacteria. ISME J. 8(5), 953-962. doi: 10.1038/ismej.2013.211.

Pande, S., Shitut, S., Freund, L., Westermann, M., Bertels, F., Colesie, C., et al. (2015). Metabolic cross-feeding via intercellular nanotubes among bacteria. Nat. Commun. 6, 6238. doi: 10.1038/ncomms7238

Pant, K., Yadav, A.K., Gupta, P., Islam, R., Saraya, A., and Venugopal, S.K. (2017). Butyrate induces ROS-mediated apoptosis by modulating miR-22/SIRT-1 pathway in hepatic cancer cells. Redox Biol. 12, 340-349. doi: 10.1016/j.redox.2017.03.006.

Patra, A., Park, T., Kim, M., and Yu, Z. (2017). Rumen methanogens and mitigation of methane emission by anti-methanogenic compounds and substances. J. Anim. Sci. Biotechnol. 8(1), 13. doi: 10.1186/s40104-017-0145-9.

Payne, A.N., Chassard, C., Zimmermann, M., Müller, P., Stinca, S., and Lacroix, C. (2011). The metabolic activity of gut microbiota in obese children is increased compared with normal-

weight children and exhibits more exhaustive substrate utilization. Nutr. Diabetes 1(7), e12. doi: 10.1038/nutd.2011.8.
Penders, J., Thijs, C., Vink, C., Stelma, F.F., Snijders, B., Kummeling, I., et al. (2006). Factors influencing the composition of the intestinal microbiota in early infancy. Pediatrics 118(2), 511-521. doi: 10.1542/peds.2005-2824.
Pfeiffer, T., and Bonhoeffer, S. (2004). Evolution of cross-feeding in microbial populations. Am. Nat. 163(6), E126-135.
Pham, V.T., Lacroix, C., Braegger, C.P., and Chassard, C. (2017). Lactate-utilizing community is associated with gut microbiota dysbiosis in colicky infants. Sci. Rep. 7(1). doi: 10.1038/s41598-017-11509-1.
Pimentel, M., Lin, H.C., Enayati, P., Van Den Burg, B., Lee, H.R., Chen, J.H., et al. (2006). Methane, a gas produced by enteric bacteria, slows intestinal transit and augments small intestinal contractile activity. Am. J. Physiol. Gastrointest. Liver Physiol. 290(6), G1089-G1095. doi: 10.1152/ajpgi.00574.2004.
Pimentel, M., Mathur, R., and Chang, C. (2013). Gas and the Microbiome. Curr. Gastroenterol. Rep. 15(12), 356. doi: 10.1007/s11894-013-0356-y.
Pitcher, M.C.L., Beatty, E.R., and Cummings, J.H. (2000). The contribution of sulphate reducing bacteria and 5-aminosalicylic acid to faecal sulphide in patients with ulcerative colitis. Gut 46(1), 64-72. doi: 10.1136/gut.46.1.64.
Pochart, P., Doré, J., Lémann, F., and Rambaud, J.C. (1992). Interrelations between populations of methanogenic archaea and sulfate-reducing bacteria in the human colon. FEMS Microbiol. Lett. 98(1-3), 225-228.
Poltak, S.R., and Cooper, V.S. (2011). Ecological succession in long-term experimentally evolved biofilms produces synergistic communities. ISME J 5(3), 369-378. doi: http://www.nature.com/ismej/journal/v5/n3/suppinfo/ismej2010136s1.html.
Porcher, E., Tenaillon, O., and Godelle, B. (2001). From metabolism to polymorphism in bacterial populations: A theoretical study. Evolution 55(11), 2181-2193.
Proctor, L., LoTempio, J., Marquitz, A., Daschner, P., Xi, D., Flores, R., et al. (2019). A review of 10 years of human microbiome research activities at the US National Institutes of Health, Fiscal Years 2007-2016. Microbiome 7, 31. doi: 10.1186/s40168-019-0620-y
Pryde, S.E., Duncan, S.H., Hold, G.L., Stewart, C.S., and Flint, H.J. (2002). The microbiology of butyrate formation in the human colon. FEMS Microbiol. Lett. 217(2), 133-139. doi: 10.1016/s0378-1097(02)01106-0.
Qin, J., Li, R., Raes, J., Arumugam, M., Burgdorf, K.S., Manichanh, C., et al. (2010). A human gut microbial gene catalogue established by metagenomic sequencing. Nature 464, 59-65.
Rainey, P.B., and Travisano, M. (1998). Adaptive radiation in a heterogeneous environment. Nature 394(6688), 69-72. doi: 10.1038/27900
Rajilić–Stojanović, M., Biagi, E., Heilig, H.G.H.J., Kajander, K., Kekkonen, R.A., Tims, S., et al. (2011). Global and Deep Molecular Analysis of Microbiota Signatures in Fecal Samples From Patients With Irritable Bowel Syndrome. Gastroenterol. 141(5), 1792-1801. doi: https://doi.org/10.1053/j.gastro.2011.07.043.
Rajilić-Stojanović, M., and De Vos, W.M. (2014). The first 1000 cultured species of the human gastrointestinal microbiota. FEMS Microbiol. Rev. 38, 996-1047.
Rakoff-Nahoum, S., Foster, K.R., and Comstock, L.E. (2016). The evolution of cooperation within the gut microbiota. Nature 533(7602), 255-259. doi: 10.1038/nature17626.
Reichardt, N., Vollmer, M., Holtrop, G., Farquharson, F.M., Wefers, D., Bunzel, M., et al. (2018). Specific substrate-driven changes in human faecal microbiota composition contrast with functional redundancy in short-chain fatty acid production. ISME J 12, 610-622.
Rey, F.E., Faith, J.J., Bain, J., Muehlbauer, M.J., Stevens, R.D., Newgard, C.B., et al. (2010). Dissecting the in vivo metabolic potential of two human gut acetogens. J. Biol. Chem. 285(29), 22082-22090. doi: 10.1074/jbc.M110.117713.
Rey, F.E., Gonzalez, M.D., Cheng, J., Wu, M., Ahern, P.P., and Gordon, J.I. (2013). Metabolic niche of a prominent sulfate-reducing human gut bacterium. Proc. Natl. Acad. Sci. USA. 110(33), 13582-13587. doi: 10.1073/pnas.1312524110.
Rios-Covian, D., Gueimonde, M., Duncan, S.H., Flint, H.J., and De Los Reyes-Gavilan, C.G. (2015). Enhanced butyrate formation by cross-feeding between *Faecalibacterium prausnitzii* and *Bifidobacterium adolescentis*. FEMS Microbiol. Lett. 362(21). doi: 10.1093/femsle/fnv176.

Rivière, A., Gagnon, M., Weckx, S., Roy, D., and De Vuyst, L. (2015). Mutual cross-feeding interactions between *Bifidobacterium longum* subsp. *longum* NCC2705 and *Eubacterium rectale* ATCC 33656 explain the bifidogenic and butyrogenic effects of arabinoxylan oligosaccharides. Appl. Environ. Microbiol. 81(22), 7767-7781. doi: 10.1128/aem.02089-15.

Rivière, A., Moens, F., Selak, M., Maes, D., Weckx, S., and De Vuyst, L. (2014). The ability of bifidobacteria to degrade arabinoxylan oligosaccharide constituents and derived oligosaccharides is strain dependent. Appl. Environ. Microbiol. 80(1), 204-217. doi: 10.1128/AEM.02853-13.

Rivière, A., Selak, M., Lantin, D., Leroy, F., and De Vuyst, L. (2016). Bifidobacteria and butyrate-producing colon bacteria: Importance and strategies for their stimulation in the human gut. Front. Microbiol. 7:979. doi: 10.3389/fmicb.2016.00979.

Robert, C., and Bernalier-Donadille, A. (2003). The cellulolytic microflora of the human colon: evidence of microcrystalline cellulose-degrading bacteria in methane-excreting subjects. FEMS Microbiol. Ecol. 46(1), 81-89. doi: 10.1016/S0168-6496(03)00207-1.

Robert, C., Del'Homme, C., and Bernalier-Donadille, A. (2001). Interspecies H2 transfer in cellulose degradation between fibrolytic bacteria and H2-utilizing microorganisms from the human colon. FEMS Microbiol. Lett. 205(2), 209-214. doi: 10.1016/s0378-1097(01)00467-0.

Roediger, W.E.W., Moore, J., and Babidge, W. (1997). Colonic sulfide in pathogenesis and treatment of ulcerative colitis. Dig. Dis. Sci. 42(8), 1571-1579. doi: 10.1023/a:1018851723920.

Rogowski, A., Briggs, J.A., Mortimer, J.C., Tryfona, T., Terrapon, N., Lowe, E.C., et al. (2015). Glycan complexity dictates microbial resource allocation in the large intestine. Nat. Commun. 6, 7481. doi: 10.1038/ncomms8481

Rosenzweig, R.F., Sharp, R.R., Treves, D.S., and Adams, J. (1994). Microbial evolution in a simple unstructured environment: Genetic differentiation in *Escherichia coli*. Genetics 137(4), 903-917.

Rossi, M., Corradini, C., Amaretti, A., Nicolini, M., Pompei, A., Zanoni, S., et al. (2005). Fermentation of fructooligosaccharides and inulin by bifidobacteria: A comparative study of pure and fecal cultures. Appl. Environ. Microbiol. 71(10), 6150-6158. doi: 10.1128/aem.71.10.6150-6158.2005.

Rowland, I., Gibson, G., Heinken, A., Scott, K., Swann, J., Thiele, I., et al. (2017). Gut microbiota functions: metabolism of nutrients and other food components. Eur. J. Nutr. 57(1), 1-24. doi: 10.1007/s00394-017-1445-8.

Rozen, D.E., and Lenski, R.E. (2000). Long-term experimental evolution in *Escherichia coli*. VIII. Dynamics of a balanced polymorphism. Am. Nat. 155(1), 24-35. doi: 10.1086/303299.

Rozen, D.E., Schneider, D., and Lenski, R.E. (2005). Long-term experimental evolution in *Escherichia coli*. XIII. Phylogenetic history of a balanced polymorphism. J. Mol. Evol. 61(2), 171-180. doi: 10.1007/s00239-004-0322-2.

Ruaud, A., Esquivel-Elizondo, S., de la Cuesta-Zuluaga, J., Waters, J.L., Angenent, L.T., Youngblut, N.D., et al. (2020). Syntrophy via Interspecies H2 Transfer between *Christensenella* and *Methanobrevibacter* Underlies Their Global Cooccurrence in the Human Gut. mBio 11(1), e03235-03219. doi: 10.1128/mBio.03235-19.

Ruppin, H., Bar-Meir, S., Soergel, K.H., Wood, C.M., and Schmitt, M.G. (1980). Absorption of short-chain fatty acids by the colon. Gastroenterol. 78(6), 1500-1507.

Sachs, J.L., and Hollowell, A.C. (2012). The origins of cooperative bacterial communities. mBio 3(3). doi: 10.1128/mBio.00099-12.

Sachs, J.L., Mueller, U.G., Wilcox, T.P., and Bull, J.J. (2004). The evolution of cooperation. Q. Rev. Biol. 79(2), 135-160. doi: 10.1086/383541.

Sahakian, A.B., Jee, S.-R., and Pimentel, M. (2010). Methane and the Gastrointestinal Tract. Dig. Dis. Sci. 55(8), 2135-2143. doi: 10.1007/s10620-009-1012-0.

Salonen, A., Lahti, L., Salojärvi, J., Holtrop, G., Korpela, K., Duncan, S.H., et al. (2014). Impact of diet and individual variation on intestinal microbiota composition and fermentation products in obese men. ISME J. 8(11), 2218-2230. doi: 10.1038/ismej.2014.63.

Samuel, B.S., and Gordon, J.I. (2006). A humanized gnotobiotic mouse model of host-archaeal-bacterial mutualism. Proc. Natl. Acad. Sci. USA. 103(26), 10011-10016. doi: 10.1073/pnas.0602187103.

Samuel, B.S., Hansen, E.E., Manchester, J.K., Coutinho, P.M., Henrissat, B., Fulton, R., et al. (2007). Genomic and metabolic adaptations of *Methanobrevibacter smithii* to the human gut. Proc. Natl. Acad. Sci. USA. 104(25), 10643-10648. doi: 10.1073/pnas.0704189104.

Sankar, S.A., Lagier, J.-C., Pontarotti, P., Raoult, D., and Fournier, P.-E. (2015). The human gut microbiome, a taxonomic conundrum. Syst. Appl. Microbiol. 38, 276-286.

Scheperjans, F., Aho, V., Pereira, P.A.B., Koskinen, K., Paulin, L., Pekkonen, E., et al. (2015). Gut microbiota are related to Parkinson's disease and clinical phenotype. Mov. Disord. 30(3), 350-358. doi: 10.1002/mds.26069.

Schiel-Bengelsdorf, B., and Dürre, P. (2012). Pathway engineering and synthetic biology using acetogens. FEBS Lett. 586(15), 2191-2198. doi: https://doi.org/10.1016/j.febslet.2012.04.043.

Schwartz, M.W., and Hoeksema, J.D. (1998). Specialization and resource trade: Biological markets as a model of mutualisms. Ecology 79(3), 1029-1038.

Schwiertz, A., Taras, D., Schäfer, K., Beijer, S., Bos, N.A., Donus, C., et al. (2010). Microbiota and SCFA in lean and overweight healthy subjects. Obesity 18(1), 190-195. doi: 10.1038/oby.2009.167.

Scott, K.P., Martin, J.C., Duncan, S.H., and Flint, H.J. (2014). Prebiotic stimulation of human colonic butyrate-producing bacteria and bifidobacteria, in vitro. FEMS Microbiol. Ecol. 87(1), 30-40. doi: 10.1111/1574-6941.12186.

Sender, R., Fuchs, S., and Milo, R. (2016). Revised Estimates for the Number of Human and Bacteria Cells in the Body. PLoS Biol. 14(8), e1002533-e1002533. doi: 10.1371/journal.pbio.1002533.

Shitut, S., Ahsendorf, T., Pande, S., Egbert, M., and Kost, C. (2019). Nanotube-mediated cross-feeding couples the metabolism of interacting bacterial cells. Environ. Microbiol. doi: 10.1111/1462-2920.14539.

Song, M., and Chan, A.T. (2017). Diet, Gut Microbiota, and Colorectal Cancer Prevention: a Review of Potential Mechanisms and Promising Targets for Future Research. Curr. Colorectal Cancer Rep. 13(6), 429-439. doi: 10.1007/s11888-017-0389-y.

Stams, A.J.M. (1994). Metabolic interactions between anaerobic bacteria in methanogenic environments. Anton. Leeuw. 66(1-3), 271-294. doi: 10.1007/BF00871644.

Stams, A.J.M., and Plugge, C.M. (2009). Electron transfer in syntrophic communities of anaerobic bacteria and archaea. Nat. Rev. Microbiol. 7(8), 568-577. doi: 10.1038/nrmicro2166.

Stewart, J.A., Chadwick, V.S., and Murray, A. (2006). Carriage, quantification, and predominance of methanogens and sulfate-reducing bacteria in faecal samples. Lett. Appl. Microbiol. 43(1), 58-63. doi: doi:10.1111/j.1472-765X.2006.01906.x.

Stipanuk, M.H., and Caudill, M.A. (2018). Biochemical, Physiological, and Molecular Aspects of Human Nutrition, Fourth Edition. Missouri, USA: Elsevier Health Sciences.

Strocchi, A., Ellis, C.J., Furne, J.K., and Levitt, M.D. (1994a). Study of constancy of hydrogen-consuming flora of human colon. Dig. Dis. Sci. 39(3), 494-497. doi: 10.1007/BF02088333.

Strocchi, A., Furne, J., Ellis, C., and Levitt, M.D. (1994b). Methanogens outcompete sulphate reducing bacteria for H2 in the human colon. Gut 35(8), 1098.

Suarez, F., Furne, J., Springfield, J., and Levitt, M. (1997). Insights into human colonic physiology obtained from the study of flatus composition. Am. J. Physiol. Gastrointest. Liver Physiol. 272(5 35-5), G1028-G1033.

Sun, Z., Koffel, T., Stump, S.M., Grimaud, G.M., and Klausmeier, C.A. (2019). Microbial cross-feeding promotes multiple stable states and species coexistence, but also susceptibility to cheaters. J. Theor. Biol. 465, 63-77. doi: https://doi.org/10.1016/j.jtbi.2019.01.009.

Sung, J., Kim, S., Cabatbat, J.J.T., Jang, S., Jin, Y.S., Jung, G.Y., et al. (2017). Global metabolic interaction network of the human gut microbiota for context-specific community-scale analysis. Nat. Commun. 8. doi: 10.1038/ncomms15393.

Tan, J., McKenzie, C., Potamitis, M., Thorburn, A.N., Mackay, C.R., and Macia, L. (2014). "Chapter Three - The Role of Short-Chain Fatty Acids in Health and Disease," in Adv. Immunol., ed. F.W. Alt. Academic Press, 91-119.

Tap, J., Mondot, S., Levenez, F., Pelletier, E., Caron, C., Furet, J.P., et al. (2009). Towards the human intestinal microbiota phylogenetic core. Environ. Microbiol. 11, 2574-2584.

Thauer, R.K., Jungermann, K., and Decker, K. (1977). Energy conservation in chemotrophic anaerobic bacteria. Bacteriol. Rev. 41(1), 100-180.

Thomas, F., Hehemann, J.-H., Rebuffet, E., Czjzek, M., and Michel, G. (2011). Environmental and Gut Bacteroidetes: The Food Connection. Front. Microbiol. 2, 93. doi: 10.3389/fmicb.2011.00093

Tolker-Nielsen, T., and Molin, S. (2000). Spatial Organization of Microbial Biofilm Communities. Microb. Ecol. 40(2), 75-84.

Tomasova, L., Konopelski, P., and Ufnal, M. (2016). Gut bacteria and hydrogen sulfide: The new old players in circulatory system homeostasis. Molecules 21(11). doi: 10.3390/molecules21111558.

Traverse, C.C., Mayo-Smith, L.M., Poltak, S.R., and Cooper, V.S. (2013). Tangled bank of experimentally evolved *Burkholderia* biofilms reflects selection during chronic infections. Proc. Natl. Acad. Sci. USA. 110(3), E250-E259. doi: 10.1073/pnas.1207025110.

Treves, D.S., Manning, S., and Adams, J. (1998). Repeated evolution of an acetate-crossfeeding polymorphism in long-term populations of *Escherichia coli*. Mol. Biol. Evol. 15(7), 789-797.

Trivers, R.L. (1971). The evolution of reciprocal altruism. Q. Rev. Biol. 46(1), 35-57.

Turnbaugh, P.J., Ley, R.E., Mahowald, M.A., Magrini, V., Mardis, E.R., and Gordon, J.I. (2006). An obesity-associated gut microbiome with increased capacity for energy harvest. Nature 444(7122), 1027-1031. doi: 10.1038/nature05414.

Turroni, F., Milani, C., Duranti, S., Mancabelli, L., Mangifesta, M., Viappiani, A., et al. (2016). Deciphering bifidobacterial-mediated metabolic interactions and their impact on gut microbiota by a multi-omics approach. ISME J. 10(7), 1656-1668. doi: 10.1038/ismej.2015.236.

Van Der Meulen, R., Adriany, T., Verbrugghe, K., and De Vuyst, L. (2006). Kinetic analysis of bifidobacterial metabolism reveals a minor role for succinic acid in the regeneration of NAD+ through its growth-associated production. Appl. Environ. Microbiol. 72(8), 5204-5210. doi: 10.1128/AEM.00146-06.

Van Der Meulen, R., Avonts, L., and De Vuyst, L. (2004). Short Fractions of Oligofructose Are Preferentially Metabolized by *Bifidobacterium animalis* DN-173 010. Appl. Environ. Microbiol. 70(4), 1923-1930. doi: 10.1128/AEM.70.4.1923-1930.2004.

van Hoek, M.J.A., and Merks, R.M.H. (2017). Emergence of microbial diversity due to cross-feeding interactions in a spatial model of gut microbial metabolism. BMC Syst. Biol. 11, Article No. 56. doi: http://dx.doi.org/10.1186/s12918-017-0430-4.

Van Wey, A., Lovatt, S., Roy, N., and Shorten, P. (2016). Determination of potential metabolic pathways of human intestinal bacteria by modeling growth kinetics resulting from cross-feeding. Food Res. Int. 88, 207-216. doi: 10.1016/j.foodres.2016.02.004.

Van Wey, A.S., Cookson, A.L., Roy, N.C., McNabb, W.C., Soboleva, T.K., and Shorten, P.R. (2011). Bacterial biofilms associated with food particles in the human large bowel. Mol. Nutr. Food Res. 55(7), 969-978. doi: 10.1002/mnfr.201000589.

Van Wey, A.S., Cookson, A.L., Soboleva, T.K., Roy, N.C., McNabb, W.C., Bridier, A., et al. (2012). Anisotropic nutrient transport in three-dimensional single species bacterial biofilms. Biotechnol. Bioeng. 109(5), 1280-1292. doi: 10.1002/bit.24390.

Velicer, G.J., and Vos, M. (2009). Sociobiology of the Myxobacteria. Annu. Rev. Microbiol. 63(1), 599-623. doi: 10.1146/annurev.micro.091208.073158.

Venema, K. (2015). "The TNO In Vitro Model of the Colon (TIM-2)," in The Impact of Food Bioactives on Health: in vitro and ex vivo models, eds. K. Verhoeckx, P. Cotter, I. López-Expósito, C. Kleiveland, T. Lea, A. Mackie, T. Requena, D. Swiatecka & H. Wichers. Springer International Publishing, 293-304.

Vernia, P., Caprilli, R., Latella, G., Barbetti, F., Magliocca, F.M., and Cittadini, M. (1988). Fecal Lactate and Ulcerative Colitis. Gastroenterol. 95(6), 1564-1568. doi: https://doi.org/10.1016/S0016-5085(88)80078-7.

Walker, A.W., Duncan, S.H., Carol McWilliam Leitch, E., Child, M.W., and Flint, H.J. (2005). pH and peptide supply can radically alter bacterial populations and short-chain fatty acid ratios within microbial communities from the human colon. Appl. Environ. Microbiol. 71(7), 3692-3700. doi: 10.1128/aem.71.7.3692-3700.2005.

Walker, A.W., Ince, J., Duncan, S.H., Webster, L.M., Holtrop, G., Ze, X., et al. (2011). Dominant and diet-responsive groups of bacteria within the human colonic microbiota. ISME J. 5(2), 220-230. doi: 10.1038/ismej.2010.118.

Wallace, J.L., and Wang, R. (2015). Hydrogen sulfide-based therapeutics: exploiting a unique but ubiquitous gasotransmitter. Nat. Rev. Drug Discov. 14(5), 329-345. doi: 10.1038/nrd4433.
Wang, Y., Huang, W.E., Cui, L., and Wagner, M. (2016). Single cell stable isotope probing in microbiology using Raman microspectroscopy. Curr. Opin. Biotechnol. 41, 34-42. doi: https://doi.org/10.1016/j.copbio.2016.04.018.
Wanner, O., Eberl, H.J., Morgenroth, E., Noguera, D.l.R., Picioreanu, C., Rittmann, B.E., et al. (2006). Mathematical Modeling of Biofilms. London: IWA Publishing.
West, S.A., Diggle, S.P., Buckling, A., Gardner, A., and Griffin, A.S. (2007a). "The social lives of microbes", in: Annu. Rev. Ecol., Evol. Syst.
West, S.A., Griffin, A.S., and Gardner, A. (2007b). Social semantics: Altruism, cooperation, mutualism, strong reciprocity and group selection. J. Evol. Biol. 20(2), 415-432. doi: 10.1111/j.1420-9101.2006.01258.x.
West, S.A., Griffin, A.S., Gardner, A., and Diggle, S.P. (2006). Social evolution theory for microorganisms. Nat. Rev. Microbiol. 4(8), 597-607. doi: 10.1038/nrmicro1461.
White, J.R., Nagarajan, N., and Pop, M. (2009). Statistical Methods for Detecting Differentially Abundant Features in Clinical Metagenomic Samples. PLoS Comp. Biol. 5(4), e1000352. doi: 10.1371/journal.pcbi.1000352.
Widder, S., Allen, R.J., Pfeiffer, T., Curtis, T.P., Wiuf, C., Sloan, W.T., et al. (2016). Challenges in microbial ecology: Building predictive understanding of community function and dynamics. ISME J. 10(11), 2557-2568. doi: 10.1038/ismej.2016.45.
Willis, C.L., Cummings, J.H., Neale, G., and Gibson, G.R. (1996). In vitro effects of mucin fermentation on the growth of human colonic sulphate-reducing bacteria. Anaerobe 2(2), 117-122. doi: 10.1006/anae.1996.0015.
Willis, C.L., Cummings, J.H., Neale, G., and Gibson, G.R. (1997). Nutritional aspects of dissimilatory sulfate reduction in the human large intestine. Curr. Microbiol. 35(5), 294-298. doi: 10.1007/s002849900257.
Windey, K., de Preter, V., and Verbeke, K. (2012). Relevance of protein fermentation to gut health. Mol. Nutr. Food Res. 56(1), 184-196. doi: 10.1002/mnfr.201100542.
Wintermute, E.H., and Silver, P.A. (2010a). Dynamics in the mixed microbial concourse. Genes Dev. 24(23), 2603-2614. doi: 10.1101/gad.1985210.
Wintermute, E.H., and Silver, P.A. (2010b). Emergent cooperation in microbial metabolism. Mol. Syst. Biol. 6, 407. doi: 10.1038/msb.2010.66.
Wolf, P.G., Parthasarathy, G., Chen, J., O'Connor, H.M., Chia, N., Bharucha, A.E., et al. (2017). Assessing the colonic microbiome, hydrogenogenic and hydrogenotrophic genes, transit and breath methane in constipation. Neurogastroenterol. Motil. 29(10), e13056. doi: 10.1111/nmo.13056.
Wolin, M.J., and Miller, T.L. (1983). Interactions of microbial populations in cellulose fermentation. Fed. Proc. 42(1), 109-113.
Yamamura, N., Higashi, M., Behera, N., and Yuichiro Wakano, J. (2004). Evolution of mutualism through spatial effects. J. Theor. Biol. 226(4), 421-428. doi: https://doi.org/10.1016/j.jtbi.2003.09.016.
Yao, C.K., Rotbart, A., Ou, J.Z., Kalantar-Zadeh, K., Muir, J.G., and Gibson, P.R. (2018). Modulation of colonic hydrogen sulfide production by diet and mesalazine utilizing a novel gas-profiling technology. Gut Microbes, 1-13. doi: 10.1080/19490976.2018.1451280.
Ze, X., Duncan, S.H., Louis, P., and Flint, H.J. (2012). Ruminococcus bromii is a keystone species for the degradation of resistant starch in the human colon. ISME J. 6(8), 1535-1543. doi: 10.1038/ismej.2012.4.
Ze, X., Le Mougen, F., Duncan, S.H., Louis, P., and Flint, H.J. (2013). Some are more equal than others: the role of "keystone" species in the degradation of recalcitrant substrates. Gut Microbes 4(3), 236-240.
Zelezniak, A., Andrejev, S., Ponomarova, O., Mende, D.R., Bork, P., and Patil, K.R. (2015). Metabolic dependencies drive species co-occurrence in diverse microbial communities. Proc. Natl. Acad. Sci. USA. 112(20), 6449-6454. doi: 10.1073/pnas.1421834112.
Ziesack, M., Gibson, T., Oliver, J.K.W., Shumaker, A.M., Hsu, B.B., Riglar, D.T., et al. (2019). Engineered Interspecies Amino Acid Cross-Feeding Increases Population Evenness in a Synthetic Bacterial Consortium. mSystems 4(4), e00352-00319. doi: 10.1128/mSystems.00352-19.

Chapter 3: Mathematical models for the growth and hydrogenotrophic metabolism of *Methanobrevibacter smithii*

Abstract

Several studies have suggested that methanogenic Archaea are present in the colon of most of adults and that the majority of these microbes are hydrogenotrophic. Their presence in the colon has been linked to several negative outcomes for the host, including irritable bowel syndrome, constipation and obesity. To complement experimental study, a mathematical model for the predominant colonic methanogen, *Methanobrevibacter smithii*, was developed, that could be used to predict the growth and methane production of this microbe under varied nutrient availabilities. Four modelling techniques were investigated for their efficacy in capturing experimental data: first order kinetics, Monod kinetics, Contois kinetics, and reversible Michaelis-Menten kinetics. Each of these models were fitted to experimental data, with or without the inclusion of an initial lag phase, before comparison to an independent validation data set. All four techniques were able to capture the first experimental data set without the inclusion of a lag phase (R^2>0.90 for fits to hydrogen, methane and growth data). The inclusion of a lag phase was minimally beneficial in some models and detrimental in others, so was not pursued further. In validation against the independent data set, only the Monod and Contois techniques were able to capture the experimental data (R^2>0.80 for fits to hydrogen, methane and growth data), implying that the other techniques were not suitable for modelling *M. smithii* dynamics. The Monod estimated maximum growth rate (0.1042 h^{-1}) and half-saturation constant (10.6 mM) compared well to literature estimates, thus this technique appears well suited for future modelling of colonic methanogens.

3.1 Introduction

Methanogenic Archaea exist in diverse habitats across the planet and their metabolic activity has wide-ranging impacts. For example, hydrogenotrophic methanogens facilitate fermentation of organic matter by microbial communities via their metabolism of hydrogen,

maintaining a low hydrogen partial pressure conducive to fermentation (Enzmann et al., 2018). The methane produced by these methanogens plays a role in climate change, energy production and human health (Thauer et al., 1977; Richards et al., 2016; Chaudhary et al., 2018). Methanogens can form methane from several carbon substrates: carbon dioxide (CO_2), formate, acetate and methylated compounds; several of these reactions require hydrogen as a co-substrate (Thauer et al., 1977; Richards et al., 2016). One habitat where understanding of methanogenic metabolism is limited is the human GIT (Chaudhary et al., 2018).

Several studies have demonstrated that methanogens are present in the colon of all adults (El Oufir et al., 1996; Suarez et al., 1997; Nava et al., 2012), and it is thought that these methanogens are predominantly hydrogenotrophic (Chaudhary et al., 2018). Their role in the colon as hydrogen consumers has proven beneficial to carbohydrate degrading microbes. The presence of a methanogen was shown to reduce the caecal NADH/NAD^+ ratio in mice, likely due to the removal of hydrogen improving the thermodynamic efficiency of NADH oxidation, and thus increasing the efficiency of carbohydrate metabolism (Samuel and Gordon, 2006). On the other hand, methanogen activity in humans has also been associated with negative effects on host function and health. Higher methane production in the colon has been associated with increased GIT transit time (El Oufir et al., 1996) and methanogenesis has also been linked to IBS-C (Chatterjee et al., 2007; Furnari et al., 2012; Ghoshal et al., 2016; Wolf et al., 2017). These studies have been limited to showing associations rather than causality, and generating a deeper understanding of the roles of methanogens in the colon is limited by the challenges associated with the study of the human colonic microbiota *in situ*. Thus, alternative methodologies that can complement experimental work are desirable.

Mathematical modelling is a valuable scientific tool that may accompany experimental work, with the goal of extracting more information from existing knowledge and data. It is therefore especially useful in fields where experimental work is challenging, expensive and labour-intensive. Study of the colonic microbiome is one such field. Faecal data are a useful proxy for the colonic microbiota as direct study and sampling of colonic microbes can be invasive and disruptive. Therefore, it is advantageous to construct mathematical models that can enhance understanding of this field as a complementary approach to *in vitro*, *in vivo* and *in situ* studies. Once validated against

experimental data, these models can be used to make rapid and high-throughput predictions about microbial dynamics.

Deterministic mathematical modelling of microbial growth is a well-established field. Perhaps the most widely used technique is Monod kinetics, which was first published over 70 years ago (Monod, 1949) and remains widely used in the field of microbiota modelling currently. There have been several other techniques developed, often similar in their formulation and adapted for specific cases (see review by Skinner et al. (1994)). As there is no universally optimal model for microbial growth, it is necessary to consider multiple candidate models for each case.

The construction of monoculture mathematical models for the study of human colonic hydrogenotrophs forms the basis for this and the following two Chapters. In each chapter, a highly abundant member of the functional group studied was taken as a representative of the group, and models were tested for their ability to capture experimental growth data for this representative. Here, four mathematical models for the growth of the predominant colonic methanogen *M. smithii* were considered. Also investigated was whether the inclusion of a lag phase in each model was beneficial to the quality of model predictions.

3.2 Methodology

3.2.1 Mathematical models

Each of the models considered is based on a system of ordinary differential equations (ODEs), including equations for the rate of change in substrate concentration (S), microbial cell concentration (X) and product concentration (P). The following model derivations were adapted from Edelstein-Keshet (2005). Logistic-type growth models to a carrying capacity were not investigated, as, in the methanogen experiments considered, microbes were not grown to saturation, therefore a carrying capacity limit was not appropriate.

It was assumed throughout the modelling that there exists some constant yield (Y) of microbial cells per unit substrate consumed, such that

$$Y = \left|\frac{dX}{dS}\right|,$$

the change in concentration of microbial cells per change in substrate concentration. Note that dS will usually be negative, since in simple microbial monocultures the substrate concentration is monotone decreasing.

Next, the specific growth rate of the microbial population, μ, is derived as

$$\mu(t) = \frac{dX}{X(t)\,dt},$$

the proportional change in microbial cell concentration over time. Note that the value of μ is time dependent, as are the concentrations of substrate, product and microbial cells. However, the notation $\mu(t)$ is henceforth replaced with μ for brevity. The same abbreviation is used for the other time dependent variables. Rearranging the equation for specific growth rate gives the ODE for the change in cell concentration:

$$\frac{dX}{dt} = \mu X\,. \tag{3.1}$$

Since $Y = \left|\frac{dX}{dS}\right|$,

$$\frac{dS}{dt} = \frac{dS}{dX}\cdot\frac{dX}{dt} = \frac{1}{-Y}\cdot\mu X = -\frac{\mu X}{Y}, \tag{3.2}$$

which is the ODE for the change in substrate concentration. Note the inclusion of the negative coefficient here, since dS/dt is negative due to the monotone decreasing nature of substrate concentration.

Equations 3.1 and 3.2 form the basis for all further modelling performed in this Chapter. One further equation is for product concentration, which is assumed to be linearly proportional to substrate concentration:

$$\frac{dP}{dt} = b_{SP}\left|\frac{dS}{dt}\right|. \tag{3.3}$$

b_{SP} is a coefficient, often determined by the stoichiometry of the reaction converting substrate into product, and P is monotone increasing as S decreases.

The next step in the construction of the mathematical model was to define the specific growth rate, μ. This value is non-constant, as growth rate depends on several factors, such as the substrate availability and population size at a given time. There are a number of established growth functions, the most applicable of which are defined here.

The concentration of substrate is essential to the growth rate, as once the substrate is depleted growth is completely halted. Therefore, set:

$$\mu = \eta S \tag{3.4}$$

for some fixed rate parameter η. This construction results in rapid growth when substrate is abundant, thereafter reducing proportionally to the reduction in substrate concentration. This model is referred to as the first order kinetics model.

Different microbes have different levels of affinity for certain substrates. In the case of hydrogen, for example, it is known that methanogens can metabolise this substrate at low concentrations at a greater rate than reductive acetogens (Leclerc et al., 1997). The Monod model captures this substrate affinity aspect (Monod, 1949):

$$\mu = \mu_{max}\left(\frac{S}{K_S + S}\right). \tag{3.5}$$

Here, the parameter μ_{max} denotes the maximum possible growth rate of this microbe on this substrate. K_S is the Monod or half-saturation constant, giving the substrate concentration at which the microbe can attain half of its maximum growth rate, μ_{max}. The Monod model is analogous to Michaelis-Menten enzyme kinetics and forces the growth rate to slow when substrate is still available, subject to the size of K_S.

A variation of the Monod model is the Contois model for reduced substrate uptake with high cell density (Contois, 1959). This may be appropriate in environments with limited physical space, where growth will be limited by the space availability. High cell density may also restrict the diffusion of metabolites through the medium or result in a build-up of toxic waste molecules. The Contois growth model is:

$$\mu = \mu_{max}\left(\frac{S}{K_{SX}X + S}\right). \tag{3.6}$$

In this growth rate equation, the half-saturation constant is replaced by the product of X and the parameter K_{SX}, which has different dimensions to K_S, as it is dependent on the cell concentration (see Table 3.1).

Table 3.1. Mathematical notation		
Notation	**Description**	**Unit**
S	Substrate (hydrogen) concentration	mM
X	Cell concentration	mg ml^{-1}
P	Product (methane) concentration	mM
Y	Growth yield	mg ml^{-1} mM^{-1}
t	Time	h
μ	Specific growth rate	h^{-1}
b_{SP}	Production coefficient	-
η	First order kinetics growth rate	mM^{-1} h^{-1}
μ_{max}	Maximum growth rate	h^{-1}
K_S	Monod half-saturation constant	mM
K_{SX}	Contois half-saturation constant	mM ml mg^{-1}
$\mu_{max,S}$	Maximum substrate metabolism rate (reversible Michaelis-Menten kinetics)	h^{-1}
$\mu_{max,P}$	Maximum product metabolism rate (reversible Michaelis-Menten kinetics)	h^{-1}
K_P	Half-saturation constant (product)	mM
q	Lag coefficient	h^{-1}
Q	Lag variable	-

The final growth rate equation presented is based on reversible Michaelis-Menten kinetics (Klipp, 2009). Here, it is assumed that the reaction converting substrate to product is a reversible one, and that the net conversion is dependent upon the metabolite concentrations on each side of the reaction:

$$\mu = \left(\frac{\mu_{max,S} \frac{S}{K_S} - \mu_{max,P} \frac{P}{K_P}}{1 + \frac{S}{K_S} + \frac{P}{K_P}} \right). \quad (3.7)$$

$\mu_{max,S}$ and K_S are the maximum rates and half-saturation constants of the substrate to product reaction, while $\mu_{max,P}$ and K_P are the corresponding values for the reverse reaction. The appropriateness of a reversible reaction for hydrogenotrophic methanogenesis is addressed in the Discussion.

In addition to the differential equations for the concentrations of substrate, product and microbial cells, it can be useful to include a lag equation in the model. Such an equation is used to account for the commonly observed lag phase, a period at the beginning of an experimental culture in which minimal growth occurs. This dynamic can be difficult to model using the previously outlined equations, as the delay may be due to factors unrelated to substrate or population size. For example, exponential population growth may be delayed due to differences between the preculture and culture media (Baranyi et al., 1993). A lag term can be used when the biological cause of the lag

phase is unconfirmed, but must be accounted for to ensure model fit (for example, Noguera et al. (1998)). To account for this delay, the following differential equation, based on (Baranyi et al., 1993), is formulated:

$$\frac{dQ}{dt} = qQ\,. \tag{3.8}$$

The lag model also requires that the specific growth rate, μ, include the following lag term:

$$\frac{Q}{1+Q}.$$

Thus, the value of Q increases exponentially over time, the rate of which is determined by the lag parameter, q. Therefore, the lag term limits the growth rate at initial time according to the initial value of Q, but approaches 1 asymptotically as time increases.

3.2.2 Biological assumptions

To evaluate model performance against experimental data, the monoculture growth of the methanogen *M. smithii* was considered. Data were obtained from Khelaifia et al. (2013) and Muñoz-Tamayo et al. (2019). *M. smithii* was chosen due to its ability to metabolise hydrogen, as well as its status as the predominant methanogen in the human colon (Eckburg et al., 2005; Dridi et al., 2009; Nava et al., 2012). *M. smithii* converts hydrogen (H_2) and carbon dioxide (CO_2) into methane (CH_4) with the following stoichiometry (Thauer et al., 1977):

$$CO_2 + 4H_2 \rightarrow CH_4 + 2H_2O.$$

M. smithii is an excellent candidate for single substrate models, as CO_2 was supplied in abundance in the experiments of Khelaifia et al. (2013) and Muñoz-Tamayo et al. (2019), and hydrogen may be considered the sole limiting substrate. It should be noted that thermodynamic considerations were not included in the model. While it is known that the thermodynamic properties of the culture environment are important for methanogen growth due to the low energy generation associated with hydrogenotrophic methanogenesis (−130 kJ mol^{-1} under standard conditions; Thauer et al. (2008), Richards et al. (2016)), it was found that the techniques used here were sufficient to capture the experimental data. The reader is referred to existing mathematical models in the literature including thermodynamic limitations on methanogenesis for descriptions of these techniques (e.g. Muñoz-Tamayo et al. (2019)). The production of water is also neglected in the models. The model

considers a single microbial strain metabolising a single substrate to a single product. The experimental data used for model calibration are shown in Figure 3.1.

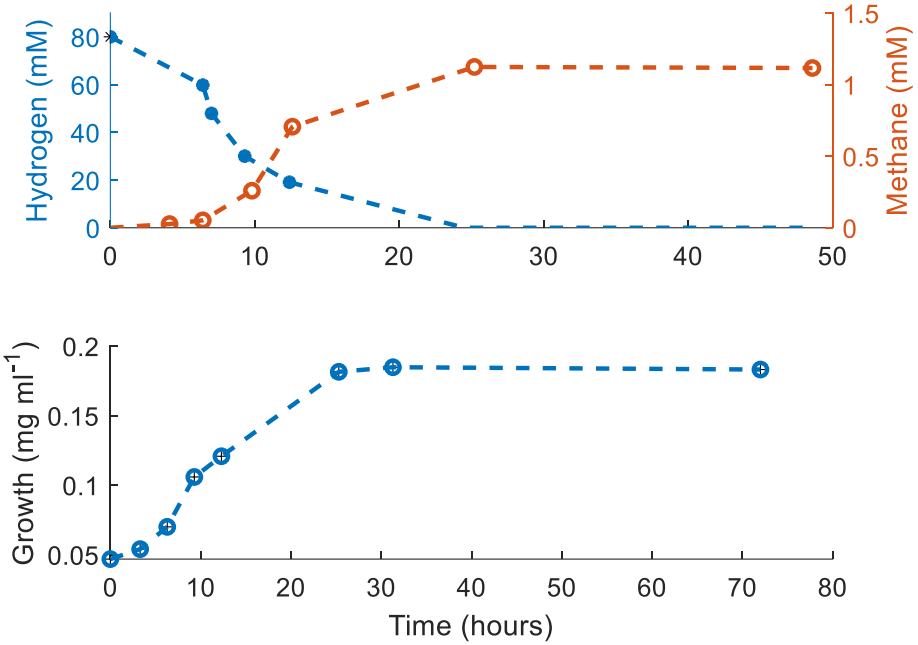

Figure 3.1. *Methanobrevibacter smithii* monoculture data from Khelaifia et al. (2013). Data points are means of triplicate experiments.

3.2.3 Data capture

MATLAB (The MathWorks; www.mathworks.com) was used to collect data from the literature via image capturing. Cell concentration in mg ml^{-1} was determined using the optical density (OD) conversion of: mg ml^{-1} = 0.465 · OD (Richards et al., 2016).

3.2.4 Model fitting

The mathematical model was fitted to the experimental data using a Markov Chain Monte Carlo (MCMC) approach, minimising the sum of the squared residuals for each respective response variable, normalised by the mean of each response variable, thus giving equal weighting to each variable. The fitting was performed using MATLAB (The MathWorks; www.mathworks.com) over 100,000 MCMC iterations. This approach gives a sample of values for each parameter fitted, with the density of samples increasing around the values that give best model fit to the data. 95% confidence intervals were found by fitting a non-parametric distribution to the MCMC sample for each

estimated parameter. Quality of model fit was assessed from R^2 values, with values above 0.80 considered good.

3.3 Results

3.3.1 Model calibration

Models consisting of equations 3.1-3.3 including each of the different growth rate expressions in equations 3.4-3.7 were fitted to the experimental data. The results are shown in Figure 3.2.

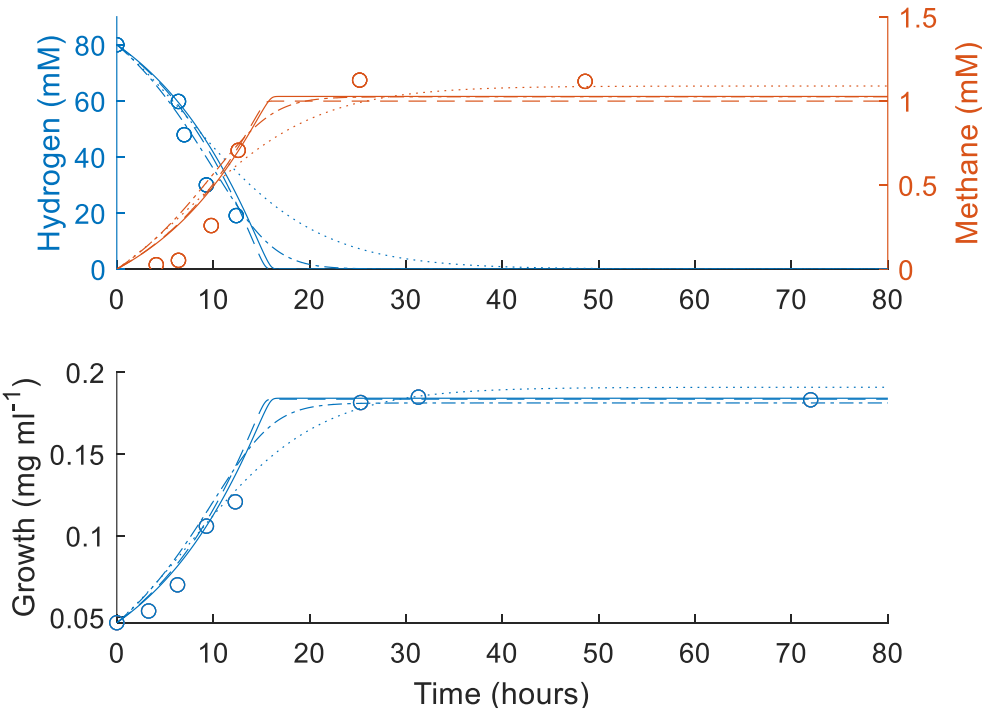

Figure 3.2. Comparison of the four growth rate structures to data from Khelaifia et al. (2013). Dash-dot line: Monod (Hydrogen R^2 = 0.95, Methane R^2 = 0.90, Growth R^2 = 0.97); dotted line: first order kinetics (Hydrogen R^2 = 0.88, Methane R^2 = 0.90, Growth R^2 = 0.98); dashed line: Contois (Hydrogen R^2 = 0.95, Methane R^2 = 0.91, Growth R^2 = 0.97); solid line: reversible Michaelis-Menten (Hydrogen R^2 = 0.92, Methane R^2 = 0.92, Growth R^2 = 0.98).

Table 3.2 lists the parameter values estimated from model fitting. Note that the parameters have units reflective of the experimental data.

Table 3.2. Best fit parameter estimates (with 95% confidence interval in parentheses) for each of the four models considered

Parameter (units)	First order kinetics	Monod	Contois	Reversible Michaelis-Menten
Y (mg ml^{-1} mM^{-1})	0.0018 (0.00097 – 0.00275)	0.00168 (0.00085 – 0.00224)	0.00171 (0.00097 – 0.00267)	0.00172 (0.00107 – 0.00311)
b_{SP} (dimensionless)	0.0136 (0.0085 – 0.0178)	0.0126 (0.0088 – 0.0175)	0.0125 (0.0084 – 0.0175)	0.0128 (0.0084 – 0.0183)
η (mM^{-1} h^{-1})	0.0014 (0.00095 – 0.00233)	-	-	-
μ_{max} (h^{-1})	-	0.1042 (0.082 – 0.304)	0.092 (0.067 – 0.187)	-
K_S (mM)	-	10.6 (15.2 – 132.5)	-	0.8 (1.5 – 52.3)
K_{SX} (mM ml mg^{-1})	-	-	7.32 (37.03 – 456.67)	-
$\mu_{max,S}$ (h^{-1})	-	-	-	0.115 (0.07 – 0.228)
$\mu_{max,P}$ (h^{-1})	-	-	-	0.0008 (0.0017 – 0.0198)
K_P (mM)	-	-	-	1.43 (0.24 – 5.26)

The yield (Y) and methane production coefficient (b_{SP}) parameters show good reliability and consistency between model structures. However, it is clear from the experimental data that the assumed stoichiometry did not match the observed stoichiometry. Following the assumed stoichiometry, approximately 20 mM of methane would be expected to be formed from 80 mM of hydrogen, whereas less than 1.5 mM was measured.

Previous work has found that there can be difficulty in estimating the value of the maximum growth rates (μ_{max}, $\mu_{max,S}$, $\mu_{max,P}$) and the half-saturation constants (K_S, K_{SX}, K_P) from experiments with a single set of initial conditions (Tamayo et al., 2008; Muñoz-Tamayo et al., 2016). In such cases it is often possible only to estimate the ratio of these two parameters. These parameters were estimated with poor repeatability in the Monod, Contois and reversible Michaelis-Menten models, as shown by the broad confidence intervals of these parameter values. There were also instances where the best fit parameter value lay outside the 95% confidence interval estimated by the MCMC. It is possible to circumvent this issue by fixing the value of one of these parameters, usually the half-saturation constant, to a value determined experimentally, where an estimate is

available. Model fitting was performed with the value of K_S fixed in the Monod model, but this did not increase the quality of the model fit to the data (data not shown).

The four models performed similarly in terms of R^2 values when fitted to the experimental data (Figure 3.2). However, all four model structures suffered from lack of fit over the first ten hours. This is noticeable for the growth fit, but most pronounced for the methane fit. This could be caused by a time delay between the production of methane and its detection in the gaseous phase during the experiment, as methane is produced in the aqueous phase but was measured in the gaseous phase. The lack of fit could also be caused by some initial lag phase in the growth and metabolism of *M. smithii*, therefore the incorporation of a lag term in the models was investigated. Figure 3.3 shows the model fits to the data when equation 3.8 and a lag term were added.

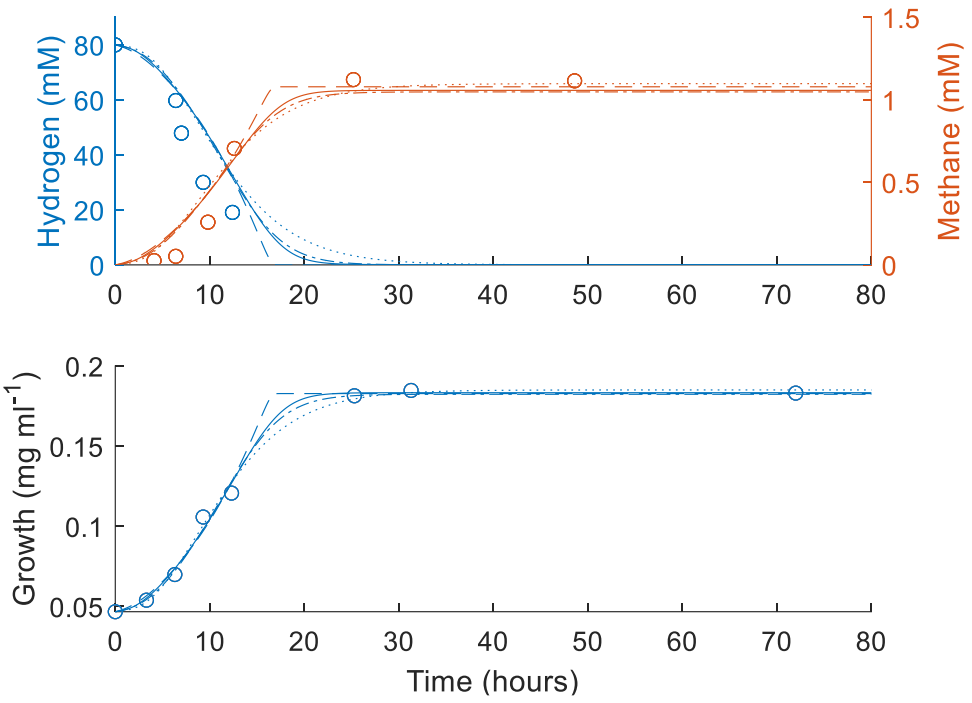

Figure 3.3. Comparison of the four growth rate structures to data from Khelaifia et al. (2013) with a lag phase included. Dash-dot line: Monod (Hydrogen R^2 = 0.85, Methane R^2 = 0.96, Growth R^2 = 0.99); dotted line: first order kinetics (Hydrogen R^2 = 0.85, Methane R^2 = 0.95, Growth R^2 = 0.99); dashed line: Contois (Hydrogen R^2 = 0.85, Methane R^2 = 0.96, Growth R^2 = 0.99); solid line: reversible Michaelis-Menten (Hydrogen R^2 = 0.85, Methane R^2 = 0.95, Growth R^2 = 0.99).

The addition of the lag phase further reduced the variation between the predictions of the four model structures. In all four cases, the fit to the growth and methane data was improved by the inclusion of the lag phase, whereas the accuracy of the fit to the hydrogen data was reduced. It is not clear what caused this discrepancy between the hydrogen and methane data, but it is possible

that gas-liquid transfer of both hydrogen and methane, which is not accounted for in this model, is responsible. If the rate of transfer of these metabolites was limiting to the reaction rate or causing a delay between methane production and its measurement in the experiment, the model would not be expected to capture this. The addition of mass transfer to the model would require further model parameters for this phenomenon, for which data were not available. Also, due to the current R^2 values of 0.85 and above, this addition would minimally improve the predictive power of this model.

Table 3.3. Best fit parameter estimates (with 95% confidence interval in parentheses) for each of the four models considered after inclusion of a lag phase

Parameter (units)	**First order kinetics**	**Monod**	**Contois**	**Reversible Michaelis-Menten**
Y (mg ml^{-1} mM^{-1})	0.0017 (0.00077 – 0.00289)	0.00169 (0.00078 – 0.00295)	0.0017 (0.00078 – 0.00293)	0.0017 (0.0008 – 0.003)
b_{SP} (dimensionless)	0.0137 (0.0074 – 0.0186)	0.0131 (0.0077 – 0.0192)	0.0135 (0.0078 – 0.019)	0.0132 (0.0076 – 0.0195)
ɳ (mM^{-1} h^{-1})	0.00192 (0.00094 – 0.02067)			
μ_{max} (h^{-1})		0.215 (0.22 – 4.685)	0.093 (0.054 – 0.219)	
K_S (mM)		58.4 (88.8 – 2390.1)		5.9 (4.1 – 143.4)
K_{SX} (mM ml mg^{-1})			7.3 (4.7 – 301.9)	
$\mu_{max,S}$ (h^{-1})				0.112 (0.074 – 0.463)
$\mu_{max,P}$ (h^{-1})				0.0071 (0.0054 – 0.1741)
K_P (mM)				0.44 (0.36 – 9.01)
q (h^{-1})	0.865 (0.029 – 10.705)	0.665 (0.296 – 9.886)	0.812 (0.115 – 9.83)	1.033 (0.214 – 9.887)
Initial Q (dimensionless)	0.069 (0.007 – 2.342)	0.189 (0.039 – 2.615)	0.484 (0.089 – 5.728)	0.171 (0.031 – 4.325)

The parameter values generated from model fitting with a lag phase are given in Table 3.3. Once again, the yield (Y) and methane production coefficient (b_{SP}) parameters are consistent across both the original and the lag model structures. The remaining parameters showed more significant variation between the original and lag models. Similar issues with the repeatability of parameter estimates were observed using either the original or the lag structure. Additionally, the confidence intervals for the lag parameter and the initial value of Q were broad, showing poor repeatability of these estimates.

3.3.2 Model validation

To validate the predictions of the models, data for the growth of *M. smithii* from independent experiments with differing culture conditions were obtained from Muñoz-Tamayo et al. (2019). The experimental data are shown in Figure 3.4.

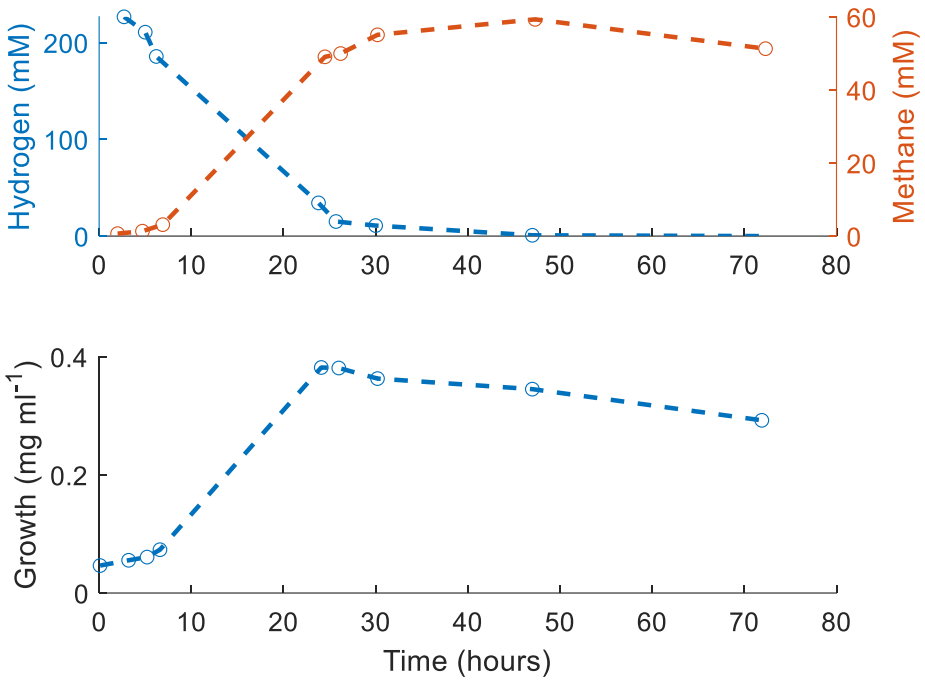

Figure 3.4. *Methanobrevibacter smithii* monoculture data from Muñoz-Tamayo et al. (2019).

The stoichiometry of methane produced per mol hydrogen consumed was not equal to the b_{SP} values obtained from the first data set. Here, this value seems to be closer to the stoichiometric value of 1 mol methane produced from 4 mol hydrogen given in section 3.2.2. Possible reasons for this are outlined in the Discussion. The value of b_{SP} was fixed at 0.25 for the validation experiments.

There also appeared to be a reduction in the cell concentration over time after a peak concentration observed between 20 and 30 hours in the validation data set. This was likely caused by cell death, which was not observed in the calibration data set, and therefore was omitted in the models.

Figure 3.5 shows the predictions of the four model structures against the validation data. The first order kinetics model predicted dynamics that were more rapid than those observed experimentally, whereas the other three models performed well. The major flaw in their predictions

was the failure to predict the decrease in cell concentration in the later stages of the experiment, which could not be captured under the model assumptions.

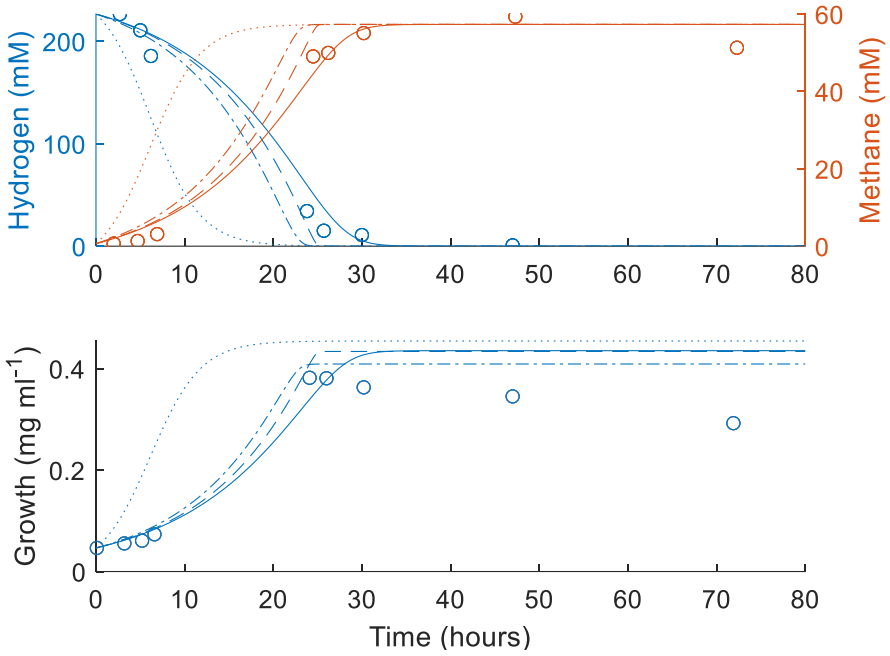

Figure 3.5. Comparison of the four growth rate structures predictions for the validation data set of Muñoz-Tamayo et al. (2019). Dash-dot line: Monod (Hydrogen R^2 = 0.98, Methane R^2 = 0.96, Growth R^2 = 0.89); dotted line: first order kinetics (Hydrogen R^2 = 0.89, Methane R^2 = 0.78, Growth R^2 = 0.47); dashed line: Contois (Hydrogen R^2 = 0.99, Methane R^2 = 0.97, Growth R^2 = 0.81); solid line: reversible Michaelis-Menten (Hydrogen R^2 = 0.98, Methane R^2 = 0.98, Growth R^2 = 0.82).

Figure 3.6 shows the predictions of the models with the inclusion of the lag phase. Once again, the first order kinetics model performed poorly, but was improved by the inclusion of the lag phase. The Contois model predictions improved, while the Monod model was less accurate with the lag phase. The reversible Michaelis-Menten kinetics model was the most affected by the inclusion of the lag phase, giving poor predictions of the experimental data. This was due to the change in the value of b_{SP}, as the specific growth rate for this model is influenced by the methane concentration, which was higher in the validation data set than in the calibration data set.

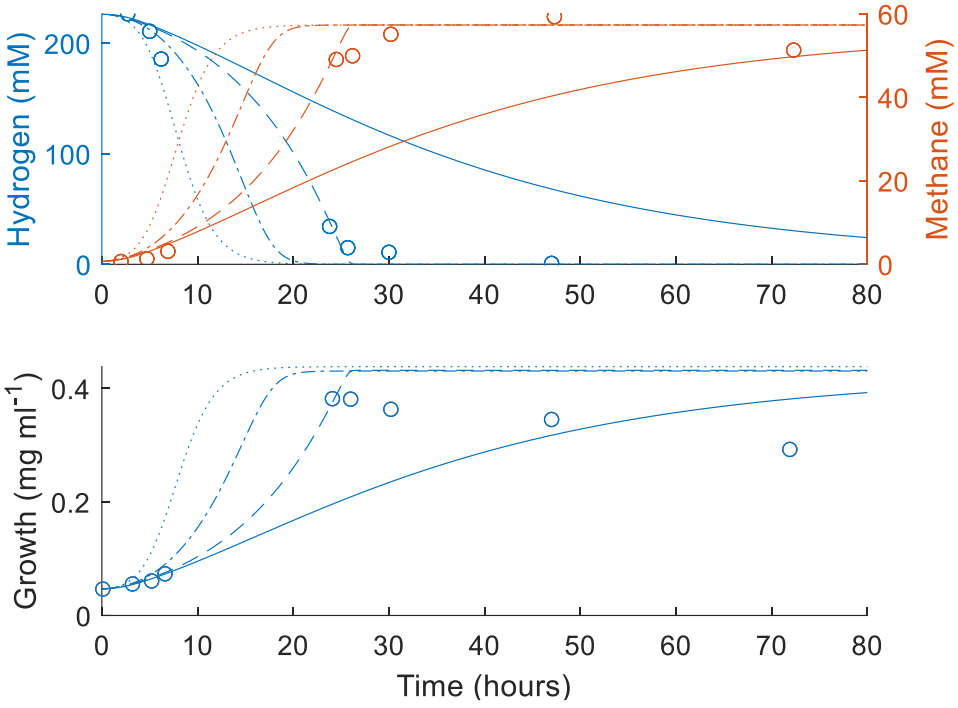

Figure 3.6. Comparison of the four growth rate structures including a lag phase to the validation data set of Muñoz-Tamayo et al. (2019). Dash-dot line: Monod (Hydrogen R^2 = 0.97, Methane R^2 = 0.96, Growth R^2 = 0.82); dotted line: first order kinetics (Hydrogen R^2 = 0.97, Methane R^2 = 0.90, Growth R^2 = 0.73); dashed line: Contois (Hydrogen R^2 = 0.99, Methane R^2 = 0.98, Growth R^2 = 0.83); solid line: reversible Michaelis-Menten (Hydrogen R^2 = 0.41, Methane R^2 = 0.52, Growth R^2 = 0.55).

3.4 Discussion

All four of the model structures considered were able to accurately capture the growth and metabolic dynamics of a simple single substrate, single product, monoculture experiment. Simplifying the metabolism of the methanogen *M. smithii* as performed here allowed for the creation of models that were both simple and accurate. Moreover, model structures that could capture the independent validation data for the same microbe grown under different conditions were identified.

Of the four model structures investigated, the Monod and Contois models were the most suitable for modelling the experiments studied here. In terms of goodness of fit, R^2 values for both models were above 0.8 in all simulations. The Monod model also has the advantage of biologically tangible parameters, which can be easily interpreted in an experimental setting. The first order kinetics model, although advantageous in that it requires the least number of fitting parameters, did not perform well against the validation data set. The reversible Michaelis-Menten kinetics model

was comparable to the Monod and Contois models in all simulations except for the prediction of the validation data set with the inclusion of a lag phase.

The addition of a lag phase to the models was of limited value. It had a minimal effect on the models during calibration, and on the Monod and Contois models in the validation simulations. It also adds a further ODE (that can be solved $Q = Q_0 \exp(qt)$, where Q_0 is the value of Q at initial time), as well as an extra initial condition (Q_0) and parameter (q) that must be fitted for each model, the values of which have no direct biological interpretation and are designed as a technique to produce slower initial dynamics. Although other lag models do exist, these are more complex and have been shown to perform similarly (Huang, 2013).

Due to the uncertainty of the cause behind the lag phase, the lag parameter and initial condition may also be expected to vary between experiments. If the lag phase were caused by differences in constituents of the culture medium, for example, different length lag phases would be expected in different media. The two data sets used here were obtained using differing culture media, therefore the availability of essential nutrients would likely not have been consistent between the two. The lag phase may reasonably be expected to differ as a result. Given the results of the models, the inclusion of a lag phase in future *M. smithii* modelling with similar data sets does not appear necessary or beneficial.

It is unclear why the value of b_{SP} was so different between the two experiments considered. For the calibration data set, b_{SP} was set as a fitting parameter, whereas in the validation experiment the stoichiometry found in the literature was sufficient. Again, this difference may be due to the growth medium used in the calibration experiment, which was more complex than that used in the validation experiment. Hydrogen may have been involved in other metabolic pathways during the calibration experiment, leading to different end metabolites, but hydrogen and methane were the only metabolites measured so this cannot be included in the models. However, the assumption of the stoichiometry is only important for the fit to the methane data; it has no influence on model fitting for the maximum growth rate, half-saturation constant or growth yield.

Another discrepancy between the two data sets was the clear reduction in cell concentration observed in the validation set, which was more pronounced than that of the

calibration data. Cell death was not included in the models, but could be included as a constant term proportional to the cell concentration. Inclusion of such a term would enable a better fit to the cell concentration data in the validation experiment but would be estimated to be negligible for the calibration data set.

The model estimates for the half-saturation constant (K_S) showed poor reliability in the MCMC estimation. Estimates of this value in the literature vary, but the Monod model estimate of 10.6 mM is comparable to the 32 mM estimated for *M. smithii* by Muñoz-Tamayo et al. (2019). Using their experimental data, Muñoz-Tamayo et al. (2019) found a maximum growth rate for *M. smithii* of 0.12 h^{-1}, which compares well with the Monod estimate of 0.1042 h^{-1} and is within the obtained 95% confidence interval. However, the poor reliability of these values is a limitation of the model that would require more detailed data to address, such as dissolved metabolite concentrations. The model is also limited to the consideration of only hydrogen and methane as metabolites, so cannot be applied to instances where CO_2 is limiting, or when methane is produced from alternative substrates. These conditions would require individual parameterisation from relevant data sources, but are beyond the scope of this study of hydrogen metabolism.

3.5 Conclusions

Four mathematical model structures for methanogen growth were constructed and compared and it was found that two of these structures could be validated against independent experimental data. The methanogen model can be combined with similar structures for other microbes to give predictions on the metabolic and growth behaviour of these organisms in the colon, where they may cross-feed or compete with one another for nutrients. The ultimate goal of these models is to provide predictions that can be used to guide experimental work and lead to a greater understanding of the role of hydrogen cross-feeding microbes in host nutrition and health.

References

Baranyi, J., Roberts, T.A., and McClure, P. (1993). A non-autonomous differential equation to model bacterial growth. Food Microbiol. 10(1), 43-59. doi: 10.1006/fmic.1993.1005.

Chatterjee, S., Park, S., Low, K., Kong, Y., and Pimentel, M. (2007). The Degree of Breath Methane Production in IBS Correlates With the Severity of Constipation. Am. J. Gastroenterol. 102, 837. doi: 10.1111/j.1572-0241.2007.01072.x.

Chaudhary, P.P., Conway, P.L., and Schlundt, J. (2018). Methanogens in humans: potentially beneficial or harmful for health. Appl. Microbiol. Biotechnol. 102(7), 3095-3104. doi: 10.1007/s00253-018-8871-2.

Contois, D. (1959). Kinetics of bacterial growth: relationship between population density and specific growth rate of continuous cultures. Microbiology 21(1), 40-50.

Dridi, B., Henry, M., El Khéchine, A., Raoult, D., and Drancourt, M. (2009). High Prevalence of *Methanobrevibacter smithii* and *Methanosphaera stadtmanae* Detected in the Human Gut Using an Improved DNA Detection Protocol. PLoS ONE 4(9), e7063. doi: 10.1371/journal.pone.0007063.

Eckburg, P.B., Bik, E.M., Bernstein, C.N., Purdom, E., Dethlefsen, L., Sargent, M., et al. (2005). Microbiology: Diversity of the human intestinal microbial flora. Science 308(5728), 1635-1638. doi: 10.1126/science.1110591.

Edelstein-Keshet, L. (2005). Mathematical models in biology. Philadelphia : Society for Industrial and Applied Mathematics, 2005.

El Oufir, L., Flourié, B., Bruley des Varannes, S., Barry, J.L., Cloarec, D., Bornet, F., et al. (1996). Relations between transit time, fermentation products, and hydrogen consuming flora in healthy humans. Gut 38(6), 870-877.

Enzmann, F., Mayer, F., Rother, M., and Holtmann, D. (2018). Methanogens: biochemical background and biotechnological applications. AMB Express 8(1), 1. doi: 10.1186/s13568-017-0531-x.

Furnari, M., Savarino, E., Bruzzone, L., Moscatelli, A., Gemignani, L., Gianini, E.G., et al. (2012). Reassessment of the role of methane production between irritable bowel syndrome and functional constipation. J. Gastrointestin. Liver Dis. 21(2), 157-163.

Ghoshal, U., Shukla, R., Srivastava, D., and Ghoshal, U.C. (2016). Irritable bowel syndrome, particularly the constipation-predominant form, involves an increase in *Methanobrevibacter smithii*, which is associated with higher methane production. Gut Liver 10(6). doi: 10.5009/gnl15588.

Huang, L. (2013). Optimization of a new mathematical model for bacterial growth. Food Control 32(1), 283-288. doi: https://doi.org/10.1016/j.foodcont.2012.11.019.

Janssen, P.H. (2010). Influence of hydrogen on rumen methane formation and fermentation balances through microbial growth kinetics and fermentation thermodynamics. Anim. Feed Sci. Technol. 160(1), 1-22. doi: https://doi.org/10.1016/j.anifeedsci.2010.07.002.

Khelaifia, S., Raoult, D., and Drancourt, M. (2013). A Versatile Medium for Cultivating Methanogenic Archaea. PLoS ONE 8(4), e61563. doi: 10.1371/journal.pone.0061563.

Klipp, E. (2009). Systems biology : a textbook. Weinheim : Wiley-VCH, 2009.

Leclerc, M., Bernalier, A., Donadille, G., and Lelait, M. (1997). H2/CO2 Metabolism in Acetogenic Bacteria Isolated From the Human Colon. Anaerobe 3(5), 307-315. doi: https://doi.org/10.1006/anae.1997.0117.

Monod, J. (1949). The Growth of Bacterial Cultures. Ann. Rev. Microbiol. 3(1), 371-394. doi: 10.1146/annurev.mi.03.100149.002103.

Muñoz-Tamayo, R., Giger-Reverdin, S., and Sauvant, D. (2016). Mechanistic modelling of in vitro fermentation and methane production by rumen microbiota. Anim. Feed Sci. Technol. 220, 1-21. doi: https://doi.org/10.1016/j.anifeedsci.2016.07.005.

Muñoz-Tamayo, R., Popova, M., Tillier, M., Morgavi, D.P., Morel, J.P., Fonty, G., et al. (2019). Hydrogenotrophic methanogens of the mammalian gut: Functionally similar, thermodynamically different-A modelling approach. PLoS ONE 14(12). doi: 10.1371/journal.pone.0226243.

Nava, G.M., Carbonero, F., Croix, J.A., Greenberg, E., and Gaskins, H.R. (2012). Abundance and diversity of mucosa-associated hydrogenotrophic microbes in the healthy human colon. ISME J. 6(1), 57-70. doi: 10.1038/ismej.2011.90.

Noguera, D.R., Brusseau, G.A., Rittmann, B.E., and Stahl, D.A. (1998). A unified model describing the role of hydrogen in the growth of *Desulfovibrio vulgaris* under different environmental conditions. Biotechnol. Bioeng. 59(6), 732-746. doi: 10.1002/(SICI)1097-0290(19980920)59:6<732::AID-BIT10>3.0.CO;2-7.

Richards, M.A., Lie, T.J., Zhang, J., Ragsdale, S.W., Leigh, J.A., and Price, N.D. (2016). Exploring Hydrogenotrophic Methanogenesis: a Genome Scale Metabolic Reconstruction of *Methanococcus maripaludis*. J. Bacteriol. 198(24), 3379. doi: 10.1128/JB.00571-16.

Samuel, B.S., and Gordon, J.I. (2006). A humanized gnotobiotic mouse model of host-archaeal-bacterial mutualism. Proc. Natl. Acad. Sci. USA. 103(26), 10011-10016. doi: 10.1073/pnas.0602187103.

Skinner, G.E., Larkin, J.W., and Rhodehamel, E.J. (1994). Mathematical Modelling of Microbial Growth: A Review. J. Food Saf. 14(3), 175-217. doi: 10.1111/j.1745-4565.1994.tb00594.x.

Suarez, F., Furne, J., Springfield, J., and Levitt, M. (1997). Insights into human colonic physiology obtained from the study of flatus composition. Am. J. Physiol. Gastrointest. Liver Physiol. 272(5 35-5), G1028-G1033.

Tamayo, R.M., Laroche, B., Leclerc, M., and Walter, E. (2008). "Modelling and identification of in vitro homoacetogenesis by human-colon bacteria", in: 2008 16th Mediterranean Conference on Control and Automation, 1717-1722.

Thauer, R.K., Jungermann, K., and Decker, K. (1977). Energy conservation in chemotrophic anaerobic bacteria. Bacteriol. Rev. 41(1), 100-180.

Thauer, R.K., Kaster, A.-K., Seedorf, H., Buckel, W., and Hedderich, R. (2008). Methanogenic archaea: ecologically relevant differences in energy conservation. Nat. Rev. Microbiol. 6(8), 579-591. doi: 10.1038/nrmicro1931.

Wolf, P.G., Parthasarathy, G., Chen, J., O'Connor, H.M., Chia, N., Bharucha, A.E., et al. (2017). Assessing the colonic microbiome, hydrogenogenic and hydrogenotrophic genes, transit and breath methane in constipation. Neurogastroenterol. Motil. 29(10), e13056. doi: 10.1111/nmo.13056.

The following chapter contains material from:

Smith NW, Shorten PR, Altermann E, Roy NC, McNabb WC (2019): A Mathematical Model for the Hydrogenotrophic Metabolism of Sulphate-Reducing Bacteria. Frontiers in Microbiology 10:1652. https://doi.org/10.3389/fmicb.2019.01652

Chapter 4: A mathematical model for the growth of the sulphate-reducing bacterium *Desulfovibrio vulgaris*

Abstract

Sulphate-reducing bacteria (SRB) are studied across a range of scientific fields due to their characteristic ability to metabolise sulphate and produce hydrogen sulphide, which can lead to significant consequences for human activities. Importantly, they are members of the human gastrointestinal microbial population, contributing to the metabolism of dietary and host secreted molecules found in this environment. The role of the microbiota in host digestion is well studied, but the full role of SRB in this process has not been established. Moreover, from a human health perspective, SRB have been implicated in a number of functional gastrointestinal disorders such as Irritable Bowel Syndrome and the development of colorectal cancer. To assist with the study of SRB, a mathematical model is presented for the growth and metabolism of the well-studied SRB, *Desulfovibrio vulgaris* in a closed system. Previous attempts to model SRB have resulted in complex or highly specific models that are not easily adapted to the study of SRB in different environments, such as the gastrointestinal tract. Here, a simpler, Monod-based model is proposed that allows for easy alteration of both key parameter values and the governing equations to enable model adaptation. To prevent any incorrect assumptions about the nature of SRB metabolic pathways, the model was structured to consider only the concentrations of initial and final metabolites in a pathway, which circumvents the current uncertainty around hydrogen cycling by SRB. The model was parameterised using experiments with varied initial substrate conditions, obtaining parameter values that compared well with experimental estimates in the literature. The model was then validated against four independent experiments involving *D. vulgaris* with further variations to substrate availability. Further use of the model will be possible in a number of settings, notably as part of larger models studying the metabolic interactions between SRB and other hydrogenotrophic microbes in the human gastrointestinal tract.

4.1 Introduction

The SRB play an important role in a variety of ecosystems, from marine sediments and oil fields to the human colon (Muyzer and Stams, 2008; Carbonero et al., 2012a). The functional group of SRB has been reported to comprise 60 genera (Barton and Fauque, 2009), and is characterised by the ability to utilise sulphate as an electron acceptor during metabolism. The presence of these microbes has both positive and negative implications on human activities, depending on the context. Much research has been performed on H_2S production in oil fields by SRB, which can lead to reduced oil quality and machinery corrosion (Magot et al., 2000), and in the treatment of industrial wastewater, as the sulphides produced by SRB facilitate the removal of contaminating heavy metals (Kiran et al., 2017). Less clear are the implications of SRB in the colon. The SRB population size in the colon has been measured at approximately 10^7 cells per gram of faeces (Doré et al., 1995), but varies between individuals and between studies (Nava et al., 2012). These microbes are widely studied due to their controversial role in a number of functional gastrointestinal disorders. Increased levels of colonic SRB and increased H_2S concentrations have been linked to IBS, IBD and CRC (for a review, see Carbonero et al. (2012b)). However, beneficial effects of H_2S have also been investigated, such as its capacity to stimulate mucous production (Motta et al., 2015) and the potential influence of this molecule on blood pressure regulation (Tomasova et al., 2016). The important connections between SRB, H_2S and the host justify further research into the metabolism of these microbes.

Another key molecule in SRB metabolism is elemental hydrogen. Alongside methanogens and reductive acetogens, SRB can metabolise free hydrogen present in the colon, utilising it in the reduction of sulphate. The sulphate metabolised by SRB can be dietary or host-derived; cross-feeding by SRB on sulphate released during mucin metabolism by other colonic microbes has been well studied (Willis et al., 1996; Rey et al., 2013). High concentrations of hydrogen in the colon are known to inhibit the metabolism of saccharolytic members of the microbiota (Wolin and Miller, 1983), therefore the presence of hydrogen cross-feeders is thought to increase the rate of carbohydrate breakdown by the wider microbial population. This has been shown in rodent models and linked to increased energy yield for the host (Samuel and Gordon, 2006; Rey et al., 2010).

Due to the importance of SRB in human health and nutrition, a greater understanding of their metabolism and growth dynamics is sought. To this end, a mathematical model for the metabolite flux and population growth of the human SRB *Desulfovibrio vulgaris*, grown on substrates found in the colon, was developed. This is not the first attempt to model SRB metabolism and growth and the predictions of the newly developed model are compared with those of the existing mathematical model of Noguera et al. (1998). Many other mathematical models of SRB have been published, but these are almost universally applied to address specific characteristics of SRB or for the investigation of competitive and syntrophic relationships between SRB and methanogens (for example, Robinson and Tiedje (1984), Okabe et al. (1995) and Stolyar et al. (2007)). The model of Noguera et al. (1998) is not targeted to a specific characteristic or environment, therefore was a good benchmark against which to compare the new model. The existing model is more complex than that proposed here: it consists of ten ODEs for aqueous and gaseous metabolite concentrations and microbial growth and is dependent on 20 parameter values that are estimated either from separate experimental work or from model fitting. While the existing model considers many aspects of the metabolism of *D. vulgaris*, it is computationally intensive and requires greater knowledge of kinetic parameters than is often available in environments such as the colon. Therefore, its structure is less readily compared or combined with other existing models for the colonic microbiota. It was also found that the existing model shows sensitivity to the initial values for dissolved hydrogen and carbonate concentrations; values that are difficult to determine experimentally and physiologically. To facilitate study of SRB in the colon, the newly developed model is simpler and requires less inputs, allowing future integration into a larger microbiota model. The new SRB model considers solely the concentrations of the initial and final metabolites in a metabolic pathway, treating the intermediate metabolites and reactions as a 'black box'. The model was calibrated using existing experimental data for the monoculture growth of a *D. vulgaris* strain and then used to predict the dynamics of separate independent experiments with both the same bacterium and a different *D. vulgaris* strain.

4.2 Methodology

4.2.1 Assumptions

For this model it was assumed that the only metabolites involved in the metabolism of *D. vulgaris* are lactate, acetate, hydrogen, sulphate and H_2S, as these metabolites represent important initial and final metabolites in the major metabolic pathways of *D. vulgaris* (Keller and Wall, 2011). Other metabolic pathways involving fermentation of alternative organic molecules, such as monosaccharides and fatty acids, and reduction of nitrogenous compounds have been studied in *Desulfovibrio* and other SRB genera, but appear to be of lesser importance and not widespread within the functional group (Barton and Fauque, 2009). While formate has been implicated in the metabolism of *Desulfovibrio* species elsewhere (da Silva et al., 2013; Junicke et al., 2015; Martins et al., 2015), here it was assumed that formate may be represented as hydrogen equivalents. This is supported by the similar reduction potentials of formate and hydrogen, allowing for interconversion of the two molecules at low energetic cost to the bacterium (Stams and Plugge, 2009; da Silva et al., 2013; Rabus et al., 2013). Formate concentrations also remained low (<0.5 mM) in previous experiments with *D. vulgaris* Hildenborough grown on either lactate and sulphate or lactate and hydrogen (da Silva et al., 2013).

It was assumed that the medium in which *D. vulgaris* was grown contained in abundance all other molecules necessary for growth and that these were not significantly depleted during the experiment. Further, it was assumed that *D. vulgaris* is able to oxidise lactate incompletely to acetate, with concurrent production of hydrogen (Keller and Wall, 2011). This hydrogen may then be utilised in the reduction of sulphate to H_2S. All metabolites were assumed to remain in the aqueous phase, with the exception of hydrogen, which may transfer between the aqueous and gaseous phases. Finally, it was assumed that all metabolites in the aqueous phase were available to the microbes in a well-mixed solution. No spatial component was considered in the model.

The assumed stoichiometries for the two reactions, expressing all protons as hydrogen molecule equivalents, are as follows (Thauer et al., 1977; Noguera et al., 1998; da Silva et al., 2013):

$$CH_3CHOHCOO^-\ (\text{Lactate}) + 2\ H_2O \rightarrow CH_3COO^-\ (\text{Acetate}) + 2.5\ H_2 + HCO_3^-\ (\text{Bicarbonate})$$

SO_4^{2-} (Sulphate) + $5H_2 \rightarrow H_2S + 4\ H_2O$

Note that the bicarbonate molecule produced in the oxidation of lactate and the water molecules produced in the reduction of sulphate were not included in the model, as they play no further role in the metabolism of *D. vulgaris*. Moreover, the culture was assumed well buffered throughout the experiment, therefore pH was not altered by changing concentrations of bicarbonate or other metabolites. There have been reports of bicarbonate as a growth-limiting molecule for other microbial strains (Dobay et al., 2018), but there is currently no evidence of this for SRB. This is further explained in the Discussion.

4.2.2 Mathematical model

The model is based on Monod kinetics for microbial growth in a batch culture environment (Monod, 1949). Monod kinetics was chosen due to the biological meaning associated with the parameters, as well as the ability to determine these values experimentally if required. The model considers the molar concentration of lactate, acetate, sulphate and H_2S, as well as the molar concentration of hydrogen in the aqueous phase and the partial pressure of hydrogen in the gaseous phase, measured in atmospheres. It also considers the concentration of the microbial population in the aqueous phase (mg L^{-1}). These units were chosen to align with data sources for both the calibration and validation of the model. Figure 4.1 shows the general structure of the model.

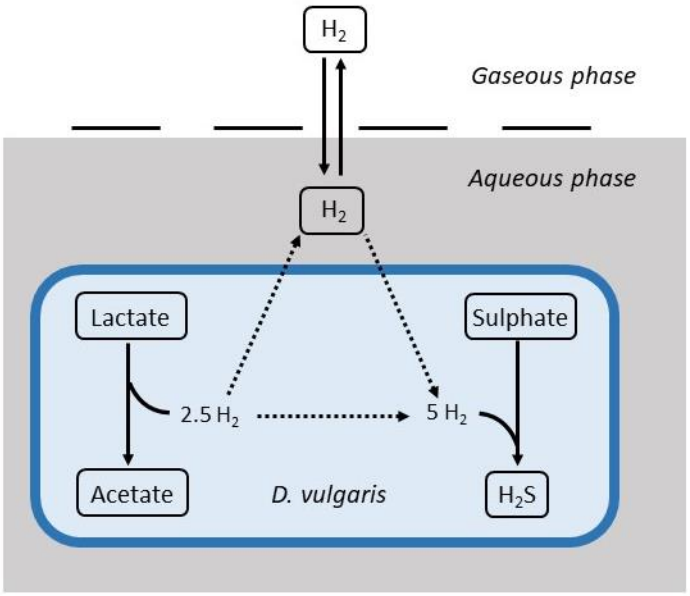

Figure 4.1 Structure of the mathematical model. Solid arrows denote modelled dynamics. Dotted arrows denote dynamics that are not explicitly modelled.

Following Monod kinetics, the rate of change in lactate concentration (L; mM) is modelled by:

$$\frac{dL}{dt} = -\frac{\mu_{max,L}\, X}{Y_L}\left(\frac{L}{K_L + L}\right) \tag{4.1}$$

where $\mu_{max,L}$ (h^{-1}) denotes the maximum growth rate and Y_L (mg L^{-1} mM^{-1}) denotes the biomass yield of *D. vulgaris* when grown on lactate. K_L (mM) is the Monod constant for this microbe and substrate, also referred to as the half-saturation constant. This value is the concentration of substrate required for the microbe to attain half of its maximum growth rate. X (mg L^{-1}) is the concentration of microbial cells in the medium.

It is known that high concentrations of hydrogen in the medium inhibit the metabolism of lactate by certain SRB, including *D. vulgaris*, although the mechanism is not clear (Pankhania et al., 1988; Junicke et al., 2015). As such, an inhibition term is added to the model that reduces the rate of lactate metabolism as the aqueous hydrogen concentration, H_{aq} (mM), increases. Equation 4.1 then becomes:

$$\frac{dL}{dt} = -\frac{\mu_{max,L}\, X}{Y_L}\left(\frac{L}{K_L + L}\right)\left(1 - \frac{H_{aq}}{H_{max}}\right) \tag{4.2}$$

where H_{max} (mM) is the aqueous hydrogen concentration above which lactate degradation is completely inhibited. This formulation also ensures that the rate of lactate degradation reduces proportionally to the aqueous hydrogen concentration. To ensure that the model is robust to hydrogen concentrations above H_{max}, the following condition is added:

$\frac{dL}{dt} = 0$ when $H_{aq} > H_{max}$.

The sulphate concentration (S; mM) is given by:

$$\frac{dS}{dt} = -\frac{\mu_{max,S}\, X}{Y_S}\left(\frac{S}{K_S + S}\right)\left(\frac{H_{aq}}{K_H + H_{aq}}\right). \tag{4.3}$$

Sulphate and hydrogen are both required for the formation of H_2S, hence the inclusion of the aqueous hydrogen concentration in Equation 4.3. The equation is adapted from the model equations of Kettle et al. (2015) for multiple essential resources. $\mu_{max,S}$ (h^{-1}) denotes the maximum growth rate and Y_S (mg L^{-1} mM^{-1}) is the biomass yield of *D. vulgaris* during sulphate reduction. K_S and K_H (mM) denote the Monod constants for sulphate and hydrogen respectively.

It is assumed that the aqueous hydrogen concentration is influenced by hydrogen production during the oxidation of lactate, hydrogen consumption in the reduction of sulphate, and liquid-gas transfer of hydrogen. The rate of change in the concentration of aqueous hydrogen is:

$$\frac{dH_{aq}}{dt} = -b_{LH}\frac{dL}{dt} + b_{HP}\frac{dS}{dt} - \frac{1}{\rho_H}\frac{dH_g}{dt}\frac{V_g}{V_{aq}} \tag{4.4}$$

where b_{LH} is the stoichiometric constant for moles of hydrogen produced per mole lactate metabolised and b_{HP} is the stoichiometric constant for moles of hydrogen required to reduce one mole of sulphate. H_g (atm) is the gaseous hydrogen concentration, measured in atmospheres, and mass transfer between the aqueous and gaseous phases is assumed to be linear, with:

$$\frac{dH_g}{dt} = k_L a(\rho_H H_{aq} - H_g)\frac{V_{aq}}{V_g} \tag{4.5}$$

Equation 4.5 represents a simple mass transfer model as explained in Kadic and Heindel (2014). Briefly, net transfer between the two phases is determined by the concentration gradient, with the rate of transfer determined by the mass transfer coefficient (MTC), k_L (calculated from the thickness of the film through which molecules must travel and the diffusivity of the molecule in question) and the surface area, a, across which mass transfer may occur. Although other, more complex models do exist for mass transfer between two phases, as only the gaseous hydrogen

concentration data were available here, this prevented parameterisation of a more complex model. Although the simplicity of this representation may result in sub-optimal representation of the hydrogen dynamics, minimising the number of fitted parameter values in the model is also desirable, and thus the film model described here is sufficient. $k_L a$ has the unit h^{-1} and V_g and V_{aq} (mL) are the fixed volumes of the gaseous and aqueous phases, respectively. ρ_H (atm mM^{-1}) is the Henry conversion constant for hydrogen. H_g is measured in atmospheres, whereas H_{aq} is given in mM concentration, therefore the gas transfer equation used in Muñoz-Tamayo et al. (2016) was adapted for this model, giving a ρ_H value of 1.364 atm mM^{-1}.

The rates of change in acetate (A; mM) and H_2S (P; mM) concentrations are proportional to the rates of change in the concentrations of lactate and sulphate, respectively:

$$\frac{dA}{dt} = -b_{LA}\frac{dL}{dt} \tag{4.6}$$

$$\frac{dP}{dt} = -b_{SP}\frac{dS}{dt} \tag{4.7}$$

where b_{LA} and b_{SP} are constants determined by the stoichiometries of each reaction stated in section 4.2.1. Note that these stoichiometries are taken directly from the literature and do not include in the model some fraction of substrate being used in the production of cell biomass. This assumption is made as, for the batch culture cases considered here, the experimentally observed stoichiometries of the metabolites closely matched those given in section 4.2.1.

Finally, the concentration of microbial cells in the medium, X ($mg\ L^{-1}$), is proportional to the change in lactate and sulphate concentrations, with consideration of the biomass yield terms (assuming the energy requirements for cell maintenance are negligible relative to the growth requirements):

$$\frac{dX}{dt} = -Y_L\frac{dL}{dt} - Y_S\frac{dS}{dt}. \tag{4.8}$$

The system consisting of Equations 4.2-4.8 fully describes the metabolism of *D. vulgaris* under the set of model assumptions.

4.2.3 Data capture

Time-course data were captured from the literature using image capturing and graphical input software in MATLAB (The MathWorks; www.mathworks.com). The mathematical model of Noguera et al. (1998) was reconstructed using the information in the original publication. This information was near complete, the only exception being the absence of initial conditions for some of the model variables. Assumptions based on other information given in the paper were used, which allowed for good reproduction of the published model fits.

4.2.4 Model fitting

In order to determine the values of several of the parameters used in the model, model fitting to existing experimental data was performed. Time-course data from Noguera et al. (1998) were collected and used to calibrate the model and estimate parameter values.

The parameter values in Table 4.1 were generated by minimising the normalised sum of squared errors between the model prediction and the data. The optimisation was performed using the fminsearch routine in MATLAB (The MathWorks; www.mathworks.com).

4.2.5 Statistical analysis

All statistics were calculated in MATLAB using the captured data and corresponding model prediction. An MCMC technique was implemented over 200,000 iterations. A non-parametric distribution was then fitted to the MCMC sample for each of the parameters estimated. The cumulative density function of this distribution was used to obtain a 95% confidence interval for each parameter.

To compare the proposed model with the existing model of Noguera et al. (1998), the corrected Akaike Information Criterion (AICc) was used (Akaike, 1974; Hurvich and Tsai, 1989):

$$\mathrm{AICc} = 2K - 2\big(\log\big(\mathcal{L}(\theta)\big)\big) + \frac{2K(K+1)}{n-K-1}$$

where n is the number of data points (63), K is the number of parameters of the model and $\log(\mathcal{L}(\theta))$ is the log likelihood function for the model. Following Burnham and Anderson (2002), the substitution:

$$\log\big(\mathcal{L}(\theta)\big) = -\frac{1}{2} n \log\left(\frac{\mathrm{RSS}}{n}\right)^2$$

was made, where RSS is the normalised residual sum of squares of the model fit to the data. Normalisation, i.e. division by the sample mean in the calculation of the RSS for each data set, was included to ensure the RSS value was not biased by the scale on which each variable was measured. Finally, the Akaike weight, w_i, for each model was calculated as follows (Burnham and Anderson, 2002):

$$w_i = \frac{l_i}{l_1 + l_2}$$

where $l_i = \exp\left(-\frac{1}{2}(\mathrm{AICc}_i - \mathrm{AICc}_{min})\right)$. Here, i is the model index (1 for the existing model of Noguera et al. (1998), 2 for the model presented here) and AICc_{min} represents the minimum AICc value of the two models.

4.3 Results

4.3.1 Model calibration

Data from two separate experiments were used simultaneously to obtain parameter values for the model (Noguera et al., 1998). The first experiment involved the growth of *D. vulgaris* in medium supplemented with lactate and sulphate (Figure 4.2), while the second experiment took place in the absence of sulphate (Figure 4.3). The mathematical model was able to describe the trends in growth and metabolite flux dynamics for both these experiments, giving comparable goodness of fit to the more complex model of Noguera et al. (1998) (Table 4.2). The parameter values used are shown in Table 4.1.

Table 4.1. Model parameter values

Parameter		Notation	Value (Best fit value with 95% confidence interval)	Source	Existing estimates[a]
Maximum growth rates	Lactate oxidation	$\mu_{max,L}$	0.116 h^{-1} (0.088 – 1.155)	Model fitting	t_d=3.7 h (≈0.21 h^{-1}) (Pankhania et al., 1986)
	Sulphate reduction	$\mu_{max,S}$	0.03 h^{-1} (0.023 – 0.212)	Model fitting	0.057 h^{-1} (Robinson and Tiedje, 1984) 0.15 h^{-1} (strain Marburg) (Badziong and Thauer, 1978) 0.15 h^{-1} (Reis et al., 1992)
Monod constants	Lactate	K_L	4.5 mM (7.3 – 136.8)	Model fitting	1.4 mM (Pankhania et al., 1988) 29 mM (Noguera et al., 1998)
	Sulphate	K_S	0.05 mM (0.02 – 0.268)	Model fitting	0.032 mM (Ingvorsen and Jørgensen, 1984) 0.21 mM (Noguera et al., 1998)
	Hydrogen	K_H	1.69 x 10^{-5} mM (2.5×10^{-4} – 3.96×10^{-3})	Model fitting	0.001 mM (Kristjansson et al., 1982) 0.0019 mM(Robinson and Tiedje, 1984) 0.0014 mM (Noguera et al., 1998)
Yield parameters	Lactate	Y_L	5.65 mg L^{-1} mM^{-1} (0.99 – 9.57)	Model fitting	5.3 mg L^{-1} mM^{-1} (Noguera et al., 1998) 5 mg L^{-1} mM^{-1} (Walker et al., 2009)
	Sulphate	Y_S	4.45 mg L^{-1} mM^{-1} (2.2 – 19.35)	Model fitting	2.8 mg L^{-1} mM^{-1} (Noguera et al., 1998) 8.3 g mol^{-1} (strain Marburg) (Badziong and Thauer, 1978) 14.3 g cell mol^{-1} (Reis et al., 1992)
Mass transfer parameter		$k_L a$	0.302 h^{-1} (0.182 – 0.914)	Model fitting	0.29 h^{-1} (Noguera et al., 1998)
Inhibitory hydrogen concentration		H_{max}	0.0216 mM (0.0341 – 0.0821)	Model fitting	0.001 atm (≈0.0007 mM) (Junicke et al., 2015)

Stoichiometric constants	Moles of hydrogen (H_2) produced per mole lactate oxidised	b_{LH}	2.5	Assumed stoichiometries	2.5 (Thauer et al., 1977; Noguera et al., 1998) 3.5 (Keller and Wall, 2011)
	Moles of hydrogen (H_2) consumed per mole H_2S produced	b_{HP}	5	Assumed stoichiometries	5 (Thauer et al., 1977; Noguera et al., 1998) 4.25 (Keller and Wall, 2011)
	Moles of acetate produced per mole lactate oxidised	b_{LA}	1	Assumed stoichiometries	1 (Thauer et al., 1977; Noguera et al., 1998; Keller and Wall, 2011)
	Moles of H_2S produced per mole sulphate reduced	b_{SP}	1	Assumed stoichiometries	1 (Thauer et al., 1977; Noguera et al., 1998; Keller and Wall, 2011)
Henry constant		ρ_H	1.364	Obtained from literature (Sander, 2015)	
[a]These estimates were obtained from different models and therefore a direct comparison cannot be made with the parameters estimated here. They are listed for reference.					

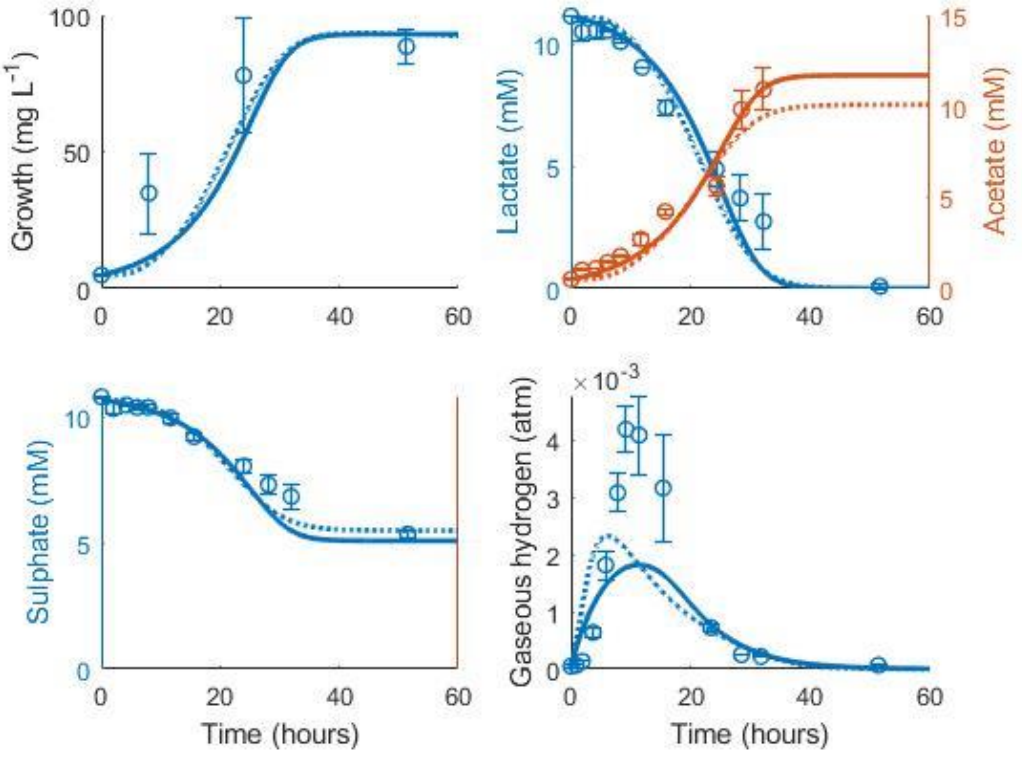

Figure 4.2. Model fits to data from Noguera et al. (1998): continuous lines display the fit of the current model; dotted lines display the fit of the model described in Noguera et al. (1998). Analysis of model fit is presented in Table 4.2.

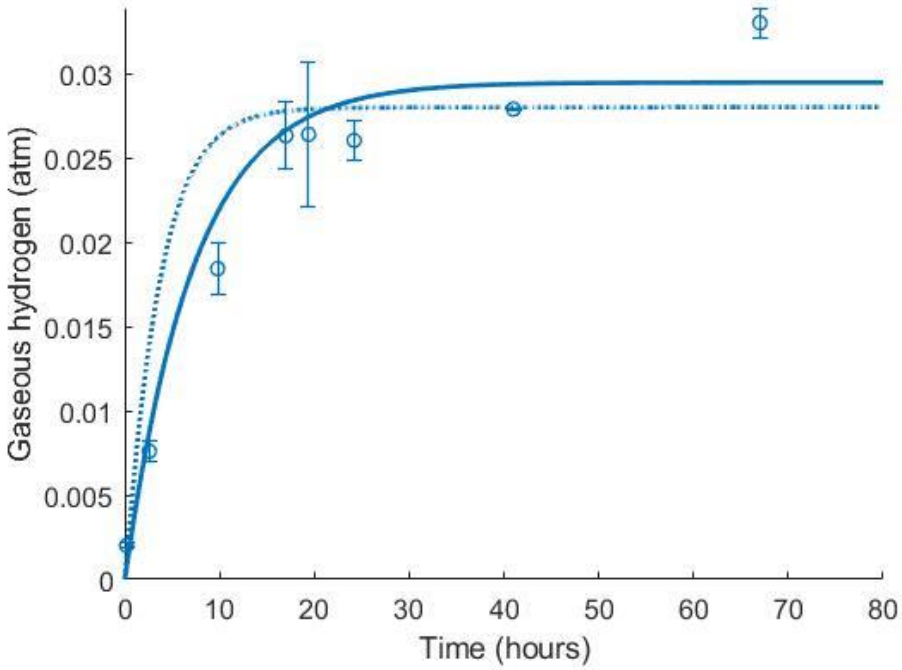

Figure 4.3. Dynamics of gaseous hydrogen in medium supplemented with 17.3 mM lactate in the absence of sulphate (Noguera et al., 1998): continuous lines display the fit of the current model; dotted lines display the fit of the model described in Noguera et al. (1998). Analysis of model fit is presented in Table 4.2.

Table 4.2. Analysis of model fits to the calibration data					
Variable	**Noguera et al. (1998) model**	**Current model**			
	R^2	R^2	Pearson's correlation coefficient (95% confidence interval)	CCC[a]	Mean bias
Figure 4.2					
Cell concentration	0.83	0.80	0.93 (-0.28, 0.99)	0.84	-10.58 mg L^{-1}
Lactate	0.95	0.96	0.98 (0.95 – 0.99)	0.96	-0.06 mM
Acetate	0.92	0.97	0.99 (0.94 – 0.99)	0.97	-0.23 mM
Sulphate	0.94	0.93	0.99 (0.94 – 0.99)	0.95	-0.26 mM
Gaseous hydrogen	<0	<0	0.93 (0.77 – 0.98)	0.57	-4.95 x 10^{-4} atm
Figure 4.3					
Gaseous hydrogen	0.83	0.96	0.98 (0.89 – 0.99)	0.96	-4.75 x 10^{-4} atm
[a]CCC: Concordance correlation coefficient (Lin, 1989).					

The model of Noguera et al. (1998) used seven model fitted parameters and a total of 20 parameters either fitted or estimated from previous experimentation, whereas the new model uses nine fitted parameters and one estimated from previous experimentation, giving a total of 10. This discrepancy is due to the increased complexity of the former model, which additionally models the aqueous concentrations and gaseous partial pressures of CO_2, H_2S and bicarbonate, as well as the mass transfer of these molecules between the two phases, and the thermodynamics of each reaction modelled. Table 4.3 details the values used for the AICc calculation. The AICc value for the new model was 263.2 compared to an AICc of 282.8 for the model of Noguera et al. (1998). This indicates the aptness of the new model to the data considered, although more complex models may be better suited for larger and more complex data sets.

Table 4.3. Akaike information criterion (AIC) calculation values						
Model	n	K	**RSS**	$\log(\mathcal{L}(\boldsymbol{\theta}))$	**AICc**	**Akaike weight**
Noguera et al. (1998)	63	20	9.6095	-111.4	282.8	0.0001
This model	63	10	8.9861	-119.5	263.2	0.9999

Some of the parameters shown in Table 4.1 were fixed to values taken from the literature. The stoichiometric constants were fixed to correspond with the assumed stoichiometries of the reactions considered and the Henry constant for hydrogen was also obtained from the literature.

It is notable that the best fit parameter values for K_L, K_H and H_{max} lie outside their respective MCMC generated 95% confidence interval. This is likely due to the difficulties in estimating half-saturation constants and maximum growth rates simultaneously, as high correlation was observed between these values. This has been observed in Monod model fitting elsewhere (for example, Muñoz-Tamayo et al. (2016)). Therefore, a second MCMC run was performed, in which the half-saturation constants were fixed at values obtained from the experimental literature. A comparison of the newly generated confidence intervals for the remaining fitted parameters with the original values is shown in Table 4.4, but the intervals are similar.

The sensitivity of the model prediction to variations in each parameter value was also analysed (Appendix A). The model prediction for growth in medium with no sulphate, shown in Figure 4.3, was not notably sensitive to small changes in any fitted parameter value except for H_{max}, which determines the final partial pressure of gaseous hydrogen. Contrastingly, the model fit to gaseous hydrogen shown in Figure 4.2 showed sensitivity to several parameters. Small variations in the maximum growth rates, half-saturation constant for lactate, yield values and the stoichiometric constants b_{LH} and b_{HP}, all resulted in relatively large changes in the quality of fit of the model to the gaseous hydrogen data. The change in the goodness of fit to the other data types was minimal. The model fit was only slightly sensitive to changes in the initial conditions for lactate, sulphate and microbial concentration and insensitive to such changes in the initial conditions for other metabolites. This was in contrast to the model of Noguera et al. (1998), which was found to be disproportionately sensitive to small changes in the initial conditions for dissolved hydrogen and carbonates: variables less likely to have a determining effect on culture dynamics than lactate, sulphate and microbial concentrations.

Table 4.4. Comparison of model parameter estimate confidence intervals when half-saturation constants were included or excluded from the estimation				
Parameter		**Notation**	**MCMC generated 95% confidence interval**	
			Fitted half-saturation parameters	Fixed half-saturation parameters
Maximum growth rates	Lactate oxidation	$\mu_{max,L}$	0.088 – 1.155	0.02 – 0.145
	Sulphate reduction	$\mu_{max,S}$	0.023 – 0.212	0.021 – 0.171
Monod constants	Lactate	K_L	7.3 – 136.8	-
	Sulphate	K_S	0.02 – 0.268	-
	Hydrogen	K_H	2.5 x 10^{-4} – 3.96 x 10^{-3}	-
Yield parameters	Lactate	Y_L	0.99 – 9.57	1.18 – 9.4
	Sulphate	Y_S	2.2 – 19.35	1.99 – 17.2
Mass transfer parameter		$k_L a$	0.182 – 0.914	0.313 – 3.724
Inhibitory hydrogen concentration		H_{max}	0.0341 – 0.0821	0.0335 – 0.0797

4.3.2 Model validation

The model was validated against several experimental data sources (Noguera et al., 1998; da Silva et al., 2013). Figure 4.4 shows the model simulation for gaseous hydrogen dynamics in medium lacking lactate, where *D. vulgaris* may only perform sulphate reduction, until the available hydrogen is depleted (data from Noguera et al. (1998)).

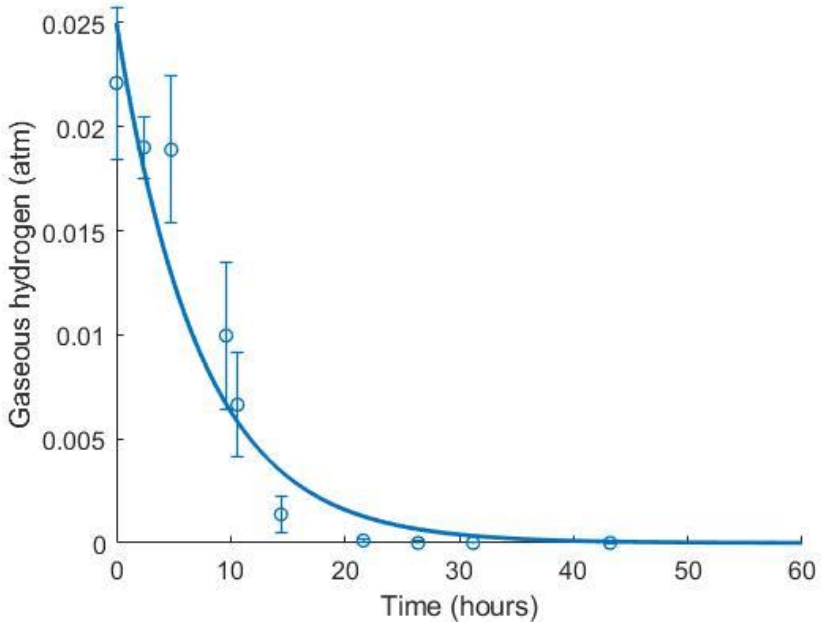

Figure 4.4. Dynamics of gaseous hydrogen in medium supplemented with 9.3 mM sulphate in the absence of lactate, with an initial hydrogen partial pressure in the gaseous phase of approximately 0.025 atm. 12 mM acetate was added as a carbon source (Noguera et al., 1998). R^2 = 0.91, r = 0.96 (0.83, 0.99), CCC = 0.92, mean bias = –0.0003 atm.

Figures 4.5 and 4.6 show the comparison between the model prediction and experimental data from further validation experiments, with altered initial conditions (data from Noguera et al. (1998)). Unfortunately, for these and the experiments from which Figures 4.3 and 4.4 were generated, data for aqueous metabolite concentrations and microbial growth were unavailable, so the model predictions for these variables cannot be verified. There was also no information regarding the concentration of microbes at the beginning of the experiment, therefore 9.4 mg L^{-1}, the initial microbial concentration in previous experiments, was assumed.

The model predicted the full utilisation of lactate and only partial consumption of sulphate in Figure 4.5, but was not able to capture the delay in hydrogen accumulation in the headspace observed in the first few hours of the experiment. The same was true of Figure 4.6. Here, the model accurately predicted the final concentration of lactate remaining in the medium at the end of the experiment as 2.98 mM, compared to the observed value of 2.58 mM. However, the model overpredicted the gaseous hydrogen accumulation. Under the model assumptions, hydrogen was expected to accumulate to the inhibitory level, whereas in the experiment hydrogen production was far lower. Given that the model accurately predicted lactate degradation, this would imply that less hydrogen was produced under the conditions shown in Figure 4.6 than under the assumed stoichiometry. Hydrogen accumulation was not measured after 48 hours in the experiment; therefore, it is not possible to know whether and at what point hydrogen accumulation peaked.

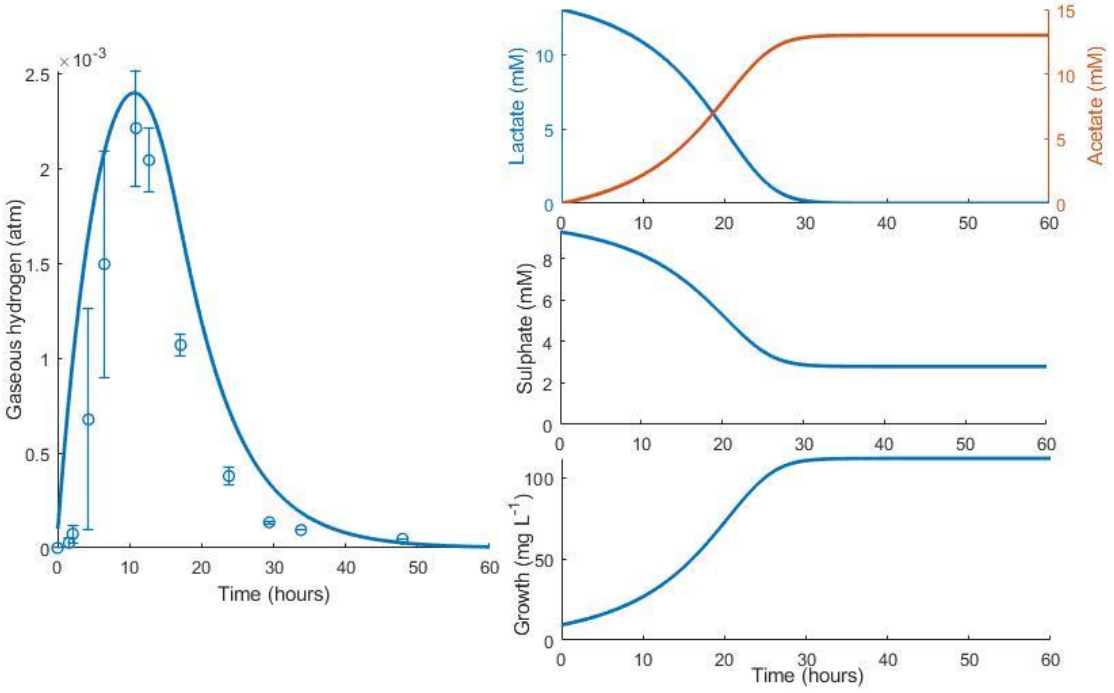

Figure 4.5. Dynamic changes in gaseous hydrogen with initial metabolite concentrations: 13 mM lactate; 9.3 mM sulphate (Noguera et al., 1998). R^2 = 0.70, r = 0.93 (0.76, 0.98), CCC = 0.77, mean bias = 0.0004 atm.

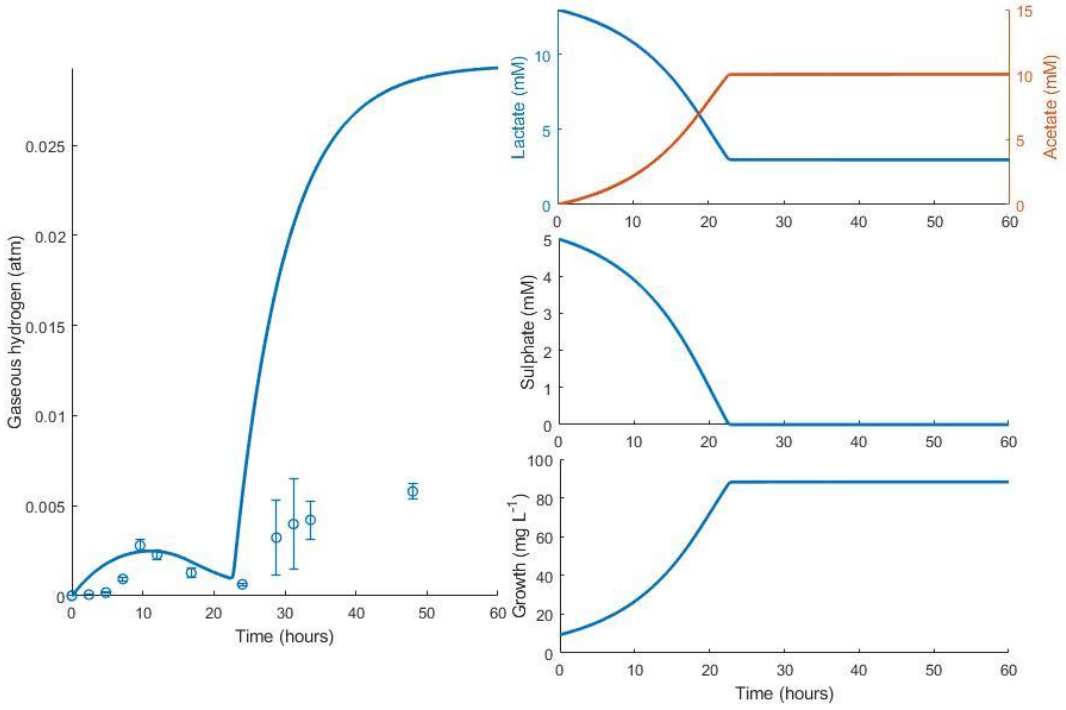

Figure 4.6. Dynamic changes in gaseous hydrogen with initial metabolite concentrations: 13 mM lactate; 5 mM sulphate (Noguera et al., 1998). R^2 = 0.22, r = 0.91 (0.72, 0.97), CCC = 0.22, mean bias = 0.0062 atm.

Figure 4.7 shows the validation of the both the new model and that of Noguera et al. (1998) against separate experimental data for *D. vulgaris* Hildenborough, taken from da Silva et al. (2013). The experimental starting microbial concentration was not stated for this data set, so this value was fitted to the data with all other parameters fixed at their previously determined values. This gave an initial microbial concentration of 6.75 mg L^{-1} for the new model and 0.038 mg L^{-1} for the model of Noguera et al. (1998). As shown in Figure 4.7, the models performed similarly with their respective initial microbial concentrations, with the exception of the gaseous hydrogen prediction, and both accurately captured the rate of lactate degradation and acetate production with no alteration to the parameter values obtained during model calibration. The large discrepancy between the obtained initial microbial concentrations for the two models prompted further investigation. The initial OD recorded for this experiment was approximately 0.025 (da Silva et al., 2013). No calibration to other units was performed by these authors and few exist in the literature for *Desulfovibrio* strains, but Bernardez and de Andrade Lima (2015) suggested a conversion of: dry weight (mg) = exp(5.12 OD – 4.987), which gives an approximate initial microbial concentration for this experiment of 7.76 mg L^{-1}. Although the conditions under which this conversion was derived differ from the experiment of da Silva et al. (2013), this estimate compares well to that of the new model.

The final acetate measurement in Figure 4.7 was not predicted by either model, and it is not clear where the remaining carbon from lactate degradation was directed in this experiment. *D. vulgaris* has the potential to use acetyl-CoA, an intermediate on the lactate oxidation pathway, in the biosynthesis of certain branched-chain amino acids and fatty acids, as well as in an incomplete citric acid cycle (Heidelberg et al., 2004), but only the metabolites shown in Figure 4.7 were measured. However, separate experiments by these authors with concentrated cell suspensions found the expected 1:1 ratio of lactate degraded to acetate produced (da Silva et al., 2013).

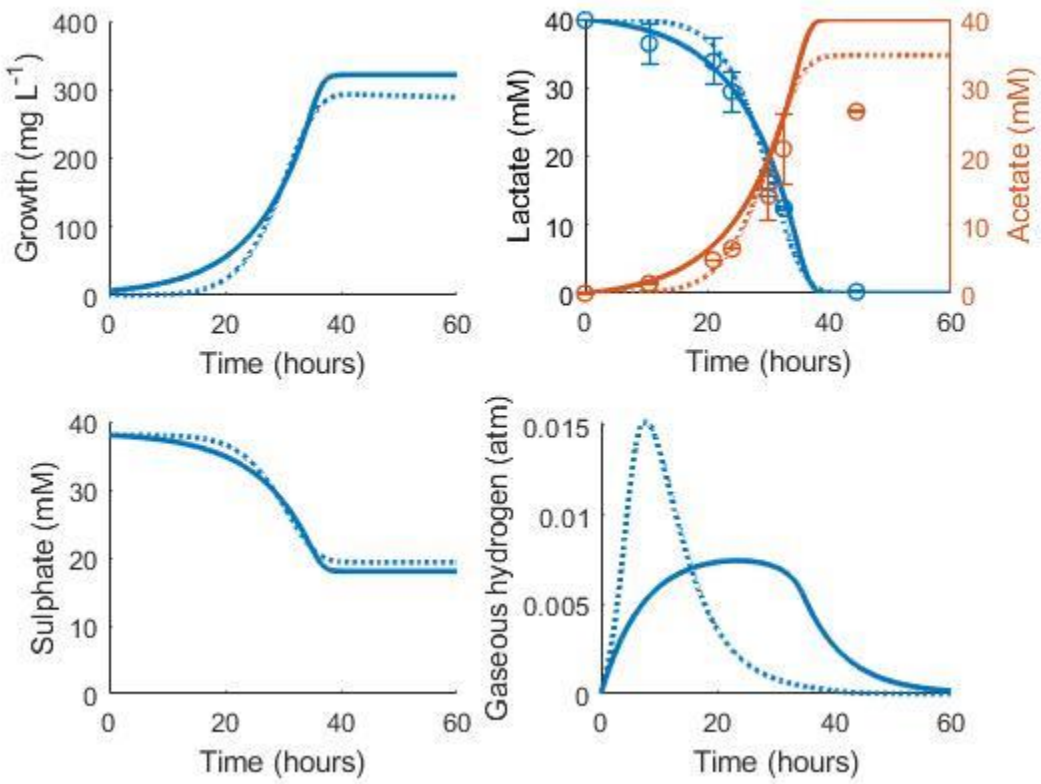

Figure 4.7. Model prediction for the consumption of lactate and production of acetate in the experimental work of da Silva et al. (2013): continuous lines display the fit of the current model; dotted lines display the fit of the model described in Noguera et al. (1998). See text for full explanation. Continuous line fit: Lactate: R^2 = 0.98, r = 0.99 (0.95, 0.99), CCC = 0.98, mean bias = 1.2 mM; Acetate: R^2 = 0.82, r = 0.99 (0.93, 0.99), CCC = 0.88, mean bias = 4.12 mM. Dotted line fit: Lactate: R^2 = 0.98, r = 0.99 (0.96, 0.99), CCC = 0.98, mean bias = 1.32 mM; Acetate: R^2 = 0.90, r = 0.99 (0.97, 0.99), CCC = 0.93, mean bias = 2.08 mM.

4.4 Discussion

This model provides a simpler mathematical representation of SRB metabolism than is currently available in the literature (Noguera et al., 1998), with similar predictive capability. As such, it can be more easily adapted to specific strains and culture conditions, not limited to SRB of the human colon. The inclusion of further characteristics of specific SRB strains could be realised with the addition of further terms to existing equations, or the inclusion of further equations if additional metabolites were considered. For example, complete growth inhibition of an SRB strain due to sulphide concentrations above 16.1 mM has been shown (Reis et al., 1992). Acetate inhibition has also been investigated for SRB, with approximately 54 mg L^{-1} undissociated acetic acid (≈45.9 mM acetate) resulting in 50% growth inhibition (Reis et al., 1990). Both these concentrations are greater than those measured in the experiments simulated here, and the H_2S concentration is greater than

that reported in faeces (Magee et al., 2000). However, the model could be adjusted to include inhibition terms for acetate and H_2S for application of the model to more extreme environments. These terms could take the form used here for hydrogen inhibition, but alternative inhibition terms could be more appropriate and should be assessed by model fitting (see Han and Levenspiel (1988) for a list of inhibition terms and a generalised form). At present, there is no time-course data involving such concentrations of these metabolites with which to parameterise the model.

It would also be useful to investigate experimentally the influence of bicarbonate on the growth rate of SRB. Several human-associated microbial strains have shown reduced growth rates when exposed to 100 mM of bicarbonate in monoculture (Dobay et al., 2018). This molecule was also shown to disrupt biofilm formation in selected strains. *D. vulgaris* is a biofilm forming organism (Clark et al., 2007), but no SRB were studied in the bicarbonate inhibition experiments, so no inference can be made about the influence of this molecule on growth rates in the model. However, following the expected stoichiometry of the *D. vulgaris* metabolic pathways, less than 20 mM of bicarbonate could be produced in the experiments of Noguera et al. (1998), and up to 40 mM in the experiments of da Silva et al. (2013), considerably lower than those found to be growth limiting by Dobay et al. (2018). Bicarbonate is secreted into the GIT lumen in humans, reaching comparable concentrations to those expected in these experiments: bicarbonate concentration at the start of the colon is estimated at around 30 mM (Gennari and Weise, 2008). Further experimental investigation is needed to determine whether, and to what extent, bicarbonate may be growth limiting to SRB before it can be included in a model.

Time-course data were also unavailable for the use of acetate as a carbon source by SRB, which has been shown in the absence of lactate (for example, Pankhania et al. (1986)). Acetate uptake is likely occurring in the data shown in Figure 4.4, as it is the sole available carbon source in the medium, but this was not measured. Experiments measuring acetate concentrations over time when this is the sole carbon source are required to determine the parameter values of acetate utilisation via model fitting.

Modelling mass transfer in experiments such as those described here is challenging. Due to limited available experimental data, a simple mass transfer model was chosen to minimise the number of fitting parameters required. Mass transfer was modelled under the assumption of linear

dynamics, but without knowledge of the concentration of dissolved hydrogen it is unclear how much this assumption biases the model. The model may be more limited in its ability to accurately capture hydrogen transfer between phases than other, more complex model structures (Kadic and Heindel, 2014). This simple structure may be partially responsible for the sensitivity of the gaseous hydrogen model fit to small changes in some of the parameter values of the model.

However, there is evidence that the model fit to the lactate, acetate and sulphate data is of greater importance than those of gaseous hydrogen and microbial growth for several reasons. The apparent initial lag phase in the gaseous hydrogen data from the experiments considered here was not captured by the model, despite the good fit to the data for other metabolites. While the inclusion of a lag phase in the model could rectify this aspect, such an addition would complicate the simplified model and there is no probable physiological cause for such a lag. The experimental data showed large variation in gaseous hydrogen pressure between replicates in both the calibration and validation data sets. The data for the concentration of microbial cells in the medium were similarly limited. Only two measurements were taken during the exponential growth phase in Figure 4.2, and the error on both measurements was greater than 25% of the mean value. It is also unclear how reliable the initial value for cell concentration was, since this was assumed from the inoculum rather than measured. Although the model proved only slightly sensitive to certain initial condition values, measuring the initial concentrations of both cells and metabolites would be of great value. The data for lactate, acetate and sulphate concentrations were more complete and more repeatable, encouraging emphasis on the model fit to these data.

Uncertainty remains in the field around the nature of hydrogen production and use by SRB. Previously, there have been arguments both for and against its status as a mandatory intermediate in the simultaneous oxidation of organic compounds and reduction of sulphate, as well as the role of various hydrogenase enzymes (Keller and Wall, 2011; Rabus et al., 2013). The importance of hydrogen in the reduction of sulphate has also been shown to differ between SRB species (see review by Rabus et al. (2015)). One of the strengths of the model is its avoidance of any biasing assumption about the nature of these relationships by using two hydrogen compartments, aqueous and gaseous, as a method to represent hydrogen equivalents that are immediately available for use in sulphate reduction or not, respectively.

The mathematical model presented here is simpler in its construction than previous attempts to capture SRB dynamics. The model uses nine fitted parameters (16 parameters in total), compared to seven fitted and three experimentally estimated parameters (20 parameters in total) in Noguera et al. (1998), and seven differential equations compared with ten in Noguera et al. (1998). The new model also showed good fits to experimental data as assessed by common measures for model analysis for two *D. vulgaris* strains from several independent experiments under varied conditions. While the model of Noguera et al. (1998) considered more factors, including the thermodynamics of the conversions performed by the microbes and the concentrations of a greater number of metabolites, these inclusions can be limiting when investigating the metabolism of SRB in environments where knowledge of these factors is not available. For example, application of the model of Noguera et al. (1998) to the human colon would be challenged by host influences on variables. The colonic model would need to consider appropriate representation of bicarbonate and CO_2 when including secretion and absorption by the host, as well as the implications of host metabolite absorption on the modelled thermodynamic inhibition of the metabolic reactions. By contrast, the relative simplicity of the new model means it can more easily be adapted to the specific environmental conditions of the colon and has greater flexibility for the inclusion of additional influences upon the metabolism of these microbes. In this way the new model could be adapted to provide a representative model for the SRB functional group in the colon.

Regarding dynamics in the colon, current existing data from rodent models support the increased efficiency of carbohydrate breakdown by saccharolytic microbes in the presence of either a methanogen or acetogen due to hydrogen metabolism by these microbes (Samuel and Gordon, 2006; Rey et al., 2010). However, there is no such evidence for the SRB, although in theory the same role could be filled by these microbes. This may be due to competition for other substrates, which could be investigated using the model presented here in combination with existing models for saccharolytic microbes (such as Kettle et al. (2015)).

The next step is to use the SRB model presented here as part of a larger model including other hydrogenotrophic and hydrogenogenic microbes of the human colon, to examine the role of hydrogen in this environment. Mathematical models for the colonic microbiota are available (Muñoz-Tamayo et al., 2010; Kettle et al., 2015; Kettle et al., 2017), but as yet do not consider the

action of SRB. The inclusion of this functional group may further enhance their predictive capabilities and could eventually be used to address the role of the SRB in human nutrition and health. Such community modelling should not be limited to the colon, as the combination of models such as that presented here with similar structures for methanogens and reductive acetogens may reveal information about the cross-feeding and competitive relationships between these hydrogenotrophs in other environments.

4.5 Conclusions

A mathematical model for lactate metabolism and sulphate reduction by the SRB *D. vulgaris* has been developed, calibrated and validated against experimental data. Comparison of the newly developed model to a more complex existing model in literature demonstrated that the simpler model performed to a similar standard in terms of quality of model fit. The newly developed model can be more easily adapted for specific purposes, such as incorporation into larger models for microbial communities.

Table 4.5. Model notation		
Notation	**Description**	**Unit**
$\mu_{max,L}$	Maximum growth rate for lactate	h^{-1}
$\mu_{max,S}$	Maximum growth rate for sulphate	h^{-1}
K_L	Half-saturation constant for lactate	mM
K_S	Half-saturation constant for sulphate	mM
K_H	Half-saturation constant for hydrogen	mM
Y_L	Yield term for lactate oxidation	mg L^{-1} mM^{-1}
Y_S	Yield term for sulphate reduction	mg L^{-1} mM^{-1}
H_{max}	Inhibitory aqueous hydrogen concentration	mM
$k_L a$	Mass transfer coefficient	h^{-1}
b_{LH}	Moles of hydrogen produced per mole lactate oxidised	-
b_{HP}	Moles of hydrogen utilised per mole H_2S produced	-
b_{LA}	Moles of acetate produced per mole lactate oxidised	-
b_{SP}	Moles of H_2S produced per mole sulphate reduced	-
L	Lactate concentration	mM
S	Sulphate concentration	mM
H_{aq}	Aqueous hydrogen concentration	mM
H_g	Gaseous hydrogen concentration	atm
A	Acetate concentration	mM
P	H_2S concentration	mM
X	Microbial cell concentration	mg L^{-1}
t	Time	h
ρ_H	Henry conversion constant for hydrogen	atm mM^{-1}
V_{aq}	Volume of the aqueous phase (50 mL for the experiments of Noguera et al. (1998), 250 mL for the experiments of da Silva et al. (2013))	mL
V_g	Volume of the gaseous phase (110 mL for the experiments of Noguera et al. (1998), 250 mL for the experiments of da Silva et al. (2013))	mL

References

Akaike, H. (1974). A New Look at the Statistical Model Identification. IEEE Trans. Automat. Contr. 19(6), 716-723. doi: 10.1109/TAC.1974.1100705.

Badziong, W., and Thauer, R.K. (1978). Growth yields and growth rates of *Desulfovibrio vulgaris* (Marburg) growing on hydrogen plus sulfate and hydrogen plus thiosulfate as the sole energy sources. Arch. Microbiol. 117(2), 209-214. doi: 10.1007/bf00402310.

Barton, L.L., and Fauque, G.D. (2009). "Biochemistry, Physiology and Biotechnology of Sulfate-Reducing Bacteria," in Adv. Appl. Microbiol.: Academic Press), 41-98.

Bernardez, L.A., and de Andrade Lima, L.R.P. (2015). Improved method for enumerating sulfate-reducing bacteria using optical density. MethodsX 2, 249-255. doi: https://doi.org/10.1016/j.mex.2015.04.006.

Burnham, K., and Anderson, D. (2002). Model selection and multimodel inference. New York: Springer-Verlag.

Carbonero, F., Benefiel, A.C., Alizadeh-Ghamsari, A.H., and Gaskins, H.R. (2012a). Microbial pathways in colonic sulfur metabolism and links with health and disease. Front. Physiol. 3:448. doi: 10.3389/fphys.2012.00448.

Carbonero, F., Benefiel, A.C., and Gaskins, H.R. (2012b). Contributions of the microbial hydrogen economy to colonic homeostasis. Nat. Rev. Gastroenterol. Hepatol. 9, 504. doi: 10.1038/nrgastro.2012.85.

Clark, M.E., Edelmann, R.E., Duley, M.L., Wall, J.D., and Fields, M.W. (2007). Biofilm formation in *Desulfovibrio vulgaris* Hildenborough is dependent upon protein filaments. Environ. Microbiol. 9(11), 2844-2854. doi: 10.1111/j.1462-2920.2007.01398.x.

da Silva, S.M., Voordouw, J., Leitão, C., Martins, M., Voordouw, G., and Pereira, I.A.C. (2013). Function of formate dehydrogenases in *Desulfovibrio vulgaris* Hildenborough energy metabolism. Microbiology (UK) 159(8), 1760-1769. doi: 10.1099/mic.0.067868-0.

Dobay, O., Laub, K., Stercz, B., Kéri, A., Balázs, B., Tóthpál, A., et al. (2018). Bicarbonate Inhibits Bacterial Growth and Biofilm Formation of Prevalent Cystic Fibrosis Pathogens. Front. Microbiol. 9**,** 2245-2245. doi: 10.3389/fmicb.2018.02245.

Doré, J., Pochart, P., Bernalier, A., Goderel, I., Morvan, B., and Rambaud, J.C. (1995). Enumeration of H2-utilizing methanogenic archaea, acetogenic and sulfate-reducing bacteria from human feces. FEMS Microbiol. Ecol. 17(4)**,** 279-284. doi: 10.1016/0168-6496(95)00033-7.

Gennari, F.J., and Weise, W.J. (2008). Acid-Base Disturbances in Gastrointestinal Disease. Clin. J. Am. Soc. Nephrol. 3(6)**,** 1861. doi: 10.2215/CJN.02450508.

Han, K., and Levenspiel, O. (1988). Extended monod kinetics for substrate, product, and cell inhibition. Biotechnol. Bioeng. 32(4)**,** 430-447. doi: 10.1002/bit.260320404.

Heidelberg, J.F., Seshadri, R., Haveman, S.A., Hemme, C.L., Paulsen, I.T., Kolonay, J.F., et al. (2004). The genome sequence of the anaerobic, sulfate-reducing bacterium *Desulfovibrio vulgaris* Hildenborough. Nat. Biotechnol. 22**,** 554. doi: 10.1038/nbt959.

Hurvich, C.M., and Tsai, C.-L. (1989). Regression and Time Series Model Selection in Small Samples. Biometrika 76(2)**,** 297-307. doi: 10.2307/2336663.

Ingvorsen, K., and Jørgensen, B.B. (1984). Kinetics of sulfate uptake by freshwater and marine species of *Desulfovibrio*. Arch. Microbiol. 139(1)**,** 61-66. doi: 10.1007/bf00692713.

Junicke, H., Feldman, H., van Loosdrecht, M.C.M., and Kleerebezem, R. (2015). Impact of the hydrogen partial pressure on lactate degradation in a coculture of *Desulfovibrio* sp. G11 and *Methanobrevibacter arboriphilus* DH1. Appl. Microbiol. Biotechnol. 99(8)**,** 3599-3608. doi: 10.1007/s00253-014-6241-2.

Kadic, E., and Heindel, T.J. (2014). An introduction to bioreactor hydrodynamics and gas-liquid mass transfer. Hoboken, New Jersey : Wiley, [2014].

Keller, K., and Wall, J. (2011). Genetics and Molecular Biology of the Electron Flow for Sulfate Respiration in *Desulfovibrio*. Front. Microbiol. 2(135). doi: 10.3389/fmicb.2011.00135.

Kettle, H., Holtrop, G., Louis, P., and Flint, H.J. (2017). microPop: Modelling microbial populations and communities in R. Methods Ecol. Evol. 9**,** 399–409. doi: 10.1111/2041-210x.12873.

Kettle, H., Louis, P., Holtrop, G., Duncan, S.H., and Flint, H.J. (2015). Modelling the emergent dynamics and major metabolites of the human colonic microbiota. Environ. Microbiol. 17(5)**,** 1615-1630. doi: 10.1111/1462-2920.12599.

Kiran, M.G., Pakshirajan, K., and Das, G. (2017). An overview of sulfidogenic biological reactors for the simultaneous treatment of sulfate and heavy metal rich wastewater. Chem. Eng. Sci. 158**,** 606-620. doi: https://doi.org/10.1016/j.ces.2016.11.002.

Kristjansson, J.K., Schönheit, P., and Thauer, R.K. (1982). Different Ks values for hydrogen of methanogenic bacteria and sulfate reducing bacteria: An explanation for the apparent inhibition of methanogenesis by sulfate. Arch. Microbiol. 131(3)**,** 278-282. doi: 10.1007/bf00405893.

Lin, L.I.-K. (1989). A concordance correlation coefficient to evaluate reproducibility. Biometrics 45(1)**,** 255-268.

Magee, E.A., Richardson, C.J., Hughes, R., and Cummings, J.H. (2000). Contribution of dietary protein to sulfide production in the large intestine: an in vitro and a controlled feeding study in humans. Am. J. Clin. Nutr. 72(6)**,** 1488-1494. doi: 10.1093/ajcn/72.6.1488.

Magot, M., Ollivier, B., and Patel, B.K.C. (2000). Microbiology of petroleum reservoirs. Anton. Leeuw. 77(2)**,** 103-116. doi: 10.1023/a:1002434330514.

Martins, M., Mourato, C., and Pereira, I.A.C. (2015). *Desulfovibrio vulgaris* Growth Coupled to Formate-Driven H2 Production. Environ. Sci. Technol. 49(24)**,** 14655-14662. doi: 10.1021/acs.est.5b02251.

Monod, J. (1949). The Growth of Bacterial Cultures. Annu. Rev. Microbiol. 3(1)**,** 371-394. doi: 10.1146/annurev.mi.03.100149.002103.

Motta, J.-P., Flannigan, K.L., Agbor, T.A., Beatty, J.K., Blackler, R.W., Workentine, M.L., et al. (2015). Hydrogen Sulfide Protects from Colitis and Restores Intestinal Microbiota Biofilm and Mucus Production. Inflamm. Bowel Dis. 21(5)**,** 1006-1017. doi: 10.1097/MIB.0000000000000345.

Muñoz-Tamayo, R., Giger-Reverdin, S., and Sauvant, D. (2016). Mechanistic modelling of in vitro fermentation and methane production by rumen microbiota. Anim. Feed Sci. Technol. 220**,** 1-21. doi: https://doi.org/10.1016/j.anifeedsci.2016.07.005.

Muñoz-Tamayo, R., Laroche, B., Walter, T., Doré, J., and Leclerc, M. (2010). Mathematical modelling of carbohydrate degradation by human colonic microbiota. J. Theor. Biol. 266(1), 189-201. doi: 10.1016/j.jtbi.2010.05.040.

Muyzer, G., and Stams, A.J.M. (2008). The ecology and biotechnology of sulphate-reducing bacteria. Nat. Rev. Microbiol. 6, 441. doi: 10.1038/nrmicro1892.

Nava, G.M., Carbonero, F., Croix, J.A., Greenberg, E., and Gaskins, H.R. (2012). Abundance and diversity of mucosa-associated hydrogenotrophic microbes in the healthy human colon. ISME J. 6(1), 57-70. doi: 10.1038/ismej.2011.90.

Noguera, D.R., Brusseau, G.A., Rittmann, B.E., and Stahl, D.A. (1998). A unified model describing the role of hydrogen in the growth of *Desulfovibrio vulgaris* under different environmental conditions. Biotechnol. Bioeng. 59(6), 732-746. doi: 10.1002/(SICI)1097-0290(19980920)59:6<732::AID-BIT10>3.0.CO;2-7.

Okabe, S., Nielsen, P.H., Jones, W.L., and Characklis, W.G. (1995). Sulfide product inhibition of *Desulfovibrio desulfuricans* in batch and continuous cultures. Water Res. 29(2), 571-578. doi: https://doi.org/10.1016/0043-1354(94)00177-9.

Pankhania, I.P., Gow, L.A., and Hamilton, W.A. (1986). The effect of hydrogen on the growth of *Desulfovibrio vulgaris* (Hildenborough) on lactate. J. Gen. Microbiol. 132(12), 3349-3356.

Pankhania, I.P., Spormann, A.M., Hamilton, W.A., and Thauer, R.K. (1988). Lactate conversion to acetate, CO2 and H2 in cell suspensions of *Desulfovibrio vulgaris* (Marburg): indications for the involvement of an energy driven reaction. Arch. Microbiol. 150(1), 26-31. doi: 10.1007/BF00409713.

Rabus, R., Hansen, T.A., and Widdel, F. (2013). "Dissimilatory sulfate- and sulfur-reducing prokaryotes," in The Prokaryotes: Prokaryotic Physiology and Biochemistry, 309-404.

Rabus, R., Venceslau, S.S., Wöhlbrand, L., Voordouw, G., Wall, J.D., and Pereira, I.A.C. (2015). "A Post-Genomic View of the Ecophysiology, Catabolism and Biotechnological Relevance of Sulphate-Reducing Prokaryotes", in: Adv. Microb. Physiol.

Reis, M.A.M., Almeida, J.S., Lemos, P.C., and Carrondo, M.J.T. (1992). Effect of hydrogen sulfide on growth of sulfate reducing bacteria. Biotechnol. Bioeng. 40(5), 593-600. doi: doi:10.1002/bit.260400506.

Reis, M.A.M., Lemos, P.C., Almeida, J.S., and Carrondo, M.J.T. (1990). Influence of produced acetic acid on growth of sulfate reducing bacteria. Biotechnol. Lett. 12(2), 145-148. doi: 10.1007/BF01022432.

Rey, F.E., Faith, J.J., Bain, J., Muehlbauer, M.J., Stevens, R.D., Newgard, C.B., et al. (2010). Dissecting the in vivo metabolic potential of two human gut acetogens. J. Biol. Chem. 285(29), 22082-22090. doi: 10.1074/jbc.M110.117713.

Rey, F.E., Gonzalez, M.D., Cheng, J., Wu, M., Ahern, P.P., and Gordon, J.I. (2013). Metabolic niche of a prominent sulfate-reducing human gut bacterium. Proc. Natl. Acad. Sci. USA. 110(33), 13582-13587. doi: 10.1073/pnas.1312524110.

Robinson, J.A., and Tiedje, J.M. (1984). Competition between sulfate-reducing and methanogenic bacteria for H2 under resting and growing conditions. Arch. Microbiol. 137(1), 26-32. doi: 10.1007/BF00425803.

Samuel, B.S., and Gordon, J.I. (2006). A humanized gnotobiotic mouse model of host-archaeal-bacterial mutualism. Proc. Natl. Acad. Sci. USA. 103(26), 10011-10016. doi: 10.1073/pnas.0602187103.

Sander, R. (2015). Compilation of Henry's law constants (version 4.0) for water as solvent. Atmospheric Chem. Phys. 15(8), 4399-4981. doi: 10.5194/acp-15-4399-2015.

Stams, A.J.M., and Plugge, C.M. (2009). Electron transfer in syntrophic communities of anaerobic bacteria and archaea. Nat. Rev. Microbiol. 7(8), 568-577. doi: 10.1038/nrmicro2166.

Stolyar, S., Van Dien, S., Hillesland, K.L., Pinel, N., Lie, T.J., Leigh, J.A., et al. (2007). Metabolic modeling of a mutualistic microbial community. Mol. Syst. Biol. 3, 92. doi: 10.1038/msb4100131

Thauer, R.K., Jungermann, K., and Decker, K. (1977). Energy conservation in chemotrophic anaerobic bacteria. Bacteriol. Rev. 41(1), 100-180.

Tomasova, L., Konopelski, P., and Ufnal, M. (2016). Gut bacteria and hydrogen sulfide: The new old players in circulatory system homeostasis. Molecules 21(11). doi: 10.3390/molecules21111558.

Walker, C.B., He, Z., Yang, Z.K., Ringbauer, J.A., He, Q., Zhou, J., et al. (2009). The Electron Transfer System of Syntrophically Grown *Desulfovibrio vulgaris*. J. Bacteriol. 191(18), 5793.

Willis, C.L., Cummings, J.H., Neale, G., and Gibson, G.R. (1996). In vitro effects of mucin fermentation on the growth of human colonic sulphate-reducing bacteria. Anaerobe 2(2), 117-122. doi: 10.1006/anae.1996.0015.

Wolin, M.J., and Miller, T.L. (1983). Interactions of microbial populations in cellulose fermentation. Fed. Proc. 42(1), 109-113.

The following chapter contains material from: ‘Smith NW, Shorten PR, Altermann E, Roy NC, McNabb Mathematical modelling supports the existence of a threshold hydrogen concentration and media-dependent yields in the growth of a reductive acetogen, Bioprocess and Biosystems Engineering, published 2020, Springer-Verlag GmbH Germany, part of Springer Nature’. https://doi.org/10.1007/s00449-020-02285-w

Chapter 5: Mathematical modelling of the reductive acetogen *Blautia hydrogenotrophica* supports the existence of a threshold hydrogen concentration and media-dependent yields

Abstract

The bacterial production of acetate via reductive acetogenesis along the Wood–Ljungdahl metabolic pathway is an important source of this molecule in several environments, ranging from industrial bioreactors to the human gastrointestinal tract. Here, mathematical modelling techniques for the prediction of bacterial growth and acetate production are considered. It was found that the incorporation of a hydrogen uptake concentration threshold into the models improves their predictions and this threshold was calculated as 86.2 mM (95% confidence interval 6.1–132.6 mM). Monod kinetics and first-order kinetics models, with the inclusion of two candidate threshold terms, and reversible Michaelis–Menten kinetics were compared to experimental data and the optimal technique for predicting both growth and metabolism was found. The models were then used to compare the efficacy of two growth media for acetogens. The recently described general acetogen medium was found to be superior to the DSMZ medium in terms of unbiased estimation of acetogen growth and the contribution of yeast extract concentration to acetate production and bacterial growth in culture was investigated. The models and their predictions will be useful to those studying both industrially and environmentally relevant reductive acetogenesis and allow for straightforward adaptation to similar cases with different organisms.

5.1 Introduction

The SCFA acetate may be formed via a number of microbial metabolic pathways, either from more complex organic compounds or from the combination of two single carbon molecules. Reductive acetogenesis via the Wood-Ljungdahl metabolic pathway is an example of the latter, in which acetate may be formed from the combination of CO_2 and/or CO with hydrogen (Drake, 1994).

Over 100 species of acetogenic bacteria that use this pathway have been isolated from a range of anaerobic habitats, such as the human and bovine GIT, oil fields and freshwater sediments (Drake et al., 2013).

In the human colon, acetogens, alongside methanogens, may cross-feed on the hydrogen and CO_2 produced by saccharolytic members of the colonic microbial population, as discussed in Chapter 2. High concentrations of hydrogen in the colon reduce the efficiency of carbohydrate breakdown by many microbes (Thauer et al., 1977; Wolin and Miller, 1983; Gibson et al., 1993) and the presence of an acetogen has been shown to mitigate this effect in rodents (Rey et al., 2010). Acetogens have also been investigated as a potential means of reducing the amount of hydrogen converted to the greenhouse gas methane in the rumen (Lopez et al., 1999; Fonty et al., 2007), since they have proven effective hydrogen consumers in the GIT of other animals (Graber and Breznak, 2004; Godwin et al., 2014).

Industrially, the use of acetogens to reduce waste and produce biofuels and other useful chemicals is an area of current development (for a review, see Bengelsdorf et al. (2018)). Waste gases containing high concentrations of CO_2 and CO can be combined with hydrogen to form synthesis gas (syngas) and then utilised as the substrate for reductive acetogenesis in bioreactors, resulting in the formation of acetate, ethanol and a number of other useful compounds (Schiel-Bengelsdorf and Dürre, 2012).

A greater understanding of the growth and metabolic dynamics of acetogenic microbes would be beneficial for several scientific fields, from human and animal nutrition and well-being, through to biotechnology and bioengineering. The research detailed in this chapter investigates an optimum method for modelling hydrogen consumption by acetogens. The established Monod model for microbial growth may be insufficient to capture hydrogen uptake by these microbes, due to the proposed existence of a minimum hydrogen concentration required for acetogen growth (Leclerc et al., 1997). Therefore, a number of mathematical modelling techniques that include a substrate threshold are presented and applied to experimental data for the acetogen *B. hydrogenotrophica*. These models are then used to investigate the growth of this microbe on different media. *B. hydrogenotrophica* was chosen due to the availability of time-course data for its growth, hydrogen consumption and acetate production in monoculture. It is also present in the human colon

(Bernalier et al., 1996), and is potentially suitable for industrial applications (Groher and Weuster-Botz, 2016a).

5.2 Methodology

5.2.1 Assumptions

The initial model considers only two of the metabolites involved in reductive acetogenesis: hydrogen and acetate. All other molecules necessary for microbial growth were assumed to be abundantly available in the medium throughout the experiment, including CO_2.

The influence of gas-liquid transfer was not considered in this model. Although the hydrogen and CO_2 necessary for reductive acetogenesis were added to the gaseous phase, it was assumed that mass transfer of these metabolites into the aqueous phase was not a limiting factor. Including mass transfer in the model would be challenging due to the lack of available data for the aqueous concentration of these molecules in the experiments considered. This assumption also reduced the complexity of the model and the number of parameters to be estimated. Experimental work has emphasised the need for aqueous metabolite data in the precise estimation of threshold concentrations under continuous metabolite inflow (Karadagli et al., 2019). Under the batch conditions considered here, the estimate of threshold concentrations should be minimally influenced by mass transfer limitation. However, the absence of mass transfer in this model may have resulted in underestimates of growth rates.

The following stoichiometry was assumed for reductive acetogenesis along the Wood-Ljungdahl pathway (Drake, 1994):

$$4H_2 + 2CO_2 \rightarrow CH_3COO^- \text{ (Acetate)} + H^+ + 2H_2O$$

5.2.2 Data capture

Data were obtained from literature sources via image capturing in MATLAB (The MathWorks; www.mathworks.com). Where necessary, cell dry weight (CDW) in g L^{-1} was determined using the OD conversion for *B. hydrogenotrophica* of CDW = 0.37 · OD (Groher and

Weuster-Botz, 2016b). Where metabolite data were given in g L^{-1}, the conversions x [mM] = $\frac{x\,[\mathrm{g\,L^{-1}}]}{2.016}$ · 1000 for hydrogen and x [mM] = $\frac{x\,[\mathrm{g\,L^{-1}}]}{59.044}$ · 1000 for acetate were used.

5.2.3 Model fitting

The model was calibrated using time-course growth and metabolite data from Bernalier et al. (1996) and validated using data from Groher and Weuster-Botz (2016b). These data were sampled using image capturing and graphical input software in MATLAB (The MathWorks; www.mathworks.com). To obtain estimates for parameter values and the reliability of these estimates, an MCMC method was employed, implemented in MATLAB. The optimisation objective function chosen was the minimisation of the sum of normalised squared differences between the model prediction and the experimental data. 10^6 iterations of the MCMC algorithm were performed for each model structure. Goodness of fit was assessed from R^2 values, with values above 0.80 considered good.

5.2.4 Mathematical model

Monod kinetics was chosen as the starting point for the investigation (Monod, 1949), with the inclusion of a constant cell death rate and the production of acetate, giving the following system of ODEs:

$$\frac{dH}{dt} = -\frac{\mu_{max}\,X}{Y}\left(\frac{H}{K_H + H}\right) \tag{5.1}$$

$$\frac{dP}{dt} = -\frac{1}{4}\frac{dH}{dt} \tag{5.2}$$

$$\frac{dX}{dt} = -Y\frac{dH}{dt} - k_d X \tag{5.3}$$

where H, P and X are the concentrations of the substrate hydrogen (mM), the product acetate (mM) and microbial cells (g L^{-1} CDW) in the medium, respectively. Time (t) is measured in hours. μ_{max} (h^{-1}) is the maximum growth rate of the microbe and Y (g L^{-1} mM^{-1}) is the yield of microbial cells per substrate consumed. K_H (mM) is the half-saturation constant for hydrogen uptake by the

microbe. Finally, k_d (h^{-1}) is the death rate, assumed to be constant throughout the experiment. It was assumed that only a negligible proportion of substrate is used for cell maintenance.

The Monod kinetics model described above is widely applied to model microbial growth. However, it is known that explicitly identifying the values of μ_{max} and K_H is not always possible using model fitting, due to strong correlation between estimates of these two parameters obtained from a typical single time-course experiment (Muñoz-Tamayo et al., 2016). Here, it was found that only estimation of the ratio of these two parameters was possible, therefore equations 5.1-5.3 were reformulated as follows:

$$\frac{dH}{dt} = -\frac{\eta XH}{Y} \tag{5.4}$$

$$\frac{dP}{dt} = -\frac{1}{4}\frac{dH}{dt} \tag{5.5}$$

$$\frac{dX}{dt} = -Y\frac{dH}{dt} - k_d X\,. \tag{5.6}$$

Here, the first order kinetics technique has been used rather than Monod kinetics, where $\eta \simeq \frac{\mu_{max}}{K_H}$ (h^{-1} mM^{-1}; (Van Wey et al., 2014)). As shown in Figure 5.1, there is negligible difference between the MCMC-generated best fit for the first order kinetics model and the Monod model when applied to monoculture data for *B. hydrogenotrophica* from Bernalier et al. (1996). Linearisation of the Monod model to first order kinetics has been successfully applied elsewhere (Van Wey et al., 2014), and the need for it is shown by the poor reliability of the estimate of K_H used in Figure 5.1. A K_H value of 37,328 mM was obtained from model fitting, with a 95% confidence interval of 1,770 – 77,680 mM and there was no chain convergence of the MCMC. The correlation coefficient between μ_{max} and K_H was 0.93, emphasising the poor reliability of estimating these two parameters individually from the available data. The first order kinetics model was therefore selected for further use due to more reliable parameter estimation with this model structure.

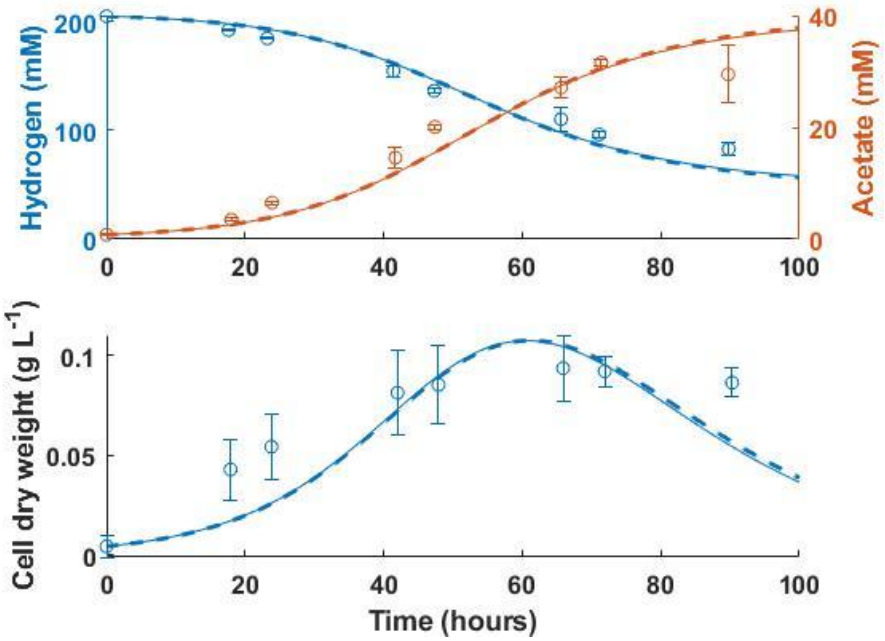

Figure 5.1. Comparison of Monod kinetics (solid line; Hydrogen R^2=0.96; Acetate R^2=0.94; CDW R^2=0.76) with first order kinetics (dashed line; Hydrogen R^2=0.96; Acetate R^2=0.94; CDW R^2=0.76) when fit to monoculture data for *Blautia hydrogenotrophica*. Error bars denote standard deviations from three experimental determinations.

One aspect of the data that was challenging to capture with either Monod or first order kinetics is the existence of a hydrogen threshold, below which the acetogen may only harvest a negligible amount of hydrogen from its environment. Both the previously presented models were insufficient to capture the dynamics of hydrogen uptake at concentrations approaching 100 mM, as seen in Figure 5.1. Previous experimentation has found the threshold value for hydrogen uptake to be 1,100 ± 200 ppm for *B. hydrogenotrophica* (Leclerc et al., 1997), which corresponds to 70 ± 12.7 mM.

There are several ways in which this threshold may be included in the model. The simplest method, variations of which have been applied in a number of comparable cases for other systems (Frame and Hu, 1991; Giraldo-Gomez et al., 1992; Kovárová et al., 1996; López-Meza et al., 2016), is to formulate equation 5.1 as follows:

$$\frac{dH}{dt} = -\frac{\mu_{max}\, X}{Y}\left(\frac{H^*}{K_H + H^*}\right) \tag{5.7}$$

where $H^* = H - H_t$, for hydrogen threshold concentration H_t. Equation 5.7 can be reformulated in the same manner as equation 5.4 to obtain:

$$\frac{dH}{dt} = -\frac{\eta H^* X}{Y} \tag{5.8}$$

Although simple and intuitive, this formulation is not robust for hydrogen concentrations below the threshold value, so is limited in its applications outside of simple monoculture cases. To prevent the model from predicting negative growth rates in such situations, the following condition was added:

$H^* = 0$ when $H < H_t$.

This threshold modelling technique is referred to as **T1**.

An alternative model was proposed by Ribes et al. (2004). They constructed the substrate equation as follows:

$$\frac{dH}{dt} = -\frac{\mu_{max} X}{Y}\left(\frac{H - H_t f}{K_H + H - H_t f} F\right) \tag{5.9}$$

where f and F are both empirical sigmoidal functions that ensure growth decreases smoothly to 0 as the substrate concentration approaches the threshold value, H_t, and remains at 0 for concentrations below this threshold:

$$f = \frac{1}{1 + \exp\left(A(H_t - H)\right)}$$

$$F = \frac{1}{1 + \exp\left(A(T - H)\right)}.$$

This technique is referred to as **T2**. Equation 5.9 may be altered in the established manner to obtain:

$$\frac{dH}{dt} = -\frac{\eta XH}{Y} F. \tag{5.10}$$

A and T are tuning parameters of the model with limited biological significance, a discussion of which may be found in the original publication (Ribes et al., 2004). This approach is robust to all possible substrate concentrations but adds considerable complexity and extra parameters to the model, which do not have a direct, biologically tangible meaning. This contrasts with the original Monod model (equations 5.1-5.3), in which all parameters may be more easily interpreted and experimentally investigated.

The final technique outlined here is the use of reversible Michaelis-Menten kinetics (Klipp, 2009). This modelling technique is referred to as **T3**. It is assumed that the conversion of hydrogen

and CO_2 to acetate is a reversible reaction, with net conversion determined by the concentrations of each metabolite. The substrate equation is then:

$$\frac{dH}{dt} = -\frac{X}{Y}\left(\frac{\mu_{max,H}\frac{H}{K_H} - \mu_{max,R}\frac{P}{K_R}}{1 + \frac{H}{K_H} + \frac{P}{K_R}}\right). \tag{5.11}$$

Here, $\mu_{max,H}$ and K_H are the maximum rate and half-saturation constant for hydrogen consumption and $\mu_{max,R}$ and K_R are the corresponding parameters for the reverse reaction. For this formulation all the parameters have a direct interpretation in terms of the forward and reverse reactions. Note that the simplification to first order kinetics is not performed in this case, as equation 5.11 cannot be converted in the same manner as were equations 5.7 and 5.9. Model **T3** therefore consists of equation 5.11 in combination with equations 5.5 and 5.6.

Importantly, the substitution of each of these techniques for a hydrogen threshold does not change the differential equations for product concentration or cell concentration.

As an extension to these model structures, the influence of a second substrate and metabolic pathway on the growth of *B. hydrogenotrophica* is briefly considered. This is used to analyse the effect of yeast extract on microbial growth, performed in Figure 5.5. It is assumed that the microbe feeds non-preferentially via both reductive acetogenesis and this second pathway. In both cases, acetate is the only product considered. Let the concentration of yeast extract be denoted by E, so that, following first order kinetics:

$$\frac{dE}{dt} = -\frac{\eta_E\, XE}{Y_E}. \tag{5.12}$$

The subscript E denotes parameters that are specific to the metabolism of yeast extract. The inclusion of this equation in any of the previous models requires no change to the differential equation for hydrogen concentration, but does require additions to the differential equations for acetate concentration and microbial growth, as follows:

$$\frac{dP}{dt} = -\frac{1}{4}\frac{dH}{dt} - b_{EP}\frac{dE}{dt} \tag{5.13}$$

$$\frac{dX}{dt} = -Y\frac{dH}{dt} - Y_E\frac{dE}{dt} - k_d X. \tag{5.14}$$

Here, b_{EP} refers to the number of moles of acetate that are produced per mole of yeast extract consumed.

5.3 Results

5.3.1 Model calibration

The four model structures outlined in the methodology were fitted to experimental data for *B. hydrogenotrophica* from Bernalier et al. (1996). Figure 5.2 shows a comparison of the model fits for the first order kinetics model, **T1**, **T2** and **T3**.

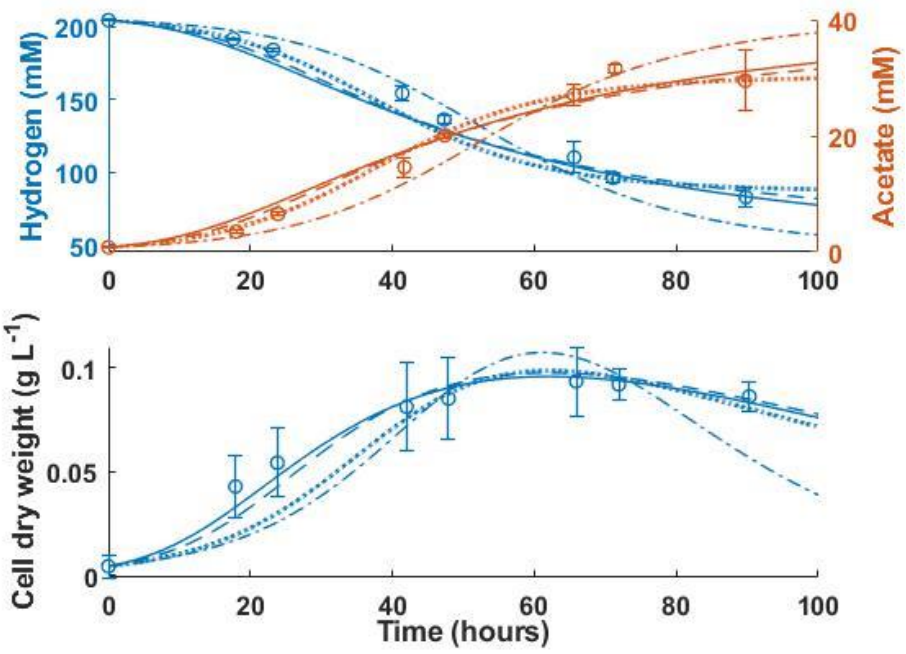

Figure 5.2. Model fits to data from Bernalier et al. (1996). Dash dot line: first order kinetics model (Hydrogen R^2=0.96; Acetate R^2=0.94; CDW R^2=0.76). Dotted line: T1 model (Hydrogen R^2=0.97; Acetate R^2=0.98; CDW R^2=0.88). Dashed line: T2 model (Hydrogen R^2=0.97; Acetate R^2=0.96; CDW R^2=0.95). Solid line: T3 model (Hydrogen R^2=0.97; Acetate R^2=0.96; CDW R^2=0.98). Error bars denote standard deviations from three experimental determinations.

Model fitting of the **T1** model gave an estimate of 86.2 mM (95% confidence interval 6.1 – 132.6 mM) for the threshold hydrogen concentration, which is comparable to the 70 ± 12.7 mM estimate of Leclerc et al. (1997). The best fits to the data were obtained using the **T2** and **T3** models,

for which the R^2 values for acetate, hydrogen and growth are all above 0.9. The parameter values obtained from model fitting are given in Table 5.1. The first order kinetics model over-predicted the consumption of hydrogen at the final data point, as well as the corresponding data point for acetate production. In contrast, all three threshold models accurately predicted the final data points for both metabolites, encouraging the use of a threshold model for this acetogen. The yield and cell death rate parameter values obtained from model fitting show good consistency between the threshold models.

Table 5.1. Best fit parameter values obtained from Markov chain Monte Carlo model fitting (95% confidence interval)

Parameter (units)	**First order kinetics**	**T1**	**T2**	**T3**
η (h^{-1} mM^{-1})	0.0008 (0.0007 – 0.0031)	0.0008 (0.0007 – 0.0032)	0.0054 (0.0018 – 0.0553)	-
Y (g L^{-1} mM^{-1})	0.0037 (0.0026 – 0.0363)	0.0014 (0.0013 – 0.0192)	0.0017 (0.0012 – 0.0274)	0.0018 (0.0009 – 0.0072)
k_d (h^{-1})	0.087 (0.067 – 0.514)	0.014 (0.011 – 0.306)	0.019 (0.012 – 0.357)	0.022 (0.004 – 0.089)
H_t (mM)	-	86.2 (6.1 – 132.6)	-	-
A (mM^{-1})	-	-	0.015 (0.0002 – 0.1096)	-
T (mM)	-	-	336 (48 – 3509)	-
$\mu_{max,H}$ (h^{-1})	-	-	-	0.451 (0.24 – 5.025)
$\mu_{max,R}$ (h^{-1})	-	-	-	0.002 (0.001 – 0.058)
K_H (mM)	-	-	-	295.8 (55.3 – 395.8)
K_R (mM)	-	-	-	4.5 (0.14 – 6.4)

The non-linearised versions of models **T1** and **T2** were also investigated using the MCMC technique. However, as noted for the original Monod model, it was not possible to estimate the maximum growth rate and half-saturation constant reliably from the available data, resulting in estimates that were not biologically feasible. The non-linearised **T1** model did show MCMC chain convergence for the threshold parameter, estimating its value at 83 mM (95% confidence interval 2.4 – 139.4 mM), comparable to the estimate of the **T1** model. The non-linearised **T2** model did not show MCMC chain convergence for the threshold parameter, therefore the non-linearised model versions were not considered further.

5.3.2 Model validation

In order to validate the threshold models, the predictions from each model were compared with separate experimental data from Groher and Weuster-Botz (2016b). Two sets of time-course data were obtained for *B. hydrogenotrophica*, one set for the microbe grown on the newly proposed general acetogen (GA) medium and a second set using the recommended DSMZ medium. A comparison of the predictions of the first order kinetics model and the three threshold models with the GA medium data is shown in Figure 5.3.

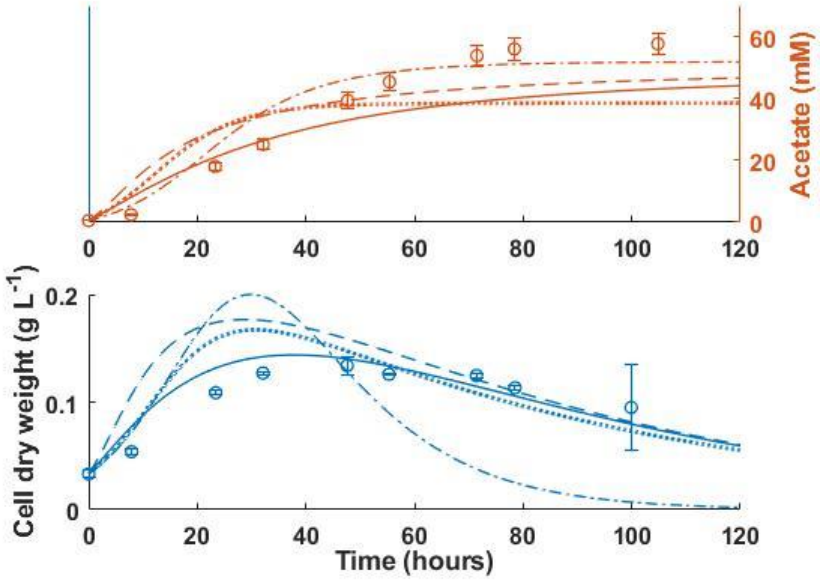

Figure 5.3. Model validation against data from Groher and Weuster-Botz (2016b) in which *Blautia hydrogenotrophica* was grown on General Acetogen medium. Dash dot line: first order kinetics model (Acetate R^2=0.91; CDW R^2=0.15). Dotted line: T1 model (Acetate R^2=0.31; CDW R^2=0.66). Dashed line: T2 model (Acetate R^2=0.63; CDW R^2=0.51). Solid line: T3 model (Acetate R^2=0.58; CDW R^2=0.84). Error bars denote standard deviations of at least three experimental replicates.

There was clear variation between the predictions of each of the four model structures. The first order kinetics model was the most accurate in predicting acetate production, but the least accurate in predicting microbial growth. The converse was true of **T3**, the reversible Michaelis-Menten kinetics model, which predicted microbial growth accurately, but underestimated acetate production.

Figure 5.4 shows the predictions of each of the four models against the DSMZ medium data. None of the models perform well in this scenario, but this may be attributed to the wide differences between the DSMZ, GA and calibration data media, explained in the Discussion.

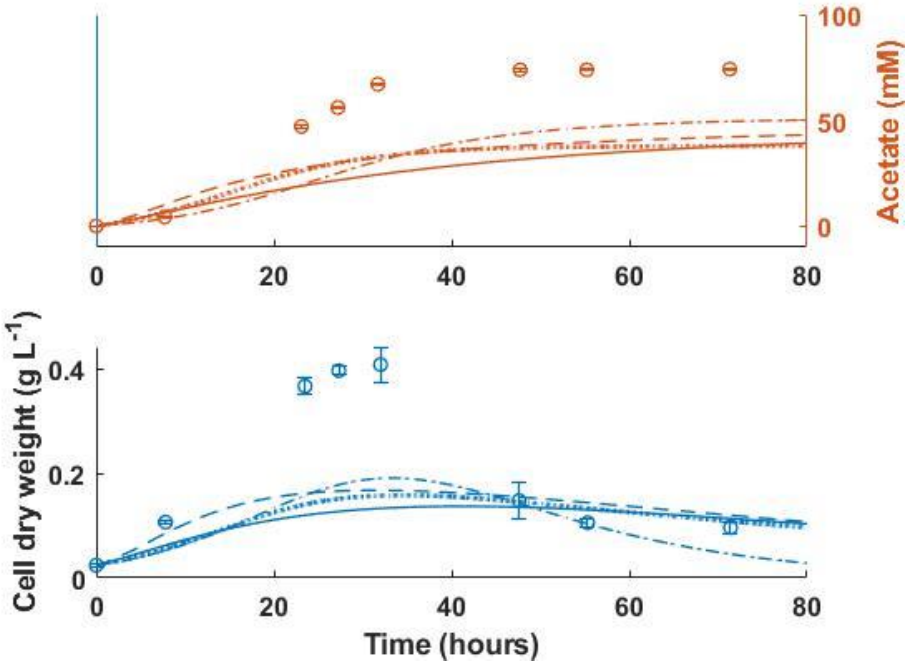

Figure 5.4. Model validation against data from Groher and Weuster-Botz (2016b) in which *Blautia hydrogenotrophica* was grown on DSMZ medium. Dash dot line: first order kinetics model. Dotted line: T1 model. Dashed line: T2 model. Solid line: T3 model. All R^2 values were <0.20. Error bars denote standard deviations of at least three experimental replicates

5.4 Discussion

The four models presented may be used to draw several conclusions on both the metabolism of *B. hydrogenotrophica* and the mathematics of the models themselves. The results of the calibration encourage the inclusion of threshold considerations in mathematical models for reductive acetogens. The threshold models presented here captured the monoculture growth kinetics of the acetogen more accurately than the first order kinetics model. This is to be expected, given that *B. hydrogenotrophica* has previously been shown to have an uptake threshold for hydrogen of approximately 70 mM (Leclerc et al., 1997), which was supported by the estimate of 86.2 mM using model **T1**. However, deciding which of the three threshold models is best suited to modelling the growth of this acetogen was challenging. Each performed similarly when compared to the calibration data, but significant variation was seen in the predictions for the validation data. Although the first order kinetics model gave a prediction of acetate production with R^2>0.9, this model structure was unable to capture the growth data. The **T1** model also yielded predictions for both metabolite concentrations and growth that were unsatisfactory for the validation data.

Between the **T2** and **T3** model structures, there was no clearly superior outcome in terms of model fit. Both require a greater number of parameters than the other models presented (two or three more parameters than the first order kinetics model for the **T2** or **T3** models respectively), some of which cannot be easily estimated experimentally. With fewer parameters, the **T2** model is the simpler of the two, but the **T3** model features parameters that are more biologically tangible. While the **T3** model was more accurate in predicting CDW, it underpredicted acetate production for the validation data set. Given further validation data from batch experiments, it may be possible to determine which of the threshold models is most effective, but these data are currently unavailable.

It should also be noted that the **T3** model is not well suited to modelling environments with high acetate concentrations and low hydrogen concentrations. Using the parameter values from Table 5.1, the non-trivial steady state for metabolite concentrations is achieved when $P \approx 3.43\ H$. This is an attraction point, stable to small perturbations in the variables. Therefore, in scenarios with a hydrogen concentration lower than the steady state value, the model would predict depletion of acetate and accumulation of hydrogen until the steady state was reached. Microbial growth yield would likely also be different when performing the reverse reaction, if indeed this reaction could be performed by the strain in question. The current model structure would predict a reduction in biomass in this situation, so would need to be altered with an appropriate yield value included. As there are no data for the culture of reductive acetogens under such conditions for comparison the use of the **T3** model would not be recommended in this scenario. Moreover, the fact that the consumption of hydrogen is limited by the acetate concentration rather than low concentrations of hydrogen is inconsistent with the results of Leclerc et al. (1997) for a hydrogen threshold. Therefore, the **T2** model with the threshold term defined by Ribes et al. (2004) is the most appropriate for the data considered here.

Ribes et al. (2004) suggested the following values for the **T2** parameters A and T:

$$A = \frac{100}{H_t}$$

$$T = 1.1H_t$$

While these values give some biological meaning to the parameters by relating them to the substrate threshold for the microbe, they are not appropriate in all cases. Using the threshold

hydrogen value of 86.2 mM, this would give values of $A \approx 1.16$ and $T = 94.82$, each of which are 773% and 30% the value of the **T2** estimates for these parameters, respectively. Use of these values in the model results in an abrupt inhibition of hydrogen metabolism and growth with poor model fit (data not shown), so is not appropriate for modelling the hydrogen threshold of *B. hydrogenotrophica*. A and T should be seen as related to H_t, and thus biologically tangible in this sense, however the exact relationship between these parameters will likely be case-dependent.

There have been previous models of *B. hydrogenotrophica* growth and metabolism. Tamayo et al. (2008) employed a Monod-based model including gas-liquid transfer and the consideration of both viable and dead cells but did not include a threshold hydrogen concentration. Their model structure and the units used mean that a direct comparison between each parameter value was impossible, but the death rates they obtained (mean rate 0.03 h^{-1}) are similar to those found here. More recently, D'Hoe et al. (2018) formulated a mathematical model for *B. hydrogenotrophica* for use in combination with models for two other colonic microbes. Their model was based on experimental data presented in the same publication but focussed on the ability of this acetogen to feed on formate and fructose, omitting its ability to consume CO_2 and H_2. The model was constructed in this manner as no detectable consumption of either metabolite was found in culture, which the authors assumed was because these metabolites did not reach sufficient concentrations for *B. hydrogenotrophica* to metabolise. Indeed, the concentration of hydrogen remained below 40 mM in monoculture and did not appear to have increased above 70 mM, the hydrogen threshold proposed by Leclerc et al. (1997) for this microbe, in any of the co-culture combinations studied. It is unclear whether this was due to depletion of formate and fructose in the medium, from which hydrogen was being produced, or whether hydrogen was metabolised by *B. hydrogenotrophica* at concentrations approaching the threshold value, thus maintaining the low concentration. It is also unclear whether *B. hydrogenotrophica* preferentially metabolises formate and fructose over hydrogen at these concentrations. However, even without consideration of hydrogen metabolism, the authors obtained a good model fit to their data. Any complete model for the acetogens must include the metabolism of all possible substrates, in order to be applicable to complex multi-substrate and multi-product environments such as the colon or a bioreactor.

The medium in which microbes are grown will have an enormous effect on experimental results and, therefore, the quality of the model prediction. The purpose of Groher and Weuster-Botz (2016b) was to present a new medium better suited to the monoculture growth of acetogens and acetate production. Indeed, they found that *B. hydrogenotrophica* was more efficient in terms of cell specific acetate formation on the GA medium than on the DSMZ recommended medium. It was notable that the acetogen achieved more rapid growth and to a greater concentration on the DSMZ medium, but the authors stated that this was almost certainly due to the greater concentration of complex constituents in the DSMZ medium compared to the GA medium. Critically, the DSMZ medium contains 25 g L^{-1} yeast extract, compared to 2 g L^{-1} in the GA medium. The medium used by Bernalier et al. (1996) contained 0.5 g L^{-1} yeast extract, making it more comparable in this respect to the GA medium than the DSMZ medium. The models developed here would therefore be expected to be more accurate in predicting growth on the GA medium, than a medium that contains more complex compounds. This justifies the lack of fit displayed in Figure 5.4. Previous experimental work with this microbe has found that the production of acetate is limited by the concentration of yeast extract in the medium, but only concentrations up to 4 g L^{-1} were considered (Leclerc et al., 1998). The additional carbon source provided by the yeast extract likely results in significant microbial feeding via pathways other than reductive acetogenesis, for which the original threshold models were not designed to account.

This is supported by considering the stoichiometry of reductive acetogenesis given the available hydrogen. At the beginning of both the GA and DSMZ experiments, the 400 mL gaseous headspace in the serum bottles used was occupied by a gas mixture of H_2:CO_2 (66:34) at 200 kPa pressure. This 0.02 mol of hydrogen could theoretically produce at most 50 mM of acetate in the 100 mL medium via the Wood-Ljungdahl pathway. This is approximately equal to the acetate yield in the GA medium, but is around 20 mM lower than the acetate yield in the DSMZ medium. This confirms that a significant proportion of the acetate produced on the DSMZ medium was not derived from reductive acetogenesis, therefore must be the result of alternative carbon source consumption.

As an additional investigation, the **T2** and **T3** models were altered by including equations 5.12-5.14 to ascertain whether growth on constituents of the added yeast extract may be

responsible for increased growth and acetate yield in the DSMZ medium. As there are no available time-course data for the growth of this microbe on yeast extract alone, the parameter values specific to yeast extract metabolism were drawn from model fitting to the *B. hydrogenotrophica* growth on DSMZ medium data. As shown in Figure 5.5, the inclusion of yeast extract metabolism allows both the **T2** and **T3** models to capture growth and acetate production on DSMZ medium.

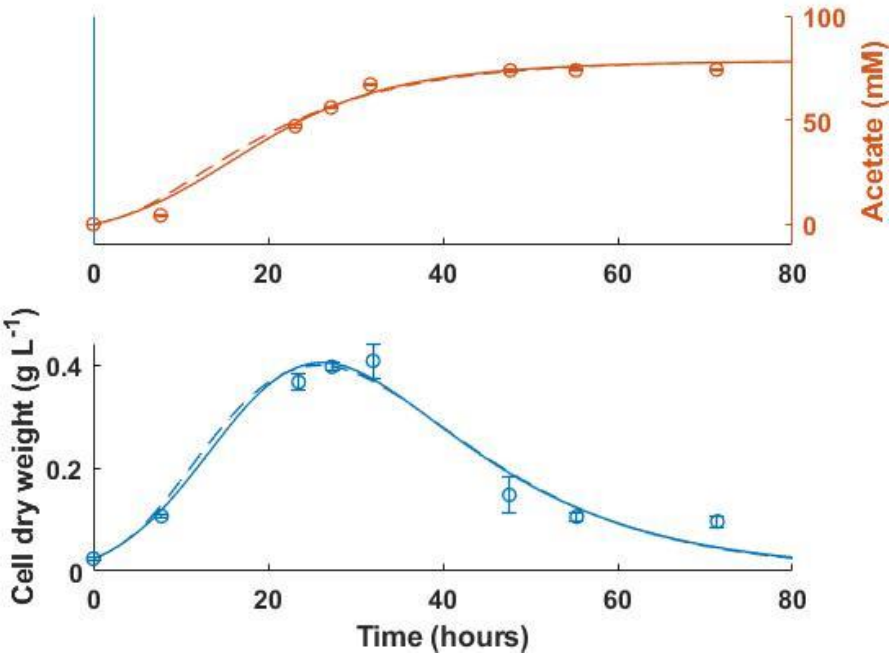

Figure 5.5. Example model prediction for *Blautia hydrogenotrophica* growth on DSMZ medium with the inclusion of yeast extract metabolism. Dashed line: T2 model (Acetate R^2=0.98; CDW R^2=0.96). Solid line: T3 model (Acetate R^2=0.99; CDW R^2=0.96). Error bars denote standard deviations of at least three experimental replicates. Parameter values used during yeast extract metabolism simulation were: $\eta_E = 0.0018$ h^{-1} mM^{-1}, $Y_E = 0.02$ g L^{-1} mM^{-1}, $b_{EP} = 0.43$ and $k_d = 0.112$ h^{-1} for T2; $\eta_E = 0.002$ h^{-1} mM^{-1}, $Y_E = 0.013$ g L^{-1} mM^{-1}, $b_{EP} = 0.5$ and $k_d = 0.08$ h^{-1} for T3.

It is impossible to draw conclusions about the growth of *B. hydrogenotrophica* on yeast extract from these data, since yeast extract concentration was not measured over time, nor were metabolites other than acetate. This leaves uncertainty around the proportion of carbon from the yeast extract that was converted to compounds other than acetate. Therefore, the parameter values for η_E, Y_E, b_{EP} and k_d used to generate Figure 5.5 and stated in the caption are hypothetical and should not be treated as accurate estimates of these parameter values. More experimental work is required to understand yeast extract metabolism by this microbe, but Figure 5.5 does demonstrate that it is possible to account for the increased production of acetate, as well as the microbial cell concentration, by including an additional carbon source in the model.

The results of this modelling support the assertion of Groher and Weuster-Botz (2016b) that their GA medium allows for culture of acetogens with less confounding factors, further recommending its use for assessment of industrial suitability of acetogenic strains. However, while these models are sufficient for the study of reductive acetogenesis under batch conditions, it is important to note that in many environments, acetogens such as *B. hydrogenotrophica* have the ability to use a number of metabolic pathways and substrates (Liu et al., 2008; D'Hoe et al., 2018). Such dynamics must be included in any mathematical model that wishes to fully capture the growth and metabolism of these microbes in more complex scenarios.

One such scenario where a modelling perspective would be useful is in the competition for hydrogen between acetogens and other hydrogenotrophs. It is thought that both SRB and methanogens should outcompete acetogens for hydrogen due to their more efficient metabolism of this substrate (Gibson et al., 1993). However, in environments such as the human colon, acetogens are observed to coexist with the other hydrogenotrophs (Nava et al., 2012). While much study has been devoted to this topic, the key factors behind colonic hydrogenotroph ecology remain unclear. Threshold models such as those presented here could be applied to the competition between the three hydrogenotroph types and may provide more insight into their coexistence in the colon.

5.5 Conclusions

The use of threshold models is a more effective way to capture acetogen growth and metabolic dynamics than the simple Monod model, although finding which threshold model is most effective requires further investigation and experimental data. The models and analyses given here provide further evidence for minimal acetogen growth below a threshold hydrogen concentration. Moreover, evidence was found to support the assertion of Groher and Weuster-Botz (2016b) that their GA medium is superior to the DSMZ medium in terms of growth assessment and cell specific acetate production, due to the reduced concentration of complex medium constituents. The differences in the results between different media discussed here will be broadly applicable to the culturing of many microbes and modelling can be a useful tool in investigating such discrepancies.

Table 5.2. Mathematical notation		
Notation	**Description**	**Unit**
H	Hydrogen concentration	mM
P	Acetate concentration	mM
X	Microbial cell concentration	g L^{-1}
t	Time	h
μ_{max} or $\mu_{max,H}$	Maximum growth rate on hydrogen	h^{-1}
$\mu_{max,R}$	Maximum rate of the reverse reaction	h^{-1}
K_H	Hydrogen half-saturation constant	mM
K_R	Half-saturation constant for the reverse reaction	mM
Y	Yield of the microbe when growing on hydrogen	g L^{-1} mM^{-1}
k_d	Microbial death rate	h^{-1}
η	First order kinetics rate	h^{-1} mM^{-1}
H_t	Threshold concentration for hydrogen uptake	mM
H^*	$H^* = H - H_t$	mM
f, F	Sigmoidal smoothing functions from Ribes et al. (2004)	Dimensionless
A	Tuning parameter from Ribes et al. (2004)	mM^{-1}
T	Tuning parameter from Ribes et al. (2004)	mM

References

Bengelsdorf, F.R., Beck, M.H., Erz, C., Hoffmeister, S., Karl, M.M., Riegler, P., et al. (2018). "Chapter Four - Bacterial Anaerobic Synthesis Gas (Syngas) and CO2+H2 Fermentation," in Adv. Appl. Microbiol., eds. S. Sariaslani & G.M. Gadd. Academic Press, 143-221.

Bernalier, A., Willems, A., Leclerc, M., Rochet, V., and Collins, M.D. (1996). *Ruminococcus hydrogenotrophicus* sp. nov., a new H2/CO2-utilizing acetogenic bacterium isolated from human feces. Arch. Microbiol. 166(3)**,** 176-183. doi: 10.1007/s002030050373.

D'Hoe, K., Vet, S., Faust, K., Moens, F., Falony, G., Gonze, D., et al. (2018). Integrated culturing, modeling and transcriptomics uncovers complex interactions and emergent behavior in a three-species synthetic gut community. eLife 7**,** e37090. doi: 10.7554/eLife.37090.

Drake, H.L. (1994). "Acetogenesis, Acetogenic Bacteria, and the Acetyl-CoA "Wood/Ljungdahl" Pathway: Past and Current Perspectives," in Acetogenesis, ed. H.L. Drake. (Boston, MA: Springer US), 3-60.

Drake, H.L., Küsel, K., and Matthies, C. (2013). "Acetogenic Prokaryotes," in The Prokaryotes: Prokaryotic Physiology and Biochemistry, eds. E. Rosenberg, E.F. DeLong, S. Lory, E. Stackebrandt & F. Thompson. (Berlin, Heidelberg: Springer Berlin Heidelberg), 3-60.

Fonty, G., Joblin, K., Chavarot, M., Roux, R., Naylor, G., and Michallon, F. (2007). Establishment and Development of Ruminal Hydrogenotrophs in Methanogen-Free Lambs. Appl. Environ. Microbiol. 73(20)**,** 6391-6403. doi: 10.1128/AEM.00181-07.

Frame, K.K., and Hu, W.-S. (1991). Kinetic study of hybridoma cell growth in continuous culture. I. A model for non-producing cells. Biotechnol. Bioeng. 37(1)**,** 55-64. doi: doi:10.1002/bit.260370109.

Gibson, G.R., MacFarlane, G.T., and Cummings, J.H. (1993). Sulphate reducing bacteria and hydrogen metabolism in the human large intestine. Gut 34(4)**,** 437-439.

Giraldo-Gomez, E., Goodwin, S., and Switzenbaum, M.S. (1992). Influence of mass transfer limitations on determination of the half saturation constant for hydrogen uptake in a mixed-culture CH4-producing enrichment. Biotechnol. Bioeng. 40(7)**,** 768-776. doi: doi:10.1002/bit.260400704.

Godwin, S., Kang, A., Gulino, L.M., Manefield, M., Gutierrez-Zamora, M.L., Kienzle, M., et al. (2014). Investigation of the microbial metabolism of carbon dioxide and hydrogen in the kangaroo foregut by stable isotope probing. ISME J. 8(9)**,** 1855-1865. doi: 10.1038/ismej.2014.25.

Graber, J.R., and Breznak, J.A. (2004). Physiology and nutrition of Treponema primitia, an H2/CO2-acetogenic spirochete from termite hindguts. Appl. Environ. Microbiol. 70(3)**,** 1307-1314. doi: 10.1128/AEM.70.3.1307-1314.2004.

Groher, A., and Weuster-Botz, D. (2016a). Comparative reaction engineering analysis of different acetogenic bacteria for gas fermentation. J. Biotechnol. 228**,** 82-94. doi: https://doi.org/10.1016/j.jbiotec.2016.04.032.

Groher, A., and Weuster-Botz, D. (2016b). General medium for the autotrophic cultivation of acetogens. Bioprocess Biosystems Eng. 39(10)**,** 1645-1650. doi: 10.1007/s00449-016-1634-5.

Karadagli, F., Marcus, A.K., and Rittmann, B.E. (2019). Role of hydrogen (H2) mass transfer in microbiological H2-threshold studies. Biodegradation 30(2)**,** 113-125. doi: 10.1007/s10532-019-09870-1.

Klipp, E. (2009). Systems biology : a textbook. Weinheim : Wiley-VCH, 2009.

Kovárová, K., Zehnder, A.J., and Egli, T. (1996). Temperature-dependent growth kinetics of *Escherichia coli* ML 30 in glucose-limited continuous culture. J. Bacteriol. 178(15)**,** 4530-4539.

Leclerc, M., Bernalier, A., Donadille, G., and Lelait, M. (1997). H2/CO2 Metabolism in Acetogenic Bacteria Isolated From the Human Colon. Anaerobe 3(5)**,** 307-315. doi: https://doi.org/10.1006/anae.1997.0117.

Leclerc, M., Elfoul-Bensaid, L., and Bernalier, A. (1998). Effect of yeast extract on growth and metabolism of H2-utilizing acetogenic bacteria from the human colon. Curr. Microbiol. 37(3)**,** 166-171. doi: 10.1007/s002849900358.

Liu, C., Finegold, S.M., Song, Y., and Lawson, P.A. (2008). Reclassification of *Clostridium coccoides*, *Ruminococcus hansenii*, *Ruminococcus hydrogenotrophicus*, *Ruminococcus luti*, *Ruminococcus productus* and *Ruminococcus schinkii* as *Blautia coccoides* gen. nov., comb. nov., *Blautia hansenii* comb. nov., *Blautia hydrogenotrophica* comb. nov., *Blautia luti* comb. nov., *Blautia producta* comb. nov., *Blautia schinkii* comb. nov. and description of *Blautia wexlerae*. Int. J. Syst. Evol. Microbiol. 58(8)**,** 1896-1902. doi: 10.1099/ijs.0.65208-0.

López-Meza, J., Araíz-Hernández, D., Carrillo-Cocom, L.M., López-Pacheco, F., Rocha-Pizaña, M.D.R., and Alvarez, M.M. (2016). Using simple models to describe the kinetics of growth, glucose consumption, and monoclonal antibody formation in naive and infliximab producer CHO cells. Cytotechnology 68(4)**,** 1287-1300. doi: 10.1007/s10616-015-9889-2.

Lopez, S., McIntosh, F.M., Wallace, R.J., and Newbold, C.J. (1999). Effect of adding acetogenic bacteria on methane production by mixed rumen microorganisms. Anim. Feed Sci. Technol. 78(1)**,** 1-9. doi: https://doi.org/10.1016/S0377-8401(98)00273-9.

Monod, J. (1949). The Growth of Bacterial Cultures. Annu. Rev. Microbiol. 3(1)**,** 371-394. doi: 10.1146/annurev.mi.03.100149.002103.

Muñoz-Tamayo, R., Giger-Reverdin, S., and Sauvant, D. (2016). Mechanistic modelling of in vitro fermentation and methane production by rumen microbiota. Anim. Feed Sci. Technol. 220**,** 1-21. doi: https://doi.org/10.1016/j.anifeedsci.2016.07.005.

Nava, G.M., Carbonero, F., Croix, J.A., Greenberg, E., and Gaskins, H.R. (2012). Abundance and diversity of mucosa-associated hydrogenotrophic microbes in the healthy human colon. ISME J. 6(1)**,** 57-70. doi: 10.1038/ismej.2011.90.

Rey, F.E., Faith, J.J., Bain, J., Muehlbauer, M.J., Stevens, R.D., Newgard, C.B., et al. (2010). Dissecting the in vivo metabolic potential of two human gut acetogens. J. Biol. Chem. 285(29)**,** 22082-22090. doi: 10.1074/jbc.M110.117713.

Ribes, J., Keesman, K., and Spanjers, H. (2004). Modelling anaerobic biomass growth kinetics with a substrate threshold concentration. Water Res. 38(20)**,** 4502-4510. doi: https://doi.org/10.1016/j.watres.2004.08.017.

Schiel-Bengelsdorf, B., and Dürre, P. (2012). Pathway engineering and synthetic biology using acetogens. FEBS Lett. 586(15)**,** 2191-2198. doi: https://doi.org/10.1016/j.febslet.2012.04.043.

Tamayo, R.M., Laroche, B., Leclerc, M., and Walter, E. (2008). "Modelling and identification of in vitro homoacetogenesis by human-colon bacteria", in: 2008 16th Mediterranean Conference on Control and Automation, 1717-1722.

Thauer, R.K., Jungermann, K., and Decker, K. (1977). Energy conservation in chemotrophic anaerobic bacteria. Bacteriol. Rev. 41(1)**,** 100-180.

Van Wey, A.S., Cookson, A.L., Roy, N.C., McNabb, W.C., Soboleva, T.K., and Shorten, P.R. (2014). Monoculture parameters successfully predict coculture growth kinetics of *Bacteroides*

thetaiotaomicron and two *Bifidobacterium* strains. Int. J. Food Microbiol. 191**,** 172-181. doi: 10.1016/j.ijfoodmicro.2014.09.006.

Wolin, M.J., and Miller, T.L. (1983). Interactions of microbial populations in cellulose fermentation. Fed. Proc. 42(1)**,** 109-113.

The following chapter contains material from the following manuscript submitted for publication in Ecological Modelling:

Co-culture modelling of a sulphate-reducing bacterium and a methanogen demonstrates altered metabolic parameters compared to monoculture. Smith NW, Shorten PR, Altermann E, Roy NC, McNabb WC.

Chapter 6: Mathematical modelling of sulphate-reducing bacteria and methanogenic archaea shows differences in metabolic parameter values between monoculture and co-culture

Abstract

Sulphate-reducing bacteria (SRB) and methanogenic archaea coexist in several environments via cross-feeding of the methanogen on products of the oxidative metabolism of SRB. This relationship has been studied experimentally, providing an opportunity for greater understanding of co-culture ecological dynamics via mathematical modelling. A co-culture Monod-based model was formulated with kinetic parameter values from previous monoculture research. The predictions of the co-culture model were then compared to experimental data for *M. maripaludis* in co-culture with either *D. vulgaris* or *Desulfovibrio alaskensis*. While the model structure was sufficient to reproduce the experimental data, monoculture metabolic parameter values did not translate to the co-culture environment. In particular, the growth yield parameters of both SRB and methanogens were estimated to be reduced by at least 50% in co-culture. With these parameter modifications, the model achieved fits with R^2 values greater than 0.90. Interspecies differences in the predominant exchange metabolite, either hydrogen or formate, for different SRB species likely contributed to the variation in parameter values estimated from monoculture versus co-culture data. Previous research has shown results both supporting and opposing the use of monoculture parameter values in co-culture modelling. This model highlights that monoculture values are inappropriate for the prediction of co-culture dynamics for SRB and methanogens. However, the same model structure may be successfully applied given appropriate modifications to parameter values such as growth yield.

6.1 Introduction

SRB and methanogens are two MFGs that are found to either compete for nutrients or cross-feed from one another depending on environmental conditions. The two coexist in many environments, from the human colon (as discussed in Chapter 2) to various naturally-occurring sediments (Muyzer and Stams, 2008) and the availability of nutrients in these environments can determine the relationship between these microbes.

The defining characteristic of SRB is their ability to use sulphate as a terminal electron acceptor, but they are also able to achieve growth by oxidising organic compounds. Such growth has been shown to be inhibited by a build-up of hydrogen in the environment, formed during the metabolism of organic compounds, which inhibits re-oxidation of cofactors important in the breakdown of these organic compounds (Noguera et al., 1998; Walker et al., 2009; Junicke et al., 2015). In the presence of excess sulphate, hydrogen build-up does not occur, due to the use of reducing power in the reduction of sulphate. In the absence of sulphate, the presence of a hydrogenotrophic methanogen that can remove the inhibitory hydrogen via metabolite cross-feeding can allow for growth of both organisms with lactate as the sole added substrate.

The study of microbial metabolism can be assisted by mathematical modelling: comparison of model predictions with experimental data complements experimentation by isolating areas that require further study. Previous research has shown that the metabolic behaviour of certain microbes in co-culture may be mathematically predicted based on their behaviour in monoculture (Van Wey et al., 2014; Louca and Doebeli, 2015). However, with different microbes, monoculture parameters were insufficient to predict dynamics in co-culture (Pinto et al., 2017; D'Hoe et al., 2018). The modelling techniques used in these studies were similar, based on either Monod or first-order kinetics, suggesting that predictability of co-culture dynamics based on monoculture parameter values may be specific to the microbes and culture conditions studied. Gene expression differences identified between organisms growing in monoculture versus co-culture have been cited as a driving factor behind these inconsistencies (D'Hoe et al., 2018).

It is unclear whether the co-culture dynamics of SRB and methanogens may be captured using mathematical models parameterised from monoculture data. Previous publications have

described transcriptional differences between monoculture and co-culture in these combinations (Walker et al., 2009; Meyer et al., 2013), which suggests that a model parameterised with monoculture parameters would not represent co-culture data well.

The hypothesis here was that the combination of monoculture models for SRB and methanogen growth and metabolic dynamics into a co-culture model could be used to identify metabolic parameters that change between monoculture and co-culture environments via comparison to experimental data. If the hypothesis holds, the model would then provide a procedure for determining the nature of environment-dependent metabolic plasticity of SRB and methanogens, yielding a novel perspective on this cross-feeding interaction.

6.2 Methodology

6.2.1 Mathematical model

The mathematical model structures from Chapters 3 and 4 were used for the initial monoculture models for the methanogen and SRB, respectively (see also Appendix B). New methanogen parameter values were obtained from fitting to monoculture data for *M. maripaludis* S2 (Appendix B, Figure B1 and Table B2), and from estimates in the literature (Ver Eecke et al., 2012; Goyal et al., 2015). The two monoculture models were combined in an additive manner to form the co-culture model.

For the experimental data considered, it was necessary to include mass transfer of hydrogen and methane between the liquid and gaseous phases. To do so, the respective MTCs were required. The MTC for methane has previously been derived from the MTC for hydrogen by considering the ratio of diffusivity between hydrogen and methane (Pauss et al., 1990). Under this assumption, the methane MTC is equal to the hydrogen MTC multiplied by 0.581. The co-culture mathematical model is as follows:

$$\frac{dL}{dt} = -\frac{\mu_{max,L}\, X_S}{Y_L}\left(\frac{L}{K_L + L}\right)\left(1 - \frac{H_{aq}}{H_{max}}\right) - DL + I_L \tag{6.1}$$

$$\frac{dH_{aq}}{dt} = b_{LH}\frac{\mu_{max,L}\, X_S}{Y_L}\left(\frac{L}{K_L + L}\right)\left(1 - \frac{H_{aq}}{H_{max}}\right) - \frac{\mu_{max,H}\, X_M}{Y_H}\left(\frac{H_{aq}}{K_{H,M} + H_{aq}}\right) - k_L a_H \left(H_{aq} - \frac{1}{\rho_H} H_g\right) - DH_{aq} \tag{6.2}$$

$$\frac{dH_g}{dt} = k_L a_H \left(\rho_H H_{aq} - H_g\right)\frac{V_{aq}}{V_g} - dH_g \tag{6.3}$$

$$\frac{dA}{dt} = b_{LA}\frac{\mu_{max,L}\, X_S}{Y_L}\left(\frac{L}{K_L + L}\right)\left(1 - \frac{H_{aq}}{H_{max}}\right) - DA \tag{6.4}$$

$$\frac{dM_{aq}}{dt} = b_{HM}\frac{\mu_{max,H}\, X_M}{Y_H}\left(\frac{H_{aq}}{K_{H,M} + H_{aq}}\right) - k_L a_M \left(M_{aq} - \frac{1}{\rho_M} M_g\right) - DM \tag{6.5}$$

$$\frac{dM_g}{dt} = k_L a_M \left(\rho_M M_{aq} - M_g\right)\frac{V_{aq}}{V_g} - dM_g \tag{6.6}$$

$$\frac{dX_S}{dt} = \mu_{max,L}\, X_S \left(\frac{L}{K_L + L}\right)\left(1 - \frac{H_{aq}}{H_{max}}\right) - DX_S \tag{6.7}$$

$$\frac{dX_M}{dt} = \mu_{max,H}\, X_M \left(\frac{H_{aq}}{K_{H,M} + H_{aq}}\right) - DX_M \tag{6.8}$$

As in the previous chapters, L, A, H and M refer to the concentrations of lactate, acetate hydrogen and methane, respectively, with the subscripts aq and g denoting aqueous and gaseous concentrations, respectively. The gaseous metabolites are given in atmospheric units; all other metabolites in mM. X_S and X_M (mg L^{-1}) are the concentrations of SRB and methanogen cells, respectively. All biological parameters and their estimated values are given in Table B2, Appendix B.

As the data to which the model was compared did not involve the metabolism of sulphate by SRB, the equations and terms involved in sulphate reduction were not reproduced in this model. Some of the data used for comparison included continuous culture conditions; thus, inflow and

outflow terms were additionally considered in the model. Metabolite addition was included at the rate given in the experimental methodology, while dilution was considered to act uniformly upon all metabolites and cells in either the gaseous or aqueous phases. The aqueous dilution rate D (h^{-1}) was applied to all model constituents in the aqueous phase, while the gaseous dilution rate d (h^{-1}) was applied to all model constituents in the gaseous phase. Lactate was the only metabolite added to the culture in the data sources used, therefore the addition term I_L (mM h^{-1}) was included in the lactate differential equation.

6.2.2 Experimental data

Experimental data for the co-culture growth of *M. maripaludis* S2 with either *D. vulgaris* Hildenborough or *Desulfovibrio alaskensis* G20 were obtained from Stolyar et al. (2007), Walker et al. (2009) and Meyer et al. (2013). Monoculture data for the methanogenic strain *M. maripaludis* were also obtained from Stolyar et al. (2007). Graphical input and image capturing software, implemented in MATLAB (The MathWorks; www.mathworks.com), were used to obtain time-course data from these sources.

Where necessary, co-culture OD data were converted to the model units of mg L^{-1} using the same conversion factor as the original publications: 1 OD unit = 385 mg L^{-1} (Stolyar et al., 2007).

6.2.3 Model fitting

The co-culture model was fitted to the experimental data in all cases using the fminsearch optimisation routine in MATLAB (The MathWorks; www.mathworks.com). The data set from each publication varied in the types of data collected. For example, Stolyar et al. (2007) did not collect data on gaseous hydrogen, whereas Meyer et al. (2013) did. For each data source A, there were response variables i (i may represent gaseous methane, lactate concentration, etc.). Data set A_i contained N_{A_i} data points. The function to be minimised, Z, was the product of the sum of squared errors of the model fit to each data set, normalised to both the measurement scale and the number of data points in the set.

$$Z = \prod_{A_i} \left(\frac{1}{N_{A_i}} \sum_{j=1}^{N_{A_i}} \frac{\left(\hat{Y}_j - Y_j\right)^2}{\bar{Y}} \right)$$

In this equation, Y_j is the data value at the j[th] time point t_j and $\hat{Y}_j$ is the corresponding model prediction at time t_j. $\bar{Y}$ is the mean value of the response variable A_i.

After comparison of the model prediction using monoculture parameters to the data, attempts were made to identify a minimal set of fitting parameters necessary to capture the experimental data. The following minimisation protocol was used in this process. A set of 10 fitting parameters was constructed: the initial ratio of SRB cell concentration to methanogen cell concentration, both the hydrogen and methane MTCs, the maximum growth rates, half-saturation constants and yield parameters for both lactate oxidation and methanogenesis, and the hydrogen inhibition parameter for lactate oxidation (see Appendix B for full details of model parameterisation). These fitting parameters were then used in the fminsearch optimisation routine described above to obtain a fit to the data. The parameter that showed the least proportional variation to its monoculture value after optimisation was then fixed to this monoculture value. The optimisation routine was then run again for the remaining parameters. This process of removing a single parameter from the optimisation routine was repeated until the quality of model fit was deemed inadequate, as determined by R^2 values below 0.80 for at least one of the OD, lactate, acetate or methane fits. When this occurred, the parameter that was fixed at the previous step was returned to the set of fitting parameters and the parameter showing the next least variation was fixed to its monoculture value for the next optimisation. This iterative process was continued until a minimal set of fitting parameters that allowed for model fit above the threshold R^2 value was found.

An MCMC approach was used to produce confidence intervals for the parameter estimates. Using the above optimisation function, Z, an MCMC algorithm was run for 500,000 iterations in MATLAB (The MathWorks; www.mathworks.com). A non-parametric distribution was fitted to the resulting sample for each parameter, allowing 95% confidence intervals to be obtained based on the cumulative density function of this distribution.

6.3 Results

6.3.1 Comparison of model predictions to experimental data using monoculture-derived parameters

Experimental data describing the co-culture growth of *M. maripaludis* with either *D. vulgaris* or *D. alaskensis* in the absence of sulphate were compared to the predictions of the co-culture model run using monoculture-derived parameter values. In each case, the initial ratio of SRB cell concentration to methanogen cell concentration (hereafter termed the initial ratio) and the MTC for hydrogen were fitted to the data. The methane MTC was assumed proportional to the hydrogen MTC, as described in the Methodology.

The experimental data were obtained from three sources. The first was a batch co-culture experiment with *D. vulgaris* Hildenborough and *M. maripaludis* S2 (Stolyar et al. (2007); Figure 6.1). The second and third sources were both chemostat experiments in which the co-cultures were run under batch conditions until reaching a specified OD, at which point continuous culture was initiated. The first of these involved a co-culture between the same two strains as above (Walker et al. (2009); Figure 6.2), whereas the final data source described *M. maripaludis* in co-culture with *D. alaskensis* (Meyer et al. (2013); Figure 6.3).

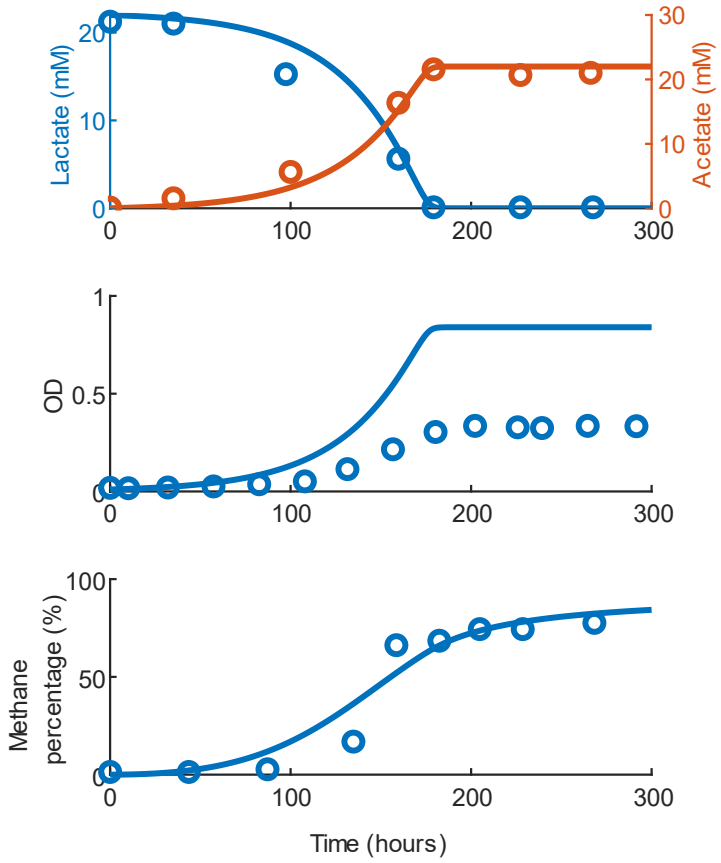

Figure 6.1 Model fit to co-culture data of *Desulfovibrio vulgaris* and *Methanococcus maripaludis* from Stolyar et al. (2007). The co-culture was run under batch conditions with approximately 22 mM lactate initially available. Monoculture-derived biological parameters were used to generate this model fit, while the mass transfer coefficients and the initial ratio of sulphate-reducing bacteria cell concentration to methanogen cell concentration were fitted to the data. Lactate R^2 = 0.98; acetate R^2 = 0.98; optical density R^2 = 0.40; gaseous methane R^2 = 0.92.

It was apparent from an inspection of the model structure conducted before running simulations that the direct use of all monoculture parameters could not accurately capture the co-culture dynamics: the half-saturation constant for hydrogen uptake by *M. maripaludis* was more than three orders of magnitude higher than the inhibitory hydrogen concentration for *D. vulgaris*. This would mean that growth by the SRB, and therefore hydrogen production, would be inhibited before sufficient hydrogen was available for meaningful growth by *M. maripaludis*. As this was clearly not reflective of the experimental data, a half-saturation constant determined experimentally for a different methanogenic strain in the literature was used as an initial approximation for use in the co-culture model, which compares well to estimates for other methanogenic strains (0.066 mM for *Methanocaldococcus* spp.; Ver Eecke et al. (2012) and references therein). This value is nearer to,

although still higher than, the SRB hydrogen inhibition parameter value. The uncertainty around this value is addressed with model fitting in section 6.3.2.

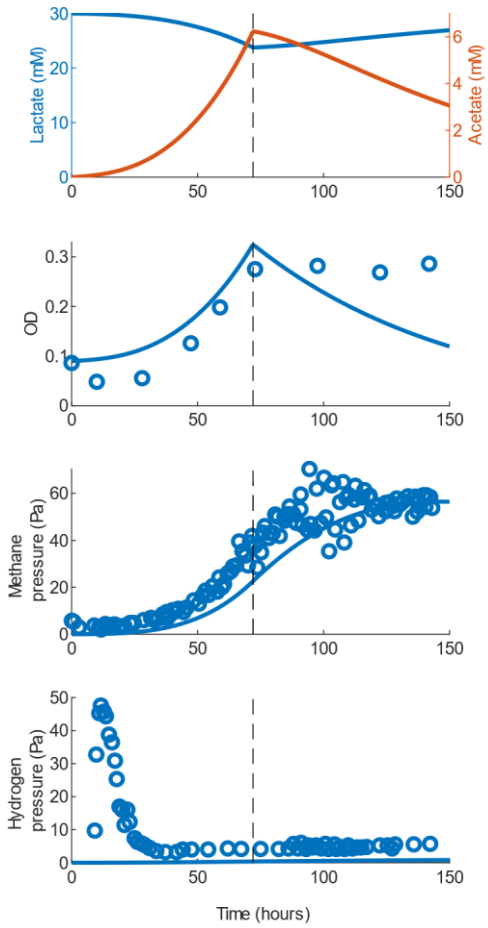

Figure 6.2. Model fit to co-culture data of *Desulfovibrio vulgaris* and *Methanococcus maripaludis* from Walker et al. (2009). The co-culture was run under batch conditions for the first 72 hours, before switching to continuous culture conditions (dashed line) with an aqueous dilution rate of 0.039 h^{-1} and a gaseous dilution rate of 0.012 h^{-1}. Monoculture-derived biological parameters were used to generate this model fit, while the hydrogen mass transfer coefficient and the initial ratio were fitted to the data. Lactate and acetate measurements were not available for this experiment; the model predictions for these metabolites are shown for illustrative purposes. optical density $R^2 = 0.05$; gaseous methane $R^2 = 0.79$; gaseous hydrogen $R^2 < 0$.

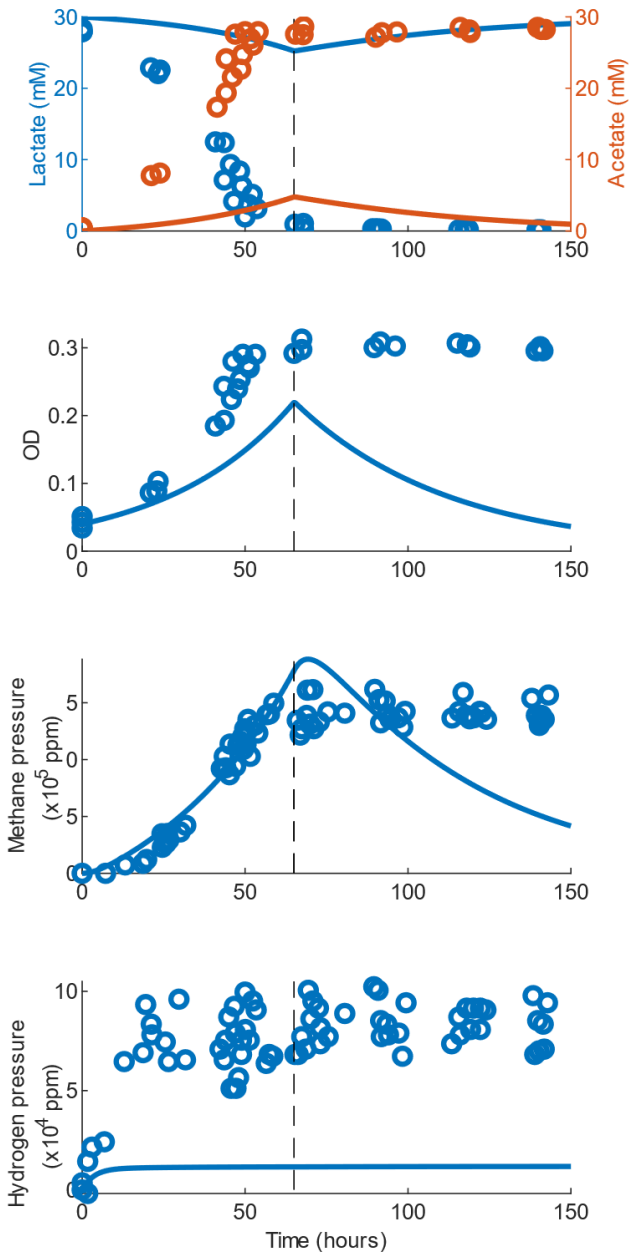

Figure 6.3. Model fit to co-culture data of *Desulfovibrio alaskensis* and *Methanococcus maripaludis* from Meyer et al. (2013). The co-culture was run under batch conditions for the first 65 hours, before switching to continuous culture conditions (dashed line) with an aqueous dilution rate of 0.047 h^{-1} and a gaseous dilution rate of 0.133 h^{-1}. Monoculture-derived biological parameters were used to generate this model fit, while the hydrogen mass transfer coefficient and the initial ratio were fitted to the data. Lactate $R^2 < 0$; acetate $R^2 < 0$; optical density $R^2 < 0$; gaseous methane $R^2 = 0.33$; gaseous hydrogen $R^2 < 0$.

Final lactate and acetate values were predicted to within 2 mM for the first data set (Figure 6.1). The OD was overpredicted, with the predicted value at the end of the experiment approximately 2.5-fold higher than the measured value. The model prediction for gaseous methane achieved an R^2 value above 0.90, although did not capture the more extended lag phase seen experimentally. The values of the initial ratio, MTCs and final ratios of SRB to methanogen cell concentrations, for this model fit and the two subsequent fits, are detailed in Table 6.1.

The model was also able to accurately capture gaseous methane pressure throughout the experiment for the second data set, with R^2 value of 0.79 (Figure 6.2). However, the trends for the other data types were not well predicted. Although time-course measurements of lactate and acetate were not available, the reported values for these molecules during steady state were 3-5 mM and 24-27 mM respectively (Walker et al., 2009), which was not predicted by the model. Moreover, OD was found to reach an equilibrium at around 0.3 experimentally, whereas the model did not reach a steady state and predicted that the OD would decrease after continuous culture was initiated. The model was also unable to capture the gaseous hydrogen burst, remaining lower than the observed data throughout the simulation.

For the third data set (Figure 6.3), similar problems with the model fit were obtained. Once again, the cause of these problems was that the model predicted gradual washout of the cultured strains once continuous culture conditions were initiated at 65 hours. As a result, the model was not able to capture the steady state dynamics observed experimentally.

Table 6.1. Comparison of model fits to experimental co-culture data using biological parameters determined from monoculture fitting

Data source	**Model fit** R^2 *Fold difference at end of experiment*[a]					**Sulphate-reducing bacteria:Methanogen ratios**			**Hydrogen mass transfer coefficient (fitted to data)**
	Optical density	Lactate	Acetate	H_2	CH_4	Model initial (fit to data)	Experimental final	Model final	
Stolyar et al. (2007) *Desulfovibrio vulgaris + Methanococcus maripaludis*	0.40 *2.5*	0.98 *BD*	0.98 *1.05*	NA	0.92 *1.06*	0.32	NA	0.63	0.00316 h^{-1}
Walker et al. (2009) *Desulfovibrio vulgaris + Methanococcus maripaludis*	0.19 *0.49*	NA	NA	<0 *0.14*	0.86 *1.04*	0.01	4	0.49	3.1955 x 10^{-6} h^{-1}
Meyer et al. (2013) *Desulfovibrio alaskensis + Methanococcus maripaludis*	<0 *0.15*	<0 *BD*	<0 *0.04*	<0 *0.12*	0.35 *0.4*	0.32	1.4	0.63	0.03527 h^{-1}

NA: Not available. BD: Experimental value was below detection limit.

[a]Calculated as: model value/experimental value. Where multiple data points were available for the final experimental value, the mean of the final three values was used.

While the model was accurate in predicting the batch culture metabolite data of Stolyar et al. (2007), the monoculture parameters were not suitable for predicting continuous culture dynamics. Concentrating on the batch culture data, a lack of fit to the OD data type was the major failing of the model prediction. This could be a result of an inaccurate conversion factor from OD units to the mg L^{-1} units of the model, or a result of decreased biomass yields in co-culture versus monoculture. To test the former possibility, the OD conversion factor was fitted to the batch culture data. The original value, taken from Stolyar et al. (2007) and also used by Walker et al. (2009), was 1 OD = 385 mg L^{-1}. The model estimate for this conversion factor was 989 mg L^{-1}, around 2.5 times larger than the experimentally determined estimate, and gave an R^2 value of 0.99 for the model fit to the OD data. The fits to the other data types were unaffected by the altered conversion factor. While an inaccurate conversion factor could therefore be responsible for the lack of fit to the batch data, it is unlikely that the experimental estimate was inaccurate by a factor of 2.5. A more likely explanation for the lack of fit is decreased biomass yields in co-culture versus monoculture, as found in previous experimental work and discussed later (Walker et al., 2009; Meyer et al., 2013). Therefore, modelling proceeded using the original conversion factor proposed by Stolyar et al. (2007).

There is variation between the MTCs for the model fits to the three data sets, particularly notable for the data from Walker et al. (2009), which was at least three orders of magnitude smaller than the other two (Table 6.1). There is no obvious physical reason why these values should be so different as the culture conditions were similar. It was also observed during model fitting that the goodness of fit to the gaseous methane data was predominantly determined by the value of the MTCs. For example, when the hydrogen MTC was fixed at 0.0032 h^{-1} (the value of the MTC determined for the data of Stolyar et al. (2007), giving a methane MTC value of 0.0019 h^{-1}) and the optimisation run again for the initial ratio in the Walker et al. (2009) simulation, the result was an overprediction of gaseous methane pressure ($R^2 < 0.0005$). Moreover, when the methane data were not included in the optimisation and both the initial ratio and the hydrogen MTC were fitted, the hydrogen MTC increased from 3.1955×10^{-6} h^{-1} to 1.7864×10^{-5} h^{-1}. Use of this new hydrogen MTC value resulted in an overprediction of gaseous methane ($R^2 = 0.12$) and the correct prediction of steady state hydrogen concentration (data not shown). Therefore, assuming a proportional

relationship between the two MTCs prevented their reliable estimation and accurate model fits to the data.

Given the clear dependency of the model gas predictions on the MTCs, both the hydrogen and methane MTCs were set as independent fitting parameters in later fitting exercises.

Despite the difficulties in predicting continuous co-culture data using monoculture-derived parameters, the accuracy of the model predictions for batch conditions imply that the true biological parameter values under co-culture conditions may be similar to those in monoculture. Several other aspects of the previous model predictions are important. Firstly, the lactate, acetate and OD aspects of the model fit were unaffected by large variations in MTC values. Therefore, mass transfer did not appear to be a limiting factor in lactate conversion to acetate or growth. Secondly, it is clear from the imprecision of the OD model fits to the batch culture data that either the yield values in co-culture were not equal to those in monoculture, or the OD conversion factor used was inaccurate. Differences in yield values were the more likely cause, as discussed above and supported by the discrepancies between the predicted and observed ratios of SRB to methanogens in the data (Table 6.1). To further investigate this, model fitting to the co-culture data sources was performed with additional parameters included in the optimisation.

6.3.2 Comparison of model predictions to experimental data using fitted metabolic parameters

For the parameter fitting to co-culture data, the data set of Meyer et al. (2013) was chosen as it includes measurements of a greater number of variables than the other data sets. A set of parameters was devised, including values that were both important determinants of model fit in these experiments and that were most likely to show variation between monoculture and co-culture. This set included all methanogen parameters, all lactate metabolism parameters for SRB and the SRB hydrogen inhibition parameter. Also included were the parameters previously considered in model fitting: both MTCs and the initial ratio. All other parameters were either fixed physical constants, biological parameters with no influence on model fit or were intentionally neglected. b_{LA},

the stoichiometric constant for moles of acetate produced per mole of lactate oxidised, was neglected as the value of this parameter appeared to be close to unity across all three data sets.

The model fitting routine was first performed using all parameters in the set, which allowed the model to capture all data types well (data not shown). However, this model fit included certain parameter values that were less than one-hundredth the size of the original values and, in some cases, not biologically plausible. In order to find the least number of parameters necessary to fit in order to capture the data, model fitting was repeated with all stoichiometric constants fixed at their monoculture values (Appendix B, Table B2). Again, this allowed for model fits with R^2 values above 0.80 for OD, lactate, acetate and methane data (data not shown). The model fitting was then iteratively repeated following the protocol described in the Methodology to identify a minimal set of fitting parameters necessary for good model fit.

Following this protocol, it was found that the minimum set of parameters necessary to obtain the threshold for goodness of fit contained the following six parameters: initial ratio, both MTCs, the yield parameters for SRB and methanogen growth, and the hydrogen inhibition parameter. However, this minimum set overpredicted the steady state lactate concentration by 4 mM and underpredicted gaseous hydrogen pressure by around 30% (Figure 6.4). In order to capture these values, it was necessary to use nine fitting parameters, which included those already listed and additionally the lactate maximum growth rate and the half-saturation constants for lactate and hydrogen (Figure 6.5). When using either parameter set, the model predicted a notable drop in gaseous hydrogen pressure once lactate became limiting, which was not observed experimentally. This drop was brief, and the model estimate returned to the steady state value by around the 75-hour mark. The cause for this feature was likely the depletion of lactate before continuous culture was initiated in the model, which appears not to have occurred in the experiments, and explains why the hydrogen prediction returned to the steady state value once continuous culture conditions were initiated.

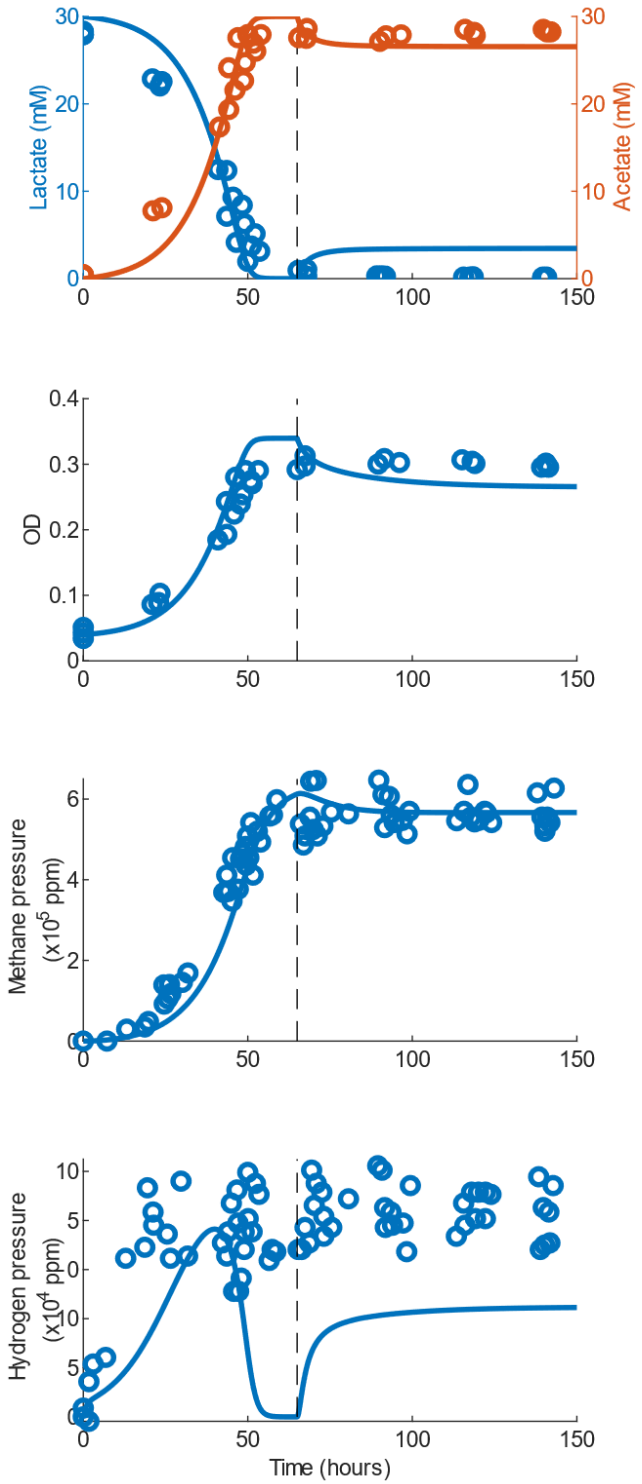

Figure 6.4. Model fit to the data of Meyer et al. (2013) using six fitting parameters: initial ratio, both mass transfer coefficients, both yield parameters and the hydrogen inhibition parameter. Lactate $R^2 = 0.91$; acetate $R^2 = 0.95$; optical density $R^2 = 0.88$; gaseous methane $R^2 = 0.92$; gaseous hydrogen $R^2 < 0$.

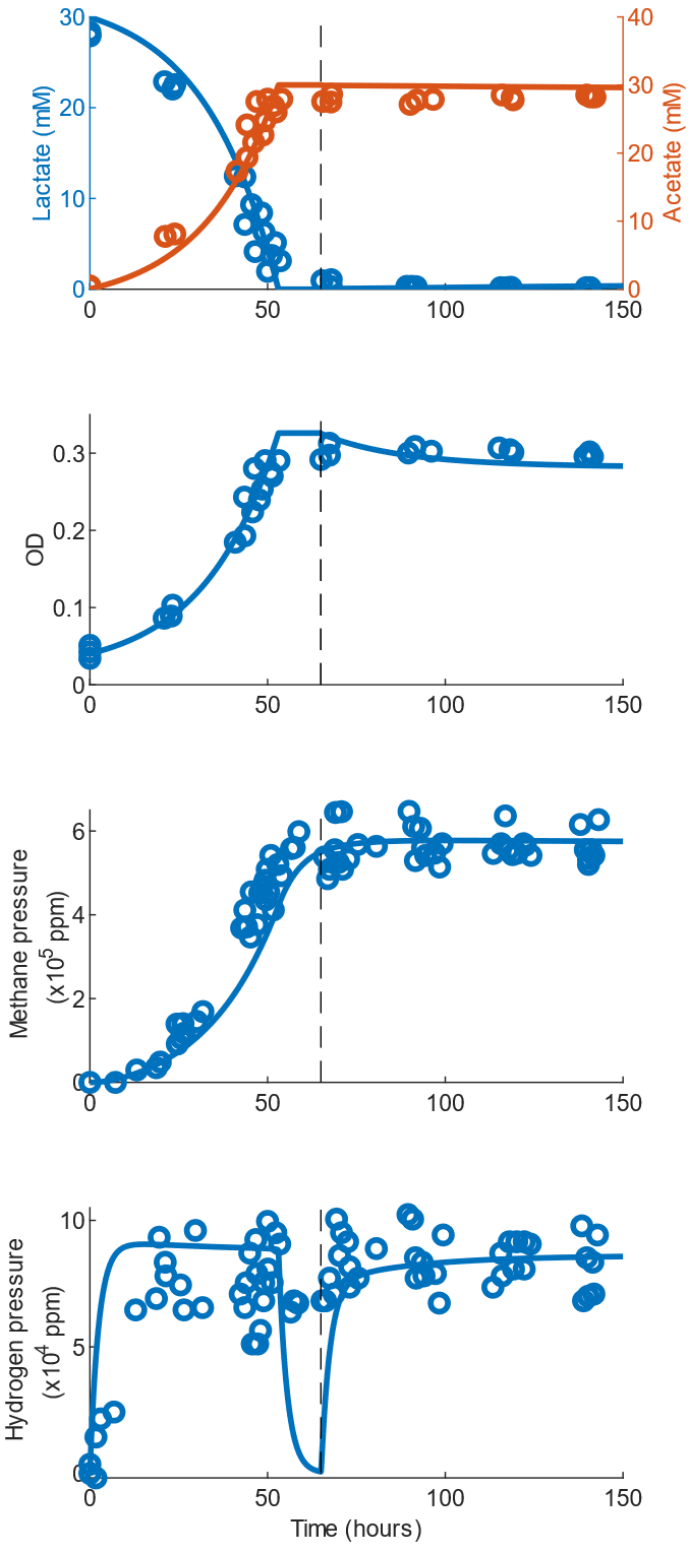

Figure 6.5. Model fit to the data of Meyer et al. (2013) using nine fitting parameters: initial ratio, both mass transfer coefficients, both yield parameters, the lactate maximum growth rate, the half-saturation constants for lactate and hydrogen and the hydrogen inhibition parameter. Lactate R^2 = 0.97; acetate R^2 = 0.95; optical density R^2 = 0.96; gaseous methane R^2 = 0.87; gaseous hydrogen R^2 = 0.06

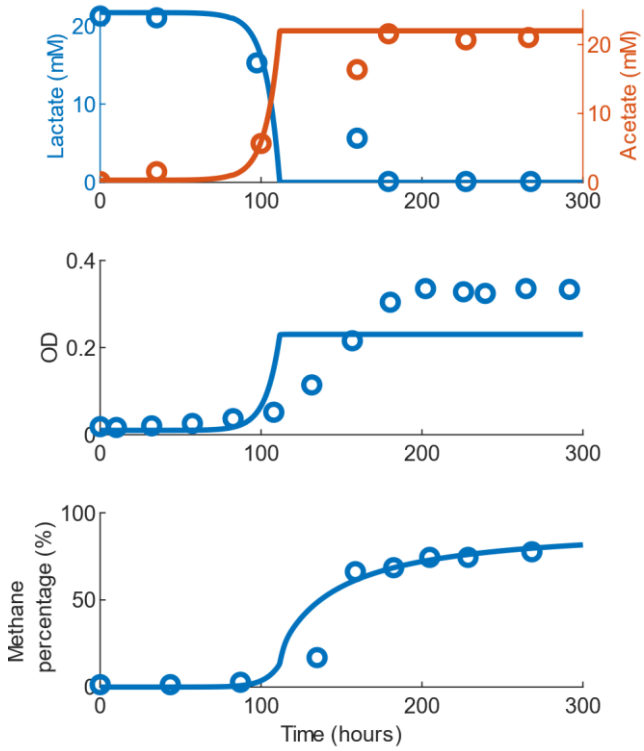

Figure 6.6. Model fit to the data of Stolyar et al. (2007) using six-parameter set parameter values. Optical density R^2 =0.49, lactate R^2 = 0.95, acetate R^2 = 0.95, gaseous methane R^2 = 0.89.

Model fit was sensitive to small variations in the six parameters of the minimised set (data not shown). Both fitted yield values were substantially lower than the monoculture values and use of either monoculture yield value resulted in an overprediction of OD. Use of the monoculture hydrogen inhibition constant resulted in earlier inhibition of lactate degradation, which prevented full lactate utilisation and therefore predicted reduced hydrogen and methane production compared to the data.

To ascertain whether the obtained parameter values for either the six- or nine-parameter sets could capture the data from the other sources, the data of Stolyar et al. (2007) and Walker et al. (2009) was used. Again, the initial ratio and MTCs were allowed to vary, but the remaining parameters were fixed at the new values obtained during optimisation to the Meyer et al. (2013) data set. Figures 6.6 and 6.7 show the model fits using the six-parameter set, while Figures 6.8 and 6.9 show the model fits using the nine-parameter set.

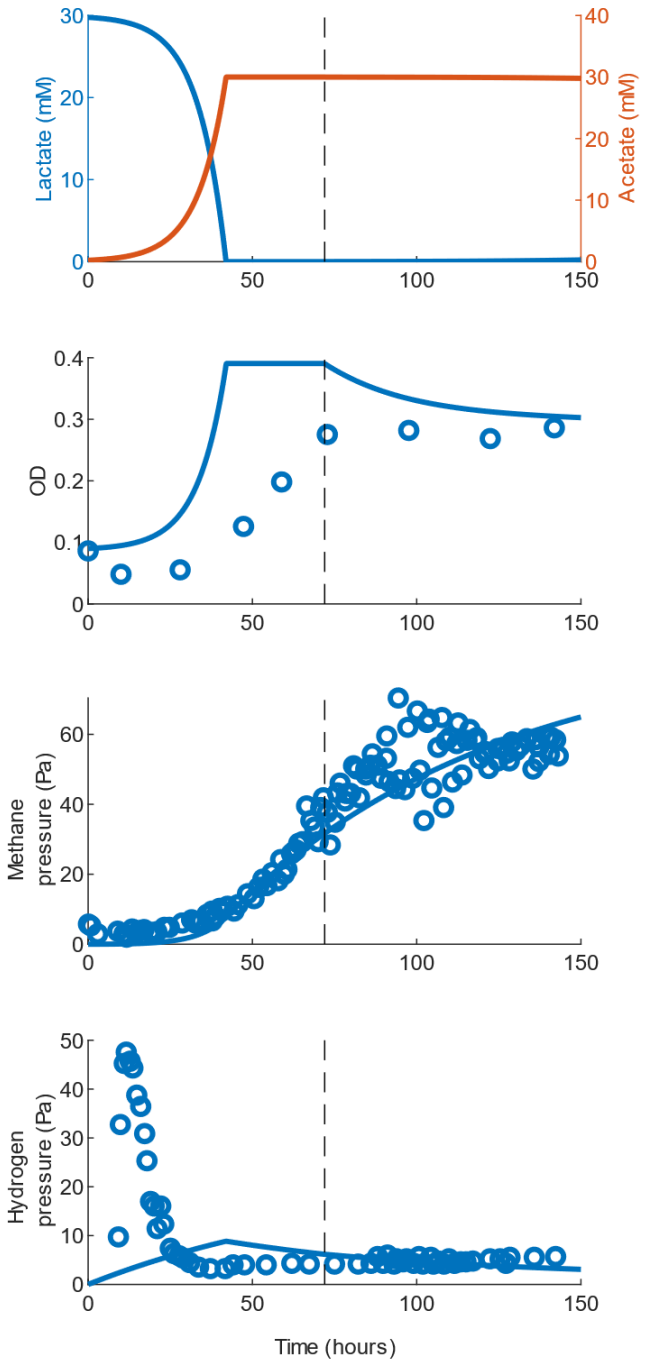

Figure 6.7. Model fit to the data of Walker et al. (2009) using six-parameter set parameter values. Optical density $R^2 = 0.34$, gaseous methane $R^2 = 0.89$, gaseous hydrogen $R^2 < 0$.

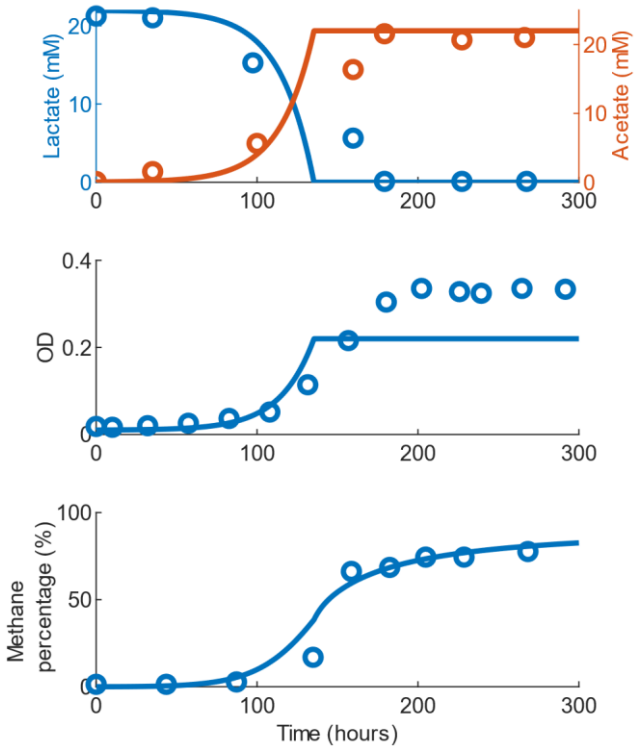

Figure 6.8. Model fit to the data of Stolyar et al. (2007) using nine-parameter set parameter values. Optical density R^2 =0.52, lactate R^2 = 0.94, acetate R^2 = 0.95, gaseous methane R^2 = 0.95.

Interestingly, the model prediction for OD against the data of Walker et al. (2009) was improved (Figures 6.7 and 6.9), with an R^2 value of 0.90 in the nine-parameter set case. The predictions for the gaseous metabolites were also good for both the six- and nine-parameter sets.

As shown in Table 6.2, the estimates for the maximum growth rate and half-saturation constant for lactate in the nine-parameter fit lie outside their MCMC generated confidence interval. These parameters also showed a positive correlation of 0.49, so are expected to have been estimated with poor repeatability. As has been seen previously (for example, Muñoz-Tamayo et al. (2016)), maximum growth rates and half-saturation constants are often strongly correlated in Monod model fitting, allowing only the ratio of the two to be repeatably estimated.

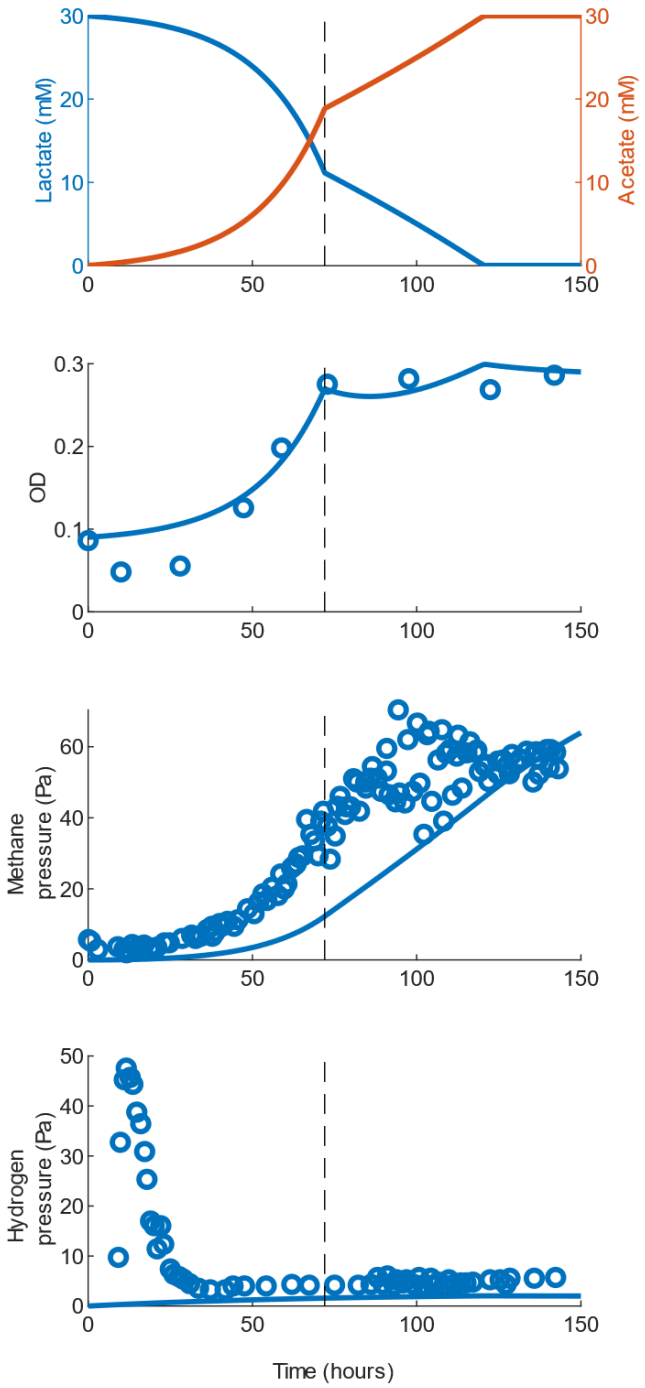

Figure 6.9. Model fit to the data of Walker et al. (2009) using nine-parameter set parameter values. Optical density $R^2 = 0.90$, gaseous methane $R^2 = 0.46$, gaseous hydrogen $R^2 < 0$.

Notable correlation was found between several of the estimated parameters from the MCMC routines (Appendix B, Tables B3 & B4). In particular, the nine-parameter set showed correlation coefficients greater than ± 0.4 for eight of the 36 pairwise combinations. These eight involved most of the estimated parameters, the only exceptions being the initial ratio and the methane MTC. A negative correlation (-0.76) between the hydrogen MTC and the hydrogen half-

saturation constant was the strongest correlation. The yield parameters were also strongly negatively correlated (-0.63), as would be expected given their linked role in determining the steady state OD value. In contrast, the six-parameter set showed minimal correlation, the greatest being a correlation coefficient of 0.39 between the initial ratio and the MTC for methane, the cause of which is not obvious and may be incidental. There was negligible correlation (-0.003) between the yield parameters in this set.

In all cases, the yield values obtained from model fitting were smaller than the monoculture estimates. These values were reduced to between 20-50% of their monoculture values, except for the SRB yield on lactate in the six-parameter fitting set, which was reduced by almost three orders of magnitude. Experimental estimates have put the co-culture yield value for *D. vulgaris* at around 80% of the monoculture value (Walker et al., 2009).

For future modelling of this co-culture, the nine-parameter set values appear to be the most applicable and biologically plausible when compared to monoculture parameter values. However, caution must be used given the case-specific initial ratios and MTCs observed here, as well as the observed differences in OD prediction precision between experimental data sets.

Table 6.2. Parameter values obtained via model fitting and Markov chain Monte Carlo generated confidence intervals

Parameter			Parameter value (95% confidence interval)		
			Monoculture values[a]	**9 fitted parameters**	**6 fitted parameters**
Initial ratio			NA	2.08 (0.06 - 4.12)	0.0002 (0 - 22)
Maximum growth rates	Lactate oxidation	$\mu_{max,L}$ (h^{-1})	0.116	0.784 (1.4 – 5.81)	0.116 [Fixed]
	Methanogenesis	$\mu_{max,H}$ (h^{-1})	0.131	0.131 [Fixed]	0.131 [Fixed]
Monod constants	Lactate (sulphate-reducing bacteria)	K_L (mM)	4.5	0.1702 (0.0028 – 0.086)	4.5 [Fixed]
	Hydrogen (Methanogen)	$K_{H,M}$ (mM)	0.066	0.168 (0.056 – 0.812)	0.066 [Fixed]
Yield parameters	Lactate (sulphate-reducing bacteria)	Y_L (mg L^{-1} mM^{-1})	5.65	1.674 (0.22 – 9.58)	0.008 (0.001 - 0.026)
	Hydrogen (Methanogen)	Y_H (mg L^{-1} mM^{-1})	3.55	0.8 (0.44 – 2.58)	1.54 (0.31 – 2.12)
Mass transfer parameters	Hydrogen	$k_L a_H$ (h^{-1})	NA	0.063 (0.005 – 0.253)	0.25 (0.181 – 1.549)
	Methane	$k_L a_M$ (h^{-1})	NA	0.0011 (0.00023 – 0.00289)	0.0012 (0.00031 – 0.00212)
Inhibitory hydrogen concentration		H_{max} (mM)	0.0216	0.1017 (0.0452 – 0.4383)	0.563 (0.172 – 2.371)

[a]Obtained from the literature or fitted to monoculture data ((Ver Eecke et al., 2012; Goyal et al., 2015); see Appendix B, Table B2).

6.4 Discussion

It is clear from the comparison of the co-culture model predictions using monoculture parameters with the experimental data that monoculture parameter values were unsuitable for predicting the co-culture dynamics displayed experimentally. However, as posed in the hypothesis for this work, it was possible to identify which parameters varied between monoculture and co-culture. The use of monoculture yield values in the co-culture model universally led to an overprediction of OD compared to the experimental data. Previous experimental work has shown that these co-cultures do have reduced yield compared to monoculture (Walker et al., 2009), but the magnitude of the reduction differs between the model and experimental estimates. Walker et al. (2009), and references therein, put the co-culture yield to monoculture yield ratio at around 0.8 for co-culture growth on lactate, while a ratio of around 0.4 was obtained for the model to achieve a good fit to the batch culture data. Accurate estimation of the yield parameters for both the SRB and the methanogen was challenged by the lack of information about the initial ratio of the strains inoculated into the culture vessels in every data set. Measurement of this value would reduce the number of fitting parameters of the model and strengthen the reliability of yield parameter estimation. Nevertheless, a reduction in the yield parameters in co-culture compared to monoculture estimates was seen consistently throughout the fitting exercises.

A less anticipated result was the discrepancies between model estimated MTCs in different experiments. Initially, a proportional relationship between the hydrogen and methane MTCs was assumed, based on calculations in the literature (Pauss et al., 1990). However, it was found that such a proportional relationship was limiting to the quality of model fit, and that this could be remedied by allowing both MTCs to be independent fitting parameters. The methane MTC to hydrogen MTC ratio obtained when these values were independently fitted ranged from 0.004 to 0.319, compared to the literature value of 0.581 (Pauss et al., 1990). This emphasises the difficulty in estimating MTCs using solely gaseous metabolite data, without knowledge of the aqueous concentrations. Time-course data for the aqueous concentrations of hydrogen and methane would allow the MTCs to be estimated with more precision. As emphasised by Karadagli et al. (2019), not only does data for dissolved metabolite concentrations aid the estimation of MTCs, these data also allow for more

accurate estimation of biological parameters, such as half-saturation constants. These authors found that previous estimates of hydrogen half-saturation constants for several methanogens were overestimates, since mass transfer limitation of hydrogen from the gaseous phase to the aqueous phase was a limiting factor not considered in the original estimations.

This difficulty in estimating half-saturation constants without aqueous metabolite data may also have prevented correct estimation of the hydrogen half-saturation constant for the methanogen from monoculture data in this study. To facilitate growth in the co-culture model, it was necessary to use a value for this parameter taken from the literature that was three orders of magnitude lower than the value estimated using monoculture model fitting. This finding thus supports the assertions of Karadagli et al. (2019) on the requirement for aqueous metabolite data in the estimation of hydrogen half-saturation constants.

In determining metabolic parameters, interspecies differences were shown to be important. Although the SRB monoculture model was originally developed for *D. vulgaris*, it was also applied here to the metabolism of *D. alaskensis*, studied experimentally by Meyer et al. (2013). Differences at the species level between these two SRB strains likely contribute to the lack of fit to this data set exhibited by the model using monoculture parameters (Figure 6.3). In particular, the omission of formate from the SRB model used here must be discussed.

In Chapter 4, good model fits to monoculture data for *D. vulgaris* were demonstrated using a model that did not include formate, but instead relied upon hydrogen as the representative of all reducing equivalents. This was likely possible due to the relatively low production and utilisation of formate by this SRB when growing on lactate, which has been well documented (Stolyar et al., 2007; Walker et al., 2009; da Silva et al., 2013).

Meyer et al. (2013) highlighted the differences between *D. vulgaris* and *D. alaskensis* in their use of formate as a means for exchange of reducing equivalents in co-culture. A sharp increase in formate concentration was observed by these authors when methanogenesis was inhibited in their established co-cultures of *D. alaskensis* and *M. maripaludis*. Before this intervention, formate concentrations were near zero, suggesting that formate was being produced by the SRB throughout the culture, but was being efficiently utilised by the methanogen prior to inhibition. Contrastingly, the flux-balance models of Stolyar et al. (2007) and accompanying experimental work predicted that

hydrogen would be the dominant electron carrier between *D. vulgaris* and the methanogen. Their simulations found that co-culture survival was possible only when the flux of hydrogen was greater than that of formate, whereas Meyer et al. (2013) calculated that, for *D. alaskensis*, at least 70% of the exchanged reducing equivalents were in the form of formate.

This key difference in exchange metabolite preference likely helps to explain why the use of hydrogen to represent all reducing equivalents in the initial co-culture model was insufficient to capture the experimental data for *D. alaskensis*. Moreover, while both Walker et al. (2009) and Meyer et al. (2013) found significant gene regulatory differences in the SRB between monoculture and co-culture, these differences were inconsistent between *D. vulgaris* and *D. alaskensis*. These results further emphasise the species-specific differences in co-culture metabolism between the two strains, potentially requiring more complex or species-specific models to capture co-culture dynamics. Future attempts to model *D. alaskensis* in co-culture must include formate as a metabolite, with corresponding metabolic parameter values for its production and consumption by a cross-feeder. Monoculture data for the production of formate by *D. alaskensis* would be required for the parameterisation of such a model, as would data for the consumption of formate by *M. maripaludis*, but such a co-culture model could then be utilised to ascertain the key parameter changes between monoculture and co-culture growth with formate as the exchange metabolite.

It is plausible to assume that the results of co-culturing would change in different environments. For example, if sulphate were available in the culture medium, the reducing power generated in the oxidation of lactate should be used in the reduction of sulphate by the SRB, thus reducing the exchange of metabolites between the SRB and the methanogen and likely resulting in the extinction of the methanogen. The outcome would be determined by the ratio of lactate to sulphate: if sulphate became depleted before lactate, then cross-feeding would be reinstated and the methanogen would be expected to coexist with the SRB. Such dynamics would be easily investigated with a mathematical model such as the one used here, with appropriate co-culture parameter values and the inclusion of sulphate-reduction from the original SRB model.

As well as the free-living strains considered here, it would be desirable to have time-course co-culture data for strains of SRB and methanogens present in the human colon, to validate model predictions against a broader range of environments. It would also be of interest to have tri-culture

data including a reductive acetogenic strain that could compete with the methanogen for hydrogen released by the SRB. While collecting such data would be challenged by the difficulty of successfully culturing these organisms together, they are known to coexist naturally, and an understanding of their interactions would be advantageous to researching the human colonic microbiota. While mathematical models of monoculture microbial dynamics can be used to help guide experimentation, scaling up these models to consider multiple species increases their usefulness and applicability to natural scenarios where the understanding of microbial interactions is sought. Moreover, an understanding of the parameter changes between monoculture and co-culture as investigated here is an important step in the establishment of reliable microbial community models.

6.5 Conclusions

The results described in this chapter demonstrated that the use of monoculture-determined parameter values alone was insufficient to capture co-culture data for the growth and metabolism of *M. maripaludis* with either *D. vulgaris* or *D. alaskensis* in the absence of sulphate. This conclusion likely extends to other SRB and methanogen combinations. While certain aspects of the co-culture data, such as lactate and acetate dynamics and accumulation of gaseous metabolites in batch culture, could be predicted using monoculture parameter values, the remaining batch data and the continuous culture data were poorly predicted. To capture these data sets, it was necessary to fit several parameter values to the data, in particular the yield parameters, which were clearly reduced in co-culture fitting compared to monoculture, in support of experimental results. Future use of co-culture models utilising monoculture-determined parameter values can be used to identify metabolic parameters that change between independent and co-culture environments.

References

Carbonero, F., Benefiel, A.C., and Gaskins, H.R. (2012). Contributions of the microbial hydrogen economy to colonic homeostasis. Nat. Rev. Gastroenterol. Hepatol. 9**,** 504. doi: 10.1038/nrgastro.2012.85.

D'Hoe, K., Vet, S., Faust, K., Moens, F., Falony, G., Gonze, D., et al. (2018). Integrated culturing, modeling and transcriptomics uncovers complex interactions and emergent behavior in a three-species synthetic gut community. eLife 7**,** e37090. doi: 10.7554/eLife.37090.

da Silva, S.M., Voordouw, J., Leitão, C., Martins, M., Voordouw, G., and Pereira, I.A.C. (2013). Function of formate dehydrogenases in *Desulfovibrio vulgaris* Hildenborough energy metabolism. Microbiology (UK) 159(8)**,** 1760-1769. doi: 10.1099/mic.0.067868-0.

Goyal, N., Padhiary, M., Karimi, I.A., and Zhou, Z. (2015). Flux measurements and maintenance energy for carbon dioxide utilization by *Methanococcus maripaludis*. Microb. Cell Fact. 14(1), 146. doi: 10.1186/s12934-015-0336-z.

Junicke, H., Feldman, H., van Loosdrecht, M.C.M., and Kleerebezem, R. (2015). Impact of the hydrogen partial pressure on lactate degradation in a coculture of *Desulfovibrio* sp. G11 and *Methanobrevibacter arboriphilus* DH1. Appl. Microbiol. Biotechnol. 99(8), 3599-3608. doi: 10.1007/s00253-014-6241-2.

Karadagli, F., Marcus, A.K., and Rittmann, B.E. (2019). Role of hydrogen (H2) mass transfer in microbiological H2-threshold studies. Biodegradation 30(2), 113-125. doi: 10.1007/s10532-019-09870-1.

Louca, S., and Doebeli, M. (2015). Calibration and analysis of genome-based models for microbial ecology. eLife 4:e08208. doi: 10.7554/eLife.08208.

Meyer, B., Kuehl, J., Deutschbauer, A.M., Price, M.N., Arkin, A.P., and Stahl, D.A. (2013). Variation among *Desulfovibrio* Species in Electron Transfer Systems Used for Syntrophic Growth. J. Bacteriol. 195(5), 990. doi: 10.1128/JB.01959-12.

Muñoz-Tamayo, R., Giger-Reverdin, S., and Sauvant, D. (2016). Mechanistic modelling of in vitro fermentation and methane production by rumen microbiota. Anim. Feed Sci. Technol. 220, 1-21. doi: https://doi.org/10.1016/j.anifeedsci.2016.07.005.

Muyzer, G., and Stams, A.J.M. (2008). The ecology and biotechnology of sulphate-reducing bacteria. Nat. Rev. Microbiol. 6, 441. doi: 10.1038/nrmicro1892.

Noguera, D.R., Brusseau, G.A., Rittmann, B.E., and Stahl, D.A. (1998). A unified model describing the role of hydrogen in the growth of *Desulfovibrio vulgaris* under different environmental conditions. Biotechnol. Bioeng. 59(6), 732-746. doi: 10.1002/(SICI)1097-0290(19980920)59:6<732::AID-BIT10>3.0.CO;2-7.

Pauss, A., Andre, G., Perrier, M., and Guiot, S.R. (1990). Liquid-to-Gas Mass Transfer in Anaerobic Processes: Inevitable Transfer Limitations of Methane and Hydrogen in the Biomethanation Process. Appl. Environ. Microbiol. 56(6), 1636-1644.

Pinto, F., Medina, D.A., Pérez-Correa, J.R., and Garrido, D. (2017). Modeling Metabolic Interactions in a Consortium of the Infant Gut Microbiome. Front. Microbiol. 8(2507). doi: 10.3389/fmicb.2017.02507.

Stolyar, S., Van Dien, S., Hillesland, K.L., Pinel, N., Lie, T.J., Leigh, J.A., et al. (2007). Metabolic modeling of a mutualistic microbial community. Mol. Syst. Biol. 3, 92. doi: 10.1038/msb4100131

Van Wey, A.S., Cookson, A.L., Roy, N.C., McNabb, W.C., Soboleva, T.K., and Shorten, P.R. (2014). Monoculture parameters successfully predict coculture growth kinetics of *Bacteroides thetaiotaomicron* and two *Bifidobacterium* strains. Int. J. Food Microbiol. 191, 172-181. doi: 10.1016/j.ijfoodmicro.2014.09.006.

Ver Eecke, H.C., Butterfield, D.A., Huber, J.A., Lilley, M.D., Olson, E.J., Roe, K.K., et al. (2012). Hydrogen-limited growth of hyperthermophilic methanogens at deep-sea hydrothermal vents. P. Natl. Acad. Sci. 109(34), 13674. doi: 10.1073/pnas.1206632109.

Walker, C.B., He, Z., Yang, Z.K., Ringbauer, J.A., He, Q., Zhou, J., et al. (2009). The Electron Transfer System of Syntrophically Grown *Desulfovibrio vulgaris*. J. Bacteriol. 191(18), 5793.

The following chapter contains material from:

Smith NW, Shorten PR, Altermann E, Roy NC, McNabb WC (2020): Competition for hydrogen prevents coexistence of human gastrointestinal hydrogenotrophs in continuous culture. Frontiers in Microbiology 11:1073. https://doi.org/10.3389/fmicb.2020.01073

Chapter 7: Competition for hydrogen prevents coexistence of human gastrointestinal hydrogenotrophs in a continuous culture environment

Abstract

Understanding the metabolic dynamics of the human gastrointestinal tract (GIT) microbiota is of growing importance as research continues to link the microbiome to host health status. Microbial strains that metabolise hydrogen have been associated with a variety of both positive and negative host nutritional and health outcomes, but limited data exist for their competition in the GIT. To enable greater insight into the behaviour of these microbes, a mathematical model was developed for the metabolism and growth of the three major hydrogenotrophic groups: sulphate-reducing bacteria (SRB), methanogens and reductive acetogens. In batch culture simulations with abundant sulphate and hydrogen, the SRB outcompeted the methanogen for hydrogen due to having a half-saturation constant 10^6 times lower than that of the methanogen. The acetogen, with a high model threshold for hydrogen uptake of around 70 mM, was the least competitive. Under high lactate and zero sulphate conditions, hydrogen exchange between the SRB and the methanogen was the dominant interaction. The methanogen grew at 70% the rate of the SRB, with negligible acetogen growth. In continuous culture simulations, both the SRB and the methanogen were washed out at dilution rates above 0.15 h^{-1} regardless of substrate availability, whereas the acetogen could survive under abundant hydrogen conditions. Specific combinations of conditions were required for survival of more than one hydrogenotroph in continuous culture, and survival of all three was not possible. The stringency of these requirements and the inability of the model to simulate survival of all three hydrogenotrophs in continuous culture demonstrates that factors outside of those modelled are vital to allow hydrogenotroph coexistence in the GIT.

7.1 Introduction

The human colon is home to a vast number of microbes that survive via metabolism of dietary and endogenous substrates, or via cross-feeding on molecules released by other members of the microbiota. Study of this metabolic network is challenged by the number of different strains and interactions present in the colonic microbiota of a single individual (Qin et al., 2010), as well as the inter-individual differences in the microbiota profile and variation in this profile over time (Healey et al., 2017). However, the increasing number of links between diet, the microbiota and host health motivate greater understanding of the microbial community (Zmora et al., 2019).

For research purposes, the microbiota is often divided into functional groups based on the metabolic substrates and products associated with that group (for example, see Kettle et al. (2015), Kalyuzhnyi and Fedorovich (1998) and Motelica-Wagenaar et al. (2014)). The metabolic activity of saccharolytic functional groups results in the release of hydrogen (Carbonero et al., 2012). The accumulation of hydrogen in the colon reduces the efficiency of carbohydrate breakdown via inhibition of coenzyme reoxidation (Thauer et al., 1977; Wolin and Miller, 1983). Hydrogen is removed from this environment via host absorption and excretion, but also via hydrogenotrophic microbes. There are three major functional groups that metabolise hydrogen: the SRB, the methanogens and the reductive acetogens. Each of these hydrogenotrophic functional groups or their metabolic products have been linked to nutritional and health impacts upon the host: H_2S, produced by the SRB, has been investigated for its genotoxic effect on the colonic epithelium (Attene-Ramos et al., 2010); methane, produced by the methanogens, has been associated with constipation (Ghoshal et al., 2016); and acetate, produced by the acetogens, is readily absorbed by the host for use as an energy source (Morrison and Preston, 2016), but can also be cross-fed upon by other members of the microbiota (Falony et al., 2006). Numerous other links between hydrogenotrophs and the host have also been researched, as discussed in Chapter 2.

To investigate the competitive and cross-feeding interactions between the three hydrogenotrophic functional groups, a mathematical model for their growth and metabolism in batch or continuous culture was developed. This model includes the hydrogenotrophic metabolic pathways of each group, as well as lactate oxidation by the SRB, which can be a source of hydrogen.

Much previous research has demonstrated a hierarchy in hydrogen uptake efficiency between these groups, with SRB having the greatest affinity for hydrogen and the acetogens the least (Carbonero et al., 2012), but there is currently no experimental data for the direct competition between the three groups for this substrate. The expectation was that the model would reveal what conditions were necessary for hydrogenotroph coexistence, as well as the conditions that would favour one group over the others.

7.2 Methodology

7.2.1 Mathematical model

The tri-culture model is the result of the additive combination of monoculture models for each of the three hydrogenotrophic functional groups. The constituent monoculture models are based on those of Chapters 3-5, with minor notation alterations and the removal of mass transfer from the SRB model. Mass transfer is not included in the tri-culture model as the emphasis was on the ultimate outcome of cultures under various conditions, rather than the dynamics of the culture over time. The model also assumes that the culture media is homogeneously mixed, with no spatial component considered. The model structure is described below, with notation summarised in Table 7.1.

The following metabolic pathways are assumed for each hydrogenotroph:

Lactate metabolism by the SRB: $CH_3CHOHCOO^-$ (Lactate) + 2 H_2O → CH_3COO^- (Acetate) + 2.5 H_2 + HCO_3^- (Bicarbonate)

Sulphate metabolism by the SRB: SO_4^{2-} (Sulphate) + 5 H_2 → H_2S (Hydrogen sulphide) + 4 H_2O

Hydrogen metabolism by the methanogen: 4 H_2 + CO_2→ CH_4 (Methane) + 2 H_2O

Hydrogen metabolism by the acetogen: 4 H_2 + 2 CO_2 → CH_3COO^- (Acetate) + H^+ + 2 H_2O

Note that the tri-culture model does not consider the concentrations of H_2O, CO_2, bicarbonate or H^+; these molecules are assumed abundant if required as substrates.

Let $\mathcal{L}$ and $\mathcal{S}$ represent the rate of lactate and sulphate metabolism by the SRB, respectively:

$$\mathcal{L} = \frac{\mu_{max,L}}{Y_{SRB,L}} \frac{L}{L + K_L} \left(1 - \frac{H}{H_{max}}\right) X_{SRB} \tag{7.1}$$

$$\mathcal{S} = \frac{\mu_{max,S}}{Y_{SRB,S}} \frac{S}{S + K_S} \frac{H}{H + K_{SRB,H}} X_{SRB} \tag{7.2}$$

These model equations are based on Monod kinetics, with the addition of a hydrogen inhibition term in the lactate metabolism equation (see Table 7.1 for definition of variables and parameters).

Next, let $\mathcal{M}$ and $\mathcal{A}$ be the rate of hydrogen metabolism by the methanogen and the acetogen respectively:

$$\mathcal{M} = \frac{\mu_{max,H}}{Y_{MET}} \frac{H}{H + K_{MET,H}} X_{MET} \tag{7.3}$$

$$\mathcal{A} = \frac{\eta}{Y_{ACE}} \frac{H}{1 + \exp\left(p_1(p_2 - H)\right)} X_{ACE} \tag{7.4}$$

The rate of hydrogen metabolism by the acetogen is not based on Monod kinetics, but rather on first order kinetics with the incorporation of a threshold term, adapted from Ribes et al. (2004). Using these rate terms, the full model is defined as the following system of ODEs:

$$\frac{dL}{dt} = -\mathcal{L} \tag{7.5}$$

$$\frac{dS}{dt} = -\mathcal{S} \tag{7.6}$$

$$\frac{dH}{dt} = b_{LH}\mathcal{L} - b_{HP}\mathcal{S} - \mathcal{M} - \mathcal{A} \tag{7.7}$$

$$\frac{dA}{dt} = b_{LA}\mathcal{L} + b_{HA}\mathcal{A} \tag{7.8}$$

$$\frac{dP}{dt} = b_{SP}\mathcal{S} \tag{7.9}$$

$$\frac{dM}{dt} = b_{HM}\mathcal{M} \tag{7.10}$$

$$\frac{dX_{SRB}}{dt} = Y_{SRB,L}\mathcal{L} + Y_{SRB,S}\,\mathcal{S} \tag{7.11}$$

$$\frac{dX_{MET}}{dt} = Y_{MET}\mathcal{M} \tag{7.12}$$

$$\frac{dX_{ACE}}{dt} = Y_{ACE}\mathcal{A} \tag{7.13}$$

Note that when the model is applied to continuous culture conditions, the following terms are appended to each ODE:

$$-Di + I_i$$

where D is the dilution rate, i denotes the state variable of the ODE to which the term is appended and I_i is the inflow rate of i. In the cases considered here, I_i is set to zero for all microbial state variables; only metabolite inflows are permitted to be non-zero.

7.2.2 Numerical simulations

For numerical analysis, the mathematical model was solved using the ode15s solver in MATLAB (The MathWorks; www.mathworks.com).

Table 7.1. Mathematical notation used in the model			
Variables	**Notation**	**Value (if a parameter)**	**Units**
Lactate concentration	L		mM
Sulphate concentration	S		mM
Hydrogen concentration	H		mM
Acetate concentration	A		mM
H_2S concentration	P		mM
Methane concentration	M		mM
Concentration of sulphate-reducing bacteria cells	X_{SRB}		g L^{-1}
Concentration of methanogen cells	X_{MET}		g L^{-1}
Concentration of acetogen cells	X_{ACE}		g L^{-1}
Rate terms			
Lactate metabolism by sulphate-reducing bacteria	$\mathcal{L}$		mM h^{-1}
Sulphate metabolism by sulphate-reducing bacteria	$\mathcal{S}$		mM h^{-1}
Hydrogen metabolism by the methanogen	$\mathcal{M}$		mM h^{-1}
Hydrogen metabolism by the acetogen	$\mathcal{A}$		mM h^{-1}
Dilution rate	D		h^{-1}
Inflow rate of metabolite variable i	I_i		mM h^{-1} (since i denotes a metabolite)
SRB parameters			
Maximum growth rate for lactate	$\mu_{max,L}$	0.116	h^{-1}
Maximum growth rate for sulphate	$\mu_{max,S}$	0.03	h^{-1}
Growth yield during growth on lactate	$Y_{SRB,L}$	0.00565	g L^{-1} mM^{-1}
Growth yield during growth on sulphate	$Y_{SRB,S}$	0.00445	g L^{-1} mM^{-1}
Hydrogen inhibition parameter	H_{max}	0.0216	mM
Half-saturation constant for lactate uptake	K_L	4.5	mM
Half-saturation constant for sulphate uptake	K_S	0.05	mM
Half-saturation constant for hydrogen uptake	$K_{SRB,H}$	1.69×10^{-5}	mM
Moles of hydrogen produced per mole lactate used	b_{LH}	2.5	-
Moles of hydrogen used per mole H_2S produced	b_{HP}	5	-
Moles of acetate produced per mole lactate used	b_{LA}	1	-
Moles of H_2S produced per mole sulphate used	b_{SP}	1	-
Methanogen parameters			
Maximum growth rate for hydrogen	$\mu_{max,H}$	0.1042	h^{-1}
Growth yield during growth on hydrogen	Y_{MET}	0.0016	g L^{-1} mM^{-1}
Half-saturation constant for hydrogen uptake	$K_{MET,H}$	10.63	mM
Moles of methane produced per mole hydrogen used	b_{HM}	0.0126	-
Acetogen parameters			
Threshold parameter	p_1	0.015	mM^{-1}
Threshold parameter	p_2	336	mM
First order kinetics rate parameter	η	0.0054	h^{-1} mM^{-1}
Growth yield during growth on hydrogen	Y_{ACE}	0.0017	g L^{-1} mM^{-1}
Moles of acetate produced per mole hydrogen used	b_{HA}	0.25	-

7.3 Results

7.3.1 Analysis of the model under batch culture conditions

A comparison of the half-saturation and threshold parameter values for the three hydrogenotrophs shows the hierarchy in affinities for this substrate: the model estimates for the hydrogen half-saturation constants of the SRB and the methanogen are 1.69×10^{-5} mM and 10.63 mM, respectively (Table 7.1), while the threshold for hydrogen uptake for the acetogen is estimated at around 70 mM (Leclerc et al., 1997). As has been established by previous research, SRB generally have a greater affinity for hydrogen than the methanogens, which in turn have a greater affinity than the reductive acetogens for this substrate (Carbonero et al., 2012). For the acetogen in this model, growth limitation due to reduced substrate availability increases rapidly once the hydrogen concentration is below 336 mM. Using the parameter values in Table 7.1, the growth rate of the acetogen at this hydrogen concentration is 0.0069 h^{-1}, which is small compared to the corresponding methanogen growth rate of 0.09 h^{-1} at this hydrogen concentration.

The complexity of the model equations, defined in the Methodology section, precludes an analytical solution, but steady state analysis may still be performed. The first case considered is the batch culturing of all three hydrogenotrophs where lactate is the sole available substrate in the model. Under batch conditions with initially abundant lactate, the SRB will metabolise lactate to acetate and hydrogen rapidly, until the inhibitory hydrogen concentration is approached and growth is slowed (Figure 7.1). Growth would be halted completely under these conditions, but for the consumption of hydrogen via metabolite cross-feeding by the other two hydrogenotrophs.

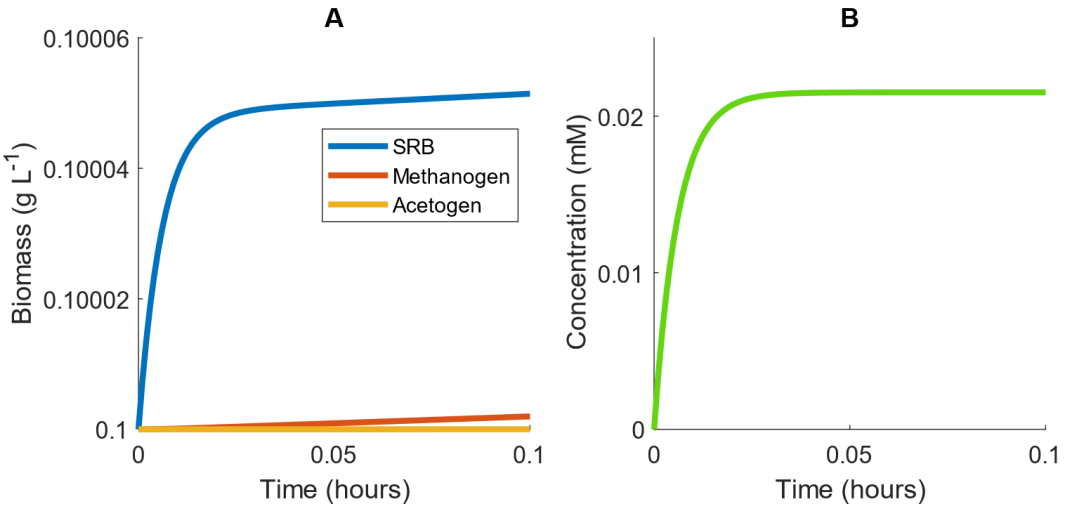

Figure 7.1. Example simulation of early stages of batch tri-culture with lactate the sole added substrate. Panel A shows the change in microbial biomass over time and Panel B shows the change in hydrogen concentration over time. The sulphate-reducing bacteria (SRB) rapidly oxidise lactate to acetate and hydrogen, resulting in SRB growth and hydrogen accumulation. Once hydrogen accumulates to a level approaching the inhibitory concentration for SRB growth, its concentration remains in a pseudo-steady state with a balance between hydrogen production by the SRB and consumption by the methanogen.

The acetogen's threshold for hydrogen uptake is greater than the inhibitory hydrogen concentration for the SRB: at the inhibitory hydrogen concentration for SRB, the growth rate of the acetogen, $\mathcal{A} = 4.41 \times 10^{-4} X_{ACE}$, is minimal, resulting in minimal acetogen growth under these conditions. The SRB inhibitory hydrogen concentration is also almost three orders of magnitude smaller than the half-saturation constant for hydrogen uptake by the methanogen, thus limiting methanogen growth, with methanogen growth rate of $\mathcal{M} = 0.13\, X_{MET}$.

A pseudo-steady state is then reached for the hydrogen concentration at a level approaching the inhibitory concentration, which is maintained by low-rate hydrogen consumption by the methanogen and hydrogen production by the SRB. Assuming this steady state and thereby nullifying $\frac{dH}{dt}$, the growth rate of the methanogen is proportional to that of the SRB at this steady state:

$$0 = b_{LH}\mathcal{L} - \mathcal{M} \;\Rightarrow\; \frac{dX_{MET}}{dt} = \frac{b_{LH}Y_{MET}}{Y_{SRB,L}}\frac{dX_{SRB}}{dt} \approx 0.7\frac{dX_{SRB}}{dt}$$

Using the monoculture parameter values in Table 7.1 and assuming negligible growth by the acetogen, the growth rate of the methanogen is around 70% of the SRB growth rate in this situation. The population continues in this hydrogen steady state until lactate becomes depleted, at

which point SRB growth is halted. As a result, hydrogen production ceases and hydrogen is then depleted by the methanogen, ultimately halting its growth (Figure 7.2).

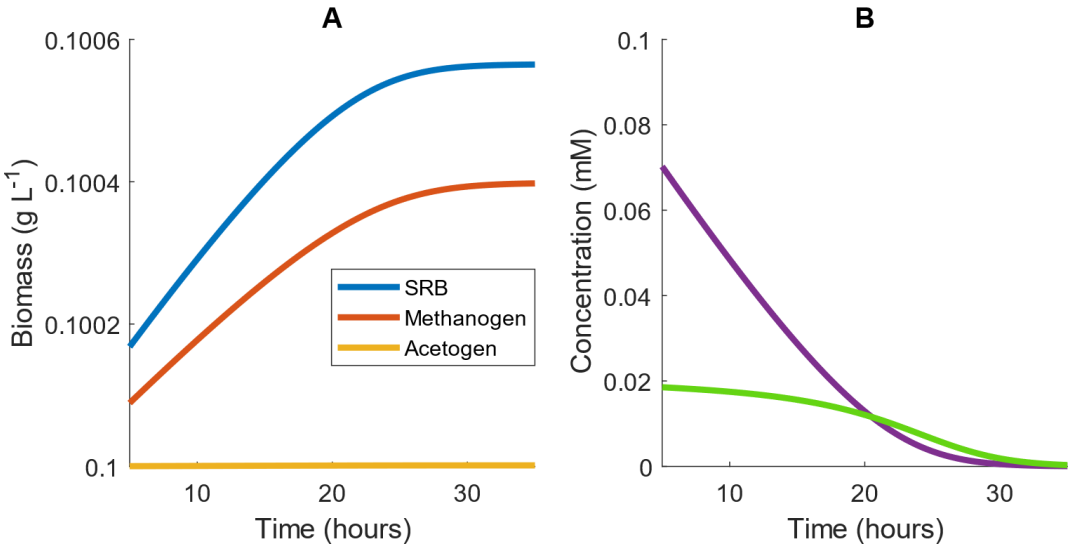

Figure 7.2. Example simulation of late stages of batch tri-culture with lactate the sole added substrate. Panel A shows the change in microbial biomass over time and Panel B shows the change in hydrogen concentration over time. As lactate is depleted, hydrogen production ceases and ultimately both lactate and hydrogen are depleted by the sulphate-reducing bacterium and the methanogen, respectively.

If sulphate is also present in the medium in excess, hydrogen does not reach the inhibitory concentration due to its further use in the reduction of sulphate (data not shown). Again, negligible acetogen growth is possible at such a low hydrogen concentration. In numerical simulations (data not shown), the methanogens achieved only an incremental increase in biomass from hydrogen metabolism in this scenario, due to the hydrogen concentration remaining much lower than the methanogen half-saturation constant.

If hydrogen is the sole model substrate available, then the SRB will not grow, due to the absence of sulphate. Both the methanogen and the acetogen grow under these conditions, but the methanogen will show greater growth at low hydrogen concentrations due to its greater affinity for this substrate. At high hydrogen concentrations, the model predicts greater growth by the acetogen, since its growth rate increases linearly with the hydrogen concentration, whereas the methanogen's growth rate is limited to $\mu_{max,H}$. However, the acetogen model was parameterised at hydrogen concentrations below 200 mM, therefore likely extrapolates poorly to concentrations above this range. For higher hydrogen concentrations, it is likely that a Monod formulation would be more

appropriate in capturing the acetogen dynamics. However, such high concentrations are not expected in the colon (Carbonero et al., 2012; Wolf et al., 2016).

Under the model assumptions on the simple tri-culture batch scenario, the acetogen achieves a growth rate of at least G g L^{-1} h^{-1} if the hydrogen and acetogen cell concentrations satisfy:

$$X_{ACE} > G\frac{1+\exp\left(p_1(p_2-H)\right)}{\eta H} \tag{7.14}$$

An interpretation of equation 14 is shown in Figure 7.3, where points above and to the right of the line indicate conditions resulting in an acetogen growth rate of at least $G = 0.1$.

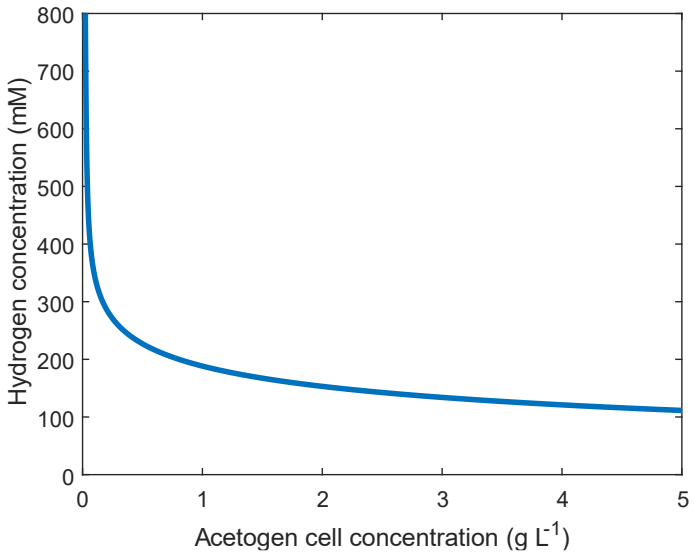

Figure 7.3. Conditions necessary for an acetogen growth rate above 0.1 g L^{-1} h^{-1}. The line indicates the threshold for this growth rate: any combination of hydrogen and cell concentrations falling to the upper/right side of this line results in a growth rate above 0.1.

It is important to note that in the batch tri-culture environment, the hydrogen concentration will rapidly decrease due to metabolism by the methanogen and the SRB (if sulphate is available). Therefore, the acetogen will only display growth in the early stages of culture when hydrogen is abundant.

Table 7.2 summarises the outcomes of various initial culture conditions on batch culture growth of the three hydrogenotrophs.

Table 7.2. Outcomes of batch culture under various initial conditions. Green represents growth of all organisms, red represents no growth of any organisms, tan represents more complex dynamics. SRB: sulphate-reducing bacterium.

		Hydrogenotrophs in culture at initial time					
		SRB + Methanogen + Acetogen	SRB + EITHER Methanogen OR Acetogen	Methanogen + Acetogen	SRB only	Methanogen only	Acetogen only
Substrates available at initial time	Lactate + Sulphate + Hydrogen	Growth of SRB, minimal growth of methanogen and negligible growth of acetogen due to out-competition for hydrogen	Growth of SRB, minimal growth of other due to out-competition for hydrogen				
	Lactate + Sulphate	Growth of SRB, minimal growth of methanogen and negligible growth of acetogen due to out-competition for hydrogen	Growth of SRB, minimal growth of other due to out-competition for hydrogen				
	Lactate + Hydrogen	Growth of SRB when $H < H_{max}$, minimal growth of methanogen and negligible growth of acetogen due to out-competition for hydrogen until $H > H_{max}$, at which point SRB growth halted, methanogen and acetogen growth	Growth of SRB when $H < H_{max}$, growth of other		Growth when $H < H_{max}$		
	Sulphate + Hydrogen	Growth of SRB, minimal growth of others due to out-competition for hydrogen	Growth of SRB, minimal growth of other due to out-competition for hydrogen				
	Lactate only	Slow growth of all as SRB dependent on hydrogen removal by others. More growth by methanogen than acetogen due to low hydrogen concentration	Slow growth of both as SRB dependent on hydrogen removal by other		Growth until H reaches H_{max}		
	Sulphate only						
	Hydrogen only	No growth of SRB, growth of methanogen, minimal growth of acetogen due to out-competition for hydrogen	No growth of SRB, growth of other				

7.3.2 Analysis of the model under continuous culture conditions

Once dilution is introduced to the model, competition between the hydrogenotrophs becomes important in determining their survival. However, it is initially of importance to investigate what dilution rates allow for survival of each microbe individually. For a microbe to have the potential to survive continuous culture, its maximum growth rate must be greater than the dilution rate. The maximum growth rates of the SRB and the methanogen are 0.146 h^{-1} and 0.1042 h^{-1} respectively (Table 7.1), so they cannot survive in continuous culture with a greater dilution rate than these values. The maximum growth rate of the reductive acetogen is not as straightforward since under the current model structure it is determined in part by the hydrogen concentration. However, the growth rate of the acetogen would be similar to the maximum growth rate of the methanogen under a hydrogen concentration of around 190 mM, therefore hydrogen concentrations exceeding this are required for the acetogen to survive a dilution rate (D) above 0.1 h^{-1}.

When growing solely by sulphate reduction in the absence of lactate, the maximum growth rate of the SRB is 0.03 h^{-1}. Washout of this microbe therefore occurs at dilution rates exceeding this value, regardless of the abundance of hydrogen and sulphate.

The first competitive scenario considered is competition for hydrogen between the methanogen and the acetogen. This is analysed via their respective non-trivial steady states. Assuming abundant hydrogen and a steady state cell concentration for the methanogen, it can be seen that:

$$D = \mu_{max,H} \frac{H}{H + K_{MET,H}} \Rightarrow H = \frac{K_{MET,H} D}{\mu_{max,H} - D}$$

Similarly, assuming steady state for the acetogen gives:

$$D = \frac{\eta H}{1 + \exp\left(p_1 (p_2 - H)\right)} \tag{7.15}$$

Plotting the dilution rate against the steady state hydrogen concentration (Figure 7.4) allows determination of the persistence of each of these two hydrogenotrophs under abundant hydrogen conditions in continuous culture. The microbe that achieves the lower steady state

hydrogen concentration at a given dilution rate will outcompete the other by reducing the concentration of this substrate below its competitor's steady state value, leading to washout of the competitor. It can be seen in Figure 7.4 that the methanogen is therefore the survivor at lower dilution rates, and the acetogen at higher dilution rates. The only dilution rate at which the two may coexist is when their steady state hydrogen concentrations intersect, at a dilution rate of approximately 0.09861 h^{-1}. At this dilution rate, the methanogen and the acetogen can coexist, given abundant hydrogen availability.

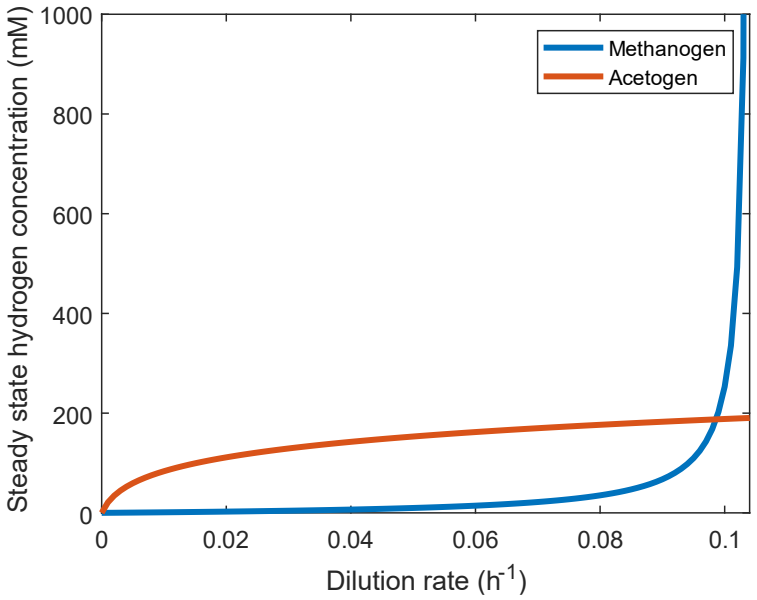

Figure 7.4. Comparison of steady state hydrogen concentrations achieved by the methanogen and the reductive acetogen. The hydrogenotroph with the lower of the two steady state hydrogen concentrations at a given dilution rate will outcompete the other for this substrate and survive while the other is washed out. Beyond D=0.1042, the methanogen growth rate cannot be greater than the dilution rate, so it is washed out irrespective of the presence of the acetogen.

The more diverse metabolic capabilities of the SRB mean that conditions for SRB survival are more complex. If no lactate is available to the SRB, then survival requires that the dilution rate $D \leq \mu_{max,s} = 0.03$, the maximum growth rate of the SRB in the absence of lactate. Moreover, a non-negative SRB growth rate, $\frac{dX_{SRB}}{dt} \geq 0$, requires that:

$$D \leq \mu_{max,S} \frac{S}{S + K_S} \frac{H}{H + K_{SRB,H}} \tag{7.16}$$

The surface plot in Figure 7.5 demonstrates these conditions on the three key variables.

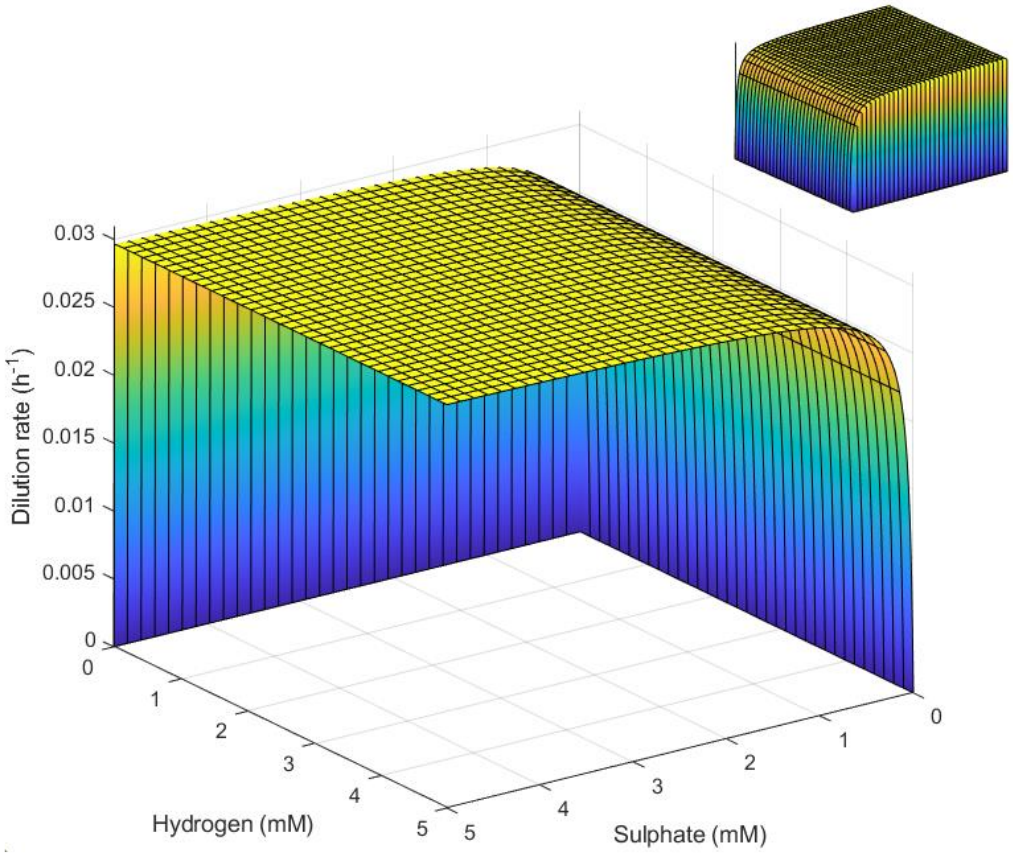

Figure 7.5. Surface representation of conditions necessary for sulphate-reducing bacterium (SRB) survival in the absence of lactate. SRB survival requires that conditions represent a point below the surface. Note the inverted sulphate and hydrogen axes. Inset: reverse view.

If lactate is available in the medium, but sulphate is not, survival requires that $D \leq \mu_{max,L} = 0.116$, the maximum growth rate of the SRB on lactate. Secondly, SRB growth is also impossible for hydrogen concentrations above H_{max}. Thirdly, there is also the requirement that:

$$D \leq \mu_{max,L} \frac{L}{L + K_L}\left(1 - \frac{H}{H_{max}}\right) \leq \mu_{max,L}\left(1 - \frac{H}{H_{max}}\right) \tag{7.17}$$

$$\Rightarrow H \leq H_{max}\left(1 - \frac{D}{\mu_{max,L}}\right) \tag{7.18}$$

Figure 7.6 shows these conditions graphically using the parameter values in Table 7.1. Clearly, the third condition encapsulates the first two and is the most stringent under these parameter values.

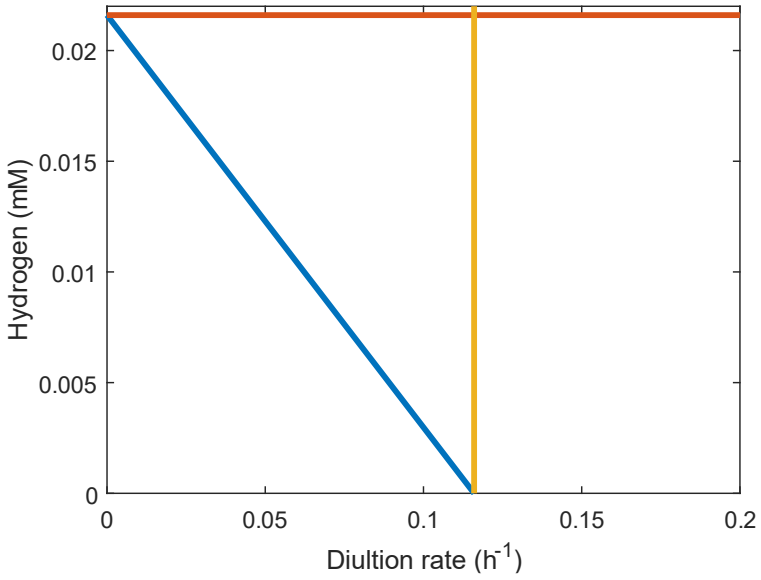

Figure 7.6. Representation of conditions necessary for sulphate-reducing bacterium (SRB) survival in the absence of sulphate. The orange line indicates $\mathbf{H = H_{max}}$, the yellow line indicates $\mathbf{D = 0.116}$ and the blue line indicates the inequality derived in the text (Equation 7.18) between dilution rate and hydrogen concentration. SRB survival requires that steady state conditions lie below and to the left of all three lines, making the blue line clearly the strongest requirement.

Further conditions for SRB growth when lactate is the sole added substrate may also be extracted. Taking the steady state for the hydrogen differential equation under abundant lactate, no hydrogen inflow and with only the SRB present gives an expression for the steady state hydrogen concentration allows derivation of the steady state hydrogen concentration:

$$0 = b_{LH}\frac{\mu_{max,L}}{Y_{SRB,L}}X_{SRB}\left(1 - \frac{H_{SS}}{H_{max}}\right) - DH_{SS}$$

$$\Rightarrow H_{SS} = b_{LH}\frac{\mu_{max,L}}{Y_{SRB,L}}X_{SRB}\left(D + b_{LH}\frac{\mu_{max,L}}{H_{max}Y_{SRB,L}}X_{SRB}\right)^{-1}$$

Substituting this value into the equation for the SRB growth rate under abundant lactate conditions and simplifying gives the SRB growth rate at steady state as:

$$\mu_{max,L}\left(1 - \frac{H_{SS}}{H_{max}}\right) = \frac{DH_{max}\mu_{max,L}Y_{SRB,L}}{\left(DH_{max}Y_{SRB,L} + b_{LH}\mu_{max,L}X_{SRB}\right)}$$

Since this growth rate must be greater than or equal to the dilution rate to prevent washout, the following condition for SRB survival may be derived:

$$D \leq \mu_{max,L}\left(1 - \frac{b_{LH}X_{SRB}}{H_{max}Y_{SRB,L}}\right) \approx 0.116 - 2376X_{SRB} \qquad (7.19)$$

Therefore, survival of the SRB requires that the cell concentration is less than approximately 4.88×10^{-5} g L^{-1}; any greater concentration would result in too rapid an

accumulation of hydrogen and subsequent SRB inhibition. This constitutes a small window for SRB survival when lactate is the sole added substrate.

Moving on to the survival of co-cultures including the SRB, next analysed is the coexistence of the SRB and the methanogen when no lactate is available. In this case, the steady state hydrogen concentrations for each in monoculture are:

$$H_{SS,SRB} = \frac{K_{SRB,H}}{\frac{\mu_{max,S}S}{D(K_S + S)} - 1} \tag{7.20}$$

for the SRB and:

$$H_{SS,MET} = \frac{K_{MET,H}D}{\mu_{max,H} - D} \tag{7.21}$$

for the methanogen. Whichever of these values is smaller under a given set of conditions will indicate the hydrogenotroph that will survive, the other being outcompeted. Similar to the case for the methanogen and the acetogen, coexistence is possible where these two steady states coincide. When sulphate is assumed abundant, this occurs at $D = 0.03$, which is intuitive since this is the value of $\mu_{max,S}$. If sulphate is not abundant, then setting the two steady state equations above equal to one another gives:

$$D \approx \frac{0.03S}{0.05 + S} \tag{7.22}$$

Thus, as the steady state sulphate concentration (S) decreases, so too must D to allow for continued coexistence of both the SRB and the methanogen. For dilution rates lower than this value, the SRB will out-compete the methanogen for hydrogen, with the converse true for dilution rates above this value.

Following the same argument for the SRB and the acetogen, once again survival of both is possible under abundant sulphate at $D = 0.03$, with acetogens out-competed below this value and SRB out-competed above this value. An analytical solution requires the use of the Lambert *W* function for the case when sulphate is limiting due to the complexity of the acetogen growth rate equation, thus is not useful for this analysis.

Next, in the case where lactate is available, but sulphate is not, clearly a steady state hydrogen concentration approaching the inhibitory concentration will be maintained if both the SRB

and the methanogen are present, analogously to the batch culture case. Assuming a steady state hydrogen concentration of H_{max}, the growth rate for the methanogen is:

$$\mathcal{M} = \frac{\mu_{max,H}}{Y_{MET}} \frac{H}{K_H + H} X_{MET} = \frac{\mu_{max,H}}{Y_{MET}} \frac{H_{max}}{K_H + H_{max}} X_{MET} \approx 0.132 X_{MET} \tag{7.23}$$

Thus, the dilution rate must be less than this growth rate for the methanogen to survive. Under these conditions, SRB growth will be limited by the hydrogen consumption rate of the methanogen. If the methanogen is growing at the upper limit rate of $0.132X_{MET}$, then hydrogen is removed from the system at the rate:

$$0.132X_{MET} + DH_{max}$$

This is therefore the rate at which the SRB produces hydrogen to maintain the steady state. Thus:

$$b_{LH}\,\mathcal{L} = 0.132X_{MET} + DH_{max} \tag{7.24}$$

and since the rate of growth of the SRB is $Y_{SRB,L}\mathcal{L}$, the SRB growth rate is:

$$Y_{SRB,L}\mathcal{L} = \frac{Y_{SRB,L}}{b_{LH}}(0.132X_{MET} + DH_{max}) \tag{7.25}$$

$$\approx 2.98 \times 10^{-4} X_{MET} + 4.88 \times 10^{-5} D$$

Since the dilution rate must be lower than the growth rate of both the SRB and the methanogen for coexistence to be sustained, coexistence of the SRB and the methanogen in the presence of excess lactate is possible only when the dilution rate is low and the methanogen cell concentration sufficiently high.

Following the same argument, co-culture survival conditions for the SRB and the acetogen may also be derived. In this case, the growth rate for the acetogen at the hydrogen inhibition concentration is $4.41 \times 10^{-4} X_{ACE}$ (g L^{-1} h^{-1}) and the corresponding SRB growth rate is approximately $4.88 \times 10^{-4} X_{ACE} + 4.88 \times 10^{-5} D$ (g L^{-1} h^{-1}).

Table 7.3 outlines the outcomes of all possible culture combinations under excess substrate inflow based on the conclusions of the analytical derivations described previously. For the cases where substrates are present, but at limiting concentrations, a computational analysis of outcomes was used.

Table 7.3. Outcomes of continuous culture under various conditions. Green represents growth of all organisms, red represents no growth of any organisms, tan represents more complex dynamics, with details given. SRB: sulphate-reducing bacterium.

		Hydrogenotrophs in culture at initial time						
		SRB + Methanogen + Acetogen	SRB + Methanogen	SRB + Acetogen	Methanogen + Acetogen	SRB only	Methanogen only	Acetogen only
Substrates supplied in abundance to culture	Lactate + Sulphate + Hydrogen	Analogous to Sulphate + Hydrogen case as high hydrogen concentration prevents lactate metabolism by SRB	Analogous to Sulphate + Hydrogen case as high hydrogen concentration prevents lactate metabolism by SRB	Analogous to Sulphate + Hydrogen case as high hydrogen concentration prevents lactate metabolism by SRB	Coexistence at $D = 0.09861$, acetogen out-competes methanogen above this and methanogen out-competes acetogen below this	Survival if $D \leq \mu_{max,S}$ as lactate metabolism inhibited by high hydrogen concentration	Survival if $D \leq \mu_{max,M}$	
	Lactate + Sulphate	SRB survival if $D \leq \mu_{max,L} + \mu_{max,S}$. Others washed out due to out-competition for hydrogen or no hydrogen production if SRB washed out	SRB survival if $D \leq \mu_{max,L} + \mu_{max,S}$. Methanogen washout due to out-competition for hydrogen or no hydrogen production if SRB washed out	SRB survival if $D \leq \mu_{max,L} + \mu_{max,S}$. Acetogen washout due to either out-competition for hydrogen or no hydrogen production if SRB washed out		Survival if $D \leq \mu_{max,L} + \mu_{max,S}$		
	Lactate + Hydrogen	SRB washout as high hydrogen concentration prevents lactate metabolism. Methanogen and acetogen coexistence at $D = 0.09861$, acetogen out-competes methanogen above this and methanogen out-competes acetogen below this	Methanogen growth. SRB washout due to hydrogen concentrations above the inhibitory concentration	Acetogen growth. SRB washout due to hydrogen concentrations above the inhibitory concentration	Coexistence at $D = 0.09861$, acetogen out-competes methanogen above this and methanogen out-competes acetogen below this	Washout as lactate metabolism inhibited by high hydrogen concentration	Survival if $D \leq \mu_{max,M}$	

	Sulphate + Hydrogen	Coexistence of SRB and methanogen at $D = 0.03$, acetogen out-competed for hydrogen. SRB only below this value. Methanogen and acetogen coexistence at $D = 0.09861$. Methanogen only between these bounds, acetogen only above the upper bound	Coexistence only possible at $D = 0.03$. Methanogens out-competed for hydrogen at lower dilution rates, SRB washed out at higher dilution rates	Coexistence only possible at $D = 0.03$. Acetogens out-competed for hydrogen at lower dilution rates, SRB washed out at higher dilution rates	Coexistence at $D = 0.09861$, acetogen out-competes methanogen above this and methanogen out-competes acetogen below this	Survival if $D \leq \mu_{max,S}$	Survival if $D \leq \mu_{max,M}$	
	Lactate only	Analogous to SRB + Methanogen case, since acetogen's hydrogen threshold for meaningful growth is much higher than methanogen's. Either survival of SRB and methanogen only, or all are washed out.	Both survive if D/X_{MET} sufficiently small. Otherwise, SRB alone may survive if at steady state D, X_{SRB} and H satisfy boundary conditions, else both will be washed out	Both survive if D/X_{ACE} sufficiently small. Otherwise, SRB alone may survive if at steady state D, X_{SRB} and H satisfy boundary conditions, else both will be washed out		Survival if at steady state D, X_{SRB} and H satisfy boundary conditions		
	Sulphate only							
	Hydrogen only	SRB washout, Methanogen and acetogen coexistence at $D = 0.09861$. Methanogen only below this value, acetogen only above	SRB washout, methanogen survival if $D \leq \mu_{max,M}$	SRB washout, acetogen growth	Coexistence at $D = 0.09861$, acetogen out-competes methanogen above this and methanogen out-competes acetogen below this		Survival if $D \leq \mu_{max,M}$	

7.3.3 Numerical analysis of the model under continuous culture conditions

In order to investigate survival of the hydrogenotrophs under mixed culture conditions, substrate inflow and dilution rate ranges were examined. These ranges were chosen as they provide coverage of conditions that allow for growth of all three hydrogenotrophs individually and allow for examination of transitions in culture dominance between the microbes. Moreover, since the aim of this study was the behaviour of hydrogenotrophs in the human colon, substrate concentrations that encompass the range of concentrations expected in this environment were deemed appropriate. The substrate inflow ranges investigated were: lactate 0-25 mM h^{-1} (Vernia et al., 1988; Macfarlane and Macfarlane, 2012); sulphate 0-10 mM h^{-1} (Florin et al., 1991); and hydrogen 0-50 mM h^{-1} (Carbonero et al., 2012; Wolf et al., 2016). The range of dilution rates was 0.01-0.15 h^{-1} (Arhan et al., 1981). The substrate inflow ranges were split into 1 mM h^{-1} intervals, and the dilution rate range was split into 0.01 h^{-1} intervals. The mathematical model was then run for all 218,790 possible combinations of these inflow and dilution rates to establish whether each hydrogenotroph survived the culture conditions. Initial cell concentration for each hydrogenotroph was set at 1 g L^{-1}, and the initial concentration of each of the three substrates was set at the maximum value of its range. Each microbe was determined to have survived if, after 1,000 hours of simulated continuous culture, its cell concentration was greater than 1×10^{-4} g L^{-1} and its population was not decreasing. The population was determined to be still decreasing if, over the final 20 hours of simulation, the cell concentration decreased by more than 1×10^{-9} g L^{-1}. If the microbe failed to satisfy these survival conditions, it was deemed extinct from the culture.

Of the 218,790 simulated metabolite inflow and dilution rate combinations, under no conditions were all three hydrogenotrophs coexisting after 1,000 hours, as suggested by the analytical investigation of the model. Similarly, under no conditions was coexistence of the acetogen with either of the other hydrogenotrophs possible. The only possible coexisting pair was the SRB and the methanogen. Each of the three hydrogenotrophs could outcompete the other two under certain conditions, and there were also many conditions under which all three were washed out.

The simplest set of conditions to examine was those in which the acetogen outcompeted the other two hydrogenotrophs. Figure 7.7 shows the maximum dilution rates under which only the

acetogen survived to 1,000 hours. Survival was independent of the lactate and sulphate inflow, but required a hydrogen inflow of at least 22 mM h^{-1}. As hydrogen inflow increased above this cut-off, the acetogen was able to outcompete the others and survive at greater dilution rates. Note that out-competition by the acetogen occurred only when the dilution rate was above 0.1 h^{-1}; it was earlier stated that 0.146 h^{-1} and 0.1042 h^{-1} were the greatest dilution rates under which the SRB and methanogen could survive, respectively.

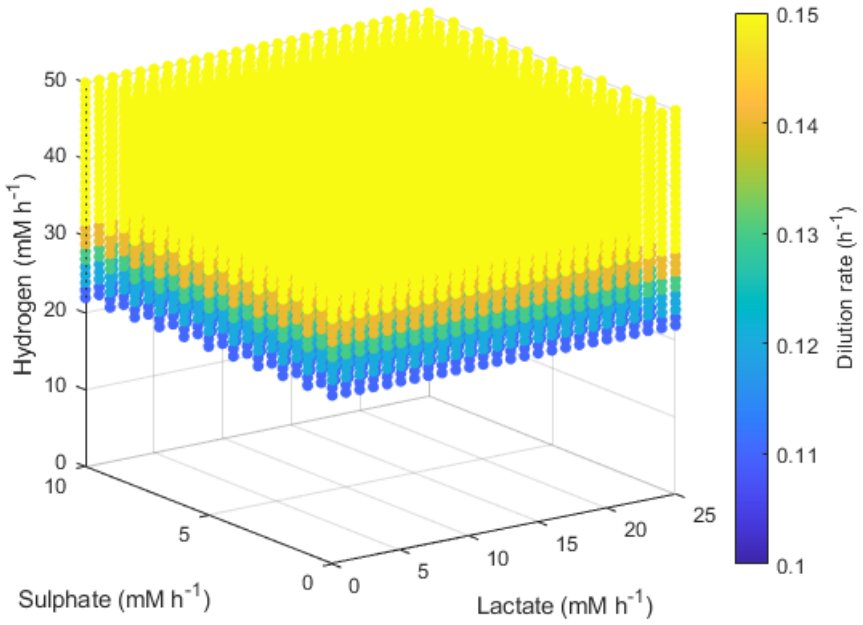

Figure 7.7. Maximum dilution rates (h^{-1}) under which the outcome of the model was survival of the acetogen only. The axes indicate the inflow rate of each of the three substrates, and the coloured points represent combinations of these inflows that resulted in survival of the acetogen only at the dilution rate shown on the colour bar.

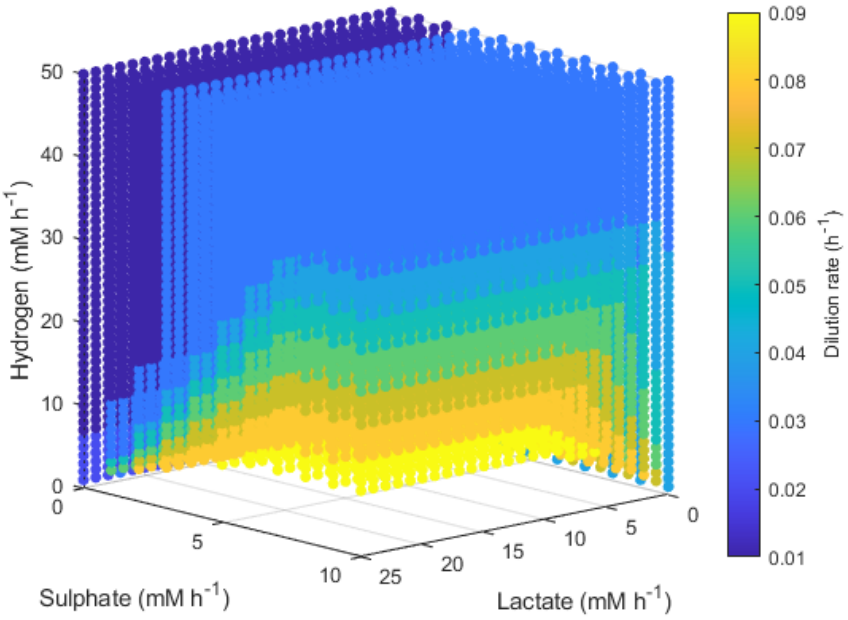

Figure 7.8. Minimum dilution rates under which the outcome of the model was survival of the methanogen only. The axes indicate the inflow rate of each of the three substrates, and the coloured points represent combinations of these inflows that resulted in survival of the acetogen only at the dilution rate shown on the colour bar. Note the inverted lactate and sulphate axes.

Conditions resulting in survival of only the methanogen took a more complex form. Figure 7.8 shows the minimum dilution rate under which only this microbe survived. At low lactate, low sulphate, high hydrogen inflows, the methanogen outcompetes the other hydrogenotrophs at most dilution rates. However, as lactate and sulphate inflows increase, only under higher dilution rates and hydrogen inflows can the methanogen outcompete the SRB; for combinations of high lactate and sulphate inflows with low hydrogen inflow, the methanogen is outcompeted by the SRB regardless of dilution rate. Conversely to Figure 7.7 for acetogen only survival, Figure 7.8 shows only dilution rates up to 0.09, as the methanogen is unable to avoid washout at dilution rates above 0.1042 h^{-1}.

Figure 7.9 shows the maximum dilution rate under which the SRB outcompetes the other hydrogenotrophs. When sulphate and lactate inflows were high and hydrogen inflow was low, the SRB was able to outcompete the other microbes at dilution rates up to 0.1 h^{-1}. This result was unaffected by lactate inflow. However, as hydrogen inflow increases, inhibition of lactate utilization by the SRB increases, thus the SRB were only able to outcompete at low dilution rates. The same was true for low sulphate inflows.

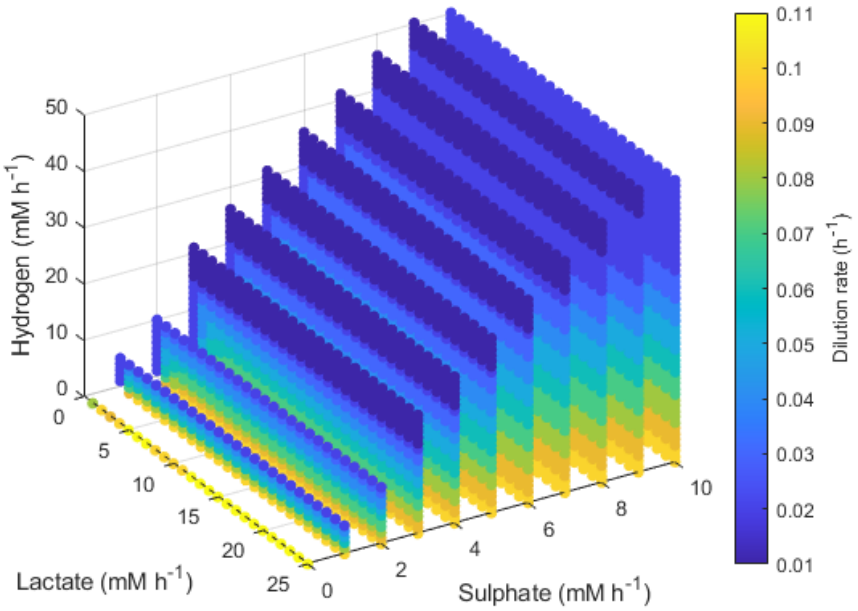

Figure 7.9. Maximum dilution rates under which the outcome of the model was survival of the sulphate-reducing bacterium only. The axes indicate the inflow rate of each of the three substrates, and the coloured points represent combinations of these inflows that resulted in survival of the acetogen only at the dilution rate shown on the colour bar. Note the inverted lactate axis.

The final set of conditions that did not result in extinction of all three hydrogenotrophs were those that enabled survival of both the SRB and the methanogen, as shown in Figure 7.10. The greatest dilution rate which resulted in this coexistence was 0.02 h^{-1}, emphasizing the low growth rates achieved by both microbes at hydrogen concentrations approaching the inhibitory concentration, as shown earlier analytically. Coexistence was unaffected by lactate concentration, but did require a relationship between the sulphate and hydrogen inflows: high hydrogen inflows had to coincide with high sulphate inflows to maintain survival of both the SRB and the methanogen. Coexistence also required a minimum hydrogen inflow of 6 mM and was not possible at zero sulphate inflow. The blue region in Figure 7.10 indicates conditions under which a dilution rate of 0.01 h^{-1} did not result in coexistence, although this is likely a result of the model not reaching steady state after 1,000 hours, as discussed below. It is anticipated that all coloured points in Figure 7.10 represent conditions that would allow for survival of both the SRB and the methanogen at either 0.01 or 0.02 h^{-1} dilution rates.

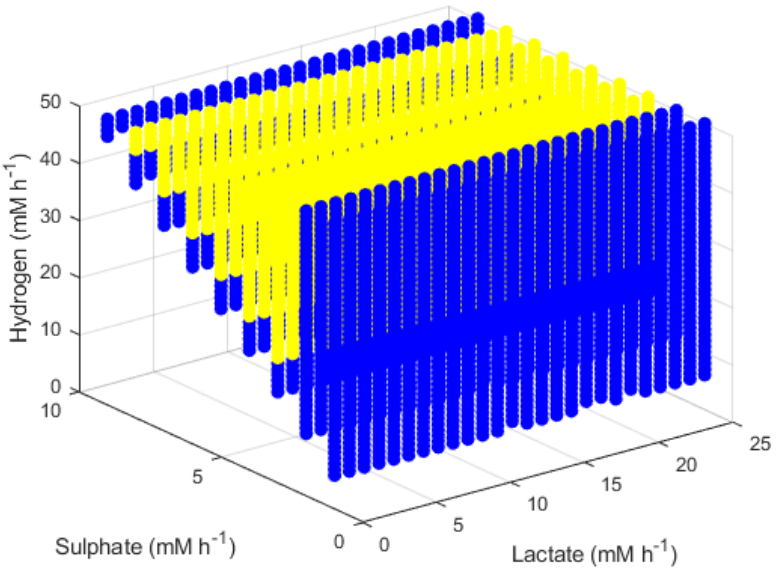

Figure 7.10. Dilution rates under which the outcome of the model was survival of the sulphate-reducing bacterium and the methanogen. The axes indicate the inflow rate of each of the three substrates. Yellow points indicate conditions where coexistence was possible at both 0.01 and 0.02 h^{-1} dilution rates and blue points indicate conditions where coexistence was only possible at a dilution rate of 0.02 h^{-1}.

The results shown in this numerical section, and in particular those shown in Figure 7.10, may not be reflective of steady state survival. Under the model assumptions, these results merely indicate survival and slow cell concentration change after 1,000 hours of simulated culture. The low dilution rates considered may result in a longer time required for the model to reach steady state under certain conditions, so the above results are not necessarily steady state results in all cases. However, when the conditions resulting in SRB and methanogen coexistence were simulated for 2,000 hours, the survival status was identical to the 1,000 hours case, making steady state survival likely. Moreover, survival of a microbial population after 1,000 hours likely translates to survival under practical, shorter timeframes.

7.4 Discussion

A number of previous studies suggested that a degree of competitive exclusion exists between hydrogenotrophs when competing for hydrogen in the human colon (Gibson et al., 1988a; Gibson et al., 1988b; Gibson et al., 1990; Gibson et al., 1993; Strocchi et al., 1994). However, more recent work has found that all three hydrogenotrophs are present in all tested individuals (Nava et al., 2012). There exists a great body of research detailing the dominant hydrogenotroph in different

human populations and in different locations in the colon, as well as the influence of dietary changes on this dominance, as discussed in Chapter 2. The modelling work presented here shows that under conditions of abundant substrate in a homogeneously mixed environment, dominance of a culture by one species is the most common result, with extinction of the others. Moreover, under low-dilution, high-substrate conditions, the model results support the established hierarchy between SRB, methanogens and acetogens in terms of their growth rates and competitiveness.

The prediction of the model that coexistence of all three hydrogenotrophs in continuous culture is impossible under any of the substrate and dilution rate combinations considered is in contrast with their observation in natural habitats, such as the human colon (Nava et al., 2012). However, the model assumption of a homogeneously mixed environment is likely partially responsible for this difference. In natural habitats, spatial separation, diffusion of metabolites, biofilm formation and many other heterogeneities will contribute both positively and negatively to the growth of each of the hydrogenotrophs. For example, being separated spatially from the methanogen would allow for better growth by the acetogen due to reduced local competition for hydrogen, whereas the same spatial separation from the SRB may be detrimental to the acetogen if it is reliant on cross-feeding for released hydrogen.

Also neglected in this model is the metabolism of substrates other than hydrogen, lactate and sulphate by the hydrogenotrophs. Several colonic SRB strains have been shown to metabolise other organic substrates (Willis et al., 1997), as have colonic acetogens (Bernalier et al., 1996). Formate is a molecule that has been shown to be metabolised by strains of all three hydrogenotrophs (Bernalier et al., 1996; Samuel et al., 2007; da Silva et al., 2013), and would be a valuable addition to the tri-culture model. However, the addition of this extra metabolite would make analytical solutions to the model more challenging to obtain, and numerical results more challenging to interpret.

It is interesting to consider the stability of the model results to small changes in the parameter values. It is not expected that the parameter values determined from monoculture experiments stated in Table 7.1 will be suitable for all hydrogenotroph strains in all environments, as gene expression changes between monoculture and co-culture have been shown in SRB and methanogen co-cultures previously, as discussed in Chapter 6 (Walker et al., 2009; Meyer et al.,

2013). However, so long as the assumptions on the model system remain unchanged, the analytical results provided here will still apply. If the assumptions change, then alterations to the model structure will necessitate a revised analysis of the model.

The applicability of the model to natural environments is also of interest. Coexistence of multiple hydrogenotrophs was shown to be possible only under a limited set of conditions in the model. Small perturbations due to external, non-modelled influences would be expected to occur in natural environments. Under the model conclusions, these small deviations would rapidly lead to extinction of all or all but one of the modelled organisms. However, the observed coexistence of hydrogenotrophs in natural environments indicates that other factors have an influence. In the human colon, these other factors may be the use of alternative metabolites, spatial separation of hydrogenotrophs and interactions with the wider microbiota and host. Also not addressed by this model was the potential for metabolite influx to follow a periodic or inconsistent pattern, as would be expected in the colon. The influence of all these factors on survival of hydrogenotrophs should be included and investigated in future models.

Inclusion of the non-modelled influences mentioned above in future modelling efforts for hydrogenotroph metabolism will be challenging, but the tools exist for such investigations. Several spatial models of microbial growth and metabolism have been developed, using both continuous (for example, see Alpkvist et al. (2006)) and discrete spatial distribution (for example, see Bauer et al. (2017)). There are also microbiome models that incorporate various host influences, such as pH buffering and water absorption (Cremer et al., 2017) and the secreted mucous layer and fluid dynamics of the colonic contents under peristaltic movement (Labarthe et al., 2019). Finally, the influence of interactions amongst the microbiota can be studied with existing microbial community models (for examples, see Motelica-Wagenaar et al. (2014), Kettle et al. (2017) and Sung et al. (2017)). Hydrogenotrophic microbes have thus far been either absent or only a minor part of these large-scale models, but both the study of these microbes and the large-scale models themselves could benefit from the inclusion of hydrogenotrophs.

The complexity of the conditions for survival derived from the relatively simple model presented here, which features only three different organisms and six metabolites (three of which had no determining effect on the model outcomes), in a homogenously mixed medium with no

gaseous phase, demonstrates the difficulty in extracting universal insight into large, complex populations from mathematical models. However, mathematical modelling has been used to successfully glean more information from experimental data for co- and tri-cultures of human colonic microbes (Van Wey et al., 2014; Pinto et al., 2017; D'Hoe et al., 2018) and for cross-feeding cultures of SRB and methanogens in the past (Archer and Powell, 1985; Stolyar et al., 2007). These successes justify the further use of modelling to explore areas that cannot easily be studied experimentally. No previous research was found in which the three hydrogenotrophs modelled here have been cultured together, thus the results of the model currently forms the best predictive capability available for what would be observed experimentally. Moreover, the simple nature of the constituent models will allow for straightforward inclusion of additional variables and conditions, such as formate metabolism. Although an increase in complexity will likely prevent analytical solutions to the model equations, model simulations can still provide useful insight into microbial community dynamics.

7.5 Conclusions

The construction of a tri-culture mathematical model using the monoculture model structures and parameters from previous Chapters allowed for predictions to be made about competitive and cross-feeding interactions between the three major hydrogenotrophic groups of the colon. The results of the model demonstrate that coexistence of all three hydrogenotrophs in the human colon must be due to selective factors outside of the hydrogen, lactate and sulphate metabolism and varied dilution rates considered here, since it was impossible to obtain coexistence of the three in continuous culture under the model assumptions. The influence of these other selective factors needs to be examined in future models investigating hydrogenotroph dynamics in the colon.

References

Alpkvist, E., Picioreanu, C., Van Loosdrecht, M.C.M., and Heyden, A. (2006). Three-dimensional biofilm model with individual cells and continuum EPS matrix. Biotechnol. Bioeng. 94(5), 961-979. doi: 10.1002/bit.20917.

Archer, D.B., and Powell, G.E. (1985). Dependence of the specific growth rate of methanogenic mutualistic cocultures on the methanogen. Arch. Microbiol. 141(2), 133-137. doi: 10.1007/BF00423273.

Arhan, P., Devroede, G., Jehannin, B., Lanza, M., Faverdin, C., Dornic, C., et al. (1981). Segmental colonic transit time. Dis. Colon Rectum 24(8), 625-629. doi: 10.1007/BF02605761.

Attene-Ramos, M.S., Nava, G.M., Muellner, M.G., Wagner, E.D., Plewa, M.J., and Gaskins, H.R. (2010). DNA damage and toxicogenomic analyses of hydrogen sulfide in human intestinal epithelial FHs 74 Int cells. Environ. Mol. Mutag. 51(4), 304-314. doi: 10.1002/em.20546.

Bauer, E., Zimmermann, J., Baldini, F., Thiele, I., and Kaleta, C. (2017). BacArena: Individual-based metabolic modeling of heterogeneous microbes in complex communities. PLoS Comp. Biol. 13(5). doi: 10.1371/journal.pcbi.1005544.

Bernalier, A., Willems, A., Leclerc, M., Rochet, V., and Collins, M.D. (1996). *Ruminococcus hydrogenotrophicus* sp. nov., a new H2/CO2-utilizing acetogenic bacterium isolated from human feces. Arch. Microbiol. 166(3), 176-183. doi: 10.1007/s002030050373.

Carbonero, F., Benefiel, A.C., and Gaskins, H.R. (2012). Contributions of the microbial hydrogen economy to colonic homeostasis. Nat. Rev. Gastroenterol. Hepatol. 9, 504. doi: 10.1038/nrgastro.2012.85.

Cremer, J., Arnoldini, M., and Hwa, T. (2017). Effect of water flow and chemical environment on microbiota growth and composition in the human colon. P. Natl. Acad. Sci. 114(25), 6438.

D'Hoe, K., Vet, S., Faust, K., Moens, F., Falony, G., Gonze, D., et al. (2018). Integrated culturing, modeling and transcriptomics uncovers complex interactions and emergent behavior in a three-species synthetic gut community. eLife 7, e37090. doi: 10.7554/eLife.37090.

da Silva, S.M., Voordouw, J., Leitão, C., Martins, M., Voordouw, G., and Pereira, I.A.C. (2013). Function of formate dehydrogenases in *Desulfovibrio vulgaris* Hildenborough energy metabolism. Microbiology (UK) 159(8), 1760-1769. doi: 10.1099/mic.0.067868-0.

Falony, G., Vlachou, A., Verbrugghe, K., and De Vuyst, L. (2006). Cross-feeding between *Bifidobacterium longum* BB536 and acetate-converting, butyrate-producing colon bacteria during growth on oligofructose. Appl. Environ. Microbiol. 72(12), 7835-7841. doi: 10.1128/aem.01296-06.

Florin, T., Neale, G., Gibson, G.R., Christl, S.U., and Cummings, J.H. (1991). Metabolism of dietary sulphate: Absorption and excretion in humans. Gut 32(7), 766-773. doi: 10.1136/gut.32.7.766.

Ghoshal, U., Shukla, R., Srivastava, D., and Ghoshal, U.C. (2016). Irritable bowel syndrome, particularly the constipation-predominant form, involves an increase in *Methanobrevibacter smithii*, which is associated with higher methane production. Gut Liver 10(6). doi: 10.5009/gnl15588.

Gibson, G.R., Cummings, J.H., and Macfarlane, G.T. (1988a). Competition for hydrogen between sulphate-reducing bacteria and methanogenic bacteria from the human large intestine. J. Appl. Bacteriol. 65(3), 241-247. doi: doi:10.1111/j.1365-2672.1988.tb01891.x.

Gibson, G.R., Cummings, J.H., Macfarlane, G.T., Allison, C., Segal, I., Vorster, H.H., et al. (1990). Alternative pathways for hydrogen disposal during fermentation in the human colon. Gut 31(6), 679-683.

Gibson, G.R., Macfarlane, G.T., and Cummings, J.H. (1988b). Occurrence of sulphate-reducing bacteria in human faeces and the relationship of dissimilatory sulphate reduction to methanogenesis in the large gut. J. Appl. Microbiol. 65(2), 103-111.

Gibson, G.R., Macfarlane, S., and Macfarlane, G.T. (1993). Metabolic interactions involving sulphate-reducing and methanogenic bacteria in the human large intestine. FEMS Microbiol. Ecol. 12(2), 117-125.

Healey, G.R., Murphy, R., Brough, L., Butts, C.A., and Coad, J. (2017). Interindividual variability in gut microbiota and host response to dietary interventions. Nutr. Rev. 75(12), 1059-1080. doi: 10.1093/nutrit/nux062.

Kalyuzhnyi, S.V., and Fedorovich, V.V. (1998). Mathematical modelling of competition between sulphate reduction and methanogenesis in anaerobic reactors. Bioresour. Technol. 65(3), 227-242. doi: 10.1016/S0960-8524(98)00019-4.

Kettle, H., Holtrop, G., Louis, P., and Flint, H.J. (2017). microPop: Modelling microbial populations and communities in R. Methods Ecol. Evol. 9, 399–409. doi: 10.1111/2041-210x.12873.

Kettle, H., Louis, P., Holtrop, G., Duncan, S.H., and Flint, H.J. (2015). Modelling the emergent dynamics and major metabolites of the human colonic microbiota. Environ. Microbiol. 17(5), 1615-1630. doi: 10.1111/1462-2920.12599.

Labarthe, S., Polizzi, B., Phan, T., Goudon, T., Ribot, M., and Laroche, B. (2019). A mathematical model to investigate the key drivers of the biogeography of the colon microbiota. J. Theor. Biol. 462**,** 552-581. doi: 10.1016/j.jtbi.2018.12.009.

Leclerc, M., Bernalier, A., Donadille, G., and Lelait, M. (1997). H2/CO2 Metabolism in Acetogenic Bacteria Isolated From the Human Colon. Anaerobe 3(5)**,** 307-315. doi: https://doi.org/10.1006/anae.1997.0117.

Macfarlane, G.T., and Macfarlane, S. (2012). Bacteria, colonic fermentation, and gastrointestinal health. J. AOAC Int. 95(1)**,** 50-60. doi: 10.5740/jaoacint.SGE-Macfarlane.

Meyer, B., Kuehl, J., Deutschbauer, A.M., Price, M.N., Arkin, A.P., and Stahl, D.A. (2013). Variation among *Desulfovibrio* Species in Electron Transfer Systems Used for Syntrophic Growth. J. Bacteriol. 195(5)**,** 990. doi: 10.1128/JB.01959-12.

Morrison, D.J., and Preston, T. (2016). Formation of short chain fatty acids by the gut microbiota and their impact on human metabolism. Gut Microbes 7(3)**,** 189-200. doi: 10.1080/19490976.2015.1134082.

Motelica-Wagenaar, A.M., Nauta, A., van den Heuvel, E.G.H.M., and Kleerebezem, R. (2014). Flux analysis of the human proximal colon using anaerobic digestion model 1. Anaerobe 28**,** 137-148. doi: 10.1016/j.anaerobe.2014.05.008.

Nava, G.M., Carbonero, F., Croix, J.A., Greenberg, E., and Gaskins, H.R. (2012). Abundance and diversity of mucosa-associated hydrogenotrophic microbes in the healthy human colon. ISME J. 6(1)**,** 57-70. doi: 10.1038/ismej.2011.90.

Pinto, F., Medina, D.A., Pérez-Correa, J.R., and Garrido, D. (2017). Modeling Metabolic Interactions in a Consortium of the Infant Gut Microbiome. Front. Microbiol. 8(2507). doi: 10.3389/fmicb.2017.02507.

Qin, J., Li, R., Raes, J., Arumugam, M., Burgdorf, K.S., Manichanh, C., et al. (2010). A human gut microbial gene catalogue established by metagenomic sequencing. Nature 464(7285)**,** 59-65. doi: 10.1038/nature08821.

Ribes, J., Keesman, K., and Spanjers, H. (2004). Modelling anaerobic biomass growth kinetics with a substrate threshold concentration. Water Res. 38(20)**,** 4502-4510. doi: https://doi.org/10.1016/j.watres.2004.08.017.

Samuel, B.S., Hansen, E.E., Manchester, J.K., Coutinho, P.M., Henrissat, B., Fulton, R., et al. (2007). Genomic and metabolic adaptations of *Methanobrevibacter smithii* to the human gut. Proc. Natl. Acad. Sci. USA. 104(25)**,** 10643-10648. doi: 10.1073/pnas.0704189104.

Stolyar, S., Van Dien, S., Hillesland, K.L., Pinel, N., Lie, T.J., Leigh, J.A., et al. (2007). Metabolic modeling of a mutualistic microbial community. Mol. Syst. Biol. 3**,** 92. doi: 10.1038/msb4100131

Strocchi, A., Furne, J., Ellis, C., and Levitt, M.D. (1994). Methanogens outcompete sulphate reducing bacteria for H2 in the human colon. Gut 35(8)**,** 1098.

Sung, J., Kim, S., Cabatbat, J.J.T., Jang, S., Jin, Y.S., Jung, G.Y., et al. (2017). Global metabolic interaction network of the human gut microbiota for context-specific community-scale analysis. Nat. Commun. 8. doi: 10.1038/ncomms15393.

Thauer, R.K., Jungermann, K., and Decker, K. (1977). Energy conservation in chemotrophic anaerobic bacteria. Bacteriol. Rev. 41(1)**,** 100-180.

Van Wey, A.S., Cookson, A.L., Roy, N.C., McNabb, W.C., Soboleva, T.K., and Shorten, P.R. (2014). Monoculture parameters successfully predict coculture growth kinetics of *Bacteroides thetaiotaomicron* and two *Bifidobacterium* strains. Int. J. Food Microbiol. 191**,** 172-181. doi: 10.1016/j.ijfoodmicro.2014.09.006.

Vernia, P., Caprilli, R., Latella, G., Barbetti, F., Magliocca, F.M., and Cittadini, M. (1988). Fecal Lactate and Ulcerative Colitis. Gastroenterol. 95(6)**,** 1564-1568. doi: https://doi.org/10.1016/S0016-5085(88)80078-7.

Walker, C.B., He, Z., Yang, Z.K., Ringbauer, J.A., He, Q., Zhou, J., et al. (2009). The Electron Transfer System of Syntrophically Grown *Desulfovibrio vulgaris*. J. Bacteriol. 191(18)**,** 5793.

Willis, C.L., Cummings, J.H., Neale, G., and Gibson, G.R. (1997). Nutritional aspects of dissimilatory sulfate reduction in the human large intestine. Curr. Microbiol. 35(5)**,** 294-298. doi: 10.1007/s002849900257.

Wolf, P.G., Biswas, A., Morales, S.E., Greening, C., and Gaskins, H.R. (2016). H2 metabolism is widespread and diverse among human colonic microbes. Gut Microbes 7(3)**,** 235-245. doi: 10.1080/19490976.2016.1182288.

Wolin, M.J., and Miller, T.L. (1983). Interactions of microbial populations in cellulose fermentation. Fed. Proc. 42(1), 109-113.
Zmora, N., Suez, J., and Elinav, E. (2019). You are what you eat: diet, health and the gut microbiota. Nat. Rev. Gastroenterol. Hepatol. 16(1), 35-56. doi: 10.1038/s41575-018-0061-2.

The following chapter contains material from the following manuscript in preparation for submission for publication in Microbiome:

Examination of hydrogen cross-feeders using a colonic microbiota model. Smith NW, Shorten PR, Altermann E, Roy NC, McNabb WC.

Chapter 8: Adaptation of the microbial community model microPop for the study of hydrogenotrophs of the human colon

Abstract

Hydrogen cross-feeding microbes form a functionally important subset of the human colonic microbiota. The three major hydrogenotrophic functional groups of the colon: sulphate-reducing bacteria (SRB), methanogens and reductive acetogens, have been linked to wide ranging impacts on host physiology, health and wellbeing. An existing mathematical model for microbial community growth and metabolism was combined with models for each of the three hydrogenotrophic functional groups. The model was further developed for application to the colonic environment via inclusion of dynamic pH, host metabolite absorption and the inclusion of a host mucins. Predictions of the model, using two existing metabolic parameter sets, were compared to three experimental faecal culture data sets. Model accuracy varied between experiments and measured variables, and was most successful in predicting the growth of high relative abundance microbial functional groups (MFGs), such as the Bacteroides, and short chain fatty acid (SCFA) production. Two versions of the colonic model were developed: one representing the colon with sequential compartments and one utilising a continuous spatial representation. When applied to the colonic environment, the model predicted pH dynamics within the ranges measured *in vivo* and SCFA ratios comparable to those in the literature. The continuous version of the model simulated the relative abundances of MFGs comparable to measured values, but predictions were sensitive to metabolic parameter values used for each MFG. Sulphate availability was found to strongly influence hydrogenotroph activity in the continuous version of the model, correlating positively with SRB and sulphide concentration and negatively with methanogen concentration, but to have no effect in the compartmentalised model version. Although the model predictions compared well to only some experimental measurements, the important features of the colon environment included in the model make it a novel and useful contribution to modelling the colonic microbiota.

8.1 Introduction

The microbial population of the human colon has wide-ranging effects on host nutrition and health. These effects include providing important metabolites that cannot be synthesised by the host, modulation of immune functions, and roles in diseases both of the colon and more distant regions of the body (see review by Nicolas and Chang (2019)). Efforts to study the colonic microbiota have included observational and interventional studies, coupled with *in vitro,* animal, and computational models. This last technique, although dependent on experimental data for model validation, has appeal as a faster, cheaper and more high-throughput method than experimentation, leading to the creation of several mathematical models for the colonic microbiota in recent years (e.g. Motelica-Wagenaar et al. (2014) and Bauer et al. (2017)). Most of these models focus on the dynamics of the dominant taxa found in the colon and their metabolites, although the importance of other, less abundant microbes is beginning to emerge. One group of microbes for which this is true is those that metabolise hydrogen. Hydrogen is produced through various microbial metabolic pathways involved in the degradation of carbohydrates, creating a niche for microbes that can cross-feed on hydrogen (Carbonero et al., 2012b). To date, computational models of the colonic microbiota have not been focussed on the study of hydrogen cross-feeding microbes. These hydrogenotrophs have demonstrated impact on both the microbiota and the host as discussed in Chapter 2, and much remains uncertain in the details of these impacts. The low colonic abundance of hydrogenotrophs, coupled with the inconsistent distribution of the microbes between individuals makes them challenging to study, thus modelling could provide useful insight into hydrogenotroph dynamics *in vivo*.

Recently, an adaptable tool for modelling the metabolism and growth of microbial communities was published, named microPop (Kettle et al., 2017). This tool was first developed as an extension of a previous model for the *in vitro* growth of the human faecal microbiota published by the same group (Kettle et al., 2015). The original authors stated that the model could be adapted for application to the colon and provided suggestions for how this might be achieved.

Here, an adaptation of the model is presented incorporating these suggestions, alongside further alterations and additions, designed to replicate the behaviour of the major MFGs of the

human colonic microbiota. The model is first compared to three *in vitro* fermentation data sets, followed by simulations of the *in vivo* environment. Adaptations include the addition of host factors: secreted mucins, buffering and absorption, as well as microbial adaptations, most notably a focus on hydrogen cross-feeding microbes. Finally, various substrate availability scenarios are simulated to give predictions for their effect on the microbiota.

8.2 Methodology

8.2.1 Consideration of hydrogen cross-feeding in microPop

The previously described mathematical models for monoculture hydrogenotroph metabolism (Chapters 3-5) were combined with the microbial community modelling tool microPop (Kettle et al., 2017). Briefly, microPop models microbial activity and metabolite concentrations by accounting for the growth and metabolism of several MFGs, each of which is representative of a subset of the wider microbial community. For each of these MFGs, microPop implements information on the different metabolic pathways available to the MFG and the corresponding parameter values for these pathways, including maximum growth rate, half-saturation constants, yield factors and stoichiometries. microPop also considers the pH preferences of each MFG, scaling metabolic activity according to environmental pH. microPop is based on Monod kinetics, constructing and solving a system of ODEs for given initial conditions relating to each MFG and each metabolite. Full details of the equations used are included in Appendix C (C1). The MFG kinetic parameter values used here were based on two different parameter sets: the Alpha set, utilising the original values of Kettle et al. (2017); and a Beta set, based on newly proposed values (Wang et al. (Under review), Personal Communication[1]). These values are included in Appendix C (C8). Use of both parameter sets allowed for comparison of the predictions of the two parameterisations.

[1] This parameter set is taken from the work of Wang et al., under review with the journal mSystems. Permission to reference the work as a personal communication was received from Harry J. Flint on 7/05/2020. Full authorship and title are included in the reference list.

The main alterations to the microPop MFGs performed here involved the representation of hydrogenotrophs: changes to the original acetogen and methanogen MFGs, as well as the addition of SRB to the model. The hydrogenotrophic metabolism of the original acetogen MFG present in microPop was replaced with the alternative model for *B. hydrogenotrophica* from Chapter 5. The SRB model from Chapter 4 was added to be representative of the SRB MFG. As a representative for the methanogens, the *M. smithii* model from Chapter 3 was used, as this is the dominant colonic methanogen.

8.2.2 Comparison of microPop to experimental data

A predecessor model to microPop has previously been validated against experimental data from human faecal fermentations (Walker et al., 2005; Kettle et al., 2015). In order to validate microPop after the alterations to the hydrogenotrophic MFGs, model predictions were compared to continuous faecal culture data from three independent sources. Data were sampled from Walker et al. (2005) (the same data used in previous model validations by Kettle et al. (2015)), Belenguer et al. (2011) and Payne et al. (2012a) using image capturing and graphical input software in MATLAB (The MathWorks; www.mathworks.com). SCFA and MFG measurements were converted to microPop values from information provided in the publications (Appendix C, C3 & C4).

8.2.3 Adaptation of microPop to the human colonic environment

To perform the theoretical study of hydrogen cross-feeding and model the activity of the microbiota in the human colon, several further alterations to microPop were introduced. Henceforth, the colon version of the model is referred to as microPop:Colon.

8.2.3.1 Physiology

In the model, the colon was divided into three sequential compartments, representative of the proximal, transverse and distal colonic sections. To make the model reflective of the colonic environment, an overall dilution rate of 1 d^{-1} was chosen for the entire colon, reflective of mean transit times in the literature (Koziolek et al., 2015; Wang et al., 2015). The dilution rate was scaled in each compartment according to the relative volume of the compartment. A fixed colonic volume

of 3.02 L was assumed, with 0.41, 0.98 and 1.63 L volumes in the proximal, transverse and distal colons, respectively (de Jong et al., 2007). Although the volume of the colon will vary *in vivo*, these assumptions on the volumes only affected transit time, metabolite absorption and bicarbonate secretion in the model.

8.2.3.2 pH

pH variation based on the metabolism of the microbiota was identified as an important inclusion. Thus, the charge balance model structures of Batstone et al. (2002) and the simplified version of Muñoz-Tamayo et al. (2016) were adapted for the colonic environment. Full details of the pH calculations are given in Appendix C (C6). Briefly, it was assumed that a charge balance is maintained between positively charged ions (H^+ ions and miscellaneous cations) and negatively charged ions (dissociated SCFAs, bicarbonate and hydroxide). Moreover, it was assumed that the host buffers the colonic lumen via secretion of bicarbonate ions, absorption of SCFAs and secretion and absorption of CO_2. Absorption of SCFAs is described in section 8.2.3.3. Bicarbonate and CO_2 was modelled to adhere to the equilibrium equation:

$$K_{a,CO_2} s_{CO2} - s_{HCO_3^-} s_{H^+} = 0,$$

where K_{a,CO_2} is the equilibrium constant for CO_2, s_{CO2}, $s_{HCO_3^-}$ and s_{H^+} are the concentrations of CO_2, bicarbonate and H^+ ions, respectively. Thus, as bicarbonate is secreted into the colonic lumen, it combines with H^+ ions to form CO_2 and H_2O to balance the equilibrium equation. This balancing also occurs during CO_2 secretion and absorption. The pH was then calculated from the concentration of H^+ ions, where s_{H^+} must satisfy both the above equilibrium equation and charge balance.

8.2.3.3 Substrates and metabolites

The influx of substrates and metabolites into the model was limited to the first compartment, with the exception of mucin and bicarbonate. Rates of substrate inflow from dietary sources were taken as equal to those from experimental estimates in the literature (Appendix C, C3). Free sulphate from the diet was included at an inflow rate of 0.86 g d^{-1} (Florin et al., 1991), which was important to the SRB MFG.

In the case of mucin, it is estimated between 2.7 – 7.3 g d^{-1} is secreted into the colon (Stephen et al., 1983; Florin et al., 1991), so 5 g d^{-1} was set as the microPop:Colon influx. Unlike the other metabolites, mucin influx was divided proportionally to the volumes of each compartment. For mucin degradation, it was assumed that mucin is made up of mostly carbohydrate, with smaller proportions of protein and sulphate (Willis et al., 1996; Kettle et al., 2015). A broad analysis of colonic microbe genomes emphasised the capacity of many *Bacteroides* strains to be effective degraders of common mucin structures (Ravcheev and Thiele, 2017). *Akkermansia muciniphila* was also implicated as a major mucin degrader and only this species and certain *Bacteroides* strains were capable of encoding mucin-desulphating sulfatases. Since microPop did not include *A. muciniphila* explicitly and this inclusion has not been made here due to a lack of parameterising data, the Bacteroides MFG was set as the sole degrader of mucin. The following pathway was selected for the breakdown of mucin by the Bacteroides MFG:

1 g Mucin -> 0.05 g Sulphate + 0.2 g Protein + *X* g Non-Starch Polysaccharide (NSP) + (0.75-*X*) g Sugars

where *X* is the unknown proportion of mucin carbohydrate that is broken down to NSP rather than simple sugars. It is unclear what proportion of mucin carbohydrate is degraded to simple sugars versus more complex polysaccharides and this likely varies between degrading strains and mucin structures (Ravcheev and Thiele, 2017). An approximate value of *X*=0.5 was used for the model. Parameter values for this Bacteroides MFG metabolic pathway were based on the metabolism of chondroitin sulphate and porcine mucin by *B. thetaiotaomicron* and are listed in Appendix C (C5; Pudlo et al. (2015)).

Finally, in order to obtain SCFA concentrations in the model compartments reflective of the concentrations in the human colon and to capture the contribution of SCFAs to host nutrition, host absorption of acetate, propionate and butyrate was included. Previous research implied minimal variation between the absorption rates of these three SCFAs in digestive environments (Ruppin et al., 1980; Topping and Clifton, 2001; Stumpff, 2018). Ruppin et al. (1980) experimentally tested the absorption rates of varied concentrations of SCFAs perfused into the colon and an absorption rate of approximately 0.4 h^{-1} was calculated from this data, which is applied to acetate, propionate and butyrate in microPop:Colon.

8.2.3.4 Microbial functional groups

The eleven MFGs of microPop:Colon were made up of the ten MFGs from the original microPop model, with the aforementioned alterations to the methanogen, acetogen and Bacteroides MFGs, and the novel SRB MFG. Unless stated as changed specifically for microPop:Colon, all values used were those of the original model. For the initial microbial population sizes, 16S rRNA probe analysis data from faecal samples detailed in Walker et al. (2005) was used, converted to microPop MFGs according to Kettle et al. (2015) (Appendix C, C4). No cell death was included in the model, as this was assumed negligible compared to washout, which was included.

8.2.4 Computation

Although microPop was used as the basis for microPop:Colon, the equations for microPop:Colon were implemented in MATLAB (The MathWorks; www.mathworks.com) rather than R, the format for the original publication, for ease of code management. The availability of microPop packages in both MATLAB and R should facilitate wider usage of the model. The mathematical structure and parameter values given in the supporting material of the microPop package were used to transition the tool between software. Upon completion, the MATLAB version was tested to ensure that its predictions were consistent with those of the R version (microPop version 1.5). This testing was carried out for the pH static experiment displayed in Figure 8.1 and the pH shift experiment displayed in Figure 8.3. For all MFGs and metabolites, the predictions of the R and MATLAB versions were identical to four significant figures. Discrepancies beyond this level of accuracy are likely due to the differing numerical solvers used in the computation and were deemed insignificant. The adaptations of the model to the human colonic environment described above were all carried out in the MATLAB environment.

8.3 Results

8.3.1 Comparison of model predictions to experimental data

To verify that the predictions of microPop were realistic for the considered MFGs and metabolite concentrations, simulated concentrations were compared with experimental data from continuous

faecal cultures. Note that both the Alpha and Beta parameter sets were used in each case, with the respective predictions shown in each figure in this section. Figures 8.1 and 8.2 show the predictions of microPop for a continuous culture with inocula from the same faecal sample but with varied peptide concentration in the added medium to investigate differences in microbiota profile caused by protein availability (Walker et al., 2005). Figure 8.1 displays the predictions of the model compared to experimental data from a continuous culture with 0.6% w/v peptide in the medium, while Figure 8.2 shows an identical culture with 0.1% w/v peptide. In both cases the pH was fixed at 6.5.

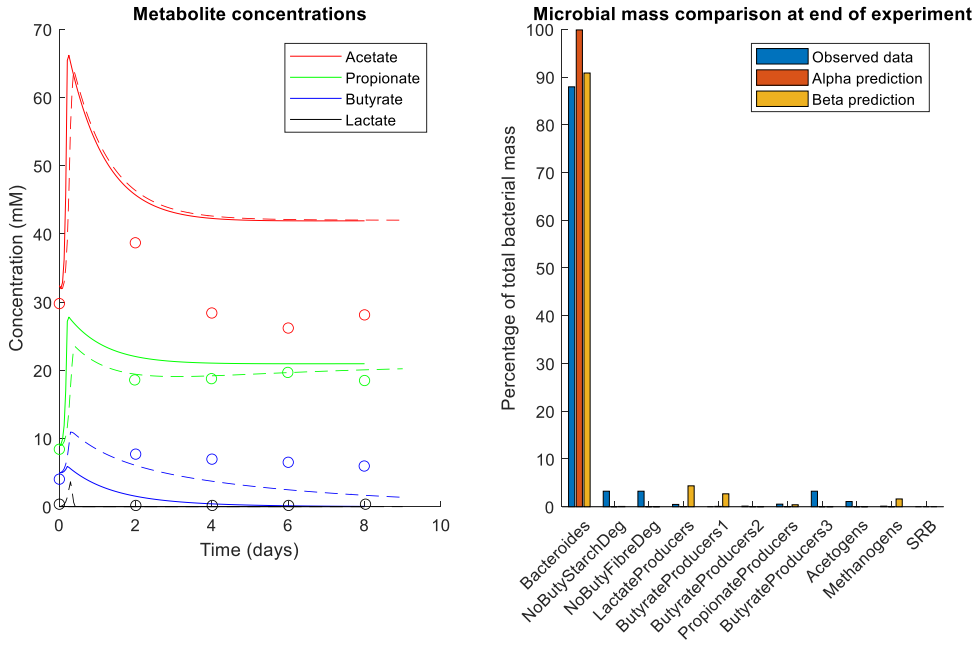

Figure 8.1. Model prediction compared with experimental data (indicated by the coloured circles) from Walker et al. (2005) for continuous culture of a faecal microbial community (Donor 2) on a medium containing 0.6% w/v peptide. The solid lines in the metabolite concentration panel display the model prediction using the Alpha parameter set, whereas the dashed lines display the prediction using the Beta parameter set.

The model correctly predicted the almost complete dominance of the Bacteroides MFG under the high peptide conditions. However, the prediction for SCFA concentrations were mostly inaccurate (see Table 8.1). Acetate was overpredicted by at least 15 mM from day 4 of culture onwards using both parameter sets. The model predicted washout of butyrate and lactate, although this was more rapid using the Alpha parameter set than the Beta parameter set, while experimentally both metabolites appeared to reach a non-zero steady state. Contrastingly,

propionate concentration was accurately predicted to within 5 mM using the Alpha parameter set and to within 2 mM using the Beta parameter set throughout the experiment.

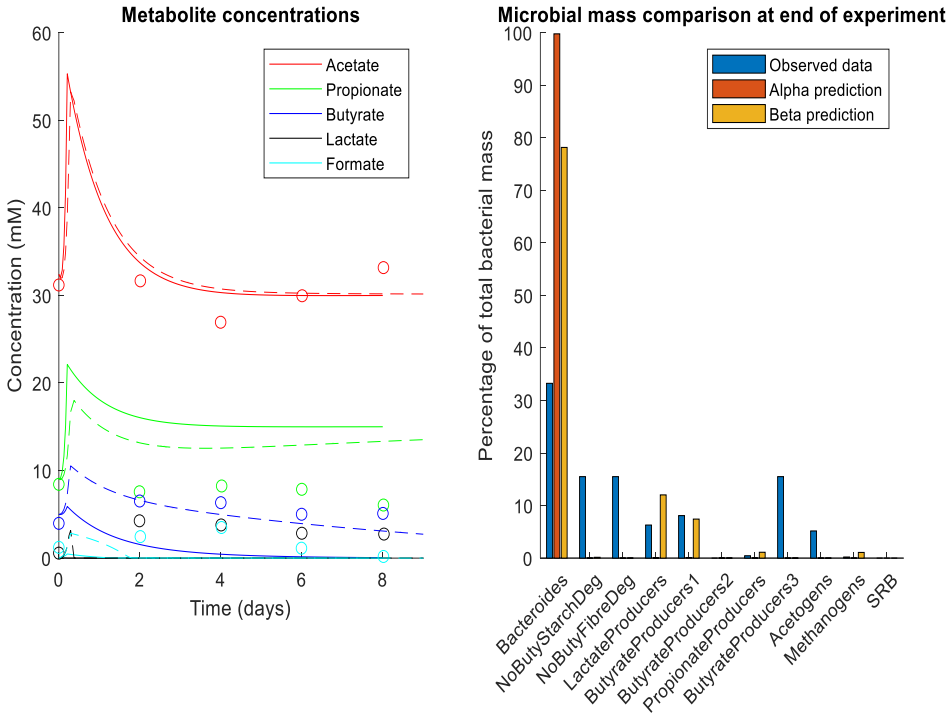

Figure 8.2. Model prediction compared with experimental data from Walker et al. (2005) for continuous culture of a faecal microbial community (Donor 2) on a medium containing 0.1% w/v peptide. The solid lines in the metabolite concentration panel display the model prediction using the Alpha parameter set, whereas the dashed lines display the prediction using the Beta parameter set.

Under low peptide conditions (Figure 8.2) the model prediction for acetate concentration was within 5 mM of the experimental values throughout the experiment using both parameter sets. However, the model predicted all other metabolites poorly, with the exception of the butyrate prediction obtained using the Beta parameter set, which was accurate to within 3 mM throughout the experiment. While the model correctly predicted that the Bacteroides MFG was also the dominant MFG in the low peptide case, it predicted more than double the Bacteroides relative abundance that was observed experimentally. While the model was able to correctly predict increases in the relative abundance of the LactateProducers and ButyrateProducers1 MFGs using the Beta parameter set, this was not possible using the Alpha parameter set.

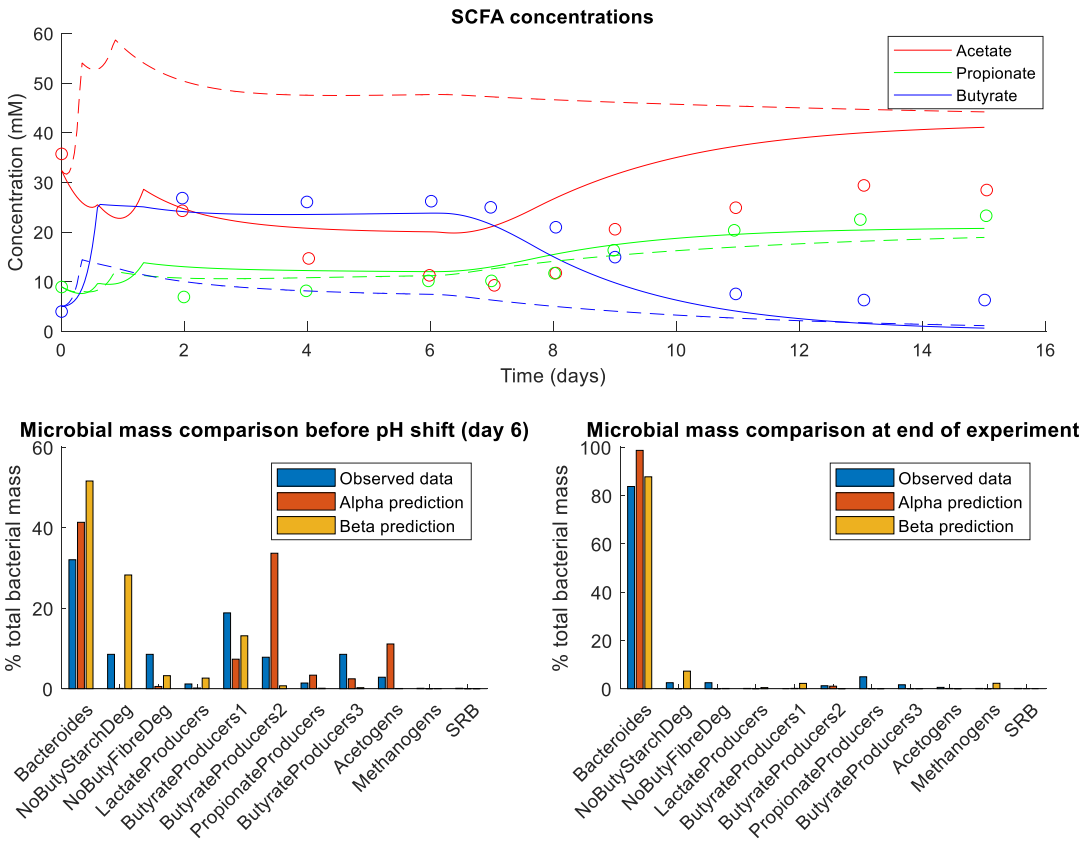

Figure 8.3. Model prediction compared with experimental data from Walker et al. (2005) for continuous culture of a faecal microbial community (Donor 1) on a medium containing 0.6% w/v peptide. A pH shift from pH 5.5 to pH 6.5 was gradually enacted between days 6 and 8. The solid lines in the short chain fatty acid concentration panel display the model prediction using the Alpha parameter set, whereas the dashed lines display the prediction using the Beta parameter set.

Data were also published for continuous culture of faecal samples with a pH shift added to the experiment. Figures 8.3 and 8.4 display the model predictions compared to these data, which were performed with faecal samples from different donors. In both experiments, the population was more evenly distributed between MFGs before the pH shift, after which the Bacteroides MFG dominated both cultures. The model captured this trend qualitatively, although quantitatively the predicted proportions did not match those observed experimentally.

For the SCFA concentrations, the mean bias values for the model prediction of each measured SCFA using the Alpha parameter set demonstrated the high quality of model fit to these data (see Table 8.1). However, using the Beta parameter set, acetate was overpredicted and butyrate underpredicted, without the dramatic change in the concentrations of these SCFAs that was observed experimentally after the pH shift.

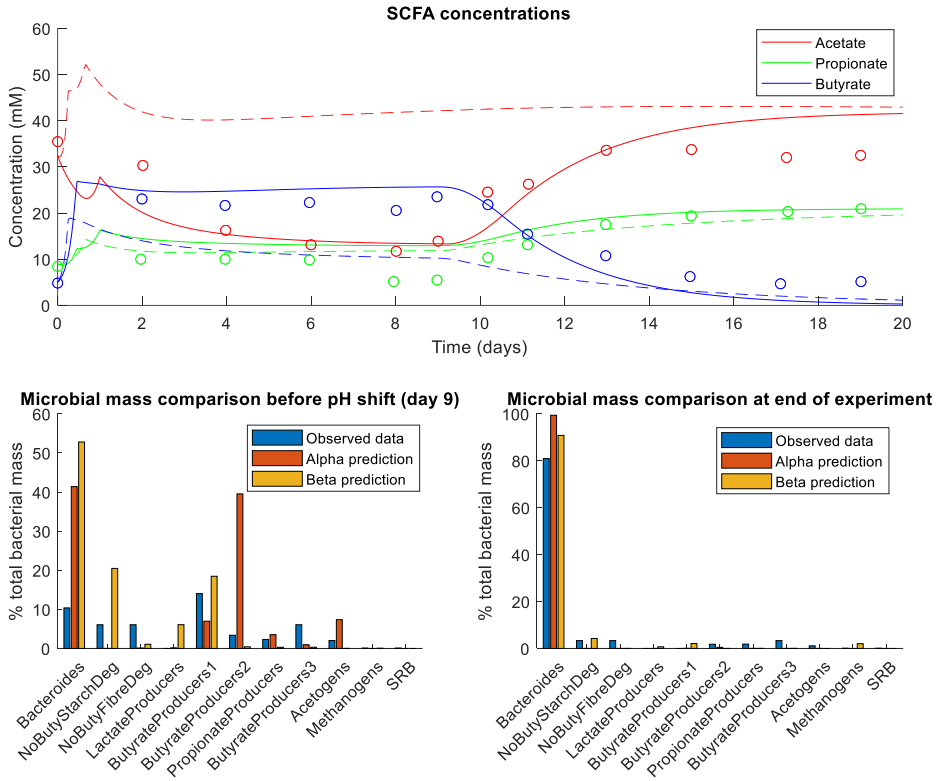

Figure 8.4. Model prediction compared with experimental data from Walker et al. (2005) for continuous culture of a faecal microbial community (Donor 2) on a medium containing 0.6% w/v peptide. A pH shift from pH 5.5 to pH 6.5 was gradually enacted between days 9 and 11. The solid lines in the short chain fatty acid concentration panel display the model prediction using the Alpha parameter set, whereas the dashed lines display the prediction using the Beta parameter set.

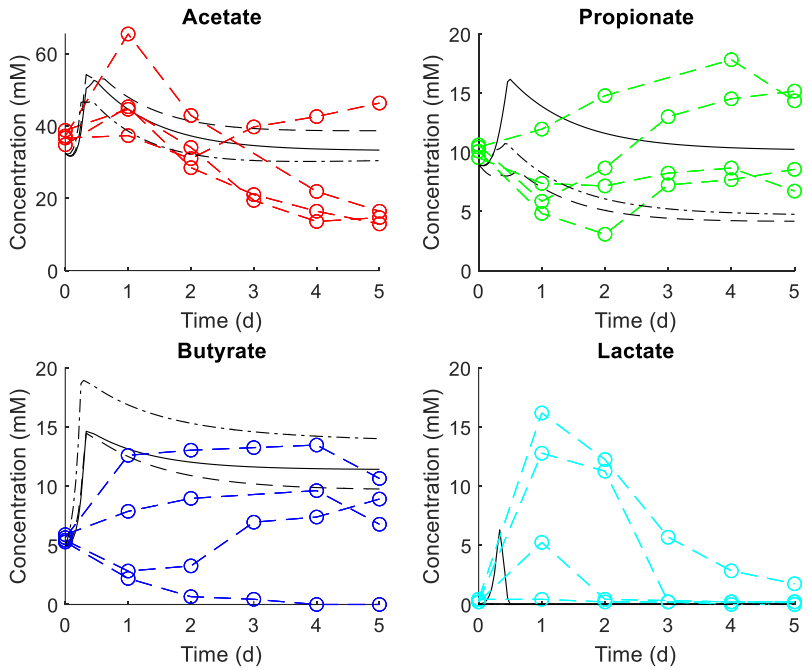

Figure 8.5. Model predictions (black lines) for short chain fatty acid production compared to experimental data (coloured lines) from Belenguer et al. (2011) for faecal cultures at pH 5.5 of faecal samples from four adult donors. The Beta parameter set was used in this instance. Note that it was not possible to convert the data on the initial inoculum to microPop microbial functional groups, thus three example faecal inocula derived from data in Walker et al. (2005) are shown instead (black lines).

The next data set to which the model was compared was that of Belenguer et al. (2011). These authors also performed continuous cultures of faecal communities at differing pH levels and recorded the SCFA production of the cultures. Faecal samples from four adults were cultured at either pH 5.5 or pH 6, with time-course SCFA concentrations recorded, alongside initial and final abundance of certain genera and species. Unfortunately, insufficient data was recorded for the microbial community makeup to allow conversion of this data to microPop MFGs. Instead, data from three faecal samples published in Walker et al. (2005) were used as example initial MFG concentrations (Appendix C, Table C8). Figure 8.5 shows the predictions of the model using the Beta parameter set compared to the pH 5.5 culture data and Figure 8.6 shows the predictions of the model using the Alpha parameter set compared to the pH 6 culture data. The predictions of the alternate parameter set at each pH value are included in Appendix C (C7).

While the example inocula used by the model may be different to those used in the experimental work, the model predictions for SCFA concentrations were mostly within the range observed experimentally. Major deviations from the experimental data were seen for acetate: overpredicted using both parameter sets at pH 6 (Figures 8.6 & C2, Appendix C), and underpredicted by the Alpha parameter set at pH 5.5 (Figure C1, Appendix C). Butyrate was overpredicted at pH 5.5 using the Alpha parameter set (Figure C1, Appendix C), but otherwise both butyrate and propionate were well predicted. Under both pH conditions, lactate was predicted by the model to remain below the experimental limit of detection using the Alpha parameter set and showed only an initial burst of less than 7 mM within the first 12 hours using the Beta parameter set. Some experimental fermentations in Figures 8.5 and 8.6 showed lactate concentrations reaching around 15 mM after 24 hours of culture, which could not be captured by the model. It is interesting to note the pronounced differences between propionate and butyrate dynamics in the model predictions given different initial MFG concentrations. However, these differences are found only temporarily: when run for several hundred days, the model predictions for each of the three initial conditions used here converged to identical values (data not shown).

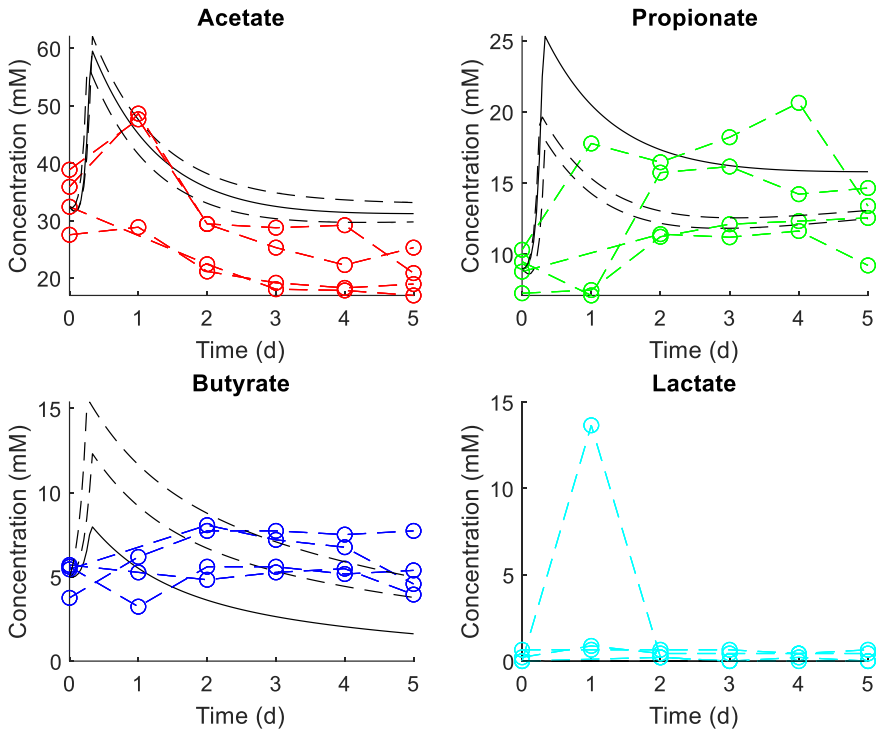

Figure 8.6. Model predictions (black lines) for short chain fatty acid production compared to experimental data (coloured lines) from Belenguer et al. (2011) for faecal cultures at pH 6 of faecal samples from four adult donors. The Alpha parameter set was used in this instance. Note that it was not possible to convert the data on the initial inoculum to microPop microbial functional groups, thus three example faecal inocula derived from data in Walker et al. (2005) are shown instead (black lines).

The final data set used for comparison was that of Payne et al. (2012a). These researchers used three-compartment sequential fermenters, inoculated with faecal material from an obese (experiment A) and a normal-weight (experiment B) child, to study the impact of high-energy (HE), normal-energy (NE) and low-energy (LE) diets on the profile of the microbiota and the SCFAs produced.

For the first compartment in experiment A (Figure 8.7), with the obese child's faecal material, total SCFA concentrations were predicted with good accuracy but low precision (see Table 8.1). Acetate concentrations were underpredicted using both parameter sets while butyrate was overpredicted. Propionate concentrations during continuous fermentation remained between 2-4 mM, while the model predicted monotone decreasing propionate concentrations throughout continuous culture. The predicted total SCFA concentration was similar to those from the observed data, although did not display the fluctuations observed within each dietary treatment experimentally. Propionate was overpredicted for all media compositions in the latter two compartments.

Interestingly, the predictions for acetate and butyrate concentrations using the Beta parameter set appeared swapped compared to the experimental data: the model prediction for acetate concentration fitted the butyrate data accurately, and vice versa. A possible explanation for this is metabolism of acetate and production of butyrate by the ButyrateProducers1 MFG, the abundance of which was consistently overpredicted by the model in all compartments when using the Beta parameter set (Figure 8.8). For the Alpha parameter set, this relationship between acetate and butyrate was not present throughout the experimental data, but could be seen from 20 hours onwards in the latter two compartments (Figure 8.7). Using the Alpha parameter set, the ButyrateProducers2 MFG was consistently overpredicted (Figure 8.8), giving a similar possible explanation.

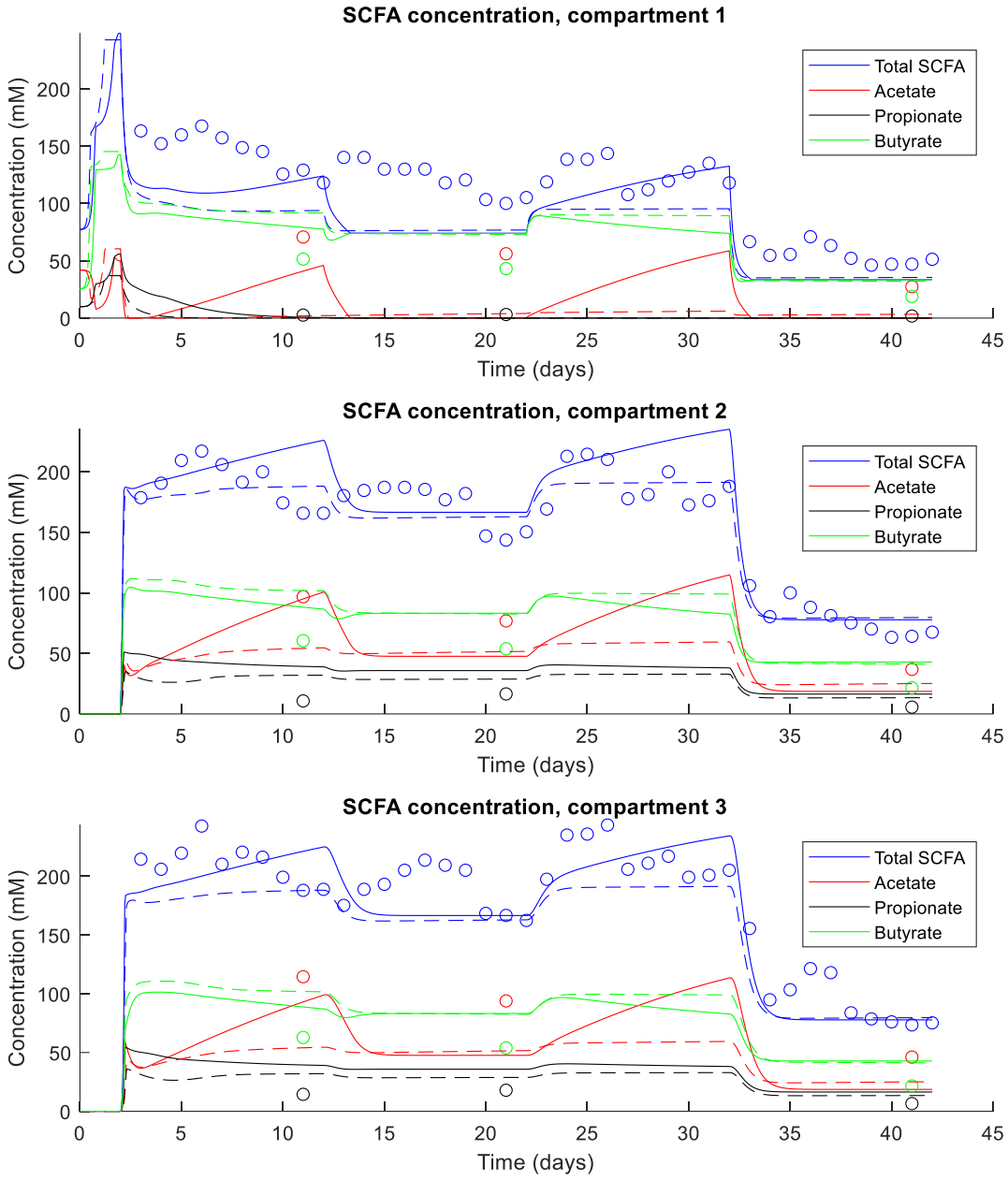

Figure 8.7. Short chain fatty acid concentrations in the three fermenter compartments over the course of the 42-day experiment of Payne et al. (2012a). This figure pertains to the A experiment, which was inoculated with faecal material from the obese child, run in batch mode with high-energy (HE) medium for 2 days, then switched to continuous fermentation. During continuous fermentation, the model was run in four 10-day slots with differing media, in the following order: HE, normal-energy, HE, low-energy. The solid lines display the model prediction using the Alpha parameter set, whereas the dashed lines display the prediction using the Beta parameter set.

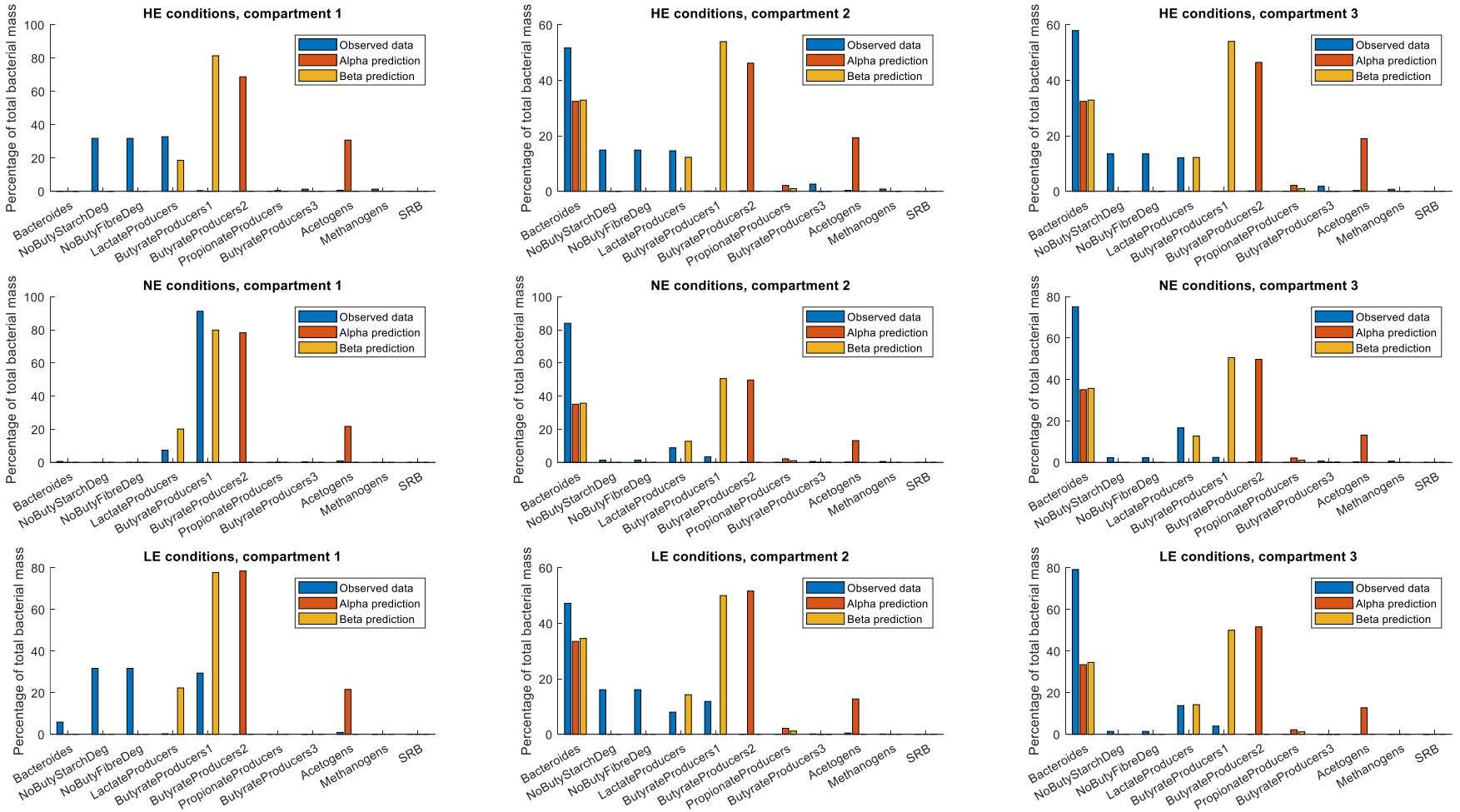

Figure 8.8. A comparison of observed and modelled microbial relative abundances in each compartment after 10 days of continuous fermentation under each medium in experiment A of Payne et al. (2012a). Observed data were measured with quantitative polymerase chain reaction and converted to microPop microbial functional groups as described in Appendix C (C4).

The SCFA results for experiment B (Figure 8.9), with the normal-weight child's faecal material, were comparable to those of experiment A. Propionate was predicted more accurately for experiment B (Table 8.1), but again an overprediction of butyrate concentration, with corresponding overprediction of butyrate-producing MFGs and underprediction of acetate, was seen in the latter two compartments.

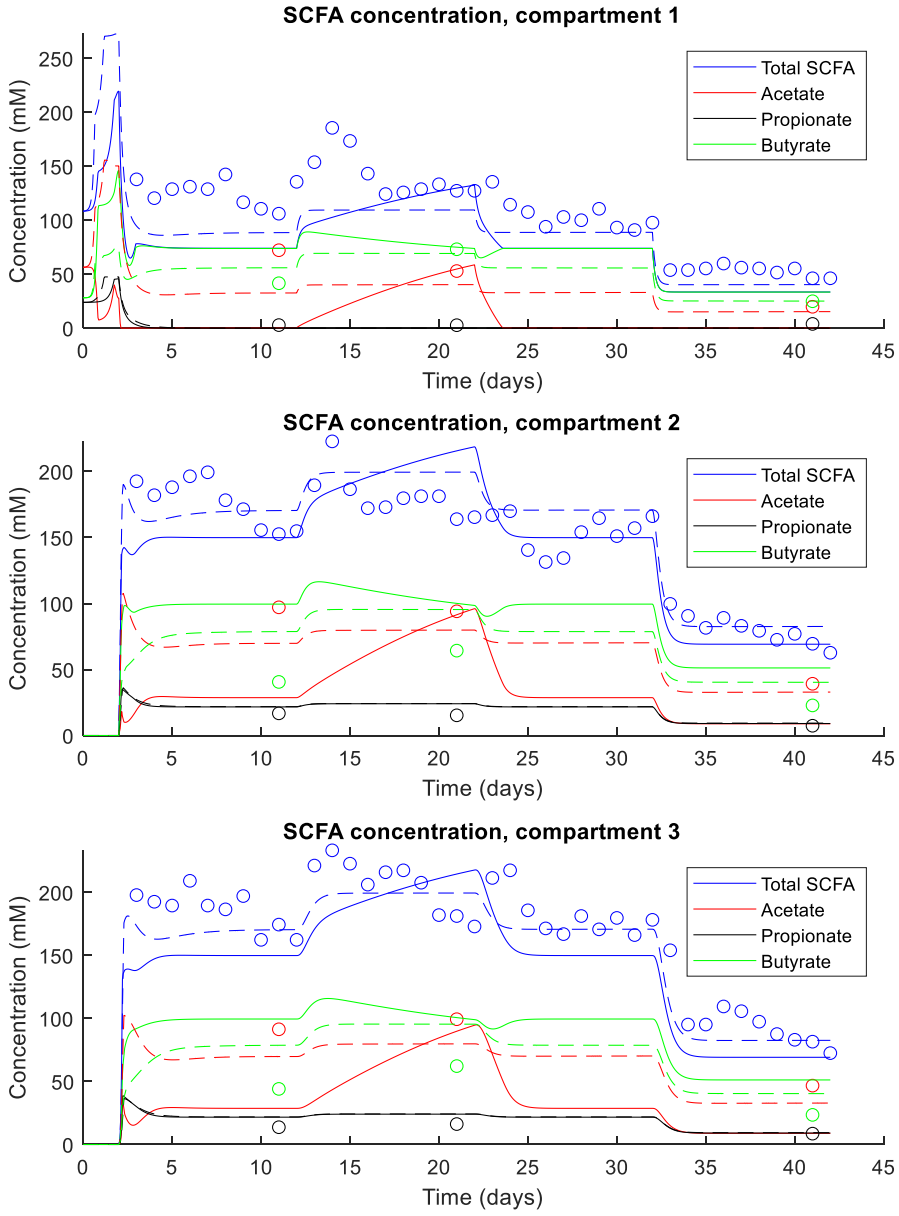

Figure 8.9. Short chain fatty acid concentrations in the three fermenter compartments over the course of the 42-day experiment of Payne et al. (2012a). This figure pertains to the B experiment, which was inoculated with faecal material from the normal-weight child, run in batch mode with high-energy (HE) medium for 2 days, then switched to continuous fermentation. During continuous fermentation, the model was run in four 10-day slots with differing media, in the following order: normal-energy (NE), HE, NE, low-energy. The solid lines display the model prediction using the Alpha parameter set, whereas the dashed lines display the prediction using the Beta parameter set.

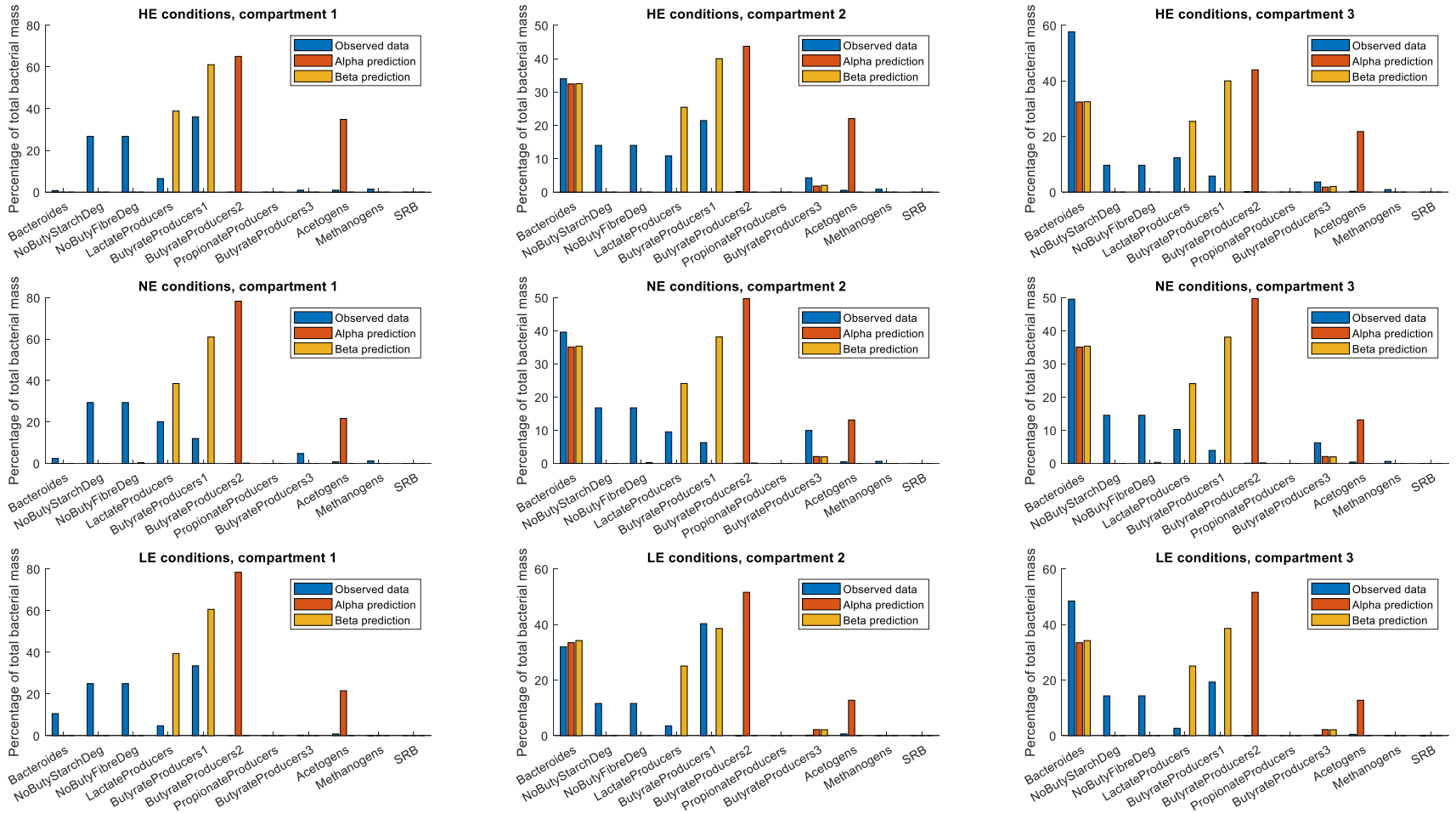

Figure 8.10. A comparison of observed and modelled microbial relative abundances in each compartment after 10 days of continuous fermentation under each medium in experiment B of Payne et al. (2012a). Observed data were measured with quantitative polymerase chain reaction and converted to microPop microbial functional groups as described in Appendix C (C4).

Table 8.1. Mean bias (mM) of the model fits to short chain fatty acid data sets using either the Alpha or Beta parameter sets. The mean absolute error (mM) is shown in parentheses where different to the absolute value of the mean bias

Walker et al. (2005) data set						
	Parameter set					
Figure 8.1	**Alpha**		**Beta**			
Acetate	10.6		10.9			
Propionate	2		0.7			
Butyrate	-4.8 (5.2)		-2.4 (2.8)			
Figure 8.2						
Acetate	0.7 (2)		1.1 (2.3)			
Propionate	6.4		4.6			
Butyrate	-3.9 (4.3)		-0.6 (1.1)			
Lactate	-2.8		-2.8			
Formate	-1.7		-1.7			
Figure 8.3						
Acetate	8.5 (9.2)		24.2 (24.9)			
Propionate	1.4 (2.5)		-0.1 (2.6)			
Butyrate	-3.4 (3.6)		-11.2 (11.4)			
Figure 8.4						
Acetate	<0.1 (4.1)		16.1 (16.6)			
Propionate	3		1.4 (2.4)			
Butyrate	<0.1 (2.6)		-7.6			
Payne et al. (2012a) data set						
	Compartment 1		**Compartment 2**		**Compartment 3**	
Experiment A (Figure 8.7)	**Alpha**	**Beta**	**Alpha**	**Beta**	**Alpha**	**Beta**
Total SCFAs	-27.5 (29.6)	-36.7	10.7 (20.1)	-3.6 (15.6)	-8.9 (20.7)	-23 (23.8)
Acetate	-37.7	-48.4	-16.4	-26.6	-31.7	-41.4
Propionate	-2.3	-2.5	19.5	13.7	17.6	11.8
Butyrate	24.3	27.8	26.1	29.9	25.5	29.2
Experiment B (Figure 8.9)						
Total SCFAs	-31.5	-24.8	-5.1 (20.1)	7.2 (16.5)	-24.9 (30.3)	-12.2 (17.2)
Acetate	-29.9 (31.2)	-18.9	-33.8	-16	-36.7	-18.4
Propionate	-3.1	-3.1	5.1	5.3	5.4	5.7
Butyrate	14.2	3.5 (6.1)	41	28.9	40.5	28.3

The SCFA predictions of the model were consistent between the two parameter sets, with the exception of the acetate predictions. Use of the Beta parameter set resulted in acetate dynamics that shifted rapidly but minimally to new steady state values after a dietary shift (Figures 8.7 & 8.9). In contrast, use of the Alpha parameter set resulted in large and continued increases in acetate concentration over the course of the HE diet. This was likely due to the increased relative abundance of the acetogen MFG seen in the use of the Alpha parameter set in all compartments under all diets,

but particularly large under the HE diet (Figures 8.8 & 8.10). This increase was not seen using the Beta parameter set.

The MFGs showing relative abundance of >10% were completely consistent between the simulations of the two experiments, demonstrating that diet rather than initial conditions was the major determinant of microbial profile in the model (Figures 8.8 & 8.10). However, this was not the case for the experimental data: the most abundant three MFGs determined from the observed data differed between the A and B experiments in eight of the nine measurements displayed in Figures 8.8 and 8.10 (LE conditions, compartment 1 was the only measurement that showed consistency between the two experiments). The most notable failings of the model displayed in these figures were its overprediction of the butyrate producing MFGs and the Acetogen MFG, and its inability to predict the high relative abundance of the NoButyStarchDeg and NoButyFibreDeg MFGs (which are capable of degrading resistant starch and NSP using differing pathways, with acetate rather than butyrate the SCFA produced).

No explicit data were available for the acetogen of the methanogen MFGs; these were simply calculated as a proportion of the total Firmicutes and total bacteria, respectively (Appendix C, C4). The SRB MFG was measured experimentally but showed a decrease from initial abundance in all cases but one: the third compartment on the LE diet, where modest increases of less than 1 $\log_{10}$ copies 16S rRNA gene g^{-1} were observed in both experiments. The model predicted a continuous decrease in the SRB MFG across all simulations, as the dilution rates of 6 d^{-1} in the first compartment and 3 d^{-1} in the latter two compartments were both greater than the maximum growth rate of the SRB MFG (2.78 d^{-1}), preventing population growth.

An important caveat to the MFG profile comparisons is that the quality of these comparisons is dependent on the assignment of experimental data to microPop MFGs, as described in Appendix C (C4). The distribution of qPCR data into MFGs was an approximation, based on similar work performed previously (Kettle et al., 2015). In simple terms, Figures 8.7-8.10 represent the quality of fit of an eleven-member microbial community model to an incomplete measurement of a microbial population that was then assigned to these eleven groups. Far more assumptions were necessary in the establishment of this comparison than were necessary for the SCFA data, therefore

the latter should be treated as the more reliable comparison between what was observed and what was simulated.

8.3.2 Simulation of the colonic microbiota

In order to study the colonic microbiota *in silico*, several adaptations were made to the original microPop structure, as detailed in the Methodology, Appendix C and illustrated in Figure 8.11. The adapted model is able to simulate the colon in two different ways: either as a series of separate compartments, representing specific regions of the colon, each with their own individual luminal conditions; or, as a continuous model in which the passage of a fixed bolus of digesta is modelled over time and space simultaneously. In the former setup, the model is run to steady state (usually after a simulation period of at least 20 days) to provide predictions, whereas in the latter setup, the model simulates the colonic dynamics over the course of a single transit. The two structures are referred to as the discrete and continuous versions of microPop:Colon, respectively.

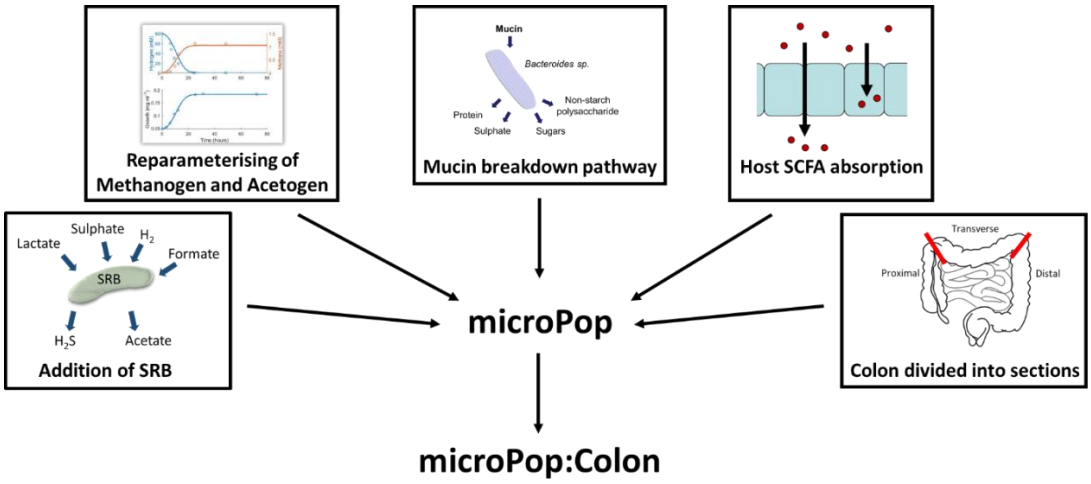

Figure 8.11. Diagrammatic explanation of the major adaptations made to microPop in the development of microPop:Colon. Note that division of the colon into sections was only performed for the discrete version of the model. See Methodology and Appendix C for a detailed description.

8.3.2.1 The discrete model

The discrete version of microPop:Colon simulates conditions in the proximal, transverse and distal colon. Selected initial dynamics from an example simulation are shown in Figures 8.12-

8.14, with steady state values obtained after 100 simulated days given in Table 8.2. The figures in this section display the results using the Alpha parameter set.

Figure 8.12 displays the changes in pH over the course of the first 10 days after model initiation. The model was initiated with the microbial community from Walker et al. (2005) used in the experiment shown in Figure 8.1 (Appendix C, Table C8), initially present only in the proximal compartment. Due to the high initial availability of substrates (Appendix C, Table C6), there was a phase of rapid population growth and metabolism during the first day after model initiation. The resulting production of SCFAs caused a rapid decrease in pH, most notable in the proximal and transverse compartments where the microbial population was at greatest abundance during this time. Due to a depletion of substrate, host buffering, SCFA absorption and washout, the pH climbed gradually thereafter, approaching steady state values between pH 6.3 and 7.2, as observed *in vivo* (Evans et al., 1988; Koziolek et al., 2015).

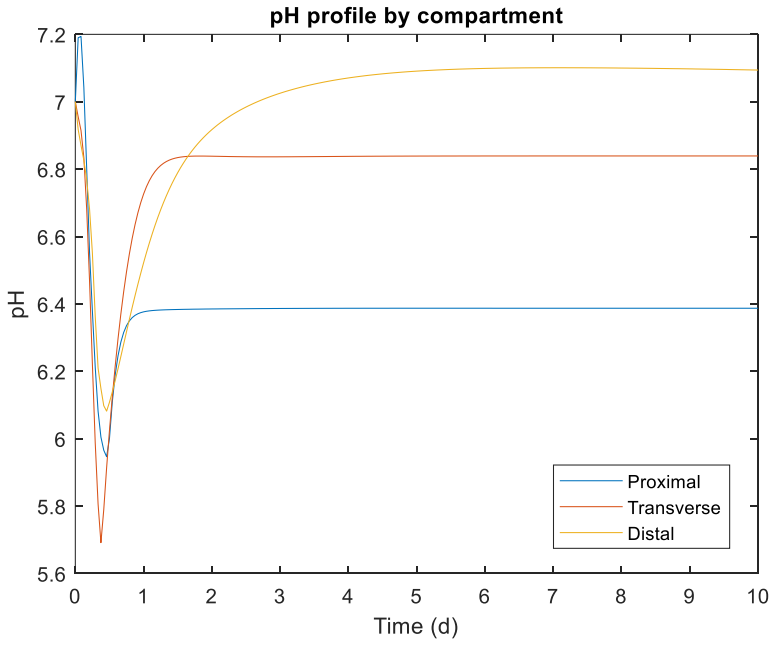

Figure 8.12. pH dynamics in each simulated compartment over the first ten days of the discrete simulation.

Figure 8.13 shows the concentration in the proximal compartment of the five most abundant MFGs over the first ten days after model initiation. The abundances of the remaining MFGs were too low to be distinguished in this plot. The Bacteroides MFG dominated this compartment from model initiation onwards, including at steady state (Table 8.2).

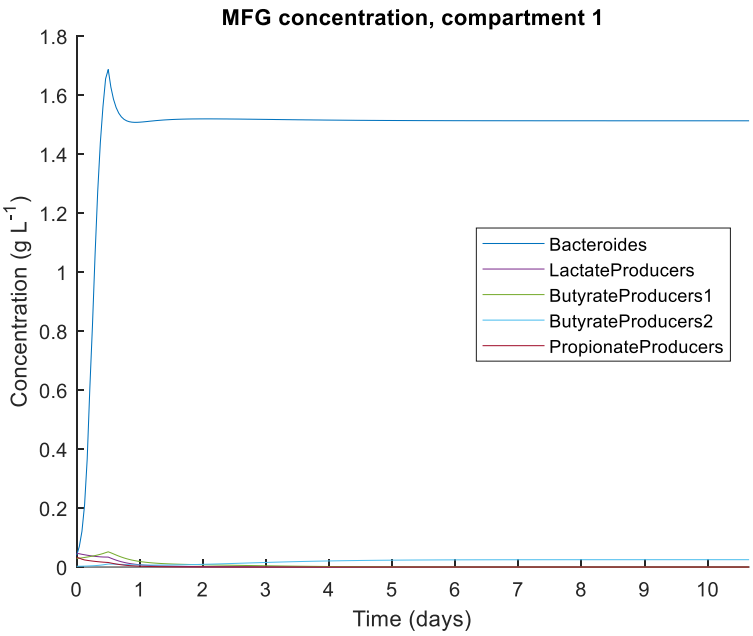

Figure 8.13. Dynamics of the five most abundant microbial functional groups in the proximal colon compartment over the first ten days of the discrete simulation.

As is clear from the pH dynamics shown in Figure 8.12, there was a drop in pH in all three compartments during the first day of simulation, due to a rapid increase in SCFA concentration. Figure 8.14 shows the change in SCFA concentration in the distal compartment over the first ten days of simulation. Increases here were the result of SCFA inflow from the transverse compartment, alongside SCFA production from what substrates were still available. SCFA removal was due to host absorption and washout.

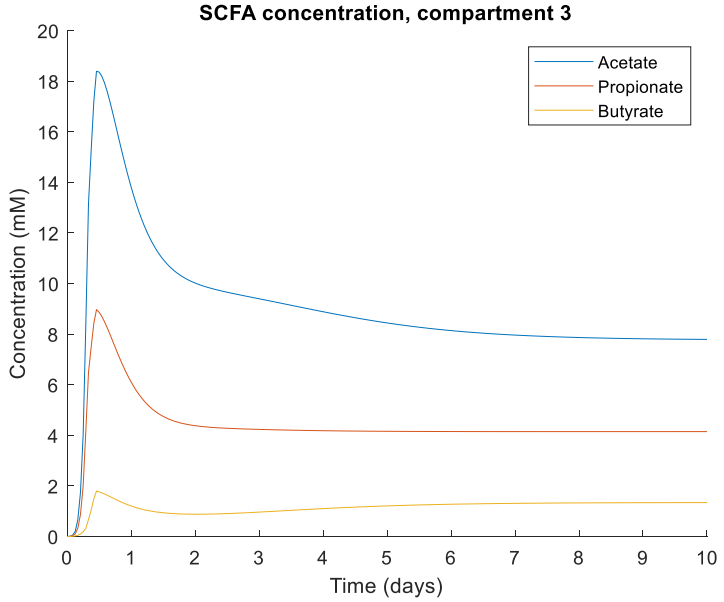

Figure 8.14. Short chain fatty acid dynamics in the distal colon compartment over the first ten days of the discrete simulation.

Under the conditions used for this simulation, the acetogen and SRB MFGs were washed out after small population increases over the first two days of the simulation. This was likely due to the dilution rates used for the simulation, which were high relative to the maximum growth rates of these MFGs, and competition for organic substrates between the acetogen MFG and other saccharolytic MFGs. The methanogen MFG was washed out of the proximal and transverse compartments, likely due to the lower pH, with no methanogen growth possible below pH 6 and limited growth below pH 6.9. However, the methanogen MFG achieved steady state concentrations in the order of 0.001 g L^{-1} in the distal compartment (Table 8.2). In comparing the results of the model with literature measurements and estimates for the colon in Table 8.2, what should be emphasised is the range of measured values present in the observational literature. microPop:Colon is deterministic, predicting a single value for each variable at each time point, and no stability analysis has been undertaken to establish what factors affect the predictions of the model, and to what degree.

The pH predictions of the model for each compartment were within 0.2 pH units of the literature measurements (Table 8.2). All SCFA concentration predictions of the model were lower than those measured in sudden death victims (Table 8.2; (Macfarlane et al., 1992)). This may be due to the substrate inflow rates, as a greater substrate inflow in the model resulted in higher SCFA concentrations (data not shown). Perhaps more important is the ratio of SCFAs, often stated as approximately 60:20:20 for acetate:propionate:butyrate *in vivo* (den Besten et al., 2013). The measurements from sudden death victims were comparable to this ratio (Table 8.2). The discrete model predicted a mean ratio across the three compartments of 63:32:5 using the Alpha parameter set, implying that acetate and propionate appear to have been overpredicted at the expense of butyrate. Remaining with the SCFA dynamics in the colon, absorption of these metabolites by the host was underpredicted by the model. The absorption parameters were calculated from perfusion studies rather than observational research; thus, the rate of absorption may be greater under normal colonic conditions. Moreover, the rate of absorption in the model increases linearly with the colonic volume, which was assumed fixed for these simulations. An increased colonic volume induced by digesta influx would increase the rate of absorption in the model.

The model predicted at least 88% relative abundance of the Bacteroides MFG in all three compartments using both parameter sets (Table 8.2). While much evidence in the literature also predicts that this MFG should be the highly abundant, 88% is significantly higher than the 3-35% estimates available in the literature and was a failing of the discrete model (see Table 8.2 for literature references). The dominance of the Bacteroides MFG also resulted in minimal relative abundances of MFGs that share substrates with the Bacteroides MFG, which is all but the methanogen MFG and the SRB MFG. As such, the estimates of MFG relative abundance did not compare well with measurements in the literature (Table 8.2).

The predictions of the discrete model using the two parameter sets were similar in most respects. The most notable discrepancy between the two sets was in the SCFA ratio, with the model predicting higher ratios of acetate when using the Beta parameter set. Regarding MFG relative abundances, use of the Beta parameter set resulted in higher predictions for the LactateProducers and ButyrateProducers1 MFGs, whereas use of the Alpha parameter set resulted in higher predictions for the ButyrateProducers2 MFG.

Although the pH profile predicted by the model was representative of *in vivo* data, the low SCFA concentrations, low SCFA absorption and the dominance of all colonic sections by the Bacteroides MFG mean that substantial changes were required in order to reflect the colonic environment. One major assumption made in the use of the discrete model was that the steady state values of the model would give the best prediction of *in vivo* conditions. The entry of digesta into the colon is not continuous and expulsion of faeces is periodic, in contrast to the model setup. Therefore, it is not feasible to expect that the variables predicted by the model at steady state will remain at this state *in vivo*. To challenge the steady state assumption, a continuous version of the model was developed.

8.3.2.2 The continuous model

To match the discrete model, a colonic transit time of 1 day was chosen for the continuous model. This is convenient as it matches the model time unit of days, and is reflective of *in vivo* transit times (Koziolek et al., 2015; Wang et al., 2015). Digesta is assumed to progress continuously along the colon over time. The dilution rates calculated from volumes used for the discrete model allowed

calculation of mean residence times in each colonic region in the model: approximately 14% (3.4 hours) for the proximal colon, 32% (7.7 hours) for the transverse colon and 54% (12.9 hours) for the distal colon. Therefore, the model estimates for each region were taken at 3, 10 and 24 hours. The concentration of inflowing substrates was set at one third of the daily influx for the discrete model, assuming this represents one of three daily meals. The continuous secretion of mucins and bicarbonate by the host was also set at one third of their daily value. The initial microbial population was again taken from Walker et al. (2005), as for the discrete model. The estimates of the model at the regional time points are given in Table 8.2 for both the Alpha and Beta parameter sets. The figures in this section show the predictions of the model using the Beta parameter set. It should be noted that these set time points are predominantly for comparison with the predictions of the discrete model; the continuous nature of this version of the model means that the colonic section has no impact on model predictions.

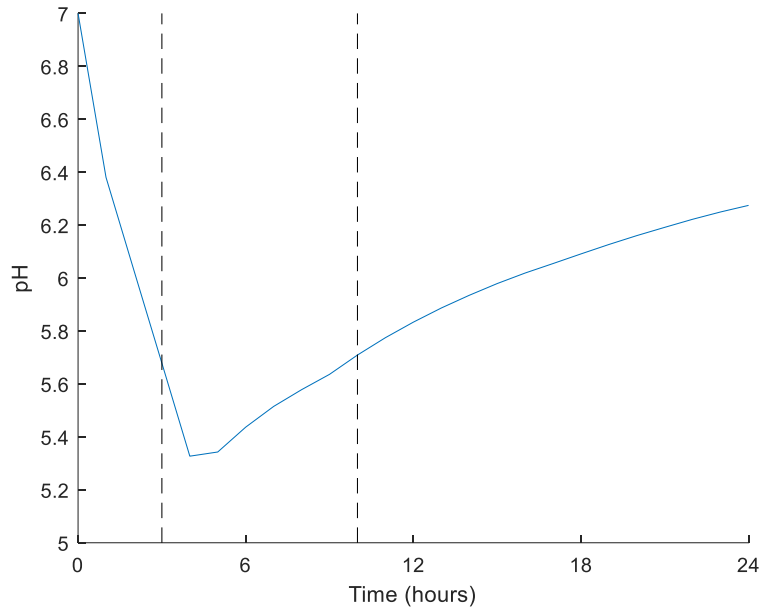

Figure 8.15. pH dynamics over a day of colonic transit simulated with the continuous model. The dashed lines display the time points at which values are taken for comparison to the proximal and transverse estimates of the discrete model in Table 8.2; the final value is taken as the estimate for the distal colon.

The pH profile followed the expected pattern established by the discrete model: there was a rapid initial decrease in pH caused by microbial production of SCFAs, which was followed by a more gradual return towards neutral pH caused by SCFA absorption and bicarbonate secretion (Figure 8.15). However, the pH did not return to neutrality during the 24 hours of simulation, finishing at pH 6.32 using the Alpha parameter set and pH 6.27 using the Beta parameter set. This is

substantially lower than the distal colonic pH estimates found in the literature (Table 8.2), perhaps reflecting inaccuracies in the bicarbonate buffering aspect of the continuous model.

As shown in Figure 8.16, the five MFGs showing the greatest population growth were identical to those shown in Figure 8.13 for the discrete model. The remaining MFGs attained population sizes too small to be distinguished in this plot. There was a more even distribution of MFGs in the continuous model predictions using either parameter set than was seen using the discrete version of the model. The MFG relative abundance values from the continuous model were similar when using the Alpha or Beta parameter sets, with the exception of the Bacteroides and LactateProducers MFGs. The Bacteroides MFG attained 42-48% relative abundance throughout transit when using the Alpha parameter set compared to the LactateProducers 20-21%, whereas these values were reversed when using the Beta parameter set, with Bacteroides relative abundances of 24-27% and LactateProducers relative abundances of 36-39% (Table 8.2).

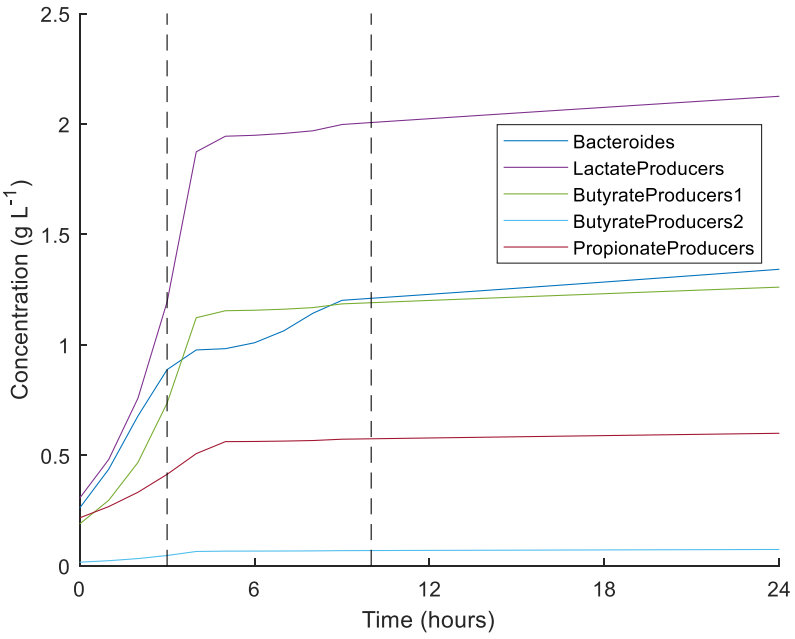

Figure 8.16. Dynamics of the five most abundant microbial functional groups over a day of colonic transit simulated with the continuous model. The dashed lines display the time points at which values are taken for comparison to the proximal and transverse estimates of the discrete model in Table 8.2; the final value is taken as the estimate for the distal colon.

The continuous model predictions for SCFA concentrations were similar in their dynamics to the steady state predictions of the discrete model, although higher maximum concentrations were achieved by the continuous model (Figure 8.17). Use of the Beta parameter set resulted in higher

acetate concentrations than did the Alpha parameter set, and also an SCFA ratio more similar to that observed *in vivo* (Table 8.2). Once again, the SCFA concentrations were substantially lower than the literature estimates for these values.

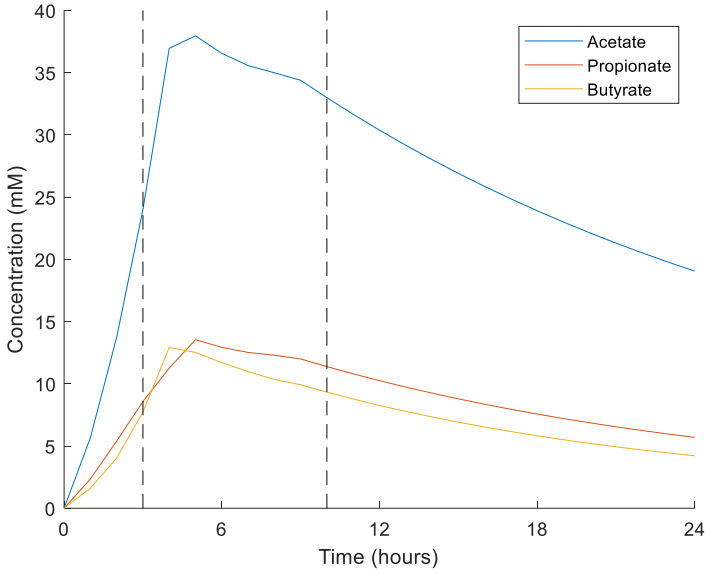

Figure 8.17. Short chain fatty acid dynamics over a day of colonic transit simulated with the continuous model. The dashed lines display the time points at which values are taken for comparison to the proximal and transverse estimates of the discrete model in Table 8.2; the final value is taken as the estimate for the distal colon.

Absorption of SCFAs was greater using the continuous model than the discrete model, with two thirds of the available SCFAs being removed from the colon by the host during transit. However, this was still less than the 95% absorption rate stated in the literature (den Besten et al., 2013).

Overall, each of the four model runs analysed here (the discrete and continuous models with each of the two parameter sets) gave the best predictions of the four for some aspects of the comparison to literature values in Table 8.2. However, the superiority of the discrete model was only seen for predictions of pH compared to literature data. The SCFA concentration and absorption predictions were poor, and the domination of all colonic sections by the Bacteroides MFG meant that little could be drawn from the microbial side of the model. Contrastingly, the continuous version of the model, while predicting lower pH values, was more accurate in predicting SCFA concentrations, absorption and the relative abundance of MFGs.

The consistent underprediction of SCFAs by each of the models would be remedied by a greater concentration of protein, NSP and resistant starch entering the colon (data not shown).

However, none of the model runs were able to achieve predictions for the NoButyStarchDeg and NoButyFibreDeg MFGs within an order of magnitude of the observed relative abundances, making this the only consistent failing of the model that could not be explained by insufficient substrate availability. Since these MFGs were also underpredicted in the comparisons to experimental data in section 8.3.1, the accuracy of the parameter values for these MFGs likely requires further investigation.

Table 8.2. Comparison of simulation predictions from the discrete and continuous microPop:Colon models. Colour coding represents: proximal, transverse and distal regions of the colon, while black text represents the total value

		Discrete model (values at 100 hours)		Continuous model (values at set time points)		Literature data	Reference
		Alpha	**Beta**	**Alpha**	**Beta**		
pH		**6.39** **6.84** **7.06**	**6.39** **6.84** **7.10**	**5.68** **5.78** **6.32**	**5.68** **5.71** **6.27**	6.37, 6.61, 7.04 (66 non-fasted subjects) 4.9/5.8, 6.2/5.7, 6.7/6[a] (2 recently deceased subjects) Mean 6.5, range 5-8 (20 fasted subjects)	Evans et al. (1988) Macfarlane et al. (1992) Koziolek et al. (2015)
SCFA concentrations (mM)	Acetate concentration	**15.4** **11.7** **7.8**	**15.9** **12.9** **11**	**23.1** **26.7** **15.3**	**24** **33** **19.1**	97.5/98 [ab] 78.4/74.6 [ab] 53.8/50.7 [ab]	Macfarlane et al. (1992)
	Propionate concentration	**7.6** **5.7** **4.1**	**7.5** **5.7** **4.4**	**13.6** **15.2** **7.2**	**8.6** **11.4** **5.7**	34.5/30 [ab] 26.7/28.5 [ab] 17.9/19.2 [ab]	Macfarlane et al. (1992)
	Butyrate concentration	**0.3** **0.6** **1.3**	**0.2** **0.2** **0.4**	**5.6** **8.1** **3.9**	**7.7** **9.3** **4.2**	41.5/36 [ab] 35.8/32.1 [ab] 16.4/25.8 [ab]	Macfarlane et al. (1992)
SCFA ratio (Acetate: Propionate: Butyrate)		**66:33:1** **65:32:3** **59:31:10**	**67:32:1** **69:30:1** **70:28:2**	**55:32:13** **54:30:16** **58:27:15**	**60:21:19** **62:21:17** **66:20:14**	56:20:24/60:18:22 [a] 56:19:25/55:21:24 [a] 61:20:19/53:20:27 [a]	Macfarlane et al. (1992)
SCFA absorption (g d^{-1})	Acetate	2.11	2.56	4.54[d]	5.45[d]	95% (≃9.4 g d^{-1} total for Alpha discrete and ≃13 g d^{-1} total for Beta	den Besten et al. (2013)
	Propionate	1.63	1.66	3.64[d]	2.78[d]		

	Butyrate	0.43	0.15	2.81[d]	3.27[d]	discrete; (≃16.3 g d^{-1} total for Alpha continuous and ≃17.3 g d^{-1} total for Beta discrete) of total produced SCFAs	
	Total	4.17	4.37	10.99	11.5		
Microbial functional group relative abundance (%)[c]	Bacteroides	98 95 88	97 95 89	48 42 42	27 24 25	23 (mean value; Bacteroidetes) 11 (mean value; *Bacteroides*) 16, 35 (mean values using different techniques; Bacteroidetes) 26, 3 (mean values; lean, obese individuals; Bacteroidetes)	Arumugam et al. (2011) Rajilić–Stojanović et al. (2011) Rajilić-Stojanović et al. (2009) White et al. (2009)
	NoButyStarchDeg	<1e-10 <1e-10 <1e-10	<1e-10 <1e-10 <1e-10	0.2 0.1 0.1	0.2 0.2 0.2	4 (mean value; *Ruminococcus bromii*) 11, 27 (mean values; lean, obese individuals; *Ruminococcus*)	Abell et al. (2008) White et al. (2009)
	NoButyFibreDeg	<1e-10 <1e-10 <1e-10	<1e-10 <1e-10 <1e-10	0.1 0.2 0.2	0.2 0.2 0.2		
	LactateProducers	<1e-10 <1e-10 <1e-10	1.8 3.5 7	20 21 21	36 39 39	5 (mean value; Actinobacteria) 4 (mean value; Actinobacteria) 2, 5 (mean values using different techniques; Bifidobacteria) <1, 4 (mean values; lean, obese individuals; Actinobacteria)	Arumugam et al. (2011) Rajilić–Stojanović et al. (2011) Rajilić-Stojanović et al. (2009) White et al. (2009)
	ButyrateProducers1	<1e-10 <1e-10 <1e-10	0.9 2 4	16 19 19	22 23 23	3 (mean value; *Roseburia*) 4 (mean values; *Roseburia intestinalis*)	Arumugam et al. (2011) Kumari et al. (2013)
	ButyrateProducers2	2 4 11	<1e-10 <1e-10 <1e-10	2 2 3	1 1 1	5 (mean value; *Faecalibacterium*) 2 (mean value; *Faecalibacterium prausnitzii*)	Arumugam et al. (2011) Kumari et al. (2013)
	PropionateProducers	<1e-10 0.2 0.5	<1e-10 0.2 0.7	14 15 15	13 11 11	4, 4 (mean values using different techniques; Veillonella)	Rajilić-Stojanović et al. (2009)

	ButyrateProducers3	<1e-10 0.001 0.004	<1e-10 0.003 0.004	0.1 0.1 0.1	0.1 0.09 0.08	0.04 (mean value; *Eubacterium hallii*) 0.5 (mean value; *E. hallii*)	Engels et al. (2016) Kumari et al. (2013)
	Acetogen	<1e-10 <1e-10 <1e-10	<1e-10 <1e-10 <1e-10	0.04 0.05 0.05	0.04 0.03 0.03	Found in all regions of the colon, but abundance varies between regions and individuals (10^4-10^5 gene copies g^{-1} in mucosal biopsies). More abundant than methanogens and sulphate-reducing bacteria in faeces. 1 (mean value; *Blautia*)	Nava et al. (2012) Rey et al. (2010) Arumugam et al. (2011)
	Methanogen	<1e-10 <1e-10 0.06	<1e-10 <1e-10 0.01	0.05 0.03 0.04	0.06 0.06 0.2	Found in all individuals, but not found in all regions of each individual. Increased population size distally.	Nava et al. (2012)
	Sulphate-reducing bacteria	<1e-10 <1e-10 <1e-10	<1e-10 <1e-10 <1e-10	0.05 0.04 0.06	0.05 0.04 0.05	Found in all regions of the colon, but abundance varies widely between regions and individuals (10^2-10^9 gene copies g^{-1} in mucosal biopsies) 0.02 (mean value; *Desulfovibrio*) 0.1, 0.03 (mean values; lean, obese individuals; *Desulfovibrio*)	Nava et al. (2012) Bartosch et al. (2004) White et al. (2009)

[a]Data from Macfarlane et al. (1992) are displayed as Subject1/Subject 2, for the two subjects analysed.
[b]mM concentrations were calculated from mmol kg^{-1} reported data assuming 1 kg faecal contents has approximately 1 L volume (Penn et al., 2018).
[c]Literature data for relative abundance were obtained from studies on faecal samples using a wide variety of techniques and various groups of faecal donors. Unless otherwise stated, the data are for healthy adults and the mean value for the indicated taxonomic group has been included, which corresponds to the assigning of microbial functional groups to taxa in Kettle et al. (2015). These values are included for comparison only and should not be interpreted as representative means for all individuals.
[d]Values from the model were tripled to give the daily total, since only one third of the daily metabolite influx into the colon was modelled using the continuous model.
SCFA: short chain fatty acid.

8.3.2.3 Investigation of varied colonic sulphate availability

The microPop:Colon model was developed for use as a tool to quickly provide predictions on the effect of changes in substrate availability on colon dynamics. As the interest was in the hydrogenotroph dynamics in the colon, it was considered what the role of inflowing sulphate quantity was on the SRB population and SRB H_2S production in the colon. Previous research has shown both positive and neutral results of increased dietary sulphate increasing the colonic SRB population (Christl et al., 1992; Lewis and Cochrane, 2007; Rey et al., 2013; Yao et al., 2018; Dostal Webster et al., 2019). The hypothesis here was that changes in sulphate inflow would have a negligible influence on SRB population size and H_2S production in the model. The reasoning was that the sulphate released during mucin metabolism would be in excess of what can be metabolised by the small SRB MFG population in the colon, therefore sulphate would not be limiting and additional sulphate would have no effect. To investigate this, microPop:Colon was run with varied sulphate inflow concentrations and transit times.

The discrete and continuous variations of the microPop:Colon model were run as described in the previous sections, using the Alpha parameter set and with sulphate inflow the only substrate factor that was altered. Conditions compared were as follows: zero sulphate (NoS), where sulphate may be derived from metabolite cross-feeding on the breakdown products of mucin only; low sulphate availability (NormS), for which the results of the previously performed model runs with 0.86 g L^{-1} d^{-1} sulphate available were used; and high sulphate availability (HighS), where the sulphate availability was increased by a factor of 10 from the NormS case. To investigate the influence of transit time on the results, colonic transit times of one day (as investigated previously), two days and four days were simulated.

Using the discrete model, variations in sulphate resulted in a maximum concentration change of less than 0.02% for those MFGs that avoided washout, including the hydrogenotrophs. Steady state differences of less than 10^{-4} g L^{-1} were observed for all metabolite concentrations, with the exception of sulphate, which increased with increasing influx levels.

The results of the continuous model showed greater differentiation between sulphate and transit time conditions (Table 8.3). Changes in the non-hydrogenotrophic MFGs and the acetogen

MFG between sulphate influx levels were minimal, as were changes in SCFA concentrations. The concentration of the methanogen MFG increased under the NoS influx level and decreased under the HighS influx level, the magnitude of this change increasing with increasing transit times. Conversely, the concentration of the SRB MFG decreased by at least 19% under the NoS influx level and increased by 1-2% under the HighS influx level, with H_2S concentration changes following the SRB trend.

Thus, the discrete and continuous models were not consistent in their predictions on the effect of varied sulphate influx on the SRB MFG. The discrete model predicted washout of the SRB MFG under all conditions simulated, whereas the continuous model predicted that increased sulphate would result in incremental increases in SRB and H_2S concentrations, while removal of sulphate inflow would result in substantial decreases in both these quantities.

Table 8.3. Summary of changes in microbiota and metabolite concentrations with varied sulphate influx and transit times in the continuous model. Percentage changes to one significant figure compared to the results under normal sulphate conditions are shown, after the full transit time

Colonic transit time	**1 day**		**2 days**		**4 days**	
Sulphate influx	**NoS**	**HighS**	**NoS**	**HighS**	**NoS**	**HighS**
Non-hydrogenotrophic MFGs	<0.02	<1e-3	<0.02	<2e-04	<0.01	<3e-04
Acetate	-5e-03	+1e-04	-4e-03	+1e-06	-3e-03	+7e-05
Propionate	-2e-03	+3e-05	-4e-04	+1e-05	+8e-04	-1e-04
Butyrate	-6e-03	+1e-04	-3e-03	+5e-05	+2e-04	-9e-06
Acetogen MFG	+0.04	-1e-3	+0.04	-8e-04	+0.01	+2e-04
Methanogen MFG	+0.7	-0.03	+3	-0.2	+10	-0.7
SRB MFG	-19	+1	-25	+2	-25	+2
H_2S	-39	+2	-35	+3	-28	+2

HighS: high sulphate availability. MFG: microbial functional group. NoS: zero sulphate availability. SRB: sulphate-reducing bacteria.

8.4 Discussion

The modelling work described here builds on the work of Kettle et al. (2015), developing and applying the microbial community model microPop (Kettle et al., 2017) for the study of the human colonic microbiota. Several features were added to the model, encompassing both human and microbial metabolites and functions. The increased attention given to hydrogen cross-feeders in

this work allows the model to provide predictions that are useful in the analysis of these microbes and their influence on human nutrition and health.

Validation of the developed model against *in vitro* faecal fermentation data was repeated for data sets originally considered by Kettle et al. (2015), followed by further validation against independent data sources. The number of sources used was limited by the requirement for time-course measurements of SCFA concentrations, detailed *in vitro* study design information, and time-course microbial population data where possible. However, the three sources and eight independent experiments used allowed for comparison of the model predictions against microbial data for the majority of MFGs in the model, and against concentration data for five microbial metabolites, namely acetate, butyrate, propionate, lactate and formate.

The accuracy of the model predictions varied both within and between sources, as well as between model parameter sets. Overall, no clearly superior parameter set was established from the validation runs: while the Beta parameter set of Wang et al. (Under review) appeared superior to the original Alpha parameter set of Kettle et al. (2017) in most cases, its poor performance in the pH shift experiments of Walker et al. (2005) prevents its recommendation as the more accurate parameter set for all cases. A similar conclusion was reached in the microPop:Colon simulations: predictions of the model using either parameter set were similar, with similar flaws. In the future, it may be possible to derive a new parameter set, incorporating the latest knowledge of the MFGs, which shows better performance than both current parameter sets. Alternatively, it could be possible to select a parameter set based on knowledge of the specific strains in the inoculum to be simulated. However, this would make for individual-specific modelling, an avenue already under research using genome-scale reconstruction and COBRA techniques (see later in the Discussion).

The major difference between the two parameter sets is the pH preferences of each MFG, which are altered for every MFG except the acetogen MFG, and in some cases by as much as 0.95 pH units. As pH varies between 5 and 7.5 in the simulations of the *in vitro* experiments and for the microPop:Colon runs, this change has a strong effect on growth. For example, when using the Alpha parameter set, growth of the Bacteroides MFG is prevented at pH 5.5, whereas up to 60% of its maximum growth rate may be achieved at this pH value using the Beta parameter set. Moreover, substantial alterations to the maximum growth rate of the Bacteroides MFG on protein, NSP and

resistant starch, as well as smaller alterations to parameter values for other MFGs, further distinguish the predictions of the model between the two parameter sets. As these changes heavily influence the Bacteroides MFG, and due to the dominance of this MFG in many of the simulations detailed here, the differences between the model predictions are to be expected.

The original setting of parameter values in the Alpha set by Kettle et al. (2015) was performed either from monoculture experimentation or assumptions based on the literature. As a result of this use of monoculture parameters, the model inherently assumes that monoculture metabolic parameter values are also accurate in a co-culture environment. Experimental and modelling evidence in the literature both supports and opposes this assumption. The FBA model of Louca and Doebeli (2015) was able to predict the cross-feeding and evolutionary dynamics of two *E. coli* strains in co-culture based on monoculture metabolite flux measurements. Similarly, Van Wey et al. (2014) were able to accurately simulate the competitive and cross-feeding dynamics of several *Bifidobacterium* strains in co-culture with *B. thetaiotaomicron* using monoculture-derived parameter values. Contrastingly, both Pinto et al. (2017) and D'Hoe et al. (2018) found that their more complex colonic representative communities required at least co-culture data for the accurate prediction of consortia dynamics. Unfortunately, the derivation of parameter values for co-culture growth is challenged by the difficulty of successfully co-culturing multiple strains *in vitro* and extracting the contributions of each to net metabolite flux. However, technologies such as FBA (Orth et al., 2010) and COBRA (Thiele et al., 2013) show promise in the further analysis of this kind of interaction.

There are obvious limitations in assuming a single set of parameter values is representative of an entire functional group, similar to those of constructing a defined microbial community to be representative of the diverse colonic microbiota for *in vitro* or animal model studies: it is never completely known what functionalities are lost in the simplified system. Kettle et al. (2015) addressed the need for greater diversity of metabolic capabilities by running their model with multiple strains in each MFG, each of which had stochastically varied parameter values within a certain range. They found that this increased diversity also increased the overall biomass of an MFG under varying environmental conditions as the growth ability of the MFG was greater than that of any single strain. Stochastic variation within each MFG was not attempted with microPop:Colon, but would be a next step in the analysis of the model. While this would likely result in quantitative

changes in the relative abundance of many MFGs, it could be speculated that this variation would be unlikely to qualitatively change aspects such as the washout of hydrogenotrophs in the discrete model, or the overall dominance of the Bacteroides MFG seen in most of the simulations.

The major addition to the original microPop model described in this Chapter was the inclusion of the SRB MFG and the alterations to the modelling of the other hydrogenotrophic MFGs. A full comparison of the developed model with the original microPop model has not been presented here, mainly due to a lack of data around hydrogenotroph dynamics: none of the data sources used here measured all three hydrogenotrophic MFGs and their metabolites, nor were the experiments designed for the study of these MFGs. Importantly, the novel SRB MFG was washed out in all simulations in section 8.3.1, due either to an absence of sulphate or mucin (Walker et al. (2005) and Belenguer et al. (2011) data sets) or high dilution rates (Payne et al. (2011) data set), thus this MFG has a negligible effect on the model predictions. The changes made to the other two MFGs also have little effect due to the incremental nature of the changes and the low abundance of these MFGs. For example, when the predictions for the developed model shown in Figures 8.1 and 8.2 were compared to those of the original microPop version, the results were nearly identical, with the exception of the acetate and acetogen MFG predictions. The developed model predicted lower acetate concentrations in both simulations (mean bias of developed model: 10.6 mM and 0.7 mM for Figure 8.1 and 8.2 respectively; corresponding mean bias of the original model: 11.1 mM and 1.1 mM, respectively), likely due to a lower abundance of the acetogen MFG in the predictions of the developed model.

Another challenge faced by the creators of the original microPop model was in determining the initial abundance of the hydrogenotrophic MFGs. Kettle et al. (2015) determined the abundance of the acetogen MFG in faecal samples as a proportion of counts from two Firmicutes-targeting 16S rRNA probes, and the abundance of the methanogen MFG simply as a proportion of the total bacterial counts. The authors acknowledged that these approximations were flawed and suggested that abundances based on functional gene counts be used in future.

Figures 8.5 and 8.6 demonstrate that initial abundance is an important determinant of model outcome, particularly in the shorter simulations shown in Figures 8.1-8.6. As such, the approximations used here and by Kettle et al. (2015) for the Walker et al. (2005) data sets may give

inaccurate initial conditions for the model, potentially leading to inaccurate predictions. Similar approximations were used here for the initial abundances in the Payne et al. (2011) data set (Appendix C (C4)). While some of the probes used match the corresponding MFGs well (e.g. Bac303 probe for the Bacteroides MFG and Fprau645 for the ButyrateProducers2 MFG), others (e.g. acetogen, methanogen, NoButyStarchDeg and NoButyFibreDeg MFGs) are not as well targeted and must be considered 'best guesses'. The fact that the simulated abundances NoButyStarchDeg and NoButyFibreDeg MFGs frequently did not match the observed abundances in the experimental data may be a result of poor approximation between microbial data and MFGs. Data collected using 16S rRNA probes targeted to specific MFGs, or the use of functional gene counts suggested by Kettle et al. (2015), would improve the accuracy of these approximations.

Moving to microPop:Colon, the adaptations to the original microPop model required for representation of the human colonic environment were far greater than the alterations to the hydrogenotrophic MFGs. The incorporation of a mucin breakdown pathway, resulting in the release of sulphate, was included both to add an important substrate for the Bacteroides MFG and as a source of non-dietary sulphate for the SRB MFG. In a recent genomic analysis of human colonic microbes, the only microbes able to produce mucin-desulfating enzymes were of the Bacteroidetes phylum, with the exception of *A. muciniphila* (Ravcheev and Thiele, 2017). Numerous other species from other phyla were capable of degrading mucin polysaccharides, which is captured in microPop:Colon by the release of NSP and sugars as mucin breakdown products. *A. muciniphila* is not included in any of the MFGs modelled in microPop and would make a good addition to future versions of the model, as it has received much study in recent years due to associations with positive host health outcomes (see review by Ottman et al. (2017)). However, this species is also found at greatest abundances in the mucous layer of the colon, which is currently not explicitly modelled in microPop:Colon.

Previous models for colonic microbiota dynamics, such as Muñoz-Tamayo et al. (2010), have included compartments representing the mucous layer and shown different dynamics in this habitat. An important feature of the mucous layer is the ability of microbes to adhere to structures in the mucous, thus increasing their residence time in a particular region of the colon and generating a population distinct from that of the lumen (Macfarlane et al., 2011). The lower dilution rates

associated with the mucous layer could be important in the persistence and greater abundance of the slower growing MFGs, such as the hydrogenotrophs (Nava et al., 2012). As the mucous layer was absent from microPop:Colon, it should be considered a model for the luminal dynamics in the colon, rather than the entire colonic environment.

The inclusion of host SCFA absorption was a way in which the effect of the microbiota on the host could be quantified. The proportion of total SCFAs absorbed was consistently lower than that observed *in vivo*, which could have been caused by several factors. Firstly, the absorption parameter used in microPop:Colon was calculated using results from perfusion experiments; colonic absorption under normal conditions may take place at a different rate. Secondly, the absorption rate in microPop:Colon was dependent on either the volume of the colonic section (for the discrete model) or the volume of the modelled digesta (for the continuous version), with greater volumes resulting in greater SCFA absorption. Estimates of adult colonic volume in the literature vary widely, from the 3.02 litres used here (de Jong et al., 2007; Muñoz-Tamayo et al., 2010) to a fasting volume of as little as 0.5 litres (Pritchard et al., 2014), thus the volume estimate may be inaccurate and biasing the absorption rate.

Moreover, water is absorbed from the intestinal lumen as digesta passes along the colon (Debongnie and Phillips, 1978). This results in changes in metabolite concentration, digesta viscosity and volume. As water absorption was not included in the model, the effects of this dynamic on microbial and metabolite concentrations were not captured. Other models for the colon have included water absorption (Cremer et al., 2017), and this would be a good addition to future versions of the colonic model.

The SCFAs are not the only metabolites exchanged between the host and the colonic lumen. Of the many other metabolites exchanged, microPop:Colon also considered bicarbonate secretion by the host, and subsequent buffering of the colonic environment. This is one of the strengths of the model, as it allows for a more physiological representation of pH than would be possible if pH were set irrespective of the metabolic activity of the microbiota. However, it was challenging to find consistent estimates of colonic bicarbonate secretion in the literature. It is known that bicarbonate ions are exchanged for SCFAs at the colonic epithelium (Charney and Donowitz, 2005; Gennari and Weise, 2008), however a 1:1 exchange implemented in microPop:Colon was

insufficient to buffer the environment (data not shown). While this was partly due to low SCFA absorption, bicarbonate is also secreted in exchange for other ions, such as chloride (Charney and Donowitz, 2005; Gennari and Weise, 2008), therefore a greater influx was required. The technique used in the final model is a constant influx of bicarbonate throughout the colon based on measurements from perfusion experiments, which again may not be representative of normal colonic function.

Although the inclusion of pH in the model adds functionality, there is also potential for this to contribute to errors in the model predictions. If the pH value is incorrect, then this will influence the growth and metabolism of the modelled MFGs, resulting in variation in the production of pH influencing metabolites. This feedback mechanism should be considered in interpreting model results and should also be an area for future development and testing of the model.

Another aspect of the model that defies consistent estimation in the literature is transit time. Total colonic transit time was important for the continuous model, with sectional transit time required in the discrete model. For microPop:Colon, a mean transit time of 24 hours was chosen based on sources in the literature (Evans et al., 1988; Wang et al., 2015). However, other research on healthy individuals has found median colonic transit times as high as 61.5 or 72 hours, with individual transit times ranging from 14 to 132 hours (Arhan et al., 1981; Graff et al., 2001; Müller et al., 2020). Moreover, these transit times were inconsistent between subject groups divided by gender or by age (see Graff et al. (2001) and Wang et al. (2015) and references therein).

Transit time has also been shown as a determining factor in hydrogenotroph abundance (El Oufir et al., 1996; Lewis and Cochrane, 2007). Both these studies saw a negative correlation between methanogen abundance and SRB abundance, with the former seen at higher abundances with slower colonic transit. There is also some evidence that the presence of colonic methane can slow colonic transit (Pimentel et al., 2006). At present, microPop:Colon uses a fixed transit rate unaffected by other model variables, but it would be possible to include these interactions for the purposes of *in silico* scenario testing.

In microPop:Colon, a longer transit time would be expected to be beneficial to both the methanogen and the SRB MFGs, as the present dilution rates leave them growing close to or below the rate required to avoid washout. This would also be reflective of results in the literature, where

abundance of Archaea was associated with harder stools, indicative of longer transit times (Tigchelaar et al., 2016; Vandeputte et al., 2016). The washout status of the acetogen and SRB MFGs were unaffected by varied transit time in the discrete model, but the methanogen MFG achieved increased steady state concentrations in the transverse and distal compartments at the higher transit times investigated in section 8.3.2.3.

microPop:Colon predicted no increase in the SRB MFG concentration in the discrete model and only minimal increases in the continuous model with increased sulphate influx. This, alongside the inverse relationship between the SRB and methanogen MFGs in terms of population size in this investigation, suggests that competition between these MFGs for other substrates may be present. This competition could be for either hydrogen or formate, but was not seen to the same extent with the acetogen MFG, perhaps due to its additional ability to metabolise carbohydrates. Competition between the hydrogenotrophic MFGs has been postulated and investigated previously, as discussed in Chapter 2, but no consensus has yet been reached on the extent to which this occurs in the colon.

The microbial community in microPop:Colon was shown to vary from the profile seen *in vivo* (Table 8.2). However, substantial differences were seen between parameter sets and between the discrete and continuous models, despite identical initial abundances of each MFG. The specific profile of the microbiota, including hydrogenotrophs, has been repeatedly shown to vary widely between individuals and even within individuals over time (for example, Nava et al. (2012), David et al. (2014a), David et al. (2014b), Healey et al. (2017)), so it is not surprising that models for this complex population exhibit high variability. This variability could potentially be minimised given a reliable estimate of the initial MFG concentrations. Currently, microPop:Colon uses faecal abundance data as the proxy for the proximal colon, due to a lack of data on the proximal colonic population. However, the population at the beginning of the colon is known to differ from the faecal population: for example, the gradually increasing pH, a strong determinant of microbial growth in microPop, is known to decrease the Bacteroides:Firmicutes ratio in the proximal colon compared to its value in the distal colon and faeces (Flint et al., 2012). Therefore, it is not expected that the faecal abundance data used to initiate microPop:Colon is representative of the proximal colonic microbiota. However, this estimate has been used in the absence of more appropriate data, and the initialisation of microPop:Colon with an initial microbial population much lower than the carrying

capacity allows for the establishment of a population with a profile appropriate to the local environment.

Moreover, the initial spike in microbial growth at initialisation of the discrete model due to low initial MFG abundances and high substrate availability, is not reflective of the colonic microbiota. Neither is the constant addition of a fixed amount of substrate into the proximal compartment, as opposed to the inconsistent inflow that would be expected *in vivo*. These issues could again be solved with knowledge of the proximal colonic microbiota population profile, and any number of inflow variations could be introduced to the model for investigation.

In the future, it may be possible to use faecal abundance data to give an estimate of the proximal colonic population using microPop:Colon. Inverting the model, so that data such as faecal pH, MFG and metabolite concentrations are the input, could allow a reverse simulation or MCMC estimation to be conducted in which the proximal colonic population could be predicted, to within some degree of accuracy. Such a model would require rigorous validation of the current model against human data, as the prediction quality of the inverted model would be dependent on its accuracy in its current form.

There are a number of existing methods for modelling microbial dynamics in the colon. Animal and *in vitro* models allow for physical data to be obtained from environments approaching the complexity of the human colon, but face ethical, financial, sampling and system control challenges. *In vitro* intestinal models such as TIM-2 or the Simulator of the Human Intestinal Microbial Ecosystem (SHIME) are widely used and accepted methods for the study of the microbiome, but are further abstractions of the living environment (Venema and van den Abbeele, 2013). Mathematical models and *in vitro* models face some similar difficulties, but also some different challenges. As observed by Payne et al. (2012b), the difficulties in obtaining an inoculum that yields both repeatable and biologically representative results is extremely challenging. In the case of microPop, simulations with the same initial MFG conditions will always result in repeatable outcomes. However, both mathematical and physical models of the colon face the same difficulty of obtaining a proximal colon inoculum representative of the microbiota in this region. Further characterisation of the proximal colonic microbiota is needed to remedy this lack of knowledge.

Contrastingly to *in vitro* models, *in silico* models can be set up and run with minimal investment, often in a fraction of the time required for experimental work, with no constraints on usage, control or data sampling. The mathematical modelling section of Chapter 2 gave an overview of previous models for the colonic microbiome. Compared to these models, microPop:Colon has the advantage of both a discrete and continuous spatial representation of the colon, as well as the uncommon inclusion of dynamic pH. However, the model is lacking in its omission of the mucous layer and gaseous phase. The most important development made by microPop:Colon compared to previous models is its greater focus on the hydrogenotrophic MFGs.

Regarding the hydrogenotrophic MFGs in microPop:Colon, the continuous model allowed for better study of these microbes than the discrete model, due to the washout observed in the compartmentalised model. However, the continuous model cannot be chosen as the superior version before simulating the discrete version with longer transit times. As the high dilution rates appeared to be the deciding factor in the washout of the SRB and the acetogen MFGs, it would be interesting to perform a detailed comparison of the results of both the discrete and continuous models using transit times at the higher end of those observed *in vivo*.

There are a number of other variations to the model that could be implemented in the future. At present, microPop gives no consideration to food structure, focussing instead on grouping metabolites into broad groups, such as protein and resistant starch. Food structure, particularly that of carbohydrates, has been shown to be a determining factor in the microbes that are able to degrade a substrate (see review by Payling et al. (2020)). For example, resistant starch has been divided into four structure types, each of which increases the relative abundance of different genera in faecal fermentations, and subclasses within these types have also been shown to illicit different microbial responses. It is challenging to know where to draw the line on the specificity of substrates in microPop, as this must also match the specificity of MFGs able to degrade these substrates. For example, it would be meaningless to include the four resistant starch types as microPop metabolites if the Bacteroides MFG, of which only a subset would be able to degrade each type, were not correspondingly subdivided.

Another important subdivision of metabolites would be on the protein breakdown pathway, which does not include the release of H_2S from sulphated amino acids, an important

source of this molecule (Carbonero et al., 2012a; Yao et al., 2016; Yao et al., 2018). Currently, the SRB MFG is the only source of H_2S in microPop:Colon. Greater detail would allow for more realistic comparison of the model predictions to dietary sulphate intervention studies.

microPop:Colon assumes that the contents of the colon are all in the liquid phase, with no gaseous headspace. In reality, gas pockets exist in the colon (Murray et al., 2014). Mass transfer of metabolites will occur between the liquid and gaseous phases, and host metabolite absorption from the gaseous phase will also occur. However, there is minimal data available for the distribution of gas pockets in the colon, or their role in the colonic environment. Thus, this aspect of the colon was not included in the model, as many assumptions would have been necessary for its inclusion.

Other straightforward aspects to investigate include diet profile, degree of host pH buffering and initial population profile, all of which would be expected to have a significant effect on the predictions of the model and could be implemented with no changes to the overall structure.

8.5 Conclusions

In this Chapter, a number of adaptations to the original microPop model of Kettle et al. (2017) have been presented, which allow it to be applied to the human colon while retaining the qualities of the original model. The inclusion of all three hydrogenotrophic MFGs is a strength of the model, as is the option to use either the discrete or continuous versions. The model predictions compared well to literature data in many respects, while pointing to potential for model improvements in others. The potential for the model to address biological questions, such as the role of sulphate in the colon, has also been demonstrated.

microPop:Colon represents a tool for the further interrogation of experimental data or investigation of hypotheses on the behaviour and function of the human colonic microbiota. Once validated against experimental data for a specific *in vitro* system, the model could be used to analyse the data from a different perspective. Example uses of the model could include: deriving an estimate for the amount of acetate produced by the acetogen MFG via reductive acetogenesis during a faecal fermentation study; estimating the effect of increased dietary resistant starch on the colonic microbiota and SCFA absorption; or providing a prediction for the best candidate prebiotics to elicit a butyrogenic effect before beginning more expensive *in vitro* tests.

The advantages of microPop:Colon over its *in vitro* and modelling alternatives are its rapid results (less than an hour runtime for 100-day simulations), relatively low cost and the ease with which new functionality can be built in. Disadvantages include the limited depth to which microbes and metabolites can currently be interrogated, in comparison to metagenomics and metabolomics approaches, and the degree of abstraction necessary in mathematical modelling, leaving the quality of model predictions dependent on the validity of its simplifying assumptions. As such, the model presented here should be viewed as complementary to experimental work. There is clear potential for both microPop and microPop:Colon to be grown, with inclusion of further metabolites and MFGs and further comparison to *in vitro* and *in vivo* data. The model has the potential to benefit microbiome research both by guiding experimental research through the provision of experimentally testable hypotheses, and in application to questions that cannot feasibly be addressed experimentally.

References

Abell, G.C.J., Cooke, C.M., Bennett, C.N., Conlon, M.A., and McOrist, A.L. (2008). Phylotypes related to *Ruminococcus bromii* are abundant in the large bowel of humans and increase in response to a diet high in resistant starch. FEMS Microbiol. Ecol. 66(3)**,** 505-515. doi: 10.1111/j.1574-6941.2008.00527.x.

Arhan, P., Devroede, G., Jehannin, B., Lanza, M., Faverdin, C., Dornic, C., et al. (1981). Segmental colonic transit time. Dis. Colon Rectum 24(8)**,** 625-629. doi: 10.1007/BF02605761.

Arumugam, M., Raes, J., Pelletier, E., Le Paslier, D., Yamada, T., Mende, D.R., et al. (2011). Enterotypes of the human gut microbiome. Nature 473(7346)**,** 174-180. doi: 10.1038/nature09944.

Bartosch, S., Fite, A., Macfarlane, G.T., and McMurdo, M.E.T. (2004). Characterization of Bacterial Communities in Feces from Healthy Elderly Volunteers and Hospitalized Elderly Patients by Using Real-Time PCR and Effects of Antibiotic Treatment on the Fecal Microbiota. Appl. Environ. Microbiol. 70(6)**,** 3575. doi: 10.1128/AEM.70.6.3575-3581.2004.

Batstone, D.J., Keller, J., Angelidaki, I., Kalyuzhnyi, S.V., Pavlostathis, S.G., Rozzi, A., et al. (2002). The IWA Anaerobic Digestion Model No 1 (ADM1). Water Sci. Technol. 45(10)**,** 65-73.

Bauer, E., Zimmermann, J., Baldini, F., Thiele, I., and Kaleta, C. (2017). BacArena: Individual-based metabolic modeling of heterogeneous microbes in complex communities. PLoS Comp. Biol. 13(5). doi: 10.1371/journal.pcbi.1005544.

Belenguer, A., Holtrop, G., Duncan, S.H., Anderson, S.E., Calder, A.G., Flint, H.J., et al. (2011). Rates of production and utilization of lactate by microbial communities from the human colon. FEMS Microbiol. Ecol. 77(1)**,** 107-119. doi: 10.1111/j.1574-6941.2011.01086.x.

Carbonero, F., Benefiel, A.C., Alizadeh-Ghamsari, A.H., and Gaskins, H.R. (2012a). Microbial pathways in colonic sulfur metabolism and links with health and disease. Front. Physiol. 3:448. doi: 10.3389/fphys.2012.00448.

Carbonero, F., Benefiel, A.C., and Gaskins, H.R. (2012b). Contributions of the microbial hydrogen economy to colonic homeostasis. Nat. Rev. Gastroenterol. Hepatol. 9**,** 504. doi: 10.1038/nrgastro.2012.85.

Charney, A.N., and Donowitz, M. (2005). "Gastrointestinal Influences on Hydrogen Ion Balance," in Acid-base disorders and their treatment, eds. F.J. Gennari, H.J. Adrogué, J.H. Galla & N.E. Madias. Taylor & Francis.

Christl, S.U., Gibson, G.R., and Cummings, J.H. (1992). Role of dietary sulphate in the regulation of methanogenesis in the human large intestine. Gut 33(9), 1234-1238.
Cremer, J., Arnoldini, M., and Hwa, T. (2017). Effect of water flow and chemical environment on microbiota growth and composition in the human colon. Proc. Natl. Acad. Sci. USA. 114, 6438.
D'Hoe, K., Vet, S., Faust, K., Moens, F., Falony, G., Gonze, D., et al. (2018). Integrated culturing, modeling and transcriptomics uncovers complex interactions and emergent behavior in a three-species synthetic gut community. eLife 7, e37090. doi: 10.7554/eLife.37090.
David, L.A., Materna, A.C., Friedman, J., Campos-Baptista, M.I., Blackburn, M.C., Perrotta, A., et al. (2014a). Host lifestyle affects human microbiota on daily timescales. Genome Biol. 15(7), R89. doi: 10.1186/gb-2014-15-7-r89.
David, L.A., Maurice, C.F., Carmody, R.N., Gootenberg, D.B., Button, J.E., Wolfe, B.E., et al. (2014b). Diet rapidly and reproducibly alters the human gut microbiome. Nature 505(7484), 559-563. doi: 10.1038/nature12820.
Debongnie, J.C., and Phillips, S.F. (1978). Capacity of the human colon to absorb fluid. Gastroenterol. 74, 698-703.
de Jong, P., Vissers, M.M.M., van der Meer, R., and Bovee-Oudenhoven, I.M.J. (2007). In Silico Model as a Tool for Interpretation of Intestinal Infection Studies. Appl. Environ. Microbiol. 73(2), 508. doi: 10.1128/AEM.01299-06.
den Besten, G., Van Eunen, K., Groen, A.K., Venema, K., Reijngoud, D.J., and Bakker, B.M. (2013). The role of short-chain fatty acids in the interplay between diet, gut microbiota, and host energy metabolism. J. Lipid Res. 54(9), 2325-2340. doi: 10.1194/jlr.R036012.
Dostal Webster, A., Staley, C., Hamilton, M.J., Huang, M., Fryxell, K., Erickson, R., et al. (2019). Influence of short-term changes in dietary sulfur on the relative abundances of intestinal sulfate-reducing bacteria. Gut Microbes. doi: 10.1080/19490976.2018.1559682.
El Oufir, L., Flourié, B., Bruley des Varannes, S., Barry, J.L., Cloarec, D., Bornet, F., et al. (1996). Relations between transit time, fermentation products, and hydrogen consuming flora in healthy humans. Gut 38(6), 870-877.
Engels, C., Ruscheweyh, H.-J., Beerenwinkel, N., Lacroix, C., and Schwab, C. (2016). The Common Gut Microbe *Eubacterium hallii* also Contributes to Intestinal Propionate Formation. Front. Microbiol. 7(713). doi: 10.3389/fmicb.2016.00713.
Evans, D.F., Pye, G., Bramley, R., Clark, A.G., Dyson, T.J., and Hardcastle, J.D. (1988). Measurement of gastrointestinal pH profiles in normal ambulant human subjects. Gut 29(8), 1035.
Flint, H.J., Scott, K.P., Louis, P., and Duncan, S.H. (2012). The role of the gut microbiota in nutrition and health. Nat. Rev. Gastroenterol. Hepatol. 9(10), 577-589. doi: 10.1038/nrgastro.2012.156.
Florin, T., Neale, G., Gibson, G.R., Christl, S.U., and Cummings, J.H. (1991). Metabolism of dietary sulphate: Absorption and excretion in humans. Gut 32(7), 766-773. doi: 10.1136/gut.32.7.766.
Gennari, F.J., and Weise, W.J. (2008). Acid-Base Disturbances in Gastrointestinal Disease. Clin. J. Am. Soc. Nephrol. 3(6), 1861. doi: 10.2215/CJN.02450508.
Graff, J., Brinch, K., and Madsen, J.L. (2001). Gastrointestinal mean transit times in young and middle-aged healthy subjects. Clin. Physiol. 21(2), 253-259. doi: 10.1046/j.1365-2281.2001.00308.x.
Healey, G.R., Murphy, R., Brough, L., Butts, C.A., and Coad, J. (2017). Interindividual variability in gut microbiota and host response to dietary interventions. Nutr. Rev. 75(12), 1059-1080. doi: 10.1093/nutrit/nux062.
Kettle, H., Holtrop, G., Louis, P., and Flint, H.J. (2017). microPop: Modelling microbial populations and communities in R. Methods Ecol. Evol. 9, 399–409. doi: 10.1111/2041-210x.12873.
Kettle, H., Louis, P., Holtrop, G., Duncan, S.H., and Flint, H.J. (2015). Modelling the emergent dynamics and major metabolites of the human colonic microbiota. Environ. Microbiol. 17(5), 1615-1630. doi: 10.1111/1462-2920.12599.
Koziolek, M., Grimm, M., Becker, D., Iordanov, V., Zou, H., Shimizu, J., et al. (2015). Investigation of pH and Temperature Profiles in the GI Tract of Fasted Human Subjects Using the Intellicap® System. J. Pharm. Sci. 104(9), 2855-2863. doi: https://doi.org/10.1002/jps.24274.

Kumari, R., Ahuja, V., and Paul, J. (2013). Fluctuations in butyrate-producing bacteria in ulcerative colitis patients of North India. World J. Gastroenterol. 19(22), 3404-3414. doi: 10.3748/wjg.v19.i22.3404.

Lewis, S., and Cochrane, S. (2007). Alteration of Sulfate and Hydrogen Metabolism in the Human Colon by Changing Intestinal Transit Rate. Am. J. Gastroenterol. 102(3), 624-633.

Louca, S., and Doebeli, M. (2015). Calibration and analysis of genome-based models for microbial ecology. eLife 4:e08208. doi: 10.7554/eLife.08208.

Macfarlane, G.T., Gibson, G.R., and Cummings, J.H. (1992). Comparison of fermentation reactions in different regions of the human colon. J. Appl. Bacteriol. 72(1), 57-64. doi: 10.1111/j.1365-2672.1992.tb04882.x.

Macfarlane, S., Bahrami, B., and Macfarlane, G.T. (2011). "Mucosal biofilm communities in the human intestinal tract", in: Advances in Applied Microbiology.

Motelica-Wagenaar, A.M., Nauta, A., van den Heuvel, E.G.H.M., and Kleerebezem, R. (2014). Flux analysis of the human proximal colon using anaerobic digestion model 1. Anaerobe 28, 137-148. doi: 10.1016/j.anaerobe.2014.05.008.

Müller, M., Hermes, G.D.A., Canfora, E.E., Smidt, H., Masclee, A.A.M., Zoetendal, E.G., et al. (2020). Distal colonic transit is linked to gut microbiota diversity and microbial fermentation in humans with slow colonic transit. American journal of physiology. Gastrointestin. Liver Physiol. 318(2), G361-G369. doi: 10.1152/ajpgi.00283.2019.

Muñoz-Tamayo, R., Giger-Reverdin, S., and Sauvant, D. (2016). Mechanistic modelling of in vitro fermentation and methane production by rumen microbiota. Anim. Feed Sci. Technol. 220, 1-21. doi: https://doi.org/10.1016/j.anifeedsci.2016.07.005.

Muñoz-Tamayo, R., Laroche, B., Walter, T., Doré, J., and Leclerc, M. (2010). Mathematical modelling of carbohydrate degradation by human colonic microbiota. J. Theor. Biol. 266(1), 189-201. doi: 10.1016/j.jtbi.2010.05.040.

Murray, K., Wilkinson-Smith, V., Hoad, C., Costigan, C., Cox, E., Lam, C., et al. (2014). Differential Effects of FODMAPs (Fermentable Oligo-, Di-, Mono-Saccharides and Polyols) on Small and Large Intestinal Contents in Healthy Subjects Shown by MRI. Am. College Gastroenterol. 109.

Nava, G.M., Carbonero, F., Croix, J.A., Greenberg, E., and Gaskins, H.R. (2012). Abundance and diversity of mucosa-associated hydrogenotrophic microbes in the healthy human colon. ISME J. 6(1), 57-70. doi: 10.1038/ismej.2011.90.

Nicolas, G.R., and Chang, P.V. (2019). Deciphering the Chemical Lexicon of Host–Gut Microbiota Interactions. Trends Pharmacol. Sci. 40(6), 430-445. doi: https://doi.org/10.1016/j.tips.2019.04.006.

Orth, J.D., Thiele, I., and Palsson, B.O. (2010). What is flux balance analysis? Nature Biotechnol. 28(3), 245-248. doi: 10.1038/nbt.1614.

Ottman, N., Geerlings, S.Y., Aalvink, S., de Vos, W.M., and Belzer, C. (2017). Action and function of *Akkermansia muciniphila* in microbiome ecology, health and disease. Best Pract. Res. Cl. Ga. 31(6), 637-642. doi: https://doi.org/10.1016/j.bpg.2017.10.001.

Payling, L., Fraser, K., Loveday, S.M., Sims, I., Roy, N., and McNabb, W. (2020). The effects of carbohydrate structure on the composition and functionality of the human gut microbiota. Trends Food Sci. Technol. 97, 233-248. doi: 10.1016/j.tifs.2020.01.009.

Payne, A.N., Chassard, C., Banz, Y., and Lacroix, C. (2012a). The composition and metabolic activity of child gut microbiota demonstrate differential adaptation to varied nutrient loads in an in vitro model of colonic fermentation. FEMS Microbiol. Ecol. 80(3), 608-623. doi: 10.1111/j.1574-6941.2012.01330.x.

Payne, A.N., Chassard, C., Zimmermann, M., Müller, P., Stinca, S., and Lacroix, C. (2011). The metabolic activity of gut microbiota in obese children is increased compared with normal-weight children and exhibits more exhaustive substrate utilization. Nutr. Diabetes 1(7), e12. doi: 10.1038/nutd.2011.8.

Payne, A.N., Zihler, A., Chassard, C., and Lacroix, C. (2012b). Advances and perspectives in in vitro human gut fermentation modeling. Trends Biotechnol. 30(1), 17-25. doi: https://doi.org/10.1016/j.tibtech.2011.06.011.

Penn, R., Ward, B.J., Strande, L., and Maurer, M. (2018). Review of synthetic human faeces and faecal sludge for sanitation and wastewater research. Water Res. 132, 222-240. doi: https://doi.org/10.1016/j.watres.2017.12.063.

Pimentel, M., Lin, H.C., Enayati, P., Van Den Burg, B., Lee, H.R., Chen, J.H., et al. (2006). Methane, a gas produced by enteric bacteria, slows intestinal transit and augments small intestinal contractile activity. Am. J. Physiol. Gastrointest. Liver Physiol. 290(6), G1089-G1095. doi: 10.1152/ajpgi.00574.2004.

Pinto, F., Medina, D.A., Pérez-Correa, J.R., and Garrido, D. (2017). Modeling Metabolic Interactions in a Consortium of the Infant Gut Microbiome. Front. Microbiol. 8(2507). doi: 10.3389/fmicb.2017.02507.

Pritchard, S.E., Marciani, L., Garsed, K.C., Hoad, C.L., Thongborisute, W., Roberts, E., et al. (2014). Fasting and postprandial volumes of the undisturbed colon: normal values and changes in diarrhea-predominant irritable bowel syndrome measured using serial MRI. Neurogastroenterol. Motility 26(1), 124-130. doi: 10.1111/nmo.12243.

Pudlo, N.A., Urs, K., Kumar, S.S., German, J.B., Mills, D.A., and Martens, E.C. (2015). Symbiotic human gut bacteria with variable metabolic priorities for host mucosal glycans. mBio 6(6). doi: 10.1128/mBio.01282-15.

Rajilić-Stojanović, M., Heilig, H.G.H.J., Molenaar, D., Kajander, K., Surakka, A., Smidt, H., et al. (2009). Development and application of the human intestinal tract chip, a phylogenetic microarray: analysis of universally conserved phylotypes in the abundant microbiota of young and elderly adults. Environ. Microbiol. 11(7), 1736-1751. doi: 10.1111/j.1462-2920.2009.01900.x.

Rajilić–Stojanović, M., Biagi, E., Heilig, H.G.H.J., Kajander, K., Kekkonen, R.A., Tims, S., et al. (2011). Global and Deep Molecular Analysis of Microbiota Signatures in Fecal Samples From Patients With Irritable Bowel Syndrome. Gastroenterol. 141(5), 1792-1801. doi: https://doi.org/10.1053/j.gastro.2011.07.043.

Ravcheev, D.A., and Thiele, I. (2017). Comparative Genomic Analysis of the Human Gut Microbiome Reveals a Broad Distribution of Metabolic Pathways for the Degradation of Host-Synthetized Mucin Glycans and Utilization of Mucin-Derived Monosaccharides. Front. Genetics 8(111). doi: 10.3389/fgene.2017.00111.

Rey, F.E., Faith, J.J., Bain, J., Muehlbauer, M.J., Stevens, R.D., Newgard, C.B., et al. (2010). Dissecting the in vivo metabolic potential of two human gut acetogens. J. Biol. 285(29), 22082-22090. doi: 10.1074/jbc.M110.117713.

Rey, F.E., Gonzalez, M.D., Cheng, J., Wu, M., Ahern, P.P., and Gordon, J.I. (2013). Metabolic niche of a prominent sulfate-reducing human gut bacterium. Proc. Natl. Acad. Sci. USA. 110(33), 13582-13587. doi: 10.1073/pnas.1312524110.

Ruppin, H., Bar-Meir, S., Soergel, K.H., Wood, C.M., and Schmitt, M.G. (1980). Absorption of short-chain fatty acids by the colon. Gastroenterol. 78(6), 1500-1507.

Stephen, A.M., Haddad, A.C., and Phillips, S.F. (1983). Passage of carbohydrate into the colon: Direct measurements in humans. Gastroenterol. 85(3), 589-595. doi: 10.1016/0016-5085(83)90012-4.

Stumpff, F. (2018). A look at the smelly side of physiology: transport of short chain fatty acids. Pflügers Archiv. 470(4), 571-598. doi: 10.1007/s00424-017-2105-9.

Thiele, I., Heinken, A., and Fleming, R.M.T. (2013). A systems biology approach to studying the role of microbes in human health. Curr. Opin. Biotech. 24(1), 4-12. doi: 10.1016/j.copbio.2012.10.001.

Tigchelaar, E.F., Bonder, M.J., Jankipersadsing, S.A., Fu, J., Wijmenga, C., and Zhernakova, A. (2016). Gut microbiota composition associated with stool consistency. Gut 65(3), 540. doi: 10.1136/gutjnl-2015-310328.

Topping, D.L., and Clifton, P.M. (2001). Short-Chain Fatty Acids and Human Colonic Function: Roles of Resistant Starch and Nonstarch Polysaccharides. Physiol. Rev. 81(3), 1031-1064. doi: 10.1152/physrev.2001.81.3.1031.

Van Wey, A.S., Cookson, A.L., Roy, N.C., McNabb, W.C., Soboleva, T.K., and Shorten, P.R. (2014). Monoculture parameters successfully predict coculture growth kinetics of *Bacteroides thetaiotaomicron* and two *Bifidobacterium* strains. Int. J. Food Microbiol. 191, 172-181. doi: 10.1016/j.ijfoodmicro.2014.09.006.

Vandeputte, D., Falony, G., Vieira-Silva, S., Tito, R.Y., Joossens, M., and Raes, J. (2016). Stool consistency is strongly associated with gut microbiota richness and composition, enterotypes and bacterial growth rates. Gut 65(1), 57-62. doi: 10.1136/gutjnl-2015-309618.

Venema, K., and van den Abbeele, P. (2013). Experimental models of the gut microbiome. Best Pract. Res. Cl. Ga. 27(1), 115-126. doi: https://doi.org/10.1016/j.bpg.2013.03.002.

Walker, A.W., Duncan, S.H., Carol McWilliam Leitch, E., Child, M.W., and Flint, H.J. (2005). pH and peptide supply can radically alter bacterial populations and short-chain fatty acid ratios within microbial communities from the human colon. Appl. Environ. Microbiol. 71(7), 3692-3700. doi: 10.1128/aem.71.7.3692-3700.2005.

Wang, S.P., Rubio, L.A., Duncan, S.H., Donachie, G., Holtrop, G., Lo, G., et al. (Under review). Pivotal roles for pH, lactate and lactate-utilizing bacteria in the stability of a human colonic microbial ecosystem. mSystems.

Wang, Y.T., Mohammed, S.D., Farmer, A.D., Wang, D., Zarate, N., Hobson, A.R., et al. (2015). Regional gastrointestinal transit and pH studied in 215 healthy volunteers using the wireless motility capsule: influence of age, gender, study country and testing protocol. Aliment. Pharmacol. Ther. 42(6), 761-772. doi: 10.1111/apt.13329.

White, J.R., Nagarajan, N., and Pop, M. (2009). Statistical Methods for Detecting Differentially Abundant Features in Clinical Metagenomic Samples. PLoS Comp. Biol. 5(4), e1000352. doi: 10.1371/journal.pcbi.1000352.

Willis, C.L., Cummings, J.H., Neale, G., and Gibson, G.R. (1996). In vitro effects of mucin fermentation on the growth of human colonic sulphate-reducing bacteria. Anaerobe 2(2), 117-122. doi: 10.1006/anae.1996.0015.

Yao, C.K., Muir, J.G., and Gibson, P.R. (2016). Review article: Insights into colonic protein fermentation, its modulation and potential health implications. Aliment. Pharmacol. Ther. 43(2), 181-196. doi: 10.1111/apt.13456.

Yao, C.K., Rotbart, A., Ou, J.Z., Kalantar-Zadeh, K., Muir, J.G., and Gibson, P.R. (2018). Modulation of colonic hydrogen sulfide production by diet and mesalazine utilizing a novel gas-profiling technology. Gut Microbes, 1-13. doi: 10.1080/19490976.2018.1451280.

Chapter 9: General discussion

"All models are wrong, but some are useful."

Box and Draper (1987)

9.1 Summary

Colonic hydrogenotrophs influence the thermodynamic efficiency of microbial fermentation in the colon via cross-feeding on hydrogen, whilst also competing for other microbial substrates. These actions impact the host either indirectly, via the metabolic influences they have on the microbiota, or directly, via the production of molecules with demonstrated or suggested roles in host digestive function and disease. Colonic microbiome research has previously described hydrogen cross-feeding in a limited capacity, focussing more on the highly abundant or pathogenic microbes and on metabolites with demonstrated impacts on the host. This is demonstrated by three recent reviews of the microbiome and human health in high-impact journals, each of which give only brief mention of hydrogen cross-feeders: as an example of a cross-feeding interaction (Zmora et al., 2019); in reference to their role in reducing the partial pressure of hydrogen (Treuren and Dodd, 2020); or in the role of methanogens in obesity (Illiano et al., 2020). By contrast, discussion of SCFAs and the microbes involved in their production was present throughout all three reviews. This is reflective of the amount of study dedicated to each topic and motivated the focus of this thesis on hydrogen cross-feeding.

In the review of the scientific literature relevant to microbial cross-feeding presented in Chapter 2, several key areas requiring further research were highlighted. Before evaluating the literature on cross-feeding of human colonic microbes, Chapter 2 recognised the inconsistent terminology used to describe different types of cross-feeding interaction. Various terminologies had been proposed and used previously (West et al., 2007), but the limitations of these terminologies in their application to cross-feeding motivated the development of a new classification scheme specific to microbial cross-feeding. Four classifications were proposed in Chapter 2, which were then used to characterise the cross-feeding relationships discussed.

Knowledge gaps were then identified in the *in vitro*, animal and human experimental literature on microbial cross-feeding by colonic microbes. It was evident that more gaps existed around hydrogen cross-feeding than the more commonly studied carbohydrate and SCFA cross-feeding relationships. In particular, the distribution of hydrogenotrophic microbes in stool samples and in direct sampling from the colon differs between individuals (Nava et al., 2012; Nishijima et al., 2016), but the causative factors behind this observation remain unclear. The use of mathematical modelling in the study of cross-feeding dynamics also appeared frequently in the literature, but these models omitted or put minimal emphasis on the role of hydrogen cross-feeding microbes.

Based on the identified knowledge gaps, the aim of this thesis was to better understand the metabolism and cross-feeding relationships of the hydrogenotrophic microbes of the human colon both at an individual level and as part of the microbial community. The method employed to address this aim was mathematical modelling, using Monod-based, deterministic models. Models were developed for each of the three main hydrogenotrophic functional groups of the human colonic microbiota, which were then combined with each other and an existing community model to obtain insights into dynamics in increasingly complex environments.

Chapters 3 to 5 detailed the development of monoculture models for a methanogen, an SRB and a reductive acetogen, respectively. Monod kinetics was a suitable technique for modelling the growth and metabolism of each of the three hydrogenotrophs. Other mathematical formulations were also considered, but it was found that Monod kinetics, with certain case-dependent extensions, was similar or superior to the other techniques investigated at accurately capturing the experimental data considered. While the presented models did not take a mass balance or thermodynamic approach, it was found that this was not necessary for the goal of developing predictive models of metabolism and growth. Indeed, the SRB model of Chapter 4 was simpler than the previous mass balance model of Noguera et al. (1998), which also considered the thermodynamics of the reactions modelled, but the two models gave nearly identical predictions. Naturally, the complexity required in a model will be determined by the type of predictions needed from it; in cases where tracing of all metabolites and both viable and dead cells is required, a model like that of Noguera et al. (1998) will be more appropriate. The field of research benefits from having the option of either modelling technique.

Further proof of the usefulness of simple Monod models with appropriate additions was provided in Chapter 5, where such a model with the inclusion of a threshold term provided insight into the contribution of substrates other than hydrogen to the acetate production of *B. hydrogenotrophica*. The results of the model supported the use of the GA medium of Groher and Weuster-Botz (2016) over the established DSMZ medium for the unbiased estimation of reductive acetogenesis. The model was also used to estimate a threshold value for hydrogen uptake by this bacterium using a basic threshold model. Using an independent data set to the original experiment that provided an estimate of 70 mM (Leclerc et al., 1997), the model estimated this threshold value at 86 mM, with a confidence interval encompassing the experimental estimate. Thus, the monoculture model provided supporting evidence for two separate biological hypotheses, with minimal complexity required to do so.

Co-culture models were also developed to investigate hydrogenotroph interactions. The model estimated hydrogen half-saturation constants for *D. vulgaris* and *M. smithii*, alongside the threshold value for *B. hydrogenotrophica*, supported the hierarchy stated in the experimental literature for hydrogen metabolism (Leclerc et al., 1997; Carbonero et al., 2012). SRB were the best able to metabolise hydrogen at low concentrations, followed by the methanogens, with the acetogen threshold value limiting their metabolism to higher concentrations.

The tri-culture modelling in Chapter 7 revealed some less intuitive dynamics. Here it was shown that the lower maximum growth rate of *D. vulgaris* on hydrogen compared to *M. smithii* resulted in a growth advantage to the methanogen under abundant hydrogen and zero lactate conditions, despite its higher half-saturation constant. However, the situation changed given limiting hydrogen or increased lactate conditions. The reduction in growth yield and alterations to other parameter values for both SRB and methanogens in co-culture compared to monoculture studied in Chapter 6 implied that drawing conclusions on community dynamics from monoculture models will not be reliable in all cases. Thus, the dynamics observed in experimental co-culture and the results predicted by the combination of simple monoculture models increase in complexity as the number of microbes included increases, making insight into community interactions difficult, regardless of the scientific approach taken.

This complexity was further compounded in the community models microPop and microPop:Colon described in Chapter 8, and previously reported by Kettle et al. (2015). The model was able to accurately capture only a subset of the experimental data considered and neither the original parameter set of Kettle et al. (2017) nor the more recent set of Wang et al. (Under review)[2] emerged as more suitable for capturing the microbial community dynamics. The development of microPop:Colon for predicting microbial and metabolite concentrations in the human colon showed promising accuracy in predicting certain measurements, such as pH, but was inaccurate in other areas, such as the high production and absorption of SCFAs observed experimentally. Comparison to the colon was challenged by the inconsistent and incomplete data on microbial and metabolite concentrations in different regions of the colon, an aspect that will need to be addressed if the model is to be more fully validated. However, the inclusion of dynamic pH, the mucin breakdown pathway of the Bacteroides MFG, and the incorporation of the three hydrogenotroph models represent novel contributions to the field.

Specific to the hydrogen cross-feeding functional groups of the colon, the predicted results of the sulphate availability investigation in Chapter 8 showed similar uncertainty to those reported in the literature. Dietary intervention research in humans has shown that increased dietary sulphate can increase faecal sulphide and decrease methanogen counts in some, but not all individuals (Christl et al., 1992; Lewis and Cochrane, 2007). Other research has shown negligible effects (Rey et al., 2013; Dostal Webster et al., 2019), or a greater effect due to fermentation of dietary sulphur amino acids (Yao et al., 2018), which was not included in the model. The two versions of microPop:Colon gave different predictions when sulphate inflow was varied: the discrete model predicted changes in microbial concentrations of less than 0.02% and metabolite concentration changes of less than 10^{-4} g L^{-1}; contrastingly, the continuous model predicted a notable influence of sulphate inflow on both SRB and methanogen relative abundance (up to 25% and 10% variation, respectively), as well as on H_2S concentration (up to 39% variation). Whether these predictions apply

[2] The work of Wang et al., from which this parameter set was taken, is under review with the journal mSystems at the time of writing. Permission to reference the work as a personal communication was received from Harry J. Flint on 7/05/2020. Full authorship and title are included in the reference list.

to dietary sulphate is unclear, as model sulphate availability was set at the start of the colon, so the actions of the upper GIT were not considered. The differing results of the two model versions mean that a conclusion cannot be drawn on whether sulphate availability is predicted to play a decisive role in the hydrogenotroph profile of an individual's microbiota. Opportunities to improve the model so that more conclusive results may be produced are described in the next section.

To summarise, this thesis makes contributions to several aspects of the field of human microbiome research. Figure 9.1 provides an overview of the main results of the thesis. The monoculture models provided tools for predicting hydrogenotroph growth and metabolism in experimental culture, as well as insight into dynamics under specific culture conditions. The co- and tri-culture modelling allowed for interactions between the hydrogenotrophs to be examined under various conditions and established growth boundaries for each. Finally, the colonic community modelling extended the existing scope of microbiota modelling in the field, with new comparisons to experimental data sets and novel methods for replicating the colonic environment *in silico*.

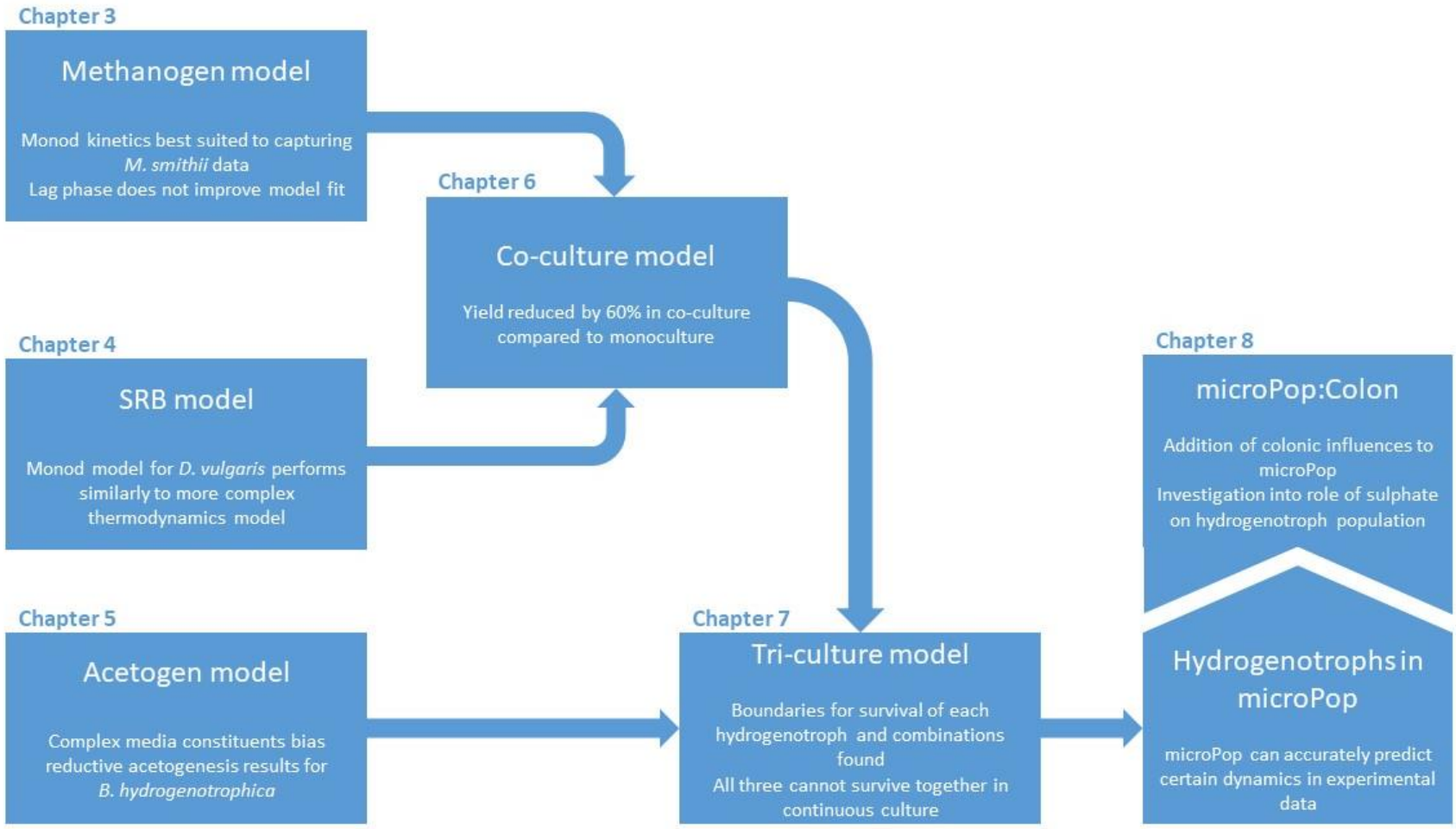

Figure 9.1. Summary of the main results of the thesis. SRB: sulphate-reducing bacteria. *M. smithii: Methanobrevibacter smithii. D. vulgaris: Desulfovibrio vulgaris. B. hydrogenotrophica: Blautia hydrogenotrophica.*

9.2 Future perspectives

The goal of microbial ecology is to understand what microbes are present in a certain environment, their individual roles in the microbial community, and their relationships with each other and their environment (Barton and Northup, 2011). This includes understanding why the present microbes survive in their environment, the influences they have on the microbes around them, and what keeps the system stable or causes it to change. Generating ecological mathematical models allows for a complex system to be converted into one that can be inspected and understood. In modelled systems, individual factors may be varied, and the outcomes of this variation inspected. This close inspection of a microbial ecological system is not always possible experimentally, particularly in complex systems or challenging environments like the GIT. The models presented in this thesis complement and extend the contribution of mathematical modelling to understanding GIT ecology. It is hoped that the models will be utilised by ecologists as well as those interested in the microbiota from nutritional and health perspectives.

As outlined in the literature review, knowledge of the role played by hydrogenotrophs in the human colon is complementary to knowledge of these microbes in the rumen. Research aiming to reduce methane production and improve animal nutrition has resulted in increased knowledge of hydrogen cross-feeding in the rumen, some of which is transferrable between this environment and the human colon. An example of this is reduced methane production with reduced transit times observed in both the rumen and human colon (Janssen, 2010; Sahakian et al., 2010). As recently reviewed by Lan and Yang (2019), sulphate-reduction and reductive acetogenesis, as well as propionate and nitrate/nitrite reduction are well studied in rumen microbiology alongside methanogens. Discussion of hydrogen cross-feeding knowledge generated from the rumen microbiology field is currently not widely observed in the colon microbiology field, as evidenced by a lack of mention in recent reviews on the subject of gas production and metabolism in the colon (Pimentel, 2013; Hylemon, 2018; Kalantar-Zadeh, 2019). The opportunity for greater knowledge sharing between the two fields is clear.

Hydrogen cross-feeding was the focus of the research in this thesis and as such the alternative substrates of the modelled hydrogenotrophs were not considered, with the exception of

lactate for *D. vulgaris*. A next inclusion for modelling these organisms would be formate metabolism, as mentioned in Chapters 4 and 6. Formate is known to be metabolised by strains of each of the three hydrogenotrophic functional groups of the human colon (Hansen et al., 2011; Martins et al., 2015; Laverde Gomez et al., 2018). More comprehensive monoculture models for these microbes would require the inclusion of formate metabolism, and it is interesting to consider what effect this inclusion would have on the predictions of the co- and tri-culture models of Chapters 6 and 7. It is possible that the monoculture parameters would provide better predictions of co-culture growth against the experimental data considered in Chapter 6 with formate included. Likewise, the conditions for survival of each member of the tri-culture in Chapter 7 would be shifted with the inclusion of a second substrate for which all three could compete. Monoculture data for formate metabolism by the strains studied here would be straightforward to produce but are not readily available in the literature currently. This lack of data, as well as the focus on hydrogen are the reasons for mostly neglecting formate in this thesis, although it was included in the community models in Chapter 8.

Microbial community modelling is a challenging task due to the complexity of these populations. The contrasting model predictions of microPop and microPop:Colon using different parameter sets, different initial relative abundances of functional groups, and a discrete versus a continuous representation of the colon emphasise the difficulty in providing consistent estimates for colonic microbiota dynamics. When the differences in colon microbiota and metabolite data sets observed experimentally between individuals are considered alongside the differences in modelling results, it can appear an insurmountable task to reliably predict the behaviour of an inconsistent population using a model with inconsistent predictions. An interesting question to consider is whether it is indeed possible to develop a mathematical model that provides accurate predictions for microbial and metabolite variables in the colon. The answer depends on the level of resolution desired from the model. For example, a three-dimensional model representing microbes at the strain level with all measurable metabolites included, against the background host processes encompassing peristaltic movement, molecular transport and immune function, is unrealistic computationally and would be impossible to validate given the lack of data on many of these variables. However, subsets of these dynamics have already been modelled: the metabolite flux of

individualised microbiota (Heinken and Thiele, 2019), and intestinal peristaltic movement in three dimensions (Sinnott et al., 2017) are examples of colonic dynamics already accounted for by highly sophisticated, specialised models. The unification of existing colonic models to capture greater complexity is already being performed (Labarthe et al., 2019), and I believe it is through these combinations that the field will increase model resolution towards the goal of an *in silico* representation of all colon dynamics.

While it is likely impossible to accurately capture all aspects of this system for every individual with a mathematical model, even capturing trends can be useful. microPop predicted the production of propionate and butyrate to within 10 mM at all time points for the experiments of Walker et al. (2005) using the Alpha parameter set, as displayed in Chapter 8; moreover, it was able to predict the dominant functional group for five out of six of these experiments. While the model gave inaccurate predictions for many of the other measured values, correct predictions of variables such as these are useful, and the number of correct predictions will only improve with model finetuning. For certain applications, prediction of one or two key variables is sufficient. For example, if multiple potentially prebiotic substances are available to test for efficacy in promoting the production of SCFAs or growth of a particular MFG in the colon, modelling could identify which of these substances show the greatest potential, and subsequently these substances could be targeted for more expensive and time-consuming experimental studies. There is no disadvantage to using modelling in this instance as a predictive tool to guide experimentation and its potential will steadily increase as the field develops.

The ability of microPop to accurately capture data from *in vitro* models should be further exploited. A possibility not addressed here was the opportunity to obtain information on the contribution of individual MFGs to overall metabolite concentrations. For example, it is possible to use microPop to provide a value for the amount of acetate produced by the acetogen MFG via reductive acetogenesis. Predictions at this level of resolution are rarely achieved experimentally, particularly for microbial communities with multiple MFGs, but would be a valuable addition to the experimental results.

A future goal of research with microPop is to compare and validate its predictions with data including the concentrations of hydrogenotroph cells and their metabolites. No data were available

for the concentration of methanogen cells in the data sets considered in Chapter 8, and only limited data for SRB and acetogens. Moreover, the experimenters had not measured concentrations of hydrogen or methane, again limiting the level of model validation that could be achieved here. Experimental faecal cultures measuring these values are currently underway in our group and this data will be used to address these limitations.

In Chapter 8, it was seen that the inclusion of the SRB and the alterations to the other hydrogenotrophic MFGs only influenced the acetate and acetogen concentrations when compared to the original microPop predictions; these alterations did not influence the dynamics of the rest of the population. This quality may change if inhibition of carbohydrate breakdown due to high hydrogen concentrations were included in the model, since there is currently no feedback on the saccharolytic MFGs from their production of hydrogen. Progress in the field of human microbiota modelling is rapid. Perhaps the most exciting recent development is that of Heinken and Thiele (2019), using genome-scale metabolic reconstructions of an individual's entire microbiota coupled with constraint-based modelling to predict metabolome dynamics at the individual level. The level of detail in this approach is large, as is the amount of data required to construct such a model. However, the results are promising for a future in which science-based personalised nutrition (the use of data to make nutritional choices tuned to the individual (Ordovas et al., 2018)) is a possibility within reach. Nonetheless, there is still value in the more generalist approach of models like microPop to make predictions about the generic colonic microbiota.

Following the idea of a generalised representation for the microbiota of a human population, numerous authors have previously proposed the classification of individuals into enterotypes based on the makeup of their microbiota (Arumugam et al., 2011; Wu et al., 2011; Bergström et al., 2014; Roager et al., 2014; Tap et al., 2017). Although there are some inconsistencies in the number and classification of these enterotypes between these studies, use of enterotypes could be a method for bridging the gap between individualised study of the microbiota and generalised study. If models like microPop:Colon were tailored to give predictions for each enterotype, the results could then be more consistent with experimental data, and thus more useful. Such a tailoring would also not require great changes to the model structure, but rather to the microbial parameter sets.

These are just some of the many possible next steps that could be taken with microPop:Colon, and mathematical modelling of the microbiome in general. Modelling at any level of simplification has the potential to be instructive, as encapsulated in the quote from Box and Draper (1987) and demonstrated by the monoculture, co-culture and community models presented in this thesis.

References

Arumugam, M., Raes, J., Pelletier, E., Le Paslier, D., Yamada, T., Mende, D.R., et al. (2011). Enterotypes of the human gut microbiome. Nature 473(7346), 174-180. doi: 10.1038/nature09944.

Barton, L.L., and Northup, D.E. (2011). "Microbial Ecology: Beginnings and the Road Forward," in Microbial Ecology.), 1-28.

Bergström, A., Skov, T.H., Bahl, M.I., Roager, H.M., Christensen, L.B., Ejlerskov, K.T., et al. (2014). Establishment of intestinal microbiota during early life: A longitudinal, explorative study of a large cohort of Danish infants. Appl. Environ. Microbiol. 80(9), 2889-2900. doi: 10.1128/aem.00342-14.

Box, G.E.P., and Draper, N.R. (1987). Empirical model-building and response surfaces. Oxford, England: John Wiley & Sons.

Carbonero, F., Benefiel, A.C., and Gaskins, H.R. (2012). Contributions of the microbial hydrogen economy to colonic homeostasis. Nat. Rev. Gastroenterol. Hepatol. 9, 504. doi: 10.1038/nrgastro.2012.85.

Christl, S.U., Gibson, G.R., and Cummings, J.H. (1992). Role of dietary sulphate in the regulation of methanogenesis in the human large intestine. Gut 33(9), 1234-1238.

Dostal Webster, A., Staley, C., Hamilton, M.J., Huang, M., Fryxell, K., Erickson, R., et al. (2019). Influence of short-term changes in dietary sulfur on the relative abundances of intestinal sulfate-reducing bacteria. Gut Microbes. doi: 10.1080/19490976.2018.1559682.

Groher, A., and Weuster-Botz, D. (2016). General medium for the autotrophic cultivation of acetogens. Bioprocess Biosystems Eng. 39(10), 1645-1650. doi: 10.1007/s00449-016-1634-5.

Hansen, E.E., Lozupone, C.A., Rey, F.E., Wu, M., Guruge, J.L., Narra, A., et al. (2011). Pan-genome of the dominant human gut-associated archaeon, *Methanobrevibacter smithii*, studied in twins. Proc. Natl. Acad. Sci. USA. 108(SUPPL. 1), 4599-4606. doi: 10.1073/pnas.1000071108.

Heinken, A., and Thiele, I. (2019). Systematic interrogation of the distinct metabolic potential in gut microbiomes of inflammatory bowel disease patients with dysbiosis. bioRxiv, 640649. doi: 10.1101/640649.

Hylemon, P.B., Harris, S.C., and Ridlon, J.M. (2018). Metabolism of hydrogen gases and bile acids in the gut microbiome. FEBS Lett. 592: 2070-2082. doi: 10.1002/1873-3468.13064

Illiano, P., Brambilla, R., and Parolini, C. (2020). The mutual interplay of gut microbiota, diet and human disease. FEBS J. 287, 833-855. doi: 10.1111/febs.15217.

Janssen, P.H. (2010). Influence of hydrogen on rumen methane formation and fermentation balances through microbial growth kinetics and fermentation thermodynamics. Anim. Feed Sci. Technol. 160, 1-22.

Kalantar-Zadeh, K., Berean, K.J., Burgell, R.E., Muir, J.G., and Gibson, P.R. (2019). Intestinal gases: influence on gut disorders and the role of dietary manipulations. Nat. Rev. Gastroenterol. Hepatol. 16, 733–747. doi: 10.1038/s41575-019-0193-z

Kettle, H., Holtrop, G., Louis, P., and Flint, H.J. (2017). microPop: Modelling microbial populations and communities in R. Methods Ecol. Evol. 9, 399–409. doi: 10.1111/2041-210x.12873.

Kettle, H., Louis, P., Holtrop, G., Duncan, S.H., and Flint, H.J. (2015). Modelling the emergent dynamics and major metabolites of the human colonic microbiota. Environ. Microbiol. 17(5), 1615-1630. doi: 10.1111/1462-2920.12599.

Labarthe, S., Polizzi, B., Phan, T., Goudon, T., Ribot, M., and Laroche, B. (2019). A mathematical model to investigate the key drivers of the biogeography of the colon microbiota. J. Theor. Biol. 462**,** 552-581. doi: 10.1016/j.jtbi.2018.12.009.

Lan, W., and Yang, C. (2019). Ruminal methane production: Associated microorganisms and the potential of applying hydrogen-utilizing bacteria for mitigation. Sci. Total Environ. 654**,** 1270-1283. doi: 10.1016/j.scitotenv.2018.11.180

Laverde Gomez, J.A., Mukhopadhya, I., Duncan, S.H., Louis, P., Shaw, S., Collie-Duguid, E., et al. (2018). Formate cross-feeding and cooperative metabolic interactions revealed by transcriptomics in co-cultures of acetogenic and amylolytic human colonic bacteria. Environ. Microbiol. 21(1), 259–271. doi: 10.1111/1462-2920.14454.

Leclerc, M., Bernalier, A., Donadille, G., and Lelait, M. (1997). H2/CO2 Metabolism in Acetogenic Bacteria Isolated From the Human Colon. Anaerobe 3(5)**,** 307-315. doi: https://doi.org/10.1006/anae.1997.0117.

Lewis, S., and Cochrane, S. (2007). Alteration of Sulfate and Hydrogen Metabolism in the Human Colon by Changing Intestinal Transit Rate. Am. J. Gastroenterol. 102(3)**,** 624-633.

Martins, M., Mourato, C., and Pereira, I.A.C. (2015). *Desulfovibrio vulgaris* Growth Coupled to Formate-Driven H2 Production. Environ. Sci. Technol. 49(24)**,** 14655-14662. doi: 10.1021/acs.est.5b02251.

Nava, G.M., Carbonero, F., Croix, J.A., Greenberg, E., and Gaskins, H.R. (2012). Abundance and diversity of mucosa-associated hydrogenotrophic microbes in the healthy human colon. ISME J. 6(1)**,** 57-70. doi: 10.1038/ismej.2011.90.

Nishijima, S., Suda, W., Oshima, K., Kim, S.-W., Hirose, Y., Morita, H., et al. (2016). The gut microbiome of healthy Japanese and its microbial and functional uniqueness. DNA Res. 23(2)**,** 125-133. doi: 10.1093/dnares/dsw002.

Noguera, D.R., Brusseau, G.A., Rittmann, B.E., and Stahl, D.A. (1998). A unified model describing the role of hydrogen in the growth of *Desulfovibrio vulgaris* under different environmental conditions. Biotechnol. Bioeng. 59(6)**,** 732-746. doi: 10.1002/(SICI)1097-0290(19980920)59:6<732::AID-BIT10>3.0.CO;2-7.

Ordovas, J.M., Ferguson, L.R., Tai, E.S., and Mathers, J.C. (2018). Personalised nutrition and health. BMJ 361**,** bmj.k2173. doi: 10.1136/bmj.k2173.

Pimentel, M., Mathur, R., and Chang, C. (2013). Gas and the Microbiome. Curr. Gastroenterol. Rep. 15**,** 356. doi: 10.1007/s11894-013-0356-y.

Rey, F.E., Gonzalez, M.D., Cheng, J., Wu, M., Ahern, P.P., and Gordon, J.I. (2013). Metabolic niche of a prominent sulfate-reducing human gut bacterium. Proc. Natl. Acad. Sci. USA. 110(33)**,** 13582-13587. doi: 10.1073/pnas.1312524110.

Roager, H.M., Licht, T.R., Poulsen, S.K., Larsen, T.M., and Bahl, M.I. (2014). Microbial Enterotypes, Inferred by the Prevotella-to-Bacteroides Ratio, Remained Stable during a 6-Month Randomized Controlled Diet Intervention with the New Nordic Diet. Appl. Environ. Microbiol. 80(3)**,** 1142. doi: 10.1128/AEM.03549-13.

Sahakian, A.B., Jee, S.-R., and Pimentel, M. (2010). Methane and the Gastrointestinal Tract. Dig. Dis. Sci. 55**,** 2135-2143. doi: 10.1007/s10620-009-1012-0

Sinnott, M.D., Cleary, P.W., and Harrison, S.M. (2017). Peristaltic transport of a particulate suspension in the small intestine. Appl. Math. Model. 44**,** 143-159. doi: https://doi.org/10.1016/j.apm.2017.01.034.

Tap, J., Derrien, M., Törnblom, H., Brazeilles, R., Cools-Portier, S., Doré, J., et al. (2017). Identification of an Intestinal Microbiota Signature Associated With Severity of Irritable Bowel Syndrome. Gastroenterol. 152(1)**,** 111-123.e118. doi: 10.1053/j.gastro.2016.09.049.

Treuren, W.V., and Dodd, D. (2020). Microbial Contribution to the Human Metabolome: Implications for Health and Disease. Ann. Rev. Pathol. 15(1)**,** 345-369. doi: 10.1146/annurev-pathol-020117-043559.

Walker, A.W., Duncan, S.H., Carol McWilliam Leitch, E., Child, M.W., and Flint, H.J. (2005). pH and peptide supply can radically alter bacterial populations and short-chain fatty acid ratios within microbial communities from the human colon. Appl. Environ. Microbiol. 71(7)**,** 3692-3700. doi: 10.1128/aem.71.7.3692-3700.2005.

Wang, S.P., Rubio, L.A., Duncan, S.H., Donachie, G., Holtrop, G., Lo, G., et al. (Under review). Pivotal roles for pH, lactate and lactate-utilizing bacteria in the stability of a human colonic microbial ecosystem. mSystems.

West, S.A., Griffin, A.S., and Gardner, A. (2007). Social semantics: Altruism, cooperation, mutualism, strong reciprocity and group selection. J. Evol. Biol. 20(2), 415-432. doi: 10.1111/j.1420-9101.2006.01258.x.

Wu, G.D., Chen, J., Hoffmann, C., Bittinger, K., Chen, Y.-Y., Keilbaugh, S.A., et al. (2011). Linking Long-Term Dietary Patterns with Gut Microbial Enterotypes. Science 334(6052), 105. doi: 10.1126/science.1208344.

Yao, C.K., Rotbart, A., Ou, J.Z., Kalantar-Zadeh, K., Muir, J.G., and Gibson, P.R. (2018). Modulation of colonic hydrogen sulfide production by diet and mesalazine utilizing a novel gas-profiling technology. Gut Microbes, 1-13. doi: 10.1080/19490976.2018.1451280.

Zmora, N., Suez, J., and Elinav, E. (2019). You are what you eat: diet, health and the gut microbiota. Nat. Rev. Gastroenterol. Hepatol. 16(1), 35-56. doi: 10.1038/s41575-018-0061-2.

Appendix A

Table A1. Percentage change in mean bias value in response to a one-at-a-time 10% variation in initial condition or parameter value to assess model sensitivity. + indicates increase in mean bias, - indicates a decrease.

	Figure 4.2					**Figure 4.3**
	Cell concentration	Lactate	Acetate	Sulphate	Gaseous hydrogen	Gaseous hydrogen
Initial condition variation						
Lactate +10%	+13%	+111%	+25%	+38%	-13%	0%
Lactate -10%	+5%	+45%	+29%	-27%	+24%	0%
Sulphate +10%	0%	0%	0%	140%	0%	-1% [a]
Sulphate -10%	0%	0%	0%	271%	0%	-
Aqueous hydrogen +10%	0%	0%	0%	0%	0%	0%
Aqueous hydrogen -10%	0%	0%	0%	0%	0%	0%
Gaseous hydrogen +10%	0%	0%	0%	0%	0%	0%
Gaseous hydrogen -10%	0%	0%	0%	0%	0%	0%
Acetate +10%	0%	0%	-4%	0%	0%	0% [a]
Acetate -10%	0%	0%	7%	0%	0%	-
H_2S +0.1 mM [a]	0%	0%	0%	0%	0%	0%
Cell concentration +10%	-9%	8%	-2%	13%	1%	-
Cell concentration -10%	11%	-3%	16%	-13%	0%	-
Parameter variation						
$\mu_{max,L}$ +10%	-6%	17%	9%	15%	-16%	1%
$\mu_{max,L}$ -10%	13%	-14%	26%	-30%	65%	-1%
$\mu_{max,S}$ +10%	-10%	8%	-2%	14%	63%	0%
$\mu_{max,S}$ -10%	18%	-4%	29%	-29%	4%	0%
K_L +10%	3%	-11%	7%	-10%	20%	0%
K_L -10%	-3%	10%	1%	9%	-15%	0%

K_S +10%	0%	0%	0%	0%	0%	0%
K_S -10%	0%	0%	0%	0%	0%	0%
K_H +10%	0%	0%	0%	0%	0%	0%
K_H -10%	0%	0%	0%	0%	0%	0%
Y_L +10%	7%	-7%	4%	-6%	62%	1%
Y_L -10%	7%	-4%	3%	-5%	-5%	0%
Y_S +10%	15%	-1%	18%	-17%	-7%	0%
Y_S -10%	-8%	1%	-7%	7%	66%	0%
$k_L a$ +10%	0%	0%	0%	0%	0%	22%
$k_L a$ -10%	0%	0%	0%	0%	3%	-18%
H_{max} +10%	0%	0%	0%	0%	-5%	78%
H_{max} -10%	0%	0%	0%	0%	4%	11%
b_{LH} +10%	15%	-1%	18%	23%	-4%	0%
b_{LH} -10%	-8%	1%	-7%	-24%	66%	-1%
b_{HP} +10%	-7%	2%	-7%	-22%	63%	0%
b_{HP} -10%	17%	-1%	20%	24%	2%	0%
b_{LA} +10%	0%	0%	26%	0%	0%	0%
b_{LA} -10%	0%	0%	36%	0%	0%	0%
b_{SP} +10%	0%	0%	0%	0%	0%	0%
b_{SP} -10%	0%	0%	0%	0%	0%	0%
ρ_H +10%	0%	0%	0%	0%	-5%	79%
ρ_H -10%	0%	0%	0%	0%	5%	11%

[a]H_2S concentration was increased by 0.1 mM rather than a 10% variation since its initial concentration was assumed to be 0 mM for the model fitting in Figure 4.2. The same was performed for sulphate and acetate concentrations for the sensitivity analysis of the model fit in Figure 4.3.

Appendix B

B1: Monoculture sulphate-reducing bacteria model

The monoculture model for SRB was adapted from Chapter 4, and is as follows:

$$\frac{dL}{dt} = -\frac{\mu_{max,L}\, X_S}{Y_L}\left(\frac{L}{K_L + L}\right)\left(1 - \frac{H_{aq}}{H_{max}}\right) \tag{B1}$$

$$\frac{dS}{dt} = -\frac{\mu_{max,S}\, X_S}{Y_S}\left(\frac{S}{K_S + S}\right)\left(\frac{H_{aq}}{K_{H,S} + H_{aq}}\right) \tag{B2}$$

$$\frac{dH_{aq}}{dt} = b_{LH}\frac{\mu_{max,L}\, X_S}{Y_L}\left(\frac{L}{K_L + L}\right)\left(1 - \frac{H_{aq}}{H_{max}}\right) - b_{HP}\frac{\mu_{max,S}\, X_S}{Y_S}\left(\frac{S}{K_S + S}\right)\left(\frac{H_{aq}}{K_{H,S} + H_{aq}}\right) - k_L a_H\left(H_{aq} - \frac{1}{\rho_H}H_g\right) \tag{B3}$$

$$\frac{dH_g}{dt} = k_L a_H(\rho_H H_{aq} - H_g)\frac{V_{aq}}{V_g} \tag{B4}$$

$$\frac{dA}{dt} = b_{LA}\frac{\mu_{max,L}\, X_S}{Y_L}\left(\frac{L}{K_L + L}\right)\left(1 - \frac{H_{aq}}{H_{max}}\right) \tag{B5}$$

$$\frac{dP}{dt} = b_{SP}\frac{\mu_{max,S}\, X_S}{Y_S}\left(\frac{S}{K_S + S}\right)\left(\frac{H_{aq}}{K_{H,S} + H_{aq}}\right) \tag{B6}$$

$$\frac{dX_S}{dt} = \mu_{max,L}\, X_S\left(\frac{L}{K_L + L}\right)\left(1 - \frac{H_{aq}}{H_{max}}\right) + \mu_{max,S}\, X_S\left(\frac{S}{K_S + S}\right)\left(\frac{H_{aq}}{K_{H,S} + H_{aq}}\right) \tag{B7}$$

All mathematical notation and parameter values are listed in Table B2.

B2: Monoculture methanogen model

A Monod model for the growth and metabolism of a methanogen, as discussed in Chapter 3, was adapted to include mass transfer of hydrogen and methane, as follows:

$$\frac{dH_{aq}}{dt} = -\frac{\mu_{max,H}\, X_M}{Y_H}\left(\frac{H_{aq}}{K_{H,M} + H_{aq}}\right) - k_L a_H \left(H_{aq} - \frac{1}{\rho_H} H_g\right) \quad \text{(B8)}$$

$$\frac{dH_g}{dt} = k_L a_H (\rho_H H_{aq} - H_g)\frac{V_{aq}}{V_g} \quad \text{(B9)}$$

$$\frac{dM_{aq}}{dt} = b_{HM}\frac{\mu_{max,H}\, X_M}{Y_H}\left(\frac{H_{aq}}{K_{H,M} + H_{aq}}\right) - k_L a_M \left(M_{aq} - \frac{1}{\rho_M} M_g\right) \quad \text{(B10)}$$

$$\frac{dM_g}{dt} = k_L a_M (\rho_M M_{aq} - M_g)\frac{V_{aq}}{V_g} \quad \text{(B11)}$$

$$\frac{dX_M}{dt} = \mu_{max,H}\, X_M \left(\frac{H_{aq}}{K_{H,M} + H_{aq}}\right) \quad \text{(B12)}$$

Note that the consumption of CO_2 is neglected as this is assumed to be abundant in the environment and therefore not limiting. The production of water is also not modelled.

To parameterise the monoculture model, data were obtained from Stolyar et al. (2007) for hydrogen and methane concentrations, as described in the Methodology section in Chapter 6. Unfortunately, biomass measurements were not available. The following best fit parameter values, with 95% confidence intervals shown in parentheses, were obtained for the metabolic parameters of *M. maripaludis*:

$\mu_{max,H} = 0.13142\ \mathrm{h}^{-1}\ (1.81 - 15.88)$

$K_{H,M} = 10.52\ \mathrm{mM}\ (85 - 1{,}273)$

$Y_H = 9.5537 \times 10^{-6}\ \mathrm{g\ L^{-1} mM^{-1}} (0.02563 - 0.08754).$

b_{HM} was fixed at 0.25 in accordance with the assumed stoichiometry, although this did lead to an underprediction of final methane concentration (Figure B1).

It is notable that all three fitted parameter values lie outside their generated 95% confidence intervals. This is most likely due to correlation between the first two parameters (Table B1) and a lack of biomass data for accurate estimation of the yield parameter. Given the strong correlation of the maximum growth rate and half-saturation constant, the ratio of these values was investigated. This ratio had mean value of 0.0165, with 95% confidence interval 0.0113 – 0.0228. The maximum growth rate and half-saturation parameter values given above were taken as the monoculture values due to their similarity to previous estimates in the literature (Goyal et al., 2015; Muñoz-Tamayo et al., 2019). For the yield parameter, since this could not be reliably estimated

mathematically without biomass data, the value of 3.549 mg L^{-1} mM^{-1} was taken from the literature (Goyal et al., 2015).

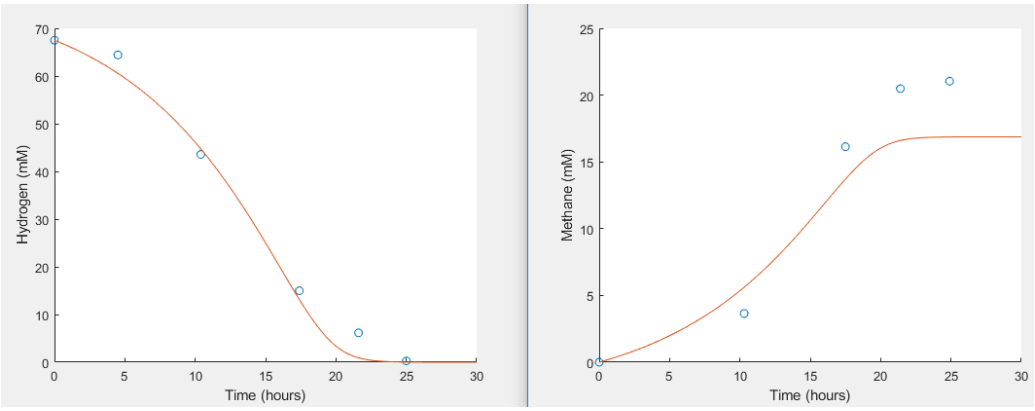

Figure B1. Best fit of monoculture Monod model to data from Stolyar et al. (2007). Biomass data were not available. Hydrogen R^2 = 0.99; Methane R^2 = 0.82.

B3: Supplementary tables

Table B1. Pearson correlation coefficients between Markov chain Monte Carlo generated parameter values for monoculture methanogen growth and metabolism			
	$\mu_{max,H}$	$K_{H,M}$	Y_H
$\mu_{max,H}$	1	0.9679	0.1104
$K_{H,M}$	-	1	0.0581
Y_H	-	-	1

Table B2. Model parameters and mathematical notation			
Parameter		**Notation**	**Value** (units)
Maximum growth rates	Lactate oxidation	$\mu_{max,L}$	0.116 (h^{-1})
	Sulphate reduction	$\mu_{max,S}$	0.03 (h^{-1})
	Methanogenesis	$\mu_{max,H}$	0.131 (h^{-1})
Monod constants	Lactate (SRB)	K_L	4.5 (mM)
	Sulphate (SRB)	K_S	0.05 (mM)
	Hydrogen (SRB)	$K_{H,S}$	1.69 x 10^{-5} (mM)
	Hydrogen (Methanogen)	$K_{H,M}$	10.52 (mM)
Yield parameters	Lactate (SRB)	Y_L	5.65 (mg L^{-1} mM^{-1})
	Sulphate (SRB)	Y_S	4.45 (mg L^{-1} mM^{-1})
	Hydrogen (Methanogen)	Y_H	3.55 (mg L^{-1} mM^{-1})
Mass transfer parameters	Hydrogen	$k_L a_H$	Fitted to data
	Methane	$k_L a_M$	Fitted to data
Inhibitory hydrogen concentration		H_{max}	0.0216 (mM)
Stoichiometric constants	Moles of hydrogen produced per mole lactate oxidised (SRB)	b_{LH}	2.5 (-)

	Moles of hydrogen consumed per mole H_2S produced (SRB)	b_{HP}	5 (-)
	Moles of acetate produced per mole lactate oxidised (SRB)	b_{LA}	1 (-)
	Moles of H_2S produced per mole sulphate reduced (SRB)	b_{SP}	1 (-)
	Moles of methane produced per mole hydrogen consumed (methanogen)	b_{HM}	0.25 (-)
Henry constants	Hydrogen	ρ_H	1.364 (atm mM^{-1})
	Methane	ρ_M	0.897 (atm mM^{-1})
State variables	Lactate concentration	L	(mM)
	Sulphate concentration	S	(mM)
	Aqueous hydrogen concentration	H_{aq}	(mM)
	Gaseous hydrogen concentration	H_g	(atm)
	Aqueous methane concentration	M_{aq}	(mM)
	Gaseous methane concentration	M_g	(atm)
	Acetate concentration	A	(mM)
	H_2S concentration	P	(mM)
	SRB cell concentration	X_S	(mg L^{-1})
	Methanogen cell concentration	X_M	(mg L^{-1})
	Volume of the aqueous phase	V_{aq}	Taken equal to experimental methods (L)
	Volume of the gaseous phase	V_g	Taken equal to experimental methods (L)
	Aqueous dilution rate	D	Taken equal to experimental methods (h^{-1})
	Gaseous dilution rate	d	Taken equal to experimental methods (h^{-1})
	Lactate inflow	I_L	Taken equal to experimental methods (mM h^{-1})
	Time	t	(h)
SRB: sulphate-reducing bacteria.			

Table B3. Markov chain Monte Carlo-determined correlations between model parameters in the 9-parameter set

	Initial ratio	$k_L a_H$	$k_L a_M$	$\mu_{max,L}$	K_L	Y_L	H_{max}	$K_{H,M}$	Y_H
Initial ratio	1	0.0418	0.3382	0.2220	0.2074	-0.2465	0.0607	0.2449	0.3947
$k_L a_H$		1	-0.0044	0.0696	-0.6275	-0.0986	-0.4354	-0.7612	-0.1317

$k_L a_M$			1	-0.2590	-0.1509	-0.2471	0.0360	0.3121	0.2252
$\mu_{max,L}$				1	0.4942	-0.0830	0.0904	-0.0361	0.2844
K_L					1	0.1349	0.1909	0.5787	0.2521
Y_L						1	-0.4817	-0.0385	-0.6256
H_{max}							1	0.4357	0.4426
$K_{H,M}$								1	0.3522
Y_H									1

Table B4. Markov chain Monte Carlo-determined correlations between model parameters in the 6-parameter set.

	Initial ratio	$k_L a_H$	$k_L a_M$	Y_L	H_{max}	Y_H
Initial ratio	1	0.0413	0.3929	0.1209	-0.0076	0.0448
$k_L a_H$		1	0.1551	0.1345	0.0583	0.0084
$k_L a_M$			1	0.1508	0.0463	0.0800
Y_L				1	0.2155	-0.0034
H_{max}					1	-0.1535
Y_H						1

References

Goyal, N., Padhiary, M., Karimi, I.A., and Zhou, Z. (2015). Flux measurements and maintenance energy for carbon dioxide utilization by *Methanococcus maripaludis*. Microb. Cell Fact. 14(1), 146. doi: 10.1186/s12934-015-0336-z.

Muñoz-Tamayo, R., Popova, M., Tillier, M., Morgavi, D.P., Morel, J.P., Fonty, G., et al. (2019). Hydrogenotrophic methanogens of the mammalian gut: Functionally similar, thermodynamically different-A modelling approach. PLoS ONE 14(12). doi: 10.1371/journal.pone.0226243.

Stolyar, S., Van Dien, S., Hillesland, K.L., Pinel, N., Lie, T.J., Leigh, J.A., et al. (2007). Metabolic modeling of a mutualistic microbial community. Mol. Syst. Biol. 3, 92.

Appendix C

C1: microPop equations

The Monod-based equations constructed and solved by microPop are fully described in the supporting materials for the R package (Kettle et al., 2017) and in a previous publication of a similar model structure (Kettle et al., 2015). Here, the general forms of the equations are briefly described.

Let X denote the concentration (g L^{-1}) of a single MFG population. The rate of change of X is given by the differential equation:

$$\frac{dX}{dt} = X_{in} + \mu X - DX \tag{C1}$$

where X_{in} is the inflow of the MFG into the model compartment, μ is the growth rate of the MFG and D is the dilution rate of the model compartment.

Each MFG has a given number of metabolic pathways available to it, N_m. The growth rate of the MFG, μ (h^{-1}), is calculated as follows:

$$\mu = \sum_{i=1}^{Nm} \frac{{\mu_i}^2}{\sum_{j=1}^{N_m} \mu_j} \tag{C2}$$

where μ_i are the growth rates (h^{-1}) of the MFG calculated for each pathway available to the MFG. The growth rate of the MFG is therefore scaled by the magnitude of the growth rate for each available pathway, rather than being the sum of all pathway growth rates.

μ_i is calculated differently depending on the nature of the substrates. If a substrate is perfectly substitutable for another on the same pathway, then each substrate is used indiscriminately according to its concentration. Let:

$$\lambda_{Ss}(S_i) = \frac{S_i/K_i}{1 + \sum_{j=1}^{N_s} S_j/K_j} \tag{C3}$$

where λ_{Ss} is the growth limitation function for the substitutable substrate S_i. K_i is the half-saturation constant for S_i. K_j is the half-saturation constant for S_j, with j representative of all

substitutable substrates available on this pathway. N_s is the number of substitutable substrates on the pathway.

If a substrate is essential, with no growth possible in its absence, then the growth limitation function is simply:

$$\lambda_{Se}(S_i) = \frac{S_i}{S_i + K_i}. \tag{C4}$$

The final substrate class is boost substrates: substrates that, if available, increase the growth rate on a certain pathway by a fixed proportion. Let f_b be the proportion of the maximum growth rate achievable by the MFG in the absence of the boost substrate. Then:

$$\lambda_b = f_b + (1 - f_b)\lambda_{Se}(S_b) \tag{C5}$$

where λ_b is the boost limitation function. Finally, pH limitation is included as the value λ_{pH}, lying in the interval [0,1], determined by the pH preferences of the MFG and the current pH value in the model compartment. Each MFG has four pH corners which define its upper and lower bounds for growth, and the upper and lower bounds for optimal growth. A λ_{pH} value of 1 is assigned if the pH is within the optimal growth bounds and a value of 0 is assigned if the pH is outside the growth bounds. If the pH is outside the optimal growth bounds but inside the growth bounds, a λ_{pH} value between 0 and 1 is assigned, with this value linearly decreasing as pH moves further from the optimal range.

The general form of μ_i is thus:

$$\mu_i = \lambda_{pH}\lambda_b \left(\mu_{ess}^m \prod_{j=1}^{N_{ess}} \lambda_{Se}(S_j) \right) \left(\sum_{l=1}^{N_s} \mu_l^m \lambda_{Ss}(S_l) \right) \tag{C6}$$

where N_{ess} is the number of essential resources on the pathway. If there exist solely substitutable resources on the pathway, then the terms relating to essential substrate metabolism are removed, but otherwise μ_{ess}^m is the maximum growth rate of this MFG on the essential pathway. μ_l^m is the maximum growth rate of the MFG on substitutable resource S_l.

The rate of change in the concentration of a resource is the sum of its inflow into the model compartment and its production by MFGs, minus its outflow from the model compartment and

uptake by MFGs. The uptake rate of a substitutable resource S_i by MFG X on the pathway with growth rate μ_i is:

$$\lambda_{pH}\lambda_b\lambda_{Ss}(S_i)\mu_i^m\frac{X}{Y_{X,S_i}} \tag{C7}$$

where Y_{X,S_i} is the growth yield of MFG X on substrate S_i. In the case of essential resources, where multiple resources are considered, the stoichiometry of the reaction is included in the uptake. Let S_k be the key resource of the pathway (one of the essential resources). Then the uptake rate of an essential resource S_i is:

$$\left(\frac{m_i n_i}{m_k n_k}\right)\lambda_{pH}\lambda_b\mu_{ess}^m\lambda_{Se}(S_k)\frac{X}{Y_{X,S_k}}. \tag{C8}$$

Here, the values m_i and n_i are the molar mass and reaction stoichiometry of S_i, and m_k and n_k the corresponding values for the key resource.

Finally, for the uptake of a boost substrate, the uptake of the substitutable resources is scaled by the reaction stoichiometry for the boost substrate to give the boost substrate uptake rate:

$$\frac{m_b n_b}{\frac{1}{N_s}\sum_{i=1}^{N_s} m_i n_i}\left(\lambda_{pH}\lambda_b\sum_{j=1}^{N_s}\left(\frac{\lambda_{Ss}(S_j)\mu_j^m}{Y_{X,S_j}}\right)X\right). \tag{C9}$$

Here, i indexes the substitutable substrates involved in the pathway, and b indexes the boost substrate.

For the production of metabolites by MFGs, let U_i denote the uptake of S_i on a given pathway. Then the production of metabolite j is given by:

$$\frac{m_j n_j}{\sum_{k=1}^{N_p} m_k n_k}\left(\sum_{i=1}^{N_{alls}} U_i - dX\right) \tag{C10}$$

where N_p and N_{alls} are the total number of products and substrates involved in the pathway, respectively, and dX is the growth rate of the MFG on this pathway.

C2: Summary of parameter values and metabolic pathways for the three hydrogenotrophic microbial functional groups

The metabolic pathways available to the Acetogen MFG are as follows:

$4\ H_2 + 2\ CO_2 \rightarrow$ Acetate $+ 2\ H_2O$

NSP/RS/Sugars + 2 Formate $\rightarrow$ 3 Acetate $+ 2\ H_2 + 2\ CO_2$

NSP/RS/Sugars $\rightarrow$ 3 Acetate.

The metabolic pathways available to the Methanogen MFG are as follows:

$4\ H_2 + CO_2 \rightarrow CH_4 + 2\ H_2O$

4 Formate $\rightarrow CH_4 + 2\ H_2O + 3\ CO_2$.

The metabolic pathways available to the SRB MFG are as follows:

$5\ H_2 +$ 1 Sulphate $\rightarrow H_2S + 4\ H_2O$

4 Formate + Sulphate $\rightarrow H_2S + 4\ H_2O + 4\ CO_2$

Lactate $+ 2\ H_2O \rightarrow$ Acetate $+ 2.5\ H_2 +$ Bicarbonate.

The SRB metabolic pathway involving formate was not studied in Chapter 4 and there is a lack of data to parameterise a monoculture model for this pathway. Therefore, the maximum growth rate and yield parameters for formate utilisation are taken as equal to those of hydrogen metabolism, while the half-saturation value for formate is taken as equal to that of the acetogens and methanogens from microPop.

Table C1. Newly derived parameter values for the hydrogenotrophic microbial functional groups. Parameter value is given, followed by the substrate to which it corresponds in brackets. Values in bold are alterations or additions to the original microPop values; all others are unchanged				
		Acetogens	Methanogens	Sulphate-reducing bacteria
Pathway 1	halfSat (g L^{-1})	**0.5975 (H_2)** 0.001 (CO_2)	**0.0214 (H_2)** 0.001 (CO_2)	**2.02 x10^{-6} (H_2)** **0.00307 (Sulphate)**
	yield (g g^{-1})	**0.9218 (H_2)**	**0.891 (H_2)**	**0.0463 (Sulphate)**
	maxGrowthRate (d^{-1})	**9.55**	**2.5**	**0.72**
Pathway 2	halfSat (g L^{-1})	0.001 (Formate) 0.001 (NSP/RS/Sugars)	0.001 (Formate)	**0.001 (Formate)** **0.00307 (Sulphate)**
	yield (g g^{-1})	0.286/0.333/0.333 (NSP/RS/Sugars)	0.00724 (Formate)	**0.0463 (Sulphate)**
	maxGrowthRate (d^{-1})	6/6/24 (NSP/RS/Sugars)	2.4	**0.72**
Pathway 3	halfSat (g L^{-1})	0.001 (NSP/RS/Sugars)	-	**0.126 (Lactate)**
	yield (g g^{-1})	0.286/0.333/0.333 (NSP/RS/Sugars)	-	**0.0627 (Lactate)**
	maxGrowthRate (d^{-1})	6/6/24 (NSP/RS/Sugars)	-	**2.784**
NSP: non-starch polysaccharide. RS: resistant starch				

C3: Metabolite influx rates for comparison to experimental data

Metabolite influx values were converted from the media contents lists in the original publications to microPop metabolites following Kettle et al. (2015). The conversion for the growth medium in Walker et al. (2005) is shown in Tables C2 and C3. The medium of Belenguer et al. (2011) is similar to that of Walker et al. (2005), except for protein influx, which was 2 g L^{-1} d^{-1}. The conversion for the growth medium of Payne et al. (2011) is shown in Tables C4 and C5.

For the simulation of the human colon, microPop:Colon influx concentrations are given in Table C6.

Table C2. Conversion of Walker et al. (2005) growth medium constituents to microPop metabolites		
Ingredient	Concentration (% wt/vol)	Conversion factors
Potato starch	0.5	100% RS
Xylan	0.06	100% NSP
Pectin	0.06	100% NSP
Amylopectin	0.06	100% RS
Arabinogalactan	0.06	100% NSP
Peptide mixture	0.1 or 0.6*	100% Protein
*Varied between experiments. NSP: non-starch polysaccharide. RS: resistant starch.		

Table C3. microPop metabolite inflow rates, based on Walker et al. (2005). Initial concentration and inflow rate for all other metabolites are set to 0		
Metabolite	**Initial concentration (g L^{-1})**	**Inflow rate (g L^{-1} d^{-1})**
Protein	1 or 6[a]	1 or 6[a]
NSP	1.8	1.8
RS	5.6	5.6
Acetate	1.95	0
Propionate	0.67	0
Butyrate	0.44	0
CO_2	10	10
H_2O	10	10
[a]Varied between experiments. NSP: non-starch polysaccharide. RS: resistant starch.		

Table C4. Conversion of Payne et al. (2012) growth medium constituents to microPop metabolites				
Ingredient	**Concentration (g L^{-1})**			**Conversion factors**
	HE medium	**NE medium**	**LE medium**	
Pectin	1	2	1.2	100% NSP
Xylan	1	2	1.2	100% NSP
Arabinogalactan	2	2	1.2	100% NSP
Guar gum	1	1	0.4	100% NSP
Inulin	1	1	0.4	100% NSP
Soluble starch	9	5	2.4	100% RS
Granular amylopectin maize starch	4	4	1	100% RS
D-fructose	6	3	1.2	100% Sugars
Mucin	4	4	4	100% Mucin
Casein acid hydrolysate	5	3	1.2	100% Protein
Peptone water	5	5	2	100% Protein
Bacto™ Tryptone	5	5	2	100% Protein
Yeast extract	4.5	4.5	1.8	100% Protein
HE: high-energy. LE: low-energy. NE: normal-energy. NSP: non-starch polysaccharide. RS: resistant starch.				

Table C5. microPop metabolite concentrations in medium, based on Payne et al. (2012). Concentrations for all other metabolites are set to 0			
Metabolite	**HE medium (g L^{-1})**	**NE medium (g L^{-1})**	**LE medium (g L^{-1})**
Protein	19.5	17.5	7
NSP	6	8	4.4
RS	13	9	3.4
Sugars	6	3	1.2
Mucin	4	4	4
CO_2	10	10	10
H_2O	10	10	10
HE: high-energy. LE: low-energy. NE: normal-energy. NSP: non-starch polysaccharide. RS: resistant starch.			

Table C6. microPop:Colon metabolite initial concentrations and inflow rates			
Metabolite	**Initial concentration in proximal compartment (g L^{-1})**	**Inflow rate (g L^{-1} d^{-1})**	**Reference/explanation**
Protein	5	5	Cummings and Macfarlane (1991)
NSP	12	12	Cummings and Macfarlane (1991)
RS	20	20	Cummings and Macfarlane (1991)
Sugars	0	0	Simple sugars assumed to have been absorbed in small intestine
H_2	0	0	[c]
CO_2	0.22[b]	0	[c]
CH_4	0	0	[c]
H_20	10	10	Set high as assumed abundant and non-limiting in the colon environment
Acetate	0	0	[c]
Propionate	0	0	[c]
Succinate	0	0	[c]
Lactate	0	0	[c]
Formate	0	0	[c]
Ethanol	0	0	[c]
Butyrate	0	0	[c]
Sulphate	0.86	0.86	Florin et al. (1991)
H_2S	0	0	[c]
Bicarbonate	1.53[b]	13.6 (g d^{-1}) [a]	Gennari and Weise (2008) Charney and Donowitz (2005) Davis et al. (1983)
Other	0	0	[c]
Mucin	5[a]	5[a]	Florin et al. (1991) Stephen et al. (1983)

[a]Divided into each of the three compartments based on their relative volume in the discrete model.
[b]CO_2 and bicarbonate concentrations were set initially at these values in all model compartments. The initial CO_2 concentration was calculated based on the bicarbonate value to ensure neutral pH at model initiation.
[c]Product of microbial metabolism assumed negligible before colon.
NSP: non-starch polysaccharide. RS: resistant starch.

C4: Microbial abundance calculations

The probe data from Walker et al. (2005) and Payne et al. (2012) were used to derive initial MFG abundances as performed by Kettle et al. (2015). The conversion used was:

Concentration (g L^{-1}) = [Counts (cells ml^{-1})] x [8.5×10^{-9}]

with the assignment of probe data to MFGs shown in Tables C7 and C9 for the Walker et al. (2005) and Payne et al. (2011) data sets, respectively. Since no data were available for the SRB from Walker et al. (2005), the initial count for this MFG was assumed equal to that of the methanogens.

Conversions from the original publication to microPop MFGs for all data used in the validations is shown in Tables C8 and C10.

For the simulation of the experimental work carried out by Payne et al. (2012), an initial inoculum concentration of 1 g L^{-1} was assumed. This was made up of all 11 MFGs, with the concentration of each determined by its proportion of the initial population, as calculated from Table C10.

Table C7. Assignment of probe counts from Walker et al. (2005) to microPop microbial functional groups (MFGs)

MFG	**Probe assignment**
Bacteroides	Bac303
NoButyStarchDeg	0.5 (Rfla729+Rbro730) + 0.3 (Erec482-Rrec584)
NoButyFibreDeg	0.5 (Rfla729+Rbro730) + 0.3 (Erec482-Rrec584)
LactateProducers	Bif164 + Ato291
ButyrateProducers1	Rrec584
ButyrateProducers2	Fprau645
PropionateProducers	Prop853
ButyrateProducers3	0.3 (Erec482 - Rrec584)
Acetogens	0.1 (Erec482 - Rrec584)
Methanogens	0.001 Eub
Sulphate-reducing bacteria	0.001 Eub

Table C8. Microbial functional group (MFG) concentrations converted from original measurements in Walker et al. (2005)										
MFG	**Concentration (g L^{-1})**									
	Figure 8.1 (6 g L^{-1} peptide, Donor 2)		**Figure 8.2 (1 g L^{-1} peptide, Donor 2)**		**Figure 8.3 (6 g L^{-1} peptide, Donor 1)**			**Figure 8.4 (6 g L^{-1} peptide, Donor 2)**		
	Initial	**Final**	**Initial**	**Final**	**Initial**	**Mid-point**	**Final**	**Initial**	**Mid-point**	**Final**
Bacteroides	0.0399	1.26	0.0399	0.0629	0.0179	0.349	1.879	0.0527	0.214	2.35
NoButyStarchDeg	0.000255	0.0464	0.000255	0.0293	0.0328	0.0928	0.0553	0.0396	0.125	0.0966
NoButyFibreDeg	0.000255	0.0464	0.000255	0.0293	0.0328	0.0928	0.0553	0.0396	0.125	0.0966
LactateProducers	0.0468	0.0068	0.0468	0.0119	0.00425	0.0128	0.00255	0.0196	BD	BD
ButyrateProducers1	0.0289	BD	0.0289	0.0153	0.0213	0.205	BD	0.0595	0.29	BD
ButyrateProducers2	0.00255	0.0017	0.00255	BD	0.0187	0.085	0.0272	0.0485	0.0697	0.0519
PropionateProducers	0.0332	0.00765	0.0332	0.00085	0.0111	0.0153	0.111	0.0315	0.0476	0.0536
ButyrateProducers3	0.000255	0.0464	0.000255	0.0293	0.0247	0.0928	0.0362	0.0337	0.125	0.0966
Acetogens	8.5e-05	0.0155	8.5e-05	0.00978	0.00825	0.0309	0.0121	0.0112	0.0417	0.0322
Methanogens	0.000232	0.00164	0.000232	0.000388	0.000428	0.00109	0.00224	0.00041	0.00207	0.0029
Sulphate-reducing bacteria	0.000232	ND	0.000232	ND	0.000428	ND	ND	0.00041	ND	ND
Note that the inocula for Figures 8.1 & 8.2 are identical, as both these experiments used a microbial population from the same faecal sample. ND: No Data. BD: Below Detection.										

Table C9. Assignment of bacterial populations from Payne et al. (2012) to microPop microbial functional groups (MFGs)	
microPop MFG	**Assignment from measured bacterial groups in original publication (primers used)**
Bacteroides	*Bacteroides* (Bac303F, Bfr-Femrev)
NoButyStarchDeg	0.5 * [Firmicutes (Firm934F, Firm1060R) - *Roseburia* sp., *E. rectale* (RrecF, Rrec630mR) - *E. hallii* (EhalF, EhalR) - *F. prausnitzii* (FPR-2F, Fprau645R) - *Veillonella* spp. (Vpa-X84005_F, Vpa_X84005_R) - *Lactobacillus* (F_Lacto 05, R_Lacto 04)]
NoButyFibreDeg	0.5 * [Firmicutes (Firm934F, Firm1060R) - *Roseburia* sp., *E. rectale* (RrecF, Rrec630mR) - *E. hallii* (EhalF, EhalR) - *F. prausnitzii* (FPR-2F, Fprau645R) - *Veillonella* spp. (Vpa-X84005_F, Vpa_X84005_R) - *Lactobacillus* (F_Lacto 05, R_Lacto 04)]
LactateProducers	*Bifidobacterium* (xfp-fw, xfp-rv) + *Lactobacillus* (F_Lacto 05, R_Lacto 04) + Enterobacteriaceae (Eco1457F, Eco1652R)
ButyrateProducers1	*Roseburia* sp., *E. rectale* (RrecF, Rrec630mR)
ButyrateProducers2	*F. prausnitzii* (FPR-2F, Fprau645R)
PropionateProducers	*Veillonella* spp. (Vpa-X84005_F, Vpa_X84005_R)
ButyrateProducers3	*E. hallii* (EhalF, EhalR)
Acetogens	0.01 * Firmicutes (Firm934F, Firm1060R)
Methanogens	0.001 * Total bacteria (Eub 338F, Eub 518R)
Sulphate-reducing bacteria	Sulphate-reducing bacteria (dsrA_290F, dsrA_660R)

Table C10. Microbial functional group (MFG) concentrations converted from original measurements in Payne et al. (2012)

MFG	Concentration (g L^{-1})																			
	Faeces		High-energy						Normal-energy						Low-energy					
			Comp. 1		Comp. R2		Comp. R3		Comp. 1		Comp. R2		Comp. R3		Comp. 1		Comp. R2		Comp. R3	
	A	B	A	B	A	B	A	B	A	B	A	B	A	B	A	B	A	B	A	B
Bacteroides	4.26E-03	3.83E-03	1.07E-06	5.36E-05	1.07E-02	6.75E-03	1.35E-02	8.50E-03	3.38E-05	2.14E-04	2.14E-02	6.75E-03	2.14E-02	8.50E-03	2.14E-03	4.26E-03	1.07E-02	1.35E-02	2.14E-02	1.35E-02
NoButyStarchDeg	5.98E-04	2.13E-03	2.61E-03	2.00E-03	3.08E-03	2.78E-03	3.14E-03	1.42E-03	0	2.61E-03	3.50E-04	2.86E-03	6.37E-04	2.49E-03	1.15E-02	1.00E-02	3.65E-03	4.88E-03	3.83E-04	3.99E-03
NoButyFibreDeg	5.98E-04	2.13E-03	2.61E-03	2.00E-03	3.08E-03	2.78E-03	3.14E-03	1.42E-03	0	2.61E-03	3.50E-04	2.86E-03	6.37E-04	2.49E-03	1.15E-02	1.00E-02	3.65E-03	4.88E-03	3.83E-04	3.99E-03
LactateProducers	1.71E-05	1.34E-04	2.69E-03	4.85E-04	3.03E-03	2.16E-03	2.81E-03	1.82E-03	4.31E-04	1.79E-03	2.23E-03	1.62E-03	4.73E-03	1.76E-03	1.05E-04	1.91E-03	1.81E-03	1.48E-03	3.72E-03	7.39E-04
ButyrateProducers1	5.36E-03	2.14E-04	3.38E-05	2.69E-03	2.69E-05	4.26E-03	1.70E-05	8.50E-04	5.36E-03	1.07E-03	8.50E-04	1.07E-03	6.75E-04	6.75E-04	1.07E-02	1.35E-02	2.69E-03	1.70E-02	1.07E-03	5.36E-03
ButyrateProducers2	1.07E-03	8.50E-04	5.36E-08	5.36E-09	3.38E-05	1.07E-05	3.38E-05	1.35E-05	8.50E-08	4.26E-09	1.07E-05	8.50E-06	1.70E-05	1.07E-05	3.38E-08	4.26E-08	8.50E-06	3.38E-06	1.70E-05	2.69E-06
PropionateProducers	8.50E-04	8.50E-13	8.50E-13	8.50E-13	1.07E-09	8.50E-13	8.50E-10	8.50E-13	8.50E-13	8.50E-13	2.14E-09	8.50E-13	8.50E-13	8.50E-13	8.50E-08	8.50E-13	5.36E-08	8.50E-13	8.50E-13	8.50E-13
ButyrateProducers3	2.14E-05	1.07E-05	1.07E-04	6.75E-05	5.36E-04	8.50E-04	4.26E-04	5.36E-04	2.14E-05	4.26E-04	1.35E-04	1.70E-03	1.70E-04	1.07E-03	2.14E-05	1.07E-04	3.38E-05	8.50E-05	1.35E-05	6.75E-05
Acetogens	8.50E-05	5.36E-05	5.36E-05	6.75E-05	6.75E-05	1.07E-04	6.75E-05	4.26E-05	5.36E-05	6.75E-05	1.70E-05	8.50E-05	2.14E-05	6.75E-05	3.38E-04	3.38E-04	1.07E-04	2.69E-04	2.14E-05	1.35E-04
Methanogens	8.50E-05	1.07E-04	1.07E-04	1.07E-04	1.70E-04	1.70E-04	1.70E-04	1.35E-04	6.75E-14	1.07E-04	1.35E-04	1.07E-04	1.70E-04	1.07E-04	1.70E-05	3.38E-05	2.69E-05	4.26E-05	1.70E-05	3.38E-05
SRB	3.38E-07	3.38E-06	4.26E-09	4.26E-09	1.07E-09	1.07E-09	2.69E-09	2.69E-09	5.36E-09	3.38E-09	1.07E-09	4.26E-09	2.69E-09	1.35E-09	1.07E-09	1.35E-09	1.07E-08	2.69E-09	2.69E-06	8.50E-06

Comp.: Compartment

C5: Addition of mucin and alterations to Bacteroides microbial functional group

Mucin was added as a metabolite in microPop, assuming a molar mass of 162.12 g mol^{-1} so that the metabolic pathway formulated maintained mass balance. Mucin would be expected to have a greater molar mass than this, but this simplification has no effect on the model output.

The following metabolic pathway was added to the Bacteroides MFG, based on literature evidence and previous modelling (Kettle et al., 2015; Sung et al., 2017):

Mucin → 0.2 Protein + 0.5 NSP + 0.25 Sugars + 0.05 Sulphate.

Since data to parameterise the growth of a *Bacteroides* strain on mucin were not available, assumptions were made based on the literature for the parameter values corresponding to this metabolic pathway. The half-saturation constant was set to 0.001 g L^{-1}, to match that of Protein, NSP and RS for the Bacteroides MFG. The yield was set to 0.01 g g^{-1}, as it was expected that this MFG grows predominantly during the subsequent metabolism of mucin constituent metabolites, rather than during mucin breakdown itself. The maximum growth rate was set to 3.3 d^{-1}, based on growth rates of *B. thetaiotaomicron*, an abundant GIT strain, cultured with porcine mucin (Pudlo et al., 2015). Finally, the pH preferences of the Bacteroides MFG was altered so that this MFG was now active down to a lower limit of pH 5.3, based on experimental evidence (Duncan et al., 2009).

C6: pH modelling

As mentioned in the main text, model pH is determined from the concentration of H^+ ions, which must satisfy both the carbonate acid-base equilibrium equation and the charge balance equation. The charge balance equation is as follows:

$$s_{cat^+} + s_{H^+} - \left(s_{HCO_3^-} + s_{SCFA^-} + s_{OH^-} + C\right) = 0 \quad \text{(C11)}$$

where s_i denotes the molar concentration of molecule i, and i may represent cat^+ (miscellaneous cations), H^+ (H^+ ions), HCO_3^- (bicarbonate), $SCFA^-$ or OH^- (hydroxide ions). C is the number of moles of bicarbonate produced from CO_2 during buffering of the colonic lumen. The value of C is determined via the carbonate acid-base equilibrium equation, as discussed later in this

section. Note that this value is negative if the net reaction is conversion of bicarbonate and H^+ ions to CO_2.

Next, the acid-base equilibrium equations for SCFA and hydroxide are defined:

$$s_{SCFA^-} = \frac{K_{SCFA} s_{SCFA}}{K_{SCFA} + s_{H^+}} \quad \text{(C12)}$$

$$s_{OH^-} = \frac{K_w}{s_{H^+}} \quad \text{(C13)}$$

where K_{SCFA} and K_w are the acid-base equilibrium constants for SCFAs and water, respectively. s_{SCFA} is the total concentration of both dissociated and undissociated SCFAs:

$$s_{SCFA} = s_{SCFA^-} + s_{HSCFA}.$$

Using these acid-base equilibrium equations, equation C11 may be rewritten as:

$$s_{cat^+} + s_{H^+} - \left(s_{HCO_3^-} + \frac{K_{SCFA} s_{SCFA}}{K_{SCFA} + s_{H^+}} + \frac{K_w}{s_{H^+}} + C \right) = 0. \quad \text{(C14)}$$

Equation C14 can be rearranged to give a polynomial of degree three in s_{H^+}, which is then solved by the model and used to calculate the pH value:

$$\text{pH} = -\log\left(s_{H^+}\right).$$

Note that the use of the charge balance equation and acid-base equilibrium equations that form the basis of this pH model are adapted from Batstone et al. (2002) and Muñoz-Tamayo et al. (2016). To capture the interconversion between $CO_2 + H_2O$ and $HCO_3^- + H^+$, the following term is appended to the microPop:Colon differential equation for bicarbonate:

$$r[\text{HCO}_3^-](K_{a,CO_2} s_{CO2} - s_{HCO_3^-} s_{H^+})$$

where $[\text{HCO}_3^-]$ is the concentration of bicarbonate in g L^{-1} and r is a rate term with units M^{-2} d^{-1}, which is set at a large value, given that the acid-base reaction it controls is assumed to take place almost instantaneously. This term is positive if the equilibrium between CO_2 and bicarbonate is unbalanced by too great a concentration of CO_2, and negative if unbalanced by too great a concentration of bicarbonate. The differential equation in C given by:

$$\frac{dC}{dt} = r s_{HCO_3^-}(K_{a,CO_2} s_{CO2} - s_{HCO_3^-} s_{H^+})$$

gives a record of the amount of bicarbonate converted to CO_2 or vice versa throughout the model simulation. It is this value that can be input into equation C14 for determining s_{H^+}.

The use of this term influences metabolite concentrations towards the balancing of the charge balance equation over short time periods, far less than a single model timestep. A corresponding term is included in the differential equation for water and CO_2, with consideration of molar masses as per the normal stoichiometric rules for microPop.

Finally, before the model is initiated, the value of s_{cat^+} and the initial CO_2 concentration are calculated to ensure that pH is neutral at initial time. The acid-base equilibrium equation for carbonates can be rearranged to give the initial CO_2 concentration:

$$s_{CO2} = \frac{10^{-7} s_{HCO_3^-}}{K_{a,CO_2}}$$

noting that pH 7 is achieved when $s_{H^+} = 10^{-7}$. Thus, the value of s_{cat^+} remains fixed at:

$$s_{cat^+} = -s_{H^+} + s_{HCO_3^-} + s_{SCFA^-} + s_{OH^-} + C$$

$$= -10^{-7} + s_{HCO_3^-} + \frac{K_{SCFA} s_{SCFA}}{K_{SCFA} + 10^{-7}} + \frac{K_w}{10^{-7}} + 0$$

where only the initial bicarbonate and SCFA concentration may vary between model runs.

Data in the literature for the absorption and secretion rates of CO_2 and bicarbonate in the colon are limited. However, it is known that colonic CO_2 absorption is rapid, hence its preferred use in medical insufflation (Cotton and Williams, 2008; Baniya et al., 2017), and that the CO_2 concentration in the canine colon tended to an equilibrium value of approximately 75 mM at a maximum rate (using the concentrations tested) of approximately 60 mM h^{-1} (Swallow and Code, 1967). While these values cannot be directly translated to the human colon, an upper estimate absorption coefficient of 65 d^{-1} was assumed in the model to allow for a rapid return to the initial concentration following perturbation by microbially produced CO_2. Thus, the following term was appended to the differential equation for CO_2:

$$-\frac{abs_{CO2}}{s_{CO2}} (s_{CO2} - s_{CO2,initial})$$

where abs_{CO2} is the absorption coefficient and $s_{CO2,initial}$ is the initial CO_2 concentration.

C7: Supplementary figures

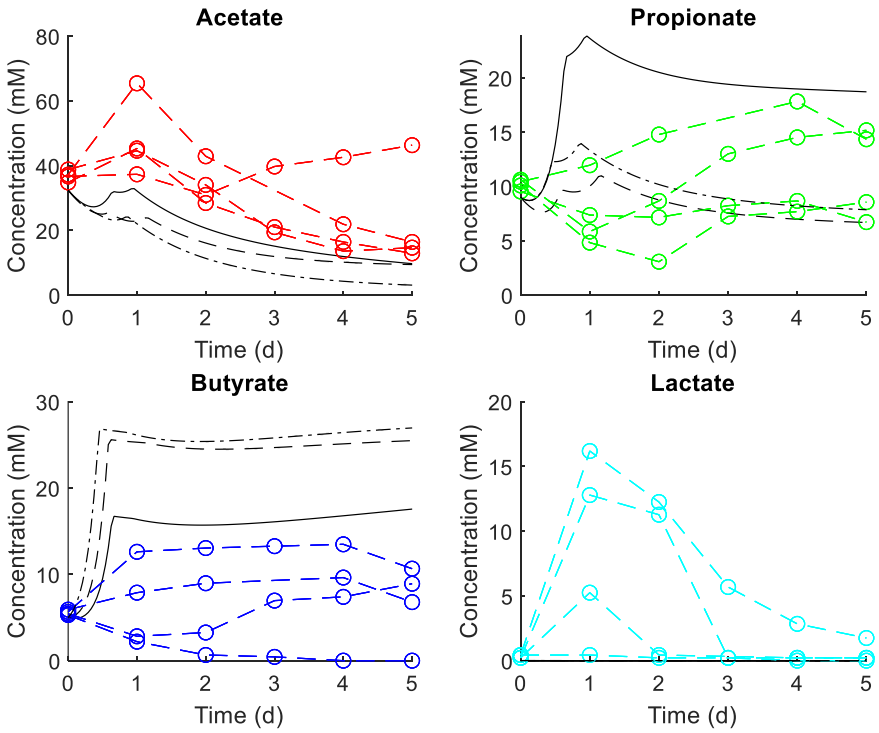

Figure C1. Model predictions (black lines) for short chain fatty acid production compared to experimental data (coloured lines represent the four subjects analysed) from Belenguer et al. (2011) for a faecal culture at pH 5.5. The Alpha parameter set was used in this instance. Note that it was not possible to convert the data on the initial inoculum to microPop microbial functional groups, thus three examples of faecal inocula derived from data in Walker et al. (2005) are shown instead (black lines).

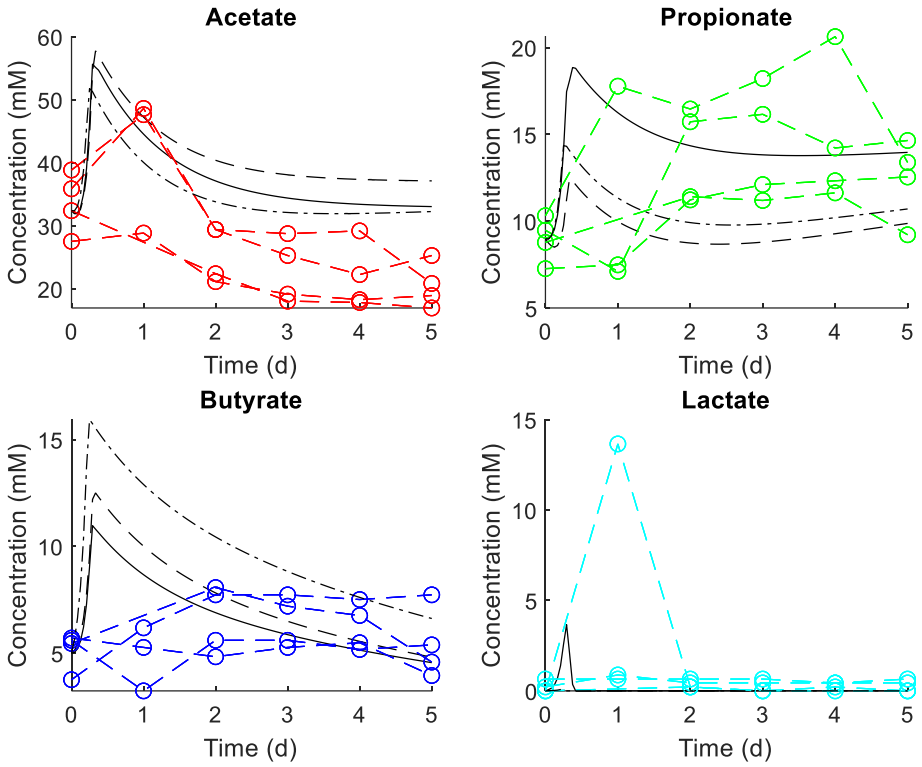

Figure C2. Model predictions (black lines) for short chain fatty acid production compared to experimental data (coloured lines represent the four subjects analysed) from Belenguer et al. (2011) for a faecal culture at pH 6. The Beta parameter set was used in this instance. Note that it was not possible to convert the data on the initial inoculum to microPop microbial functional groups, thus three examples of faecal inocula derived from data in Walker et al. (2005) are shown instead (black lines).

C8: Parameter values for the Beta parameter set

The alterations to the parameter values of the original microPop MFGs made by Wang et al. (Under review) and used in the construction of the Beta parameter set are listed in Table C11. Note that only those parameter values that were changed are listed here; all other parameters retain the Alpha parameter set value. Moreover, the parameter changes made to the hydrogenotrophic MFGs and the Bacteroides MFG detailed in Table C1 and section C5 supersede those detailed below.

In addition to these MFG parameter changes, the molar mass of 'Protein' was changed from 134 to 111 g mol^{-1} and the molar mass of 'other' was changed from 41 to 1 g mol^{-1}. Both of these metabolites are only involved in pathway 2 of the Bacteroides MFG.

Table C11. Alterations to microbial functional group (MFG) parameter values between Alpha and Beta parameter sets

MFG	Parameter	Alpha parameter set values	Beta parameter set values
Bacteroides	Maximum growth rates on pathway 1	NSP: 12 RS: 24	NSP: 16 RS: 16
	Maximum growth rates on pathway 2	Protein: 24	Protein: 9
	Stoichiometry on pathway 2	3 Protein -> 2 Acetate + 1 Propionate + 1 Succinate + 2 H2 + 1 CO2 + 1 other	6 Protein -> 2 Acetate + 1 Propionate + 1 Succinate + 2 H2 + 1 CO2 + 305.68 other
	pH corners	[5.6; 6.35; 7.85; 8.6]	[5.05; 5.8; 7.2; 7.4]
NoButyStarchDeg	Maximum growth rates on pathway 1	NSP: 3.6 RS: 14.4	NSP: 3 RS: 15
	pH corners	[5.35; 6.1; 7.6; 8.35]	[4.75; 5.5; 7.2; 7.4]
NoButyFibreDeg	Maximum growth rates on pathway 1	NSP: 16.8 RS: 3.6	NSP: 16 RS: 6
	pH corners	[5; 5.75; 7.25; 8]	[4.75; 5.5; 7.2; 7.4]
LactateProducers	Maximum growth rates on pathway 1	NSP: 7.2 RS: 6	NSP: 9 RS: 12
	pH corners	[4.95; 5.7; 7.2; 7.95]	[4.5; 5.25; 7.2; 7.4]
ButyrateProducers1	Maximum growth rates on pathway 1	NSP: 8.4 RS: 8.4	NSP: 9 RS: 12
	Stoichiometry on pathway 1	2 Hexose (+ 2 Acetate boost) -> 3 Butyrate + 2 H2 + 4 CO2 + 2 H2O	4 Hexose (+ 2 Acetate boost) -> 5 Butyrate + 6 H2 + 8 CO2 + 2 H2O
	pH corners	[4.95; 5.7; 7.2; 7.95]	[4.75; 5.5; 7.2; 7.4]
ButyrateProducers2	Maximum growth rates on pathway 1	NSP: 14.4 RS: 7.2	NSP: 12 RS: 6
	pH corners	[4.85; 5.6; 7.1; 7.85]	[4.75; 5.5; 7.2; 7.4]
PropionateProducers	Maximum growth rates on pathway 1	NSP: 7.2 RS: 7.2	NSP: 6 RS: 6
	Maximum growth rates on pathway 2	Lactate: 4.8	Lactate: 4
	pH corners	[4.75; 5.5; 7; 7.75]	[4.75; 5.5; 7.2; 7.4]
ButyrateProducers3	Maximum growth rates on pathway 1	NSP: 7.2 RS: 7.2	NSP: 6 RS: 6
	Maximum growth rates on pathway 2	Lactate: 4.8	Lactate: 4
	pH corners	[4.85; 5.6; 7.1; 7.85]	[4.75; 5.5; 7.2; 7.4]
Acetogens	Maximum growth rates on pathway 1	NSP: 7.2 RS: 7.2	NSP: 6 RS: 6

	Maximum growth rates on pathway 3	NSP: 7.2 RS: 7.2	NSP: 6 RS: 6
	pH corners	[5.25, 6, 7.5, 8.25]	[4.75, 5.5, 7.2, 7.4]
Methanogens	pH corners	[5.25; 6; 7.5; 8.25]	[5.05; 5.8; 7.2; 7.4]
NSP: non-starch polysaccharide. RS: resistant starch.			

References

Baniya, R., Upadhaya, S., Khan, J., Subedi, S.K., Mohammed, T.S., Ganatra, B.K., et al. (2017). Carbon dioxide versus air insufflation in gastric endoscopic submucosal dissection: A systematic review and meta-analysis of randomized controlled trials. Clin. Endosc. 50(5), 464-472. doi: 10.5946/ce.2016.161.

Batstone, D.J., Keller, J., Angelidaki, I., Kalyuzhnyi, S.V., Pavlostathis, S.G., Rozzi, A., et al. (2002). The IWA Anaerobic Digestion Model No 1 (ADM1). Water Sci. Technol. 45(10), 65-73.

Belenguer, A., Holtrop, G., Duncan, S.H., Anderson, S.E., Calder, A.G., Flint, H.J., et al. (2011). Rates of production and utilization of lactate by microbial communities from the human colon. FEMS Microbiol. Ecol. 77(1), 107-119. doi: 10.1111/j.1574-6941.2011.01086.x.

Charney, A.N., and Donowitz, M. (2005). "Gastrointestinal Influences on Hydrogen Ion Balance," in Acid-base disorders and their treatment, eds. F.J. Gennari, H.J. Adrogué, J.H. Galla & N.E. Madias. Taylor & Francis.

Cotton, P.B., and Williams, C.B. (2008). Practical Gastrointestinal Endoscopy: The Fundamentals. Wiley-Blackwell.

Cummings, J.H., and Macfarlane, G.T. (1991). The control and consequences of bacterial fermentation in the human colon. J. Appl. Bacteriol. 70(6), 443-459. doi: 10.1111/j.1365-2672.1991.tb02739.x.

Davis, G.R., Morawski, S.G., Santa Ana, C.A., and Fordtran, J.S. (1983). Evaluation of chloride/bicarbonate. Exchange in the human colon in vivo. J. Clin. Invest. 71(2), 201-207. doi: 10.1172/JCI110760.

Duncan, S.H., Louis, P., Thomson, J.M., and Flint, H.J. (2009). The role of pH in determining the species composition of the human colonic microbiota. Environ. Microbiol. 11(8), 2112-2122. doi: 10.1111/j.1462-2920.2009.01931.x.

Florin, T., Neale, G., Gibson, G.R., Christl, S.U., and Cummings, J.H. (1991). Metabolism of dietary sulphate: Absorption and excretion in humans. Gut 32(7), 766-773. doi: 10.1136/gut.32.7.766.

Gennari, F.J., and Weise, W.J. (2008). Acid-Base Disturbances in Gastrointestinal Disease. Clin. J. Am. Soc. Nephrol. 3(6), 1861. doi: 10.2215/CJN.02450508.

Kettle, H., Holtrop, G., Louis, P., and Flint, H.J. (2017). microPop: Modelling microbial populations and communities in R. Methods Ecol. Evol. 9, 399–409. doi: 10.1111/2041-210x.12873.

Kettle, H., Louis, P., Holtrop, G., Duncan, S.H., and Flint, H.J. (2015). Modelling the emergent dynamics and major metabolites of the human colonic microbiota. Environ. Microbiol. 17(5), 1615-1630. doi: 10.1111/1462-2920.12599.

Muñoz-Tamayo, R., Giger-Reverdin, S., and Sauvant, D. (2016). Mechanistic modelling of in vitro fermentation and methane production by rumen microbiota. Anim. Feed Sci. Technol. 220, 1-21. doi: https://doi.org/10.1016/j.anifeedsci.2016.07.005.

Payne, A.N., Chassard, C., Banz, Y., and Lacroix, C. (2012). The composition and metabolic activity of child gut microbiota demonstrate differential adaptation to varied nutrient loads in an in vitro model of colonic fermentation. FEMS Microbiol. Ecol. 80(3), 608-623. doi: 10.1111/j.1574-6941.2012.01330.x.

Payne, A.N., Chassard, C., Zimmermann, M., Müller, P., Stinca, S., and Lacroix, C. (2011). The metabolic activity of gut microbiota in obese children is increased compared with normal-weight children and exhibits more exhaustive substrate utilization. Nutr. Diabetes 1(7), e12. doi: 10.1038/nutd.2011.8.

Pudlo, N.A., Urs, K., Kumar, S.S., German, J.B., Mills, D.A., and Martens, E.C. (2015). Symbiotic human gut bacteria with variable metabolic priorities for host mucosal glycans. mBio 6(6). doi: 10.1128/mBio.01282-15.

Stephen, A.M., Haddad, A.C., and Phillips, S.F. (1983). Passage of carbohydrate into the colon: Direct measurements in humans. Gastroenterol. 85(3), 589-595. doi: 10.1016/0016-5085(83)90012-4.

Sung, J., Kim, S., Cabatbat, J.J.T., Jang, S., Jin, Y.S., Jung, G.Y., et al. (2017). Global metabolic interaction network of the human gut microbiota for context-specific community-scale analysis. Nat. Commun. 8. doi: 10.1038/ncomms15393.

Swallow, J.H., and Code, C.F. (1967). Intestinal transmucosal fluxes of bicarbonate. Am. J. Physiol. 212(3), 717-723. doi: 10.1152/ajplegacy.1967.212.3.717.

Walker, A.W., Duncan, S.H., Carol McWilliam Leitch, E., Child, M.W., and Flint, H.J. (2005). pH and peptide supply can radically alter bacterial populations and short-chain fatty acid ratios within microbial communities from the human colon. Appl. Environ. Microbiol. 71(7), 3692-3700. doi: 10.1128/aem.71.7.3692-3700.2005.

Wang, S.P., Rubio, L.A., Duncan, S.H., Donachie, G., Holtrop, G., Lo, G., et al. (Under review). Pivotal roles for pH, lactate and lactate-utilizing bacteria in the stability of a human colonic microbial ecosystem. mSystems.

Appendix D

Included in this appendix are the DRC 16 forms describing the contribution of published material to this thesis.

MASSEY UNIVERSITY
GRADUATE RESEARCH SCHOOL

STATEMENT OF CONTRIBUTION
DOCTORATE WITH PUBLICATIONS/MANUSCRIPTS

We, the candidate and the candidate's Primary Supervisor, certify that all co-authors have consented to their work being included in the thesis and they have accepted the candidate's contribution as indicated below in the *Statement of Originality*.

Name of candidate:	Nick William Smith
Name/title of Primary Supervisor:	Professor Warren McNabb
Name of Research Output and full reference:	
Smith NW, Shorten PR, Altermann E, Roy NC and McNabb WC (2019) The Classification and Evolution of Bacterial Cross-Feeding. Front. Ecol. Evol. 7:153. doi: 10.3389/fevo.2019.00153	
In which Chapter is the Manuscript /Published work:	Chapter 2
Please indicate:	
• The percentage of the manuscript/Published Work that was contributed by the candidate:	75%
and	
• Describe the contribution that the candidate has made to the Manuscript/Published Work:	
The candidate performed the literature search, read and analysed the relevant literature and drafted the manuscript. All authors decided upon the terminology framework outlined and contributed to critical revision of the manuscript before	
For manuscripts intended for publication please indicate target journal:	
Candidate's Signature:	Nick Smith Digitally signed by Nick Smith Date: 2020.05.18 11:32:38 +12'00'
Date:	18/05/2020
Primary Supervisor's Signature:	Warren McNabb Digitally signed by Warren McNabb Date: 2020.05.19 12:08:37 +12'00'
Date:	19/05/2020

(This form should appear at the end of each thesis chapter/section/appendix submitted as a manuscript/ publication or collected as an appendix at the end of the thesis)

MASSEY UNIVERSITY
GRADUATE RESEARCH SCHOOL

STATEMENT OF CONTRIBUTION
DOCTORATE WITH PUBLICATIONS/MANUSCRIPTS

We, the candidate and the candidate's Primary Supervisor, certify that all co-authors have consented to their work being included in the thesis and they have accepted the candidate's contribution as indicated below in the *Statement of Originality*.

Name of candidate:	Nick William Smith
Name/title of Primary Supervisor:	Professor Warren McNabb
Name of Research Output and full reference:	
Nick W. Smith, Paul R. Shorten, Eric H. Altermann, Nicole C. Roy & Warren C. McNabb (2019) Hydrogen cross-feeders of the human gastrointestinal tract, Gut Microbes, 10:3, 270-288, DOI: 10.1080/19490976.2018.1548622	
In which Chapter is the Manuscript /Published work:	Chapter 2
Please indicate:	
• The percentage of the manuscript/Published Work that was contributed by the candidate:	75%
and	
• Describe the contribution that the candidate has made to the Manuscript/Published Work:	
The candidate performed the literature search, read and analysed the relevant literature and drafted the manuscript. All authors contributed to critical revision of the manuscript before submission to the journal.	
For manuscripts intended for publication please indicate target journal:	
Candidate's Signature:	Nick Smith Digitally signed by Nick Smith Date: 2020.05.18 10:36:36 +12'00'
Date:	18/05/2020
Primary Supervisor's Signature:	Warren McNabb Digitally signed by Warren McNabb Date: 2020.05.19 12:07:48 +12'00'
Date:	19/05/2020

(This form should appear at the end of each thesis chapter/section/appendix submitted as a manuscript/ publication or collected as an appendix at the end of the thesis)

MASSEY UNIVERSITY
GRADUATE RESEARCH SCHOOL

STATEMENT OF CONTRIBUTION
DOCTORATE WITH PUBLICATIONS/MANUSCRIPTS

We, the candidate and the candidate's Primary Supervisor, certify that all co-authors have consented to their work being included in the thesis and they have accepted the candidate's contribution as indicated below in the *Statement of Originality*.

Name of candidate:	Nick William Smith
Name/title of Primary Supervisor:	Professor Warren McNabb
Name of Research Output and full reference:	
Smith NW, Shorten PR, Altermann E, Roy NC and McNabb WC (2019) A Mathematical Model for the Hydrogenotrophic Metabolism of Sulphate-Reducing Bacteria. Front. Microbiol. 10:1652. doi: 10.3389/fmicb.2019.01652	
In which Chapter is the Manuscript /Published work:	Chapter 4
Please indicate:	
• The percentage of the manuscript/Published Work that was contributed by the candidate:	75%
and	
• Describe the contribution that the candidate has made to the Manuscript/Published Work:	
The candidate performed the mathematical modelling and drafted the manuscript. All authors contributed to model and manuscript revision, and read and approved the submitted version.	
For manuscripts intended for publication please indicate target journal:	
Candidate's Signature:	Nick Smith Digitally signed by Nick Smith Date: 2020.05.18 11:35:37 +12'00'
Date:	18/05/2020
Primary Supervisor's Signature:	Warren McNabb Digitally signed by Warren McNabb Date: 2020.05.19 09:34:22 +12'00'
Date:	19/05/2020

(This form should appear at the end of each thesis chapter/section/appendix submitted as a manuscript/ publication or collected as an appendix at the end of the thesis)

MASSEY UNIVERSITY
GRADUATE RESEARCH SCHOOL

STATEMENT OF CONTRIBUTION
DOCTORATE WITH PUBLICATIONS/MANUSCRIPTS

We, the candidate and the candidate's Primary Supervisor, certify that all co-authors have consented to their work being included in the thesis and they have accepted the candidate's contribution as indicated below in the *Statement of Originality*.

Name of candidate:	Nick William Smith
Name/title of Primary Supervisor:	Professor Warren McNabb
Name of Research Output and full reference:	
[illegible]	
In which Chapter is the Manuscript /Published work:	Chapter 5
Please indicate:	
• The percentage of the manuscript/Published Work that was contributed by the candidate:	75%
and	
• Describe the contribution that the candidate has made to the Manuscript/Published Work:	
The candidate performed the mathematical modelling and drafted the manuscript. All authors contributed to model and manuscript revision, and read and approved the submitted version.	
For manuscripts intended for publication please indicate target journal:	
Candidate's Signature:	Nick Smith Digitally signed by Nick Smith Date: 2020.05.18 11:37:25 +12'00'
Date:	18/05/2020
Primary Supervisor's Signature:	Warren McNabb Digitally signed by Warren McNabb Date: 2020.05.19 12:10:18 +12'00'
Date:	19/05/2020

(This form should appear at the end of each thesis chapter/section/appendix submitted as a manuscript/ publication or collected as an appendix at the end of the thesis)

MASSEY UNIVERSITY
GRADUATE RESEARCH SCHOOL

STATEMENT OF CONTRIBUTION
DOCTORATE WITH PUBLICATIONS/MANUSCRIPTS

We, the candidate and the candidate's Primary Supervisor, certify that all co-authors have consented to their work being included in the thesis and they have accepted the candidate's contribution as indicated below in the *Statement of Originality*.

Name of candidate:	Nick William Smith
Name/title of Primary Supervisor:	Professor Warren McNabb
Name of Research Output and full reference:	
Co-culture modelling of a sulphate-reducing bacterium and a methanogen demonstrates altered metabolic parameters compared to monoculture. Smith NW, Shorten PR, Altermann E, Roy NC, McNabb WC	
In which Chapter is the Manuscript /Published work:	Chapter 6
Please indicate:	
• The percentage of the manuscript/Published Work that was contributed by the candidate:	75%
and	
• Describe the contribution that the candidate has made to the Manuscript/Published Work:	
The candidate performed the mathematical modelling and drafted the manuscript. All authors contributed to model and manuscript revision, and read and approved the submitted version.	
For manuscripts intended for publication please indicate target journal:	
Ecological Modelling	
Candidate's Signature:	Nick Smith Digitally signed by Nick Smith Date: 2020.05.18 11:39:58 +12'00'
Date:	18/05/2020
Primary Supervisor's Signature:	Warren McNabb Digitally signed by Warren McNabb Date: 2020.05.19 12:09:39 +12'00'
Date:	19/05/2020

(This form should appear at the end of each thesis chapter/section/appendix submitted as a manuscript/ publication or collected as an appendix at the end of the thesis)

MASSEY UNIVERSITY
GRADUATE RESEARCH SCHOOL

STATEMENT OF CONTRIBUTION
DOCTORATE WITH PUBLICATIONS/MANUSCRIPTS

We, the candidate and the candidate's Primary Supervisor, certify that all co-authors have consented to their work being included in the thesis and they have accepted the candidate's contribution as indicated below in the *Statement of Originality*.

Name of candidate:	Nick William Smith
Name/title of Primary Supervisor:	Professor Warren McNabb
Name of Research Output and full reference:	
[illegible]	
In which Chapter is the Manuscript /Published work:	Chapter 7
Please indicate:	
• The percentage of the manuscript/Published Work that was contributed by the candidate:	75%
and	
• Describe the contribution that the candidate has made to the Manuscript/Published Work:	
The candidate performed the mathematical modelling and drafted the manuscript. All authors contributed to model and manuscript revision, and read and approved the submitted version.	
For manuscripts intended for publication please indicate target journal:	
Candidate's Signature:	Nick Smith Digitally signed by Nick Smith Date: 2020.05.18 11:41:51 +12'00'
Date:	18/05/2020
Primary Supervisor's Signature:	Warren McNabb Digitally signed by Warren McNabb Date: 2020.05.19 09:32:21 +12'00'
Date:	19/05/2020

(This form should appear at the end of each thesis chapter/section/appendix submitted as a manuscript/ publication or collected as an appendix at the end of the thesis)

MASSEY UNIVERSITY
GRADUATE RESEARCH SCHOOL

STATEMENT OF CONTRIBUTION
DOCTORATE WITH PUBLICATIONS/MANUSCRIPTS

We, the candidate and the candidate's Primary Supervisor, certify that all co-authors have consented to their work being included in the thesis and they have accepted the candidate's contribution as indicated below in the *Statement of Originality*.

Name of candidate:	Nick William Smith
Name/title of Primary Supervisor:	Professor Warren McNabb
Name of Research Output and full reference:	
Examination of hydrogen cross-feeders using a colonic microbiota model. Smith NW, Shorten PR, Altermann E, Roy NC, McNabb WC	
In which Chapter is the Manuscript /Published work:	Chapter 8
Please indicate:	
• The percentage of the manuscript/Published Work that was contributed by the candidate:	75%
and	
• Describe the contribution that the candidate has made to the Manuscript/Published Work:	
The candidate performed the mathematical modelling and drafted the manuscript. All authors contributed to model and manuscript revision, and read and approved the submitted version.	
For manuscripts intended for publication please indicate target journal:	
Microbiome	
Candidate's Signature:	Nick Smith Digitally signed by Nick Smith Date: 2020.05.18 11:43:59 +12'00'
Date:	18/05/2020
Primary Supervisor's Signature:	Warren McNabb Digitally signed by Warren McNabb Date: 2020.05.19 12:07:06 +12'00'
Date:	19/05/2020

(This form should appear at the end of each thesis chapter/section/appendix submitted as a manuscript/ publication or collected as an appendix at the end of the thesis)